



On the Development of Power Drive Trains for Hydrogen Fuel Cell Electric Vehicles

Stephen M. Naylor

**School of Electrical & Electronic Engineering
Newcastle University**

**Submitted for the degree of Doctor of Philosophy
May 2013**

The world faces a major problem. Fossil fuel sources are finite and the economic and environmental cost of those that actually remain make finding an alternative one of the great technological challenges of our age. Nearly 70% of refined oil is used for transportation making it one of the key sectors where change could yield large-scale global benefits. Combustion engine passenger vehicle technology is after a long period of stagnation progressing at a pace. Hybrid electric vehicles (HEVs) and battery electric vehicles (BEVs) are also starting to penetrate the mass market. Unfortunately, HEVs do not remove our dependency on oil and the prospects of battery technology advancing sufficiently to allow BEVs to progressively replace the entire oil fuelled vehicles are currently slim. Their limited range and long recharge times prohibit them being useful for most modes of driving.

One solution to the problem may be hydrogen fuel cell electric vehicles (H_2 FCEVs) as they offer great promise, but realistically face many challenges. The fuel cell allowed man to voyage to the moon in the 1960s and recent material advances have enabled them to be packaged into motor vehicles, so providing a zero emission replacement for the internal combustion engine. However, substantial infrastructure and geopolitical changes are required to make hydrogen production and delivery economic but this gas potentially offers a clean and sustainable energy pathway to entirely replace fossil fuels in motor vehicles.

Few reported studies have comprehensively examined the optimal method of building power drive train subsystems and integrating them into an architecture that delivers energy from a fuel cell into driven road wheels. This project investigated the optimisation on the most efficient drive train topology using critical analysis and computer modeling to determine a practical system. No single drivetrain was found suitable for all driving modes and worldwide markets as the current ones typically offered either optimal performance or optimal efficiency. Consequently, a new drivetrain topology was proposed, developed, tested with a simulation environment that yielded efficiency and performance gains over existing systems. Also analysed was the effect of wider vehicle design optimisation to the development of sustainable hydrogen powered passenger vehicles and this was set against the wider social, scientific and engineering challenges that fuel cell adoption will face.

Keywords

Hydrogen, fuel cell, power train, drive train, topology, simulation, control, electric vehicle, alternative fuel, low carbon vehicle, sustainable transport.

Table of Contents

Abstract	ii
Keywords	iii
Table of Contents	iv
Table of Figures	vii
Table of Tables.....	xi
Table of Equations	xv
List of Abbreviations.....	xvii
Acknowledgements.....	xix
1 Introduction	1
1.1 Crisis	1
1.2 Research Problem & Hypothesis	2
1.3 Aims & Objectives	4
1.4 Outline of the Thesis	5
1.5 Limitations of Scope and Key Assumptions.....	6
2 The Future of Transportation Energy	8
2.1 Introduction	8
2.2 We Need to Talk About Oil	8
2.3 Environmental Targets	10
2.4 Alternative Fuels	10
2.5 A Vision of The Future	25
3 The Hydrogen Vehicle	27
3.1 Hydrogen Pathways.....	27
3.2 Hydrogen Internal Combustion Engines	28
3.3 Hydrogen Linear Free Piston Engines	30
3.4 Hydrogen Fuel Cells.....	32
3.5 Hydrogen Storage	42
3.6 Hydrogen Vehicles – The State of the Art & Summary.....	47
4 A Review of FCEV Drive Trains	53

4.1	Introduction	53
4.2	System Architecture	54
4.3	Drive Train Topology Architecture Overview	58
4.4	Detailed Topology Analysis	72
4.5	Topology Review Summary	108
5	Simulation Model Design.....	110
5.1	Choice of Simulation Software.....	110
5.2	Simulation Model Construction	115
5.3	Vehicle Chassis & Vehicle Dynamics Model	118
5.4	Motor & Inverter Drive.....	125
5.5	Transmission	133
5.6	Direct Hydrogen PEM Fuel Cell	134
5.7	Battery Pack.....	144
5.8	DC-DC Converters	158
5.9	Driving Cycles	166
5.10	Simulation Operation & Control	176
5.11	Simulation Model Test Procedures.....	185
6	Results	189
6.1	Introduction	189
6.2	Vehicle Driving Range.....	189
6.3	Vehicle Performance.....	196
6.4	Drivetrain Efficiency.....	201
6.5	Electrical Performance	204
6.6	Control Performance	209
6.7	Validation.....	213
6.8	Results Summary	218
7	Discussion	219
7.1	Introduction	219
7.2	Simulation Outcomes	219
7.3	Component Sizing & Hybridisation Ratio.....	220
7.4	Energy Storage System	221
7.5	Not Such a Global Market?	222
7.6	Performance or Efficiency?	224
7.7	New Topology	225
7.8	Vehicle Design Optimisation.....	233

7.9	Consumer Acceptance	238
7.10	Manufacturing Considerations	241
7.11	Regenerative Braking Simulation	242
8	Conclusions	244
8.1	Introduction	244
8.2	Analysis of Fuel Cell Vehicle Power Drive Train Topologies.....	244
8.3	Development of New Topology	245
8.4	Assessment of the Potential for Hydrogen	246
8.5	The Need for Open Dialogue	247
8.6	Future Work	248
8.7	Summary	249
9	References	250
Appendix i		i
Appendix ii		xvii
Appendix iii		xxii
Appendix iv		xxiii

Table of Figures

Figure 2.7 – Types of HEV Drivetrains	12
Figure 2.8 - HEV Operating Modes	13
Figure 2.9 - Toyota Prius HEV Engine Cross Section [27]	14
Figure 3.1 - Hydraulic dual piston free-piston engine [85]	30
Figure 3.2 - Linear Free Piston Engine Generator [85]	31
Figure 3.3 – Hydrogen Polymer Electrolyte Membrane Fuel Cell.....	33
Figure 3.4 - NuCellSys/Ballard HY-80 PEMFC Engine System [90]	35
Figure 3.5 - The Hindenburg Disaster, 1937 [104]	43
Figure 3.6 - Type IV Compressed H ₂ Cylinder [108]	44
Figure 3.7 - The General Motors Electrovan [112]	47
Figure 4.1 - HEV Drivetrains	59
Figure 4.2 - BEV	61
Figure 4.3 – Basic H ₂ FCEV Drivetrain	61
Figure 4.4 – Basic H ₂ FC Battery Hybrid Drivetrain.....	62
Figure 4.5 – Fuel Cell Determined DC Bus System.....	63
Figure 4.6 – Battery Determined DC Bus System.....	64
Figure 4.7 - Fuel Cell Output Voltage vs. Current	66
Figure 4.8 - Battery Cell Output Voltage vs. Current	66
Figure 4.9 - Torque Speed Curves for 75kW Induction Motor & Drive.....	67
Figure 4.10 - Fixed DC Bus Voltage System	68
Figure 4.11 – Charge Efficiency Optimised Fixed DC Bus Voltage System.....	68
Figure 4.12 – AC Bus Drivetrain System with Matrix Converter Motor Drive.....	69
Figure 4.13 – Dual DC-AC Inverter AC Bus Drivetrain System.....	70
Figure 4.14 - AC Bus ICE HEV Drivetrain	70
Figure 4.15 - Multiple Drive AC Bus Drivetrain	71
Figure 4.16 - Topology A	73
Figure 4.17 - Topology B.....	75
Figure 4.18 - Topology C.....	77
Figure 4.19 - Topology D	79
Figure 4.20 - Topology E.....	81
Figure 4.21 - Topology F	83
Figure 4.22 - Topology G	85
Figure 4.23 - Topology H	87

Figure 4.24 - Topology I.....	89
Figure 4.25 - Topology J.....	91
Figure 4.26 - Topology K.....	93
Figure 4.27 - Topology L.....	95
Figure 4.28 - Topology M.....	98
Figure 4.29 - Topology N.....	100
Figure 4.30 - Topology O.....	102
Figure 4.31 - Topology P.....	104
Figure 4.32 - Topology Q.....	106
Figure 5.1 - Forces Acting on Vehicle on Level Ground.....	119
Figure 5.2 - Forces Acting on Vehicle on Incline.....	119
Figure 5.3 - Michelin 195/65 R15 Tyre Co-efficient of Friction Data.....	120
Figure 5.4 - Rotating Components in Power Drive Train.....	122
Figure 5.5 - Maximum Motor Torque vs DC Bus Voltage.....	126
Figure 5.6 - Motor Power Loss Calculating Simulation Model.....	127
Figure 5.7 - Motor Torque Output Calculating Simulation Model.....	128
Figure 5.8 - Motor & Inverter Drive Efficiency Map.....	131
Figure 5.9 - Total Motor Power Consumption at all Operating Points and DC-Link Voltages.....	132
Figure 5.10 - Fuel Cell System Model Overview.....	135
Figure 5.11 - Fuel Cell Stack Loss Regions.....	136
Figure 5.12 - Fuel Cell System IV Characteristic.....	137
Figure 5.13 - Fuel Cell System Output Current Step Response.....	138
Figure 5.14 - Fuel Cell System Efficiency.....	138
Figure 5.15 - Fuel Cell Reactant Delivery System.....	140
Figure 5.16 - Fuel Cell System Output Power vs. Auxillary Load Power Loss.....	141
Figure 5.17 - Gas Mass Flow Rate vs System Current.....	142
Figure 5.18 - Stack vs. System Efficiency of PEMFC System.....	142
Figure 5.19 - Kokam SLPB75106100 Cell IV Characteristic.....	147
Figure 5.20 - Battery Pack Design.....	148
Figure 5.21 - Battery System VI Characteristic.....	149
Figure 5.22 – Battery Management System.....	151
Figure 5.23 - MATLAB Simulink Battery Model Subsystem.....	152
Figure 5.24 – Boeing 787 APU Lithium Ion Battery.....	155
Figure 5.25 - Failed Boeing 787 APU Lithium Ion Battery.....	155
Figure 5.26 - Uni-Directional DC-DC Converter.....	161

Figure 5.27 - Bi-Directional DC-DC Converter	162
Figure 5.28 - DC-DC Converter Simulation Model.....	163
Figure 5.29 - 80kW Uni-Directional DC-DC Converter Efficiency Map.....	164
Figure 5.30 - 50kW Bi-Directional DC-DC Converter Efficiency Map	164
Figure 5.31- US06 Driving Cycle.....	167
Figure 5.32 - NEDC Driving Cycle	167
Figure 5.33 - ECE-15 Driving Cycle.....	167
Figure 5.34 - EUDC Driving Cycle.....	167
Figure 5.35 - J10-15 Mode Driving Cycle	167
Figure 5.36 - J10 Mode Driving Cycle.....	168
Figure 5.37 - J15 Mode Driving Cycle.....	168
Figure 5.38 - US Highway Cycle.....	168
Figure 5.39 - NYCC Driving Cycle.....	168
Figure 5.40 - Artemis Urban Driving Cycle.....	168
Figure 5.41 - Artemis Road Driving Cycle.....	169
Figure 5.42 - Hyzem Motorway Driving Cycle	169
Figure 5.43 - AMS Driving Cycle	169
Figure 5.44 - UDDS Driving Cycle.....	169
Figure 5.45 - US FTP-75 Driving Cycle.....	169
Figure 5.46 - J10 Driving Cycle Setpoint Scatter Plot.....	171
Figure 5.47 - NEDC Driving Cycle Setpoint Scatter Plot.....	171
Figure 5.48 - NYCC Driving Cycle Setpoint Scatter Plot	172
Figure 5.49 - Hyzem Urban Driving Cycle Setpoint Scatter Plot	172
Figure 5.50 - J10 Driving Cycle Frequency Distribution Plot	173
Figure 5.51 - NEDC Driving Cycle Frequency Distribution Plot	174
Figure 5.52 - Hyzem Urban Driving Cycle Frequency Distribution Plot.....	174
Figure 5.53 - NYCC Driving Cycle Frequency Distribution Plot.....	175
Figure 5.54 - High Level Simulation System Abstraction.....	176
Figure 5.55 - Detailed Vehicle Simulation System Overview	177
Figure 5.56 - Quasi-Static Simulation Methodology.....	178
Figure 5.57 - Battery Charging Rule.....	180
Figure 5.58 - Simulation Operation Flow Diagram.....	183
Figure 5.59 - MATLAB Simulink Simulation Model	184
Figure 5.60 - 0-60mph Acceleration Test Cycle.....	187
Figure 5.61 - 50-70mph Overtaking Test Cycle.....	187
Figure 6.1 - H ₂ FCHEV Range by Driving Mode	194

Figure 6.2 - H ₂ FCHEV Range by Driving Mode (Excluding Aggressive Highway Driving)	195
Figure 6.3 - H ₂ FCHEV Range by Market	196
Figure 6.4 - Topology A US06 Driving Cycle Speed Deficit	200
Figure 6.5 - Topology A US06 Driving Cycle Current Deficit	200
Figure 6.6 - Topology B US06 Driving Cycle Fuel Cell & Battery Currents	201
Figure 6.7 - Power Consumption During US Highway Driving Cycle	205
Figure 6.8 - Topology B US Highway Cycle Fuel Cell & Battery Current	207
Figure 6.9 - Topology B ECE Cycle Fuel Cell & Battery Current	207
Figure 6.10 - Topology B US Highway Cycle Energy Source Terminal Voltages	208
Figure 6.11 - Topology B US06 Cycle Energy Source Terminal Voltages	209
Figure 6.12 - NEDC Driving Cycle	210
Figure 6.13 - Topology B Actual Speed During NEDC Driving Cycle Simulation	210
Figure 6.14 - New York City Cycle Driving Cycle	210
Figure 6.15 - Actual Vehicle Speed for Section of NYCC	210
Figure 6.16 - Section of ECE Driving Cycle Simulation	211
Figure 6.17 - Topology B ECE Cycle Motor Power vs. Speed	212
Figure 6.18 - Sankey Diagram - Validation of Power Losses in Topology C at 70.5kph	216
Figure 7.1 - Topology C - The Most Efficient Drivetrain	224
Figure 7.2 - Topology B - The Highest Performance Drivetrain	224
Figure 7.3 - Topology Q	226
Figure 7.4 - New Topology	227
Figure 7.5 - New Topology System Voltage vs. Power	228
Figure 7.6 - Topology C US06 Driving Cycle System Voltage	229
Figure 7.7 - New Toplogy US06 Driving Cycle Speed vs. Voltage	229
Figure 7.8 - Vehicle Weight Reduction by Application of Lightweight Materials [252]	236
Figure 8.1 - Popular Mechanics July 1960	246
Figure 9.1 - Oil Price Index Jan 1990 - Jun 2012 (US EIA Oil Index)	i
Figure 9.2 - Effect of Oil Price on US & World GDP (Data: World Bank, US EIA)	ii
Figure 9.3 - Hubbert Curve vs Actual US Production Data [263]	iv
Figure 9.4 – The increasing gap between oil discovery and production [268]	iv
Figure 9.5 - How Oil Prices Are Linked to Geo-Political Events [2]	ix
Figure 9.6 - The Persian Gulf & Expanded View of the Straits of Hormuz[275, 276]	xi

Table of Tables

Table 2.1 - Comparison of Current HEV and ICEV Models (UK RRP as of August 2012)	14
Table 2.2 - Comparison of Alternative Transport Fuels	22
Table 3.1 - Types of Hydrogen Fuel Cell	41
Table 3.2 - Comparison of H ₂ Fuel Storage Systems	46
Table 3.3 - Existing Fuel Cell Vehicles	49
Table 4.1 - Power Drive Train Topology Components	60
Table 4.2 - Topology A Power Flow Analysis	73
Table 4.3 - Topology A Control & Performance Characteristics	73
Table 4.4 - Topology A Driver Experience Characteristics	73
Table 4.5 - Topology A Manufacture & Packaging Characteristics	73
Table 4.6 - Topology B Power Flow Analysis	75
Table 4.7 - Topology B Control & Performance Characteristics	75
Table 4.8 - Topology B Driver Experience Characteristics	75
Table 4.9 - Topology B Manufacture & Packaging Characteristics	76
Table 4.10 - Topology C Power Flow Analysis	77
Table 4.11 - Topology C Control & Performance Characteristics	77
Table 4.12 - Topology C Driver Experience Characteristics	77
Table 4.13 - Topology C Manufacture & Packaging Characteristics	77
Table 4.14 - Topology D Power Flow Analysis	79
Table 4.15 - Topology D Control & Performance Characteristics	79
Table 4.16 - Topology D Driver Experience Characteristics	79
Table 4.17 - Topology D Manufacture & Packaging Characteristics	80
Table 4.18 - Topology E Power Flow Analysis	81
Table 4.19 - Topology E Control & Performance Characteristics	81
Table 4.20 - Topology E Driver Experience Characteristics	81
Table 4.21 - Topology E Manufacture & Packaging Characteristics	82
Table 4.22 - Topology F Power Flow Analysis	83
Table 4.23 - Topology F Control & Performance Characteristics	83
Table 4.24 - Topology F Driver Experience Characteristics	83
Table 4.25 - Topology F Manufacture & Packaging Characteristics	83
Table 4.26 - Topology G Power Flow Analysis	85
Table 4.27 - Topology G Control & Performance Characteristics	85

Table 4.28 - Topology G Driver Experience Characteristics.....	85
Table 4.29 - Topology G Manufacture & Packaging Characteristics	85
Table 4.30 - Topology H Power Flow Analysis	87
Table 4.31 - Topology H Control & Performance Characteristics	87
Table 4.32 - Topology H Driver Experience Characteristics.....	87
Table 4.33 - Topology H Manufacture & Packaging Characteristics	87
Table 4.34 - Topology I Power Flow Analysis	89
Table 4.35 - Topology I Control & Performance Characteristics	89
Table 4.36 – Topology I Driver Experience Characteristics.....	89
Table 4.37 - Topology I Manufacture & Packaging Characteristics	90
Table 4.38 - Topology J Power Flow Analysis	91
Table 4.39 - Topology J Control & Performance Characteristics	91
Table 4.40 - Topology J Driver Experience Characteristics.....	91
Table 4.41 - Topology J Manufacture & Packaging Characteristics	91
Table 4.42 - Topology K Power Flow Analysis	93
Table 4.43 - Topology K Control & Performance Characteristics	93
Table 4.44 - Topology K Driver Experience Characteristics.....	93
Table 4.45 - Topology K Manufacture & Packaging Characteristics.....	93
Table 4.46 - Topology L Power Flow Analysis	95
Table 4.47 - Topology L Control & Performance Characteristics	95
Table 4.48 - Topology L Driver Experience Characteristics	96
Table 4.49 - Topology L Manufacture & Packaging Characteristics	96
Table 4.50 - Topology M Power Flow Analysis.....	98
Table 4.51 – Topology M Control & Performance Characteristics	98
Table 4.52 - Topology M Driver Experience Characteristics	98
Table 4.53 - Topology M Manufacture & Packaging Characteristics	99
Table 4.54 - Topology N Power Flow Analysis	100
Table 4.55 - Topology N Control & Performance Characteristics	100
Table 4.56 - Topology N Driver Experience Characteristics.....	100
Table 4.57 - Topology N Manufacture & Packaging Characteristics	100
Table 4.58 - Topology O Power Flow Analysis.....	102
Table 4.59 - Topology O Control & Performance Characteristics	102
Table 4.60 - Topology O Driver Experience Characteristics.....	102
Table 4.61 - Topology O Manufacture & Packaging Characteristics	102
Table 4.62 - Topology P Power Flow Analysis	104
Table 4.63 - Topology P Control & Performance Characteristics	104

Table 4.64 - Topology P Driver Experience Characteristics.....	104
Table 4.65 - Topology P Manufacture & Packaging Characteristics	104
Table 4.66 - Topology Q Power Flow Analysis	106
Table 4.67 - Topology Q Control & Performance Characteristics	106
Table 4.68 - Topology Q Driver Experience Characteristics.....	106
Table 4.69 - Topology Q Manufacture & Packaging Characteristics	106
Table 4.70 - Topology Simple Power Flow Analysis Summary Table	108
Table 5.1 - Simulation Software Not Considered For Use	111
Table 5.2 - Kokam SLPB75106100 Lithium Ion Polymer Cell Specification	146
Table 5.3 - Battery System Specification	149
Table 5.4 - Driving Cycle Summary	166
Table 6.1 - Urban Driving Range	190
Table 6.2 - Extra-Urban Driving Range.....	191
Table 6.3 - Highway Driving Range.....	191
Table 6.4 - Real World Driving Range	191
Table 6.5 - Combined Driving Range.....	192
Table 6.6 - European Market Driving Range	192
Table 6.7 - North American Market Driving Range	193
Table 6.8 - Japanese Market Driving Range	193
Table 6.9 – 0-60mph Acceleration Test Results	197
Table 6.10 – 50-70mph Passing Speed Test Results	198
Table 6.11 - Vehicle Gradeability Test Result	198
Table 6.12 - Driving Mode Efficiency.....	202
Table 6.13 – Relative Driving Mode Efficiency.....	203
Table 6.14 - Efficiency by Market.....	203
Table 6.15 - Relative Efficiency by Market.....	204
Table 6.16 - Electrical Performance.....	205
Table 6.17 - Vehicle Energy Consumption in MPGe	206
Table 6.18 - Simulation Driving Distance Accuracy	211
Table 6.19 - Vehicle Range Ahluwalia et al. vs. Topology C Validation	217
Table 6.20 – Vehicle Efficiency Hauer vs. Topology C Validation	218
Table 7.1 - Driving Mode Efficiency - New Topology.....	230
Table 7.2 - Drivetrain Electrical Efficiency - New Topology.....	230
Table 7.3 - Range by World Market - New Topology	231
Table 7.4 - New Topology Passing Speed Comparison.....	231
Table 7.5 - New Topology 0-60mph Acceleration Test Comparison	231

Table 7.6 - New Topology vs. Ahluwalie et. al Literature Validation.....	232
Table 7.7 - New Topology vs. Hauer Literature Validation.....	232
Table 7.8 - Driving Mode Efficiency - Low Drag Vehicle.....	234
Table 7.9 - Driving Mode Efficiency	236
Table 7.10 - Relative Driving Mode Efficiency.....	237
Table 7.11 - Modified Gear Ratio Performance Data.....	238

Table of Equations

Equation 3.1 – Fuel Cell Anode Reaction	32
Equation 3.2 – Fuel Cell Cathode Reaction	32
Equation 3.3 – Fuel Cell System Reaction.....	33
Equation 3.4 – DMFC Anode Equation.....	38
Equation 3.5 – DMFC Cathode Equation.....	38
Equation 3.6 – DMFC System Equation	38
Equation 3.7 – AFC Anode Equation.....	39
Equation 3.8 – AFC Cathode Equation.....	39
Equation 3.9 – AFC System Equation	39
Equation 5.1 - Wind Resistance Force	119
Equation 5.2 - Rolling Resistance Force	120
Equation 5.3 - Grade Resistance Force.....	121
Equation 5.4 - Vehicle Braking Force	121
Equation 5.5 - Braking Force Calculation.....	121
Equation 5.6 - Linear Inertial Resistance Force.....	122
Equation 5.7 - Inertial Resistance Force	122
Equation 5.8 - Equivalent Mass of Rotating Components	122
Equation 5.9 - Total Resistance Forces at Rest.....	123
Equation 5.10 - Total Resistance Forces During Acceleration	123
Equation 5.11 - Total Resistance Forces at Constant Velocity	123
Equation 5.12 - Total Resistance Forces During Acceleration on a Gradient.....	123
Equation 5.13 - Total Resistance Forces at Constant Velocity on a Gradient.....	123
Equation 5.14 - Vehicle Angular Acceleration	123
Equation 5.15 - Vehicle Angular Velocity.....	124
Equation 5.16 - Vehicle Linear Acceleration.....	124
Equation 5.17 - Vehicle Linear Velocity	124
Equation 5.18 - Motor Power.....	126
Equation 5.19 - Motor Input Current.....	127
Equation 5.20 - Motor Efficiency Calculation	127
Equation 5.21 - Maximum Drive Speed & Torque	133
Equation 5.22 - Maximum Vehicle Speed.....	133
Equation 5.23 - Fuel Cell Transient Response Limit Factor.....	137
Equation 5.24 - Reactant Mass Flow Rates	141

Equation 5.25 - Battery System Characterisation.....	150
Equation 5.26 - SOC Calculation	152
Equation 5.27 - Peukert Battery Capacity Calculation	153
Equation 5.28 - Peukert Modified SOC Calculation	153
Equation 5.29 - Battery Losses	154
Equation 5.30 - DC-DC Converter Efficiency Calculation	163
Equation 5.31 - DC-DC Converter Power Output.....	163
Equation 5.32 - Hybridisation Ratio	179
Equation 5.33 - Power Split	180
Equation 5.34 - Vehicle Range	185
Equation 5.35 - Miles per kg of Hydrogen	186
Equation 5.36 - kg Hydrogen per 100km.....	186
Equation 5.37 - MPGe	187

List of Abbreviations

AC	Alternating current
AER	All electric range
AFC	Alkaline fuel cell
AFV	Alternative Fuel Vehicle
BDCM	Brushless permanent magnet direct current motor
BEV	Battery electric vehicle
BMS	Battery management system
CH ₂	Compressed Hydrogen
CHP	Combined heat and power
CNG	Compressed natural gas
DC	Direct current
DMFC	Direct methanol fuel cell
ESS	Energy storage system
EV	Electric vehicle
FCBHEV	Fuel cell battery-hybrid electric vehicle
FCPHEV	Fuel cell plug-in hydrogen electric vehicle
FCUHVE	Fuel cell ultra-capacitor hybrid electric vehicle
Fracking	Hydraulic fracturing of rock to release gas
GBa	Giga-Barrels of Oil
GDP	Gross domestic product
GHG	Green House Gases
GNP	Gross national product
H ₂ FCEV	Hydrogen fuel cell electric vehicle
H ₂ ICE	Hydrogen internal combustion engine
H ₂ LFPEG	Hydrogen linear free piston engine generator
HEV	Hybrid electric vehicle
ICE	Internal combustion engine
ICEV	Internal combustion engine vehicle
IGBT	Insulated gate bi-polar transistor
IM	Induction motor
LFPE	Linear free piston engine

LH ₂	Liquid hydrogen
LHV	Lower heating value
LPG	Liquid petroleum gas
MCFC	Molten oxide fuel cell
MPG	Miles per gallon
MPGGE/MPGe	Miles per gallon gasoline equivalent
NASA	National Aeronautics & Space Administration
NO _x	Nitrogen oxides
OPEC	Organisation of the Petroleum Exporting Countries
PAFC	Phosphoric acid fuel cell
PEMFC	Proton exchange membrane fuel cell
PEV	Pure electric vehicle
PHEV	Plug-in hybrid electric vehicle
PM	Permanent magnet
R&D	Research and development
RON	Research octane number
RPM	Revolutions per minute
SOC	State of charge
SOFC	Solid oxide fuel cell
SRM	Switched reluctance motor
STP	Standard temperature and pressure
T [†] TW	Tank-to-wheel
US EIA	US Energy Information Administration
VA-NCNT	Vertically aligned nitrogen doped carbon nanotubes
WTW	Wheel-to-well
ZCS	Zero current switching
ZVS	Zero voltage switching

Acknowledgements

This thesis has been a significant part of a personal journey in recent years that became very different to the one I originally envisaged, now some 8 years ago. Its completion owes much to many people and I would like to take this opportunity to acknowledge and thank them for the parts they all played.

Firstly I would like to express my appreciation for the support, experience, knowledge and encouragement of my supervisors Professor Volker Pickert and Dr. Dave Atkinson. Their help, direction and patience was invaluable throughout.

To my parents, Deirdre and Ian, and brother and sister Jon and Helen I owe an indescribable debt for their love and support both in life and in education. I could not have wished for a more inspiring and caring family and this thesis is testament to their endless love and encouragement that have always supported and guided me without question. Joanna, your love, friendship, support and endless patience this past year has been one of the few things to preserve my sanity. I will be eternally grateful for your good humour, gentle persuasion, cooking and tolerance of working all hours that you provided and that played such a large part in seeing this work finally completed.

This thesis has also been a story of medical endurance as well as academic. Newcastle University has shown an exceptional understanding and supported me throughout and I would like to express my heartfelt thanks to the Dean of the SAgE faculty, Dr. Byrn Jones, his staff and the support staff in the Department of Electrical, Electronic and Computer Engineering.

I likely owe my ability to write this acknowledgement to the surgeons, doctors and medical staff of Bradford Royal Infirmary, Newcastle Royal Victoria Infirmary, The Yorkshire Clinic and St. James Hospital Leeds. To my friends Rick, Matt and Anthony, your actions on that eventful trip to buy a sandwich after a lecture will truly never be forgotten. Much is also owed to Matt and Cris and all my friends who have all played a role in encouraging me to persist and complete this thesis.

The Engineering & Physical Sciences Research Council (EPSRC) sponsored this project.

Stephen M. Naylor

May 2013

1 Introduction

“Humanity stands before a great problem of finding new raw materials and new sources of energy that shall never become exhausted. In the meantime we must not waste what we have, but must leave as much as possible for coming generations.”

Svante Arrhenius (1925)

1.1 Crisis

Humanity faces many challenges but the biggest threat to our way of life is not global terrorism, nor the financial crisis, it is a crisis that we already live in the midst of yet many do not know of its existence, appreciate its significance or understand how its consequences could touch every aspect of the modern world. It is a crisis of energy.

Energy underpins nearly all-human activity. Current energy demands are overwhelming obtained from hydrocarbon fossil fuels. At the centre of that hydrocarbon economy is oil. It goes into life saving medicines, it powers the majority of our transportation; it grows our food, packages it and moves it to our plates; it heats our homes and it is involved in the manufacturing of nearly all the goods we put in them. The human race has a *de facto* dependency on oil.

For many years, resources had been able to feed this addiction cheaply and plentifully. These resources enabled a rapid development in the standard of living, technology and the global economy, fuelling consumer and industrial demand throughout the developed world. By fulfilling this demand a new industrial revolution was sparked in developing nations and hundreds of millions of people have been able to change their standard of living faster than at any time in human history. This has led to an unrelenting thirst for more energy and more oil. Once plentiful resources are being depleted at an ever increasing rate and the cost of energy is rising almost continuously. Whilst we are not yet near the immediate end of our supply of fossil fuels the economic need to find alternatives is clear.

Concurrently, the world’s climate has changed significantly in recent decades. The exact causes, its significance and the likely consequences are the matter of significant scientific and political debate. The overwhelming majority of the scientific community is in

agreement that global warming has been caused by human activity, mainly the generation of atmospheric pollution from the consumption of energy and that unabated, the consequences will be wide reaching and potentially devastating. However much of the debate in the political arena where change will be led is heated, partisan and highly contentious.

Reducing energy consumption to any great extent through either efficiency savings or limiting human activity has so far proved impossible in the face of rapidly growing global consumption. The worlds leading nations have not been able to agree on controlling emissions of polluting greenhouse gases and the dominating influence of financial self interest on both global policy and individual activity can not be understated. There are many noble and determined efforts to address both climate change and the diversification of energy supply throughout the world but the fear of climate change alone will not drive change unless a viable and affordable alternative to fossil fuels can be presented to enable change without limiting human or commercial activity.

This thesis is a body of work that contributes to the development of personal transportation that is not dependant on oil and this chapter will outline the research and engineering challenges we face to enable and deliver change in the near to midterm future. It will show such change is technically possible and how its application could enable step changes in the way we produce and consume energy that will solve at least one aspect of the energy crisis before it negatively impacts on the health of the human race and the global economy. The issues have many external stimuli that could easily influence and change how the future will proceed in contrast to the scenarios presented herewith. There are few certainties, other than that the time to do nothing has long since passed.

1.2 Research Problem & Hypothesis

The hypothesis that underpins this thesis is that hydrogen fuel cell vehicles can entirely replace the internal combustion engine and power all passenger cars. By using renewably sourced hydrogen the greenhouse gas emissions from these vehicles would be zero.

The primary research question this presents is to devise a method for quantitatively and qualitatively analysing current designs of hydrogen fuel cell vehicles to determine which designs offer the most promise for vehicles that can achieve mass-market adoption.

Previous alternative fuel vehicles have had success with consumers typically categorised as innovators but little or no success with the next category, early adopters, and have failed to take off. In order to entirely replace fossil fuel powered vehicles, fuel cell vehicles will also need to meet the requirements of the early adopters who can then influence the early and late majority consumers to take them beyond being niche products and truly revolutionise personal mobility throughout the world.

Everett Rogers defined five characteristics of the diffusion of innovations that influence whether they are adopted or rejected [1]:

1. Relative advantage – what benefits does the innovation give over existing options.
2. Compatibility – the level of compatibility that an innovation has with the experience of current and previous technology.
3. Simplicity – if the innovation is perceived as complicated or difficult to use, it is unlikely to be adopted.
4. Trialability – if the innovation is easy to demonstrate it is more likely to be adopted.
5. Observability – how visible is the innovation, the more demonstrable and visible it is, the more likely it is to achieve widespread adoption.

Rogers highlights the first two categories as being the most critical. At appropriate junctures this thesis will test and benchmark its ideas and findings against Rogers criteria to determine their potential within the context of the primary research question.

The secondary research question is to develop new features to overcome the problems and limitations of the current technology and to conceptualise and introduce them into a new drive train topology and analyse their impact on future vehicle development.

To answer these questions, the research problems that will be addressed include:

1. A comprehensive examination of the state of the art of hydrogen fuel cell power drive train topologies.
2. Analysis of the data to determine the challenges and problems facing current topologies.
3. Development of existing topology/topologies to increase efficiency, performance or ease of manufacturer.

1.3 Aims & Objectives

The aims of the thesis are designed to distil the research questions into smaller steps and specific objectives defined so as to enable the progress of the thesis to be measured.

The aims of the thesis are:

1. To prove the need for a change in the energy supply used for automotive transport.
2. To investigate the alternative forms of energy and that establish that hydrogen is a viable alternative energy source.
3. To establish the current design trends and consumer demand requirements of passenger vehicles.
4. To research published literature and public discourse to discover all the current topologies of hydrogen fuel cell power drive trains.
5. To carry out a comprehensive review and analysis of all the topologies against common metrics and to then draw conclusions about the relative merits of each.
6. To improve upon one or more of these topologies or conceptualise and introduce a new topology that addresses problems discovered with existing drive trains.
7. To show that hydrogen fuel cell vehicles can fill the requirement for clean energy transportation in the future.

The objectives of the thesis are:

1. To establish the need for an alternative energy source and make the case for hydrogen.
2. To document, evaluate and classify all current topologies.
3. To build a simulation environment to enable the topologies to be evaluated within a computer environment against established automotive benchmarks.
4. To report the results of the simulation, derive conclusions about each of the topologies and identify which topologies hold the most promise for fuel cell vehicles and which topologies can be taken forward and improved further.
5. To present improvements of existing topologies and new topologies to address the limitations and problems of current systems.
6. To test the new and improved technologies to determine if they deliver significant improvements in performance and evaluate the implications on cost, manufacture and consumer acceptance.

7. To contextualise the potential for the new topologies and hydrogen fuel cell vehicles as a whole by detailing the likely path to hydrogen powered vehicles becoming the market leader. This will include a full and comprehensive analysis of the infrastructure, engineering and social challenges that lie ahead.

1.4 Outline of the Thesis

The thesis is divided into chapters around the key subjects and parts of the research project as follows:

1. Chapter 1 outlines the research project and its aims and objectives.
2. Chapter 2 makes the case for the need for an alternative energy source and establishes hydrogen as the pre-eminent choice.
3. Chapter 3 provides a comprehensive review of hydrogen fuel cell vehicle power drive train topologies in current usage, from the past, and in development.
4. Chapter 4 looks at the current ways that a vehicle power drive train can be simulated by computer software and chooses MATLAB-Simulink as the most suitable tool.
5. Chapter 5 explains how the simulation model and its components were constructed and the methodology used to test the simulation models of each topology.
6. Chapter 6 analyses the results of the simulation, compares them to each other and other forms of automotive traction power and draws conclusions about the various fuel cell drive train systems creating a novel comprehensive review of all existing drive train topologies.
7. Chapter 7 introduces a new topology that improves upon existing topologies. It explains the power electronic principles it operates on and derives a control strategy to operate it. A simulation model of it is then implemented and tested.
8. Chapter 8 concludes the thesis, presenting the main findings of the research and identifies areas of future work and problems that the work has highlighted.

1.4.1 Contributions to Knowledge

In light of the literature and wider discourse review carried out as part of this thesis, it will set out what the author believes to be two novel contributions to the subject.

1. A comprehensive review and analysis of different hydrogen fuel cell vehicle drive train architectures on a common simulation platform.
2. The conceptualisation and introduction of a new drive train topology with improved efficiency and performance.

1.4.2 Published Papers

During this study, several papers have been published based on its work.

- “Fuel Cell Drive Train Topologies – Computer Analysis of Potential Systems” *The 3rd IET International Conference on Power Electronics, Machines and Drives, 2006*. Naylor, S.M. ; Pickert, V. ; Atkinson, D.J.
- “Fuel Cell Drive Train Systems – Driving Cycle Evaluation of Potential Topologies” *IEEE Vehicle Power and Propulsion Conference, 2006*. Naylor, S.M. ; Pickert, V. ; Atkinson, D.J.
- “Optimization of Compressor Power Supply and Control Systems for Automotive Fuel Cell Drive Train Applications” *IEEE Vehicle Power and Propulsion Conference, 2006*. Naylor, S.M. ; Pickert, V. ; Atkinson, D.J.
- “A review of Power Drive Trains for Hybrid Fuel Cell Electric Vehicles” *3rd IET Conference on Automotive Electronics, 2007*. Pickert, V. ; Naylor, S.M.
- “A Highly Modular simulation Model for Hybrid Electric Fuel Cell Power Drive Trains”, *UKACC International Conference on Control, 2008*. Naylor, S.M. ; Pickert, V.

1.5 Limitations of Scope and Key Assumptions

The design of the simulation model is discussed in Chapter 5. The main focus of this work is as an engineering evaluation of differing electric power drive topologies of hydrogen fuel cell vehicles. Since all are tested with a common vehicle, components and sub-systems it is not necessary to simulate some of the real world forces that act on a car and its subsystems beyond key forces and factors that influence the power needed to propel the vehicle at a given speed. These forces, losses and factors would act equally on all the given topologies in the simulation and therefore ignoring them has no adverse consequence on the ability to produce valid and useful data.

A number of assumptions have therefore been made to abstract and delimit the scope of the simulation to aid both computation speed and intelligibility of the simulation model:

1. The vehicle travels in a straight line at all times and does not turn any corners, bank or experience any loss of traction.
2. The weather conditions are held constant and the wind velocity is 0 m/s and the road co-efficient of friction is assumed as that of a dry tarmacadam road.
3. The hydrogen storage tank does not leak any hydrogen to the ambient surroundings.
4. A controller that follows standard driving cycles represents the vehicle driver. Human reaction times and are not simulated the controller deliberately follows the driving cycles without including any variances that a human driver would generate doing the same task to ensure that all tests against any given driving cycle are identical.
5. The temperature during simulation is constant and that a cooling system maintains the temperature of the power sources and power conversion devices. Transient effects of temperature on the components are therefore ignored.

2 The Future of Transportation Energy

2.1 Introduction

This chapter introduces the reader to the need for alternative energy sources in transport and presents a critical analysis of all the alternatives that are currently available or foreseen. It discusses every aspect of the need for an alternative and as such the scope of subjects discussed could initially seem to be detracting from the main focus and science of this thesis, the electrical and electronic engineering challenges that face hydrogen fuel cell vehicles.

Being an engineering research project though, and not one of pure science alone, it is imperative that the relevant social, economic and political factors that surround the broader context of the subject are understood to ensure that the problem is real and so that the application of science to solve the problem is delivered in the most efficient manner whilst also ensuring that the solution is responsible and ethical.

Throughout this chapter, and generally through the thesis, the economic impact of factors is attended to in some detail because they are currently the greatest stimulus for change in the world. Human and ecological concerns typically have mid-long term effects that are rarely the main priority of political leaders and business and it is they who will have to enable the changes required in many areas to change the way we approach transportation.

2.2 We Need to Talk About Oil

The world's transportation is almost entirely powered by fuels produced from oil. From super tankers to super minis, oil distillates power 95% of the movement of everything from the oil itself to the weekly grocery shop. In the automotive field specifically, this equates to the consumption of around 16.5 billion oil equivalent barrels of gasoline, diesel and liquid petroleum gas fuel per year. 7.3 billion of those are used in personal vehicles. Vehicle fuels accounted for 67% of refined oil derivatives in 2011 [2].

Gasoline and diesel are in many ways ideal vehicle fuels. They are easier to extract, transport, store, dispense and use than nearly all of the available alternatives. The problem with a dependency on them is that the supply of oil is finite; the demand for it is rising; the planets tolerance to their effects on the environment seems limited and the ability of the world to pay an ever increasing price, whilst expanding the world economy and furthering social development, is uncertain.

Oil is a highly dynamic commodity; discussions about it's future it evoke a wide range of highly polarising opinions and diametric views. Broadly speaking the impetus for change is often viewed quite simplistically as either an environmental or resource issue - alternatives need to be found as the supply will run out or using them is causing climate change. However, there is far from being a consensus on either of those views and it is a far more complicated subject than either of those views can effectively communicate.

As an engineering thesis, it is important to consider the practical requirements of the problem at hand in order to inform the thinking that determines proposed solution. Replacing oil as the primary source of transportation fuel will be an endeavour of breath taking scale and cost and it is vital to ask the question of whether it actually needs to be considered in the first place. There are many issues and problems with oil that there is broad agreement need addressing, be it now or in years to come, but they can be broadly categorised as Economic; Political; Resource; Security of Supply; Environmental, Health & Social Impact. Each of these areas have many been researched and discussed in great detail, some of them for many decades. The author considers it important to thesis to have an informed understanding of them but a detailed consideration of each within this chapter would be a distraction from the issue at hand and so a discussion about oil has been included in Appendix i.

The position of this thesis is that although the world is in no immediate danger of running out of oil, the age of cheap oil is almost certainly over. With ever advancing living standards across the globe, consumption is only going to increase and the margin between demand and available supply will grow smaller. New resources to meet additional demand are being discovered but are likely to require technologically advanced techniques to extract. This will make new resources costlier to extract and cause further price inflation. The economic effects of continual price increases on the world economy are likely to be profound and have the potential to stifle growth and cause recession. Security of supply is a major concern for nations dependant on oil imports and the risk of destabilising conflicts

in oil producing areas is an ever-present threat to the world oil supply and regional and world peace. Whether fossil fuels are a major contributor to climate change is contested but the negative health effects of particulate air pollution are beyond doubt. The causes of economics, social advancement and ecology are now, albeit independently, aligned in a common cause of promoting and finding an alternative to oil to reduce the risk inherent in continuing to be dependant on it.

2.3 Environmental Targets

Various legislative organisations around the world have laid down targets for vehicle emissions performance that vehicle manufacturers are expected to meet by defined dates. In the European Union a target of 130g CO₂/km for the average emissions of the entire by 2015 new vehicle fleet was agreed in 2009. In 2012 it was agreed that by 2020 the average emissions should be 95g CO₂/km [3]. Throughout the rest of the world the United States has set a target of 93 g CO₂/km by 2025, China 117g CO₂/km by 2020 and Japan 105 g CO₂/km by 2020 [4].

The introduction of legislative targets has actually increased the rate at which manufacturers have reduced the emissions of their vehicles, with the annual reduction rate now around twice the rate it was before the targets were introduced [4, 5]. It is important to consider these targets and requirements so that an assessment can be made of what technologies will be needed to achieve them. Although it looks likely that the targets out to 2020 can be met by combustion engine technology, the UK governments Office for Low Emission Vehicles (OLEV) envisages a target of 50g CO₂/km for passenger vehicles by 2050 [6]. Even with advances in technology, it is high unlikely this target can be met by a fleet of combustion engine powered vehicles and therefore all roadmaps, be they from manufacturers or governments feature alternative fuelled vehicles becoming an increasingly large part of the future fleet [4, 5].

2.4 Alternative Fuels

One of the main reasons that the internal combustion engine vehicle (ICEV) has been so successful is because of the technical qualities of its fuels. It was not the first to market, the electric vehicle beat it by a few decades in the early nineteenth century and initially they had

much higher performance with an electric vehicle (EV) even being the first vehicle to exceed 60mph whilst setting a new land speed record of 61mph in 1899 [7]. But as the ICEV matured and developed superior range and low refuelling times, less than a hundred years later the EV was banished to history [8]. The ICEV is now firmly entrenched as the dominant source of motive power for most road transport with 150 years of supporting development and innovation. This provides any technology wishing to gain market share with several challenges based on customer expectations largely derived from their experience with ICEVs.

Ignoring the supply and environmental drawbacks Petrol and Diesel are ideal fuels. They have high energy densities and are relatively easy to transport in bulk, store and dispense. A typical modern family ICEV with a 60-litre tank can expect to travel around 500-700km on a single tank of fuel that takes around five minutes to refuel. Vehicle technology has reached a maturity that makes travelling by car comfortable, enjoyable and safe. This enables families to purchase affordable vehicles with which they can commute short distances or travel long distances.

Alternative fuel vehicle face several challenges to compete with ICEVs. The huge size of the automotive industry and massive investment in the production and sales of ICEVs act as the primary barrier to change [7]. Automotive manufacturers do however face regulatory and consumer demands to develop alternative fuel vehicles (AFV) and most major manufacturers have active research and development programs which have seen steadily increasing amounts of investment. Though the manufacturers often promote these schemes as their leading the way to a new automotive future, these programs should be considered alongside manufacturers resisting or manipulating regulatory efficiency targets [9-11] and producing increasingly large vehicles that act to counteract improvements in efficiency [12-15] and consideration be given as to whether the investments is of a level sufficient to develop alternative technology as quickly as possible to deliver eco-benefit, or the minimum amount needed to give the outward appearance of innovation being eco-led [16].

The second problem is linked to the first. As at most for-profit companies in mature market places, innovation within the automotive sector is largely risk averse and incremental. It is unlikely that manufacturers will produce large-scale production runs of AFVs ahead of the infrastructure to provide them [12, 16]. Even if the cars were the same

price and offered a similar or improved driving experience, the majority of consumers will not buy cars that they cannot refuel and service wherever they wish to drive [17-22].

Alternative fuels fit loosely into two categories, those that utilise existing engine technologies with no or a few minor changes, and those that require a completely new design of vehicle engine. Each is presented and briefly discussed in the following pages

2.4.1 Electric Hybridisation

Hybrid electric vehicles (HEV) are already with us in the market place. The central principal is the addition of an electrical power source, usually a battery, and motor and generator or combined motor-generator into the vehicle drive train in one of two topologies, either in parallel or series with the existing internal combustion engine.

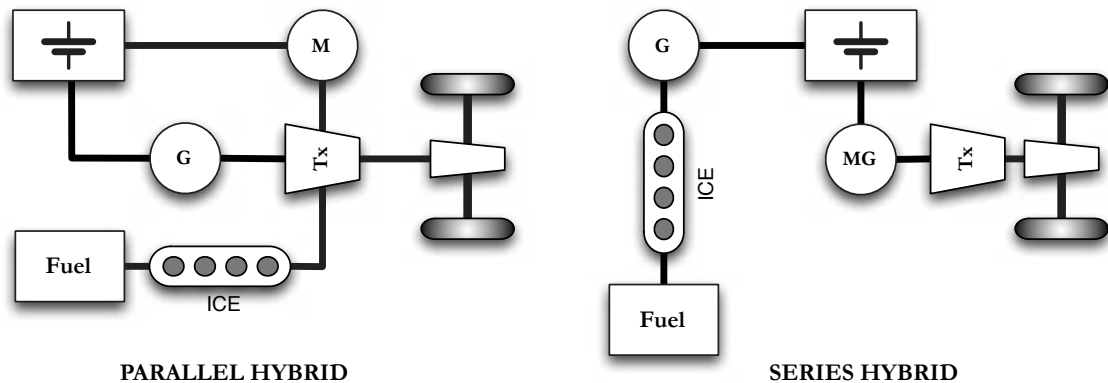


Figure 2.1 – Types of HEV Drivetrains

In the parallel HEV the vehicle is powered by a combination of mechanical power developed by an ICE and an electric motor, a transmission system combines the power from both and allows the ICE to drive the final transmission and the electrical generator, and the motor to drive the final transmission and in some cases the ICE as well.

In the series hybrid, the ICE drives a generator that makes electricity to power a motor to drive the vehicle. The principle idea behind both though is to optimise use of the ICE so that it is used mainly at efficient operating points. The electrical power source is then used to drive the vehicle in areas of operation where the engine is inefficient, generally at low speeds and during idling; and to provide a power boost during high-speed acceleration. The generator is used to recharge the battery and regenerative braking recovers power that would otherwise be dissipated as heat by the vehicles friction brakes and uses it during electric phases of driving, further increasing the efficiency of the HEV [23-26].

There are also two general classifications of hybrid vehicles independent of the drivetrain topology, mild and full. A mild hybrid offers some limited electrical functionality to increase efficiency, such as regenerative braking and stopping the motor when idle and restarting using the stored energy in the battery. A full hybrid is capable of driving the vehicle on electrical power alone.

The majority of hybrids sold have been based on the Toyota designed Hybrid Synergy Drive, a mixed series-parallel hybrid. For the parallel hybrid there are four distinct modes of operation and power flows as shown in Figure 2.2.

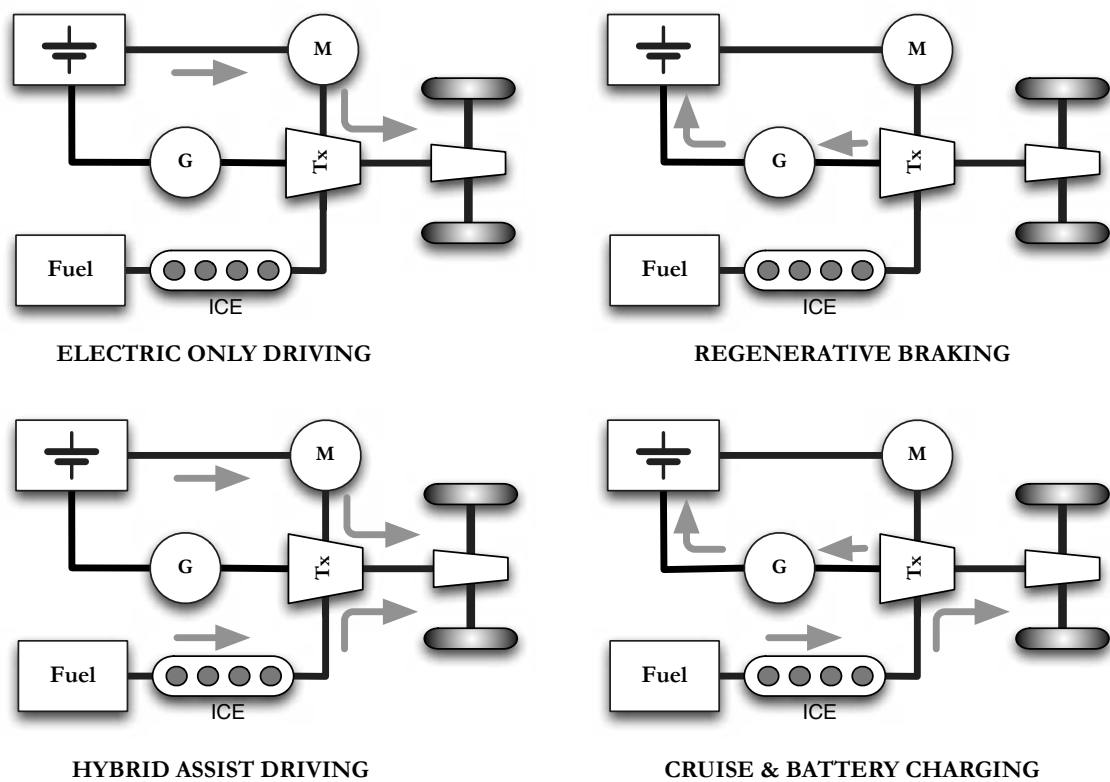


Figure 2.2 - HEV Operating Modes

Although the two power sources can be combined electrically or mechanically, most current models arrange the power sources in parallel and combine the output power of each mechanically through a planetary transmission system such as that in the Toyota Prius, shown in Figure 2.3.

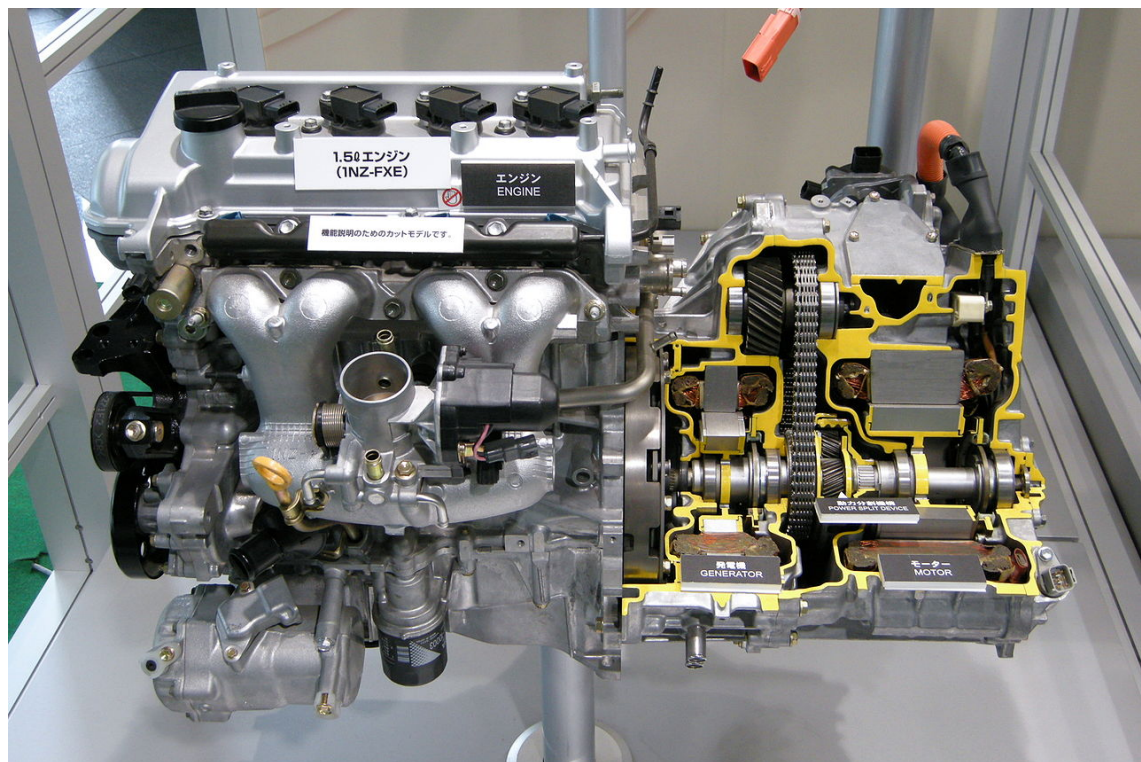


Figure 2.3 - Toyota Prius HEV Engine Cross Section [27]

Hybridisation of an ICEV offers an available solution to reduce the fuel consumption now, though there are still some issues with them and despite extensive marketing and celebrity endorsements, the HEV market is still considered niche. Vehicles like the Prius are still more expensive than comparable ICE powered models, and despite economic incentives such as reduced or zero road tax and exemption from certain tolls or road charges have in themselves not been sufficient to overcome the cost barrier to large scale adoption [26]. Although more efficient than gasoline ICE vehicles, there are many diesel ICE vehicles which are more efficient, have a higher performance and lower cost than the Prius. Table 2.1 compares the cost and specifications of the Toyota Prius with current models from Volkswagen, BMW and Seat.

Parameter	Toyota Prius T ₃ HEV	VW Golf 1.6TDI Blue Motion	BMW 116d EfficientDynamics	Seat Leon Copa TDI Ecomotive
<i>Basic OTR Price</i>	£21,600	£19,430	£20,885	£17,880
<i>CO₂ Emissions</i>	89 g/km	99 g/km	99 g/km	99g/km
<i>0-62mph Speed</i>	10.4s	11.3s	10.5s	11.5s
<i>Consumption</i>	72.4 mpg	74.3mpg	74.3 mpg	74.3mpg

Table 2.1 - Comparison of Current HEV and ICEV Models (UK RRP as of August 2012)

It should be noted that the efficiency and CO₂ emissions figures quoted in the table are derived from NEDC driving cycle testing, which is not optimised for hybrid vehicles. However it is the basis of comparison for all new vehicles currently sold and is the only benchmark available to consumers to compare and contrast the relative fuel efficiency of each vehicle. Furthermore the test vehicles supplied by the manufacturers for testing are often specially selected and highly optimised before testing and the testing itself is done on a rolling road with all possible electrical loads in the vehicle turned off. The net result is that real world performance is usually worse than that quoted by the manufacturers but until the legislative driving cycles and test procedures are changed then they remain the basis for comparing different vehicles.

In the UK market, VW and especially BMW are viewed as premium brands compared to Toyota so the comparison of the Prius against the Seat Leon Copa Ecomotive is perhaps the most illustrative of the price premium (£3720 or 20%) that consumers have to pay to drive a HEV in 2012. All the compared ICEV models feature similar engine start/stop mild hybrid systems as part of efficiency technologies that each firm has given a different but similarly evocative marketing name. VW call it BlueMotion; BMW, Efficient Dynamics; and Seat, Ecomotive.

Nevertheless, hybrid sales are increasing. In 2006, 8,957 new HEVs were sold in the UK. In 2011, 23,373 were sold, representing 1.2% of new UK vehicle sales [28]. Petrol and then diesel powered HEVs will be the first stage of the likely pathway [29-31] to an alternatively fuelled future.

Importantly, the technology that is developed for them will be transferrable. The petrol engine in the parallel HEV could be fuelled with gas, bio-fuel or hydrogen. It may even be replaced with another power source altogether such as a gas turbine or linear free piston engine. The series hybrid is the most suited format to the all-electric vehicle, where two or more electrical power sources are combined, doing so electrically and using a single, larger motor is usually more efficient than using multiple smaller motors.

The next step in the evolution of hybrids is almost certain to be the plug-in HEV (PHEV). By adding an interface to allow the vehicle to be plugged into and charged by a grid connected domestic or industrial electrical power outlet no longer is the HEV entirely dependent on gasoline as its power source, the PHEV is the first major step towards

sustainable transport [23, 24, 29-36] with some studies estimating that 70-80% of all car journeys could be done on electrical energy sourced from the grid alone [30, 34, 36, 37].

2.4.2 Liquid Bio-Fuels

Bio-fuels are another alternative to oil already in the market. Liquid vehicle fuels are produced from crops and plant or animal waste. Bio-diesel is available in many countries in Europe and bio-ethanol is a popular vehicle fuel in North and South America. Although some adaption of the ICE is necessary to ensure proper operation, there are few technology challenges to the large-scale adoption of bio-fuels. The main challenge is the sustainable manufacturer of the fuels without causing adverse environmental impacts.

In the United States, bio-ethanol has been produced mainly from spare corn capacity. It is blended with gasoline to form E85 fuel, an 85% gasoline, 15% bio-ethanol mixed fuel. In Brazil, bio-ethanol is produced from sugar cane and used pure form or blended with gasoline. Both programs have been heavily supported by government subsidies and incentives, though the industry in Brazil is now relatively self-supporting due to the success of the government back programs in driving adoption of alternatively fuelled vehicles. In the US, bio-ethanol fuels are largely confined to the mid-west areas where they are produced and E85 is only available in 1.3% of US filling stations [38]. In Europe, Bio-Diesel is produced from processing the oils of soya and rapeseed crops and is mostly used in a 95% petroleum diesel, 5% bio-diesel blend. It is also produced on relatively small scale from waste vegetable cooking oils. Both forms of bio-diesel are available as 100% bio-diesel fuels but most manufacturers do not warranty their vehicles with its use, especially in the new high performance, highly efficient and highly popular fourth generation common rail diesel engines, mostly due to the large variation in fuel quality.

Bio-fuels allow countries with large agriculture sectors to supplant petroleum fuels and both the Brazilian and US programs were government funded to reduce dependence on oil imports. They reduce CO₂ emissions as the carbon released during the fuels use is absorbed from the atmosphere during the plants growth by photosynthesis. They will likely play a small but significant part in the near term drive to replace oil. BP estimates that in 2030, bio-fuels will provide 7% of total world transport fuels [39].

However they do not reduce the local air pollution generated by vehicles and the growth of crops for bio-fuels production is an energy intensive process but more critically, a land and

water intensive process. Large-scale use of bio-fuels would require huge swathes of land currently used to grow food be diverted to fuel production. Studies [20, 40] have shown that this would have an impact on food prices in some countries; generally developing countries where food price increases would be most keenly felt. The scarcity of water in many countries would require large-scale irrigation projects that would likely impact on water availability, price and marine eco-systems [20, 41, 42]. The vast land requirements, although easily met in countries like Canada, the United States and Russia can also have adverse consequences that could result in large-scale deforestation and loss of arable land [20, 40, 43]. In Brazil, large areas of the rainforest have been destroyed to provide land for crops. Aside from the obvious paradox, destroying one of the planets most precious ecosystems and largest carbon sinks in the name of sustainable fuels appears to be nothing short of lunacy to this author. China has wisely adopted a policy of not allowing fuel crops to be grown on land used for food crops [44].

From a security point of view, whilst it is easy to secure for countries to secure the land on which fuel crops are grown, bio-fuels have a security vector not applicable to most fossil fuel production. The weather, probably influenced by climate change, has become increasingly volatile. Crop yields and price are directly related to the weather and 2012 is a fantastic year to illustrate this point. Press reports of the heat wave and drought in the United States suggest that 40-50% of US soya and corn crops will be seriously affected and there are calls to divert crops grown for fuel into the food market to reduce the impact on food prices [45]. Linking fuel prices to the weather introduces complex uncertainties into production and supply significantly harder to control and compensate for than disruption in fossil fuel supply and a moral food vs. fuel dilemma that could have severe impacts on social order in times of crisis.

2.4.3 Bio-Gas

Methane is amongst the most damaging of GHGs. The main human related sources are livestock and landfill waste sites. Aside from the practical issues of fitting cattle with gas capture devices; the mere idea is only ever going to be one exploding cow away from ridicule and this thesis could not seriously suggest it as a method of obtaining sustainable gas supplies. Waste gas from landfill and sewerage sites however, is already a serious proposition that is producing gas that is used to power plant, vehicles, heating and generate electricity [46]. As the world develops, waste per capita is likely to increase for a while until sustainable waste dispose and recycling reaches all corners of the globe. Though a viable

sustainable form of energy, with bio-gas at certain sites able meet some local energy requirements, current levels of bio-gas production are minuscule in the context of transportation energy demands and not considered a realistic part of a future sustainable transport energy mix.

2.4.4 Liquid Petroleum Gas (LPG)

LPG has been used in vehicles for some time and under the name Autogas is the most common alternative fuel seen next to petrol and diesel on filling station forecourts in the UK. It is typically around 50% cheaper per litre than gasoline. It is a by-product of petroleum refining and as such its price is linked to oil and as it is also used for home heating in areas where there is no grid gas supply and its price can increase suddenly during periods of unexpected or sustained cold weather [22]. Most gasoline ICEVs can be converted to run on LPG for around £1,000 - £2,000. Previous government incentives in the UK saw manufacturers offering LPG or dual fuel LPG/gasoline powered vehicles; the end of these incentives though has reduced the number of new vehicles available with LPG as an option.

As an energy carrier, at 26MJ per litre, LPG carries around 24% less energy per unit volume than gasoline. As it is a pressurised liquid, the typical LPG vehicle fuel tank is larger and heavier than a gasoline or diesel tank and provides less range for a given vehicle packaging volume between refuelling stops. Performance drops slightly and the efficiency also decreases, typically by 5-10% of the gasoline rated MPG. As a by-product of petroleum, LPG is not viewed as a sustainable fuel for the future.

2.4.5 Compressed Natural Gas (CNG)

Recent developments in unconventional gas resources have reinvigorated the natural gas market in Europe and the United States. Driven by the high price of energy and the desire to secure local supplies of energy, Fracking of shale gas reserves is thought to offer certain countries new, secure and abundant supplies of natural gas.

Natural gas generates lower CO₂ emissions per unit of energy than oil and coal. It is an important part of most countries drives to reduce emissions of electricity generation plants and it is better used for this than as a vehicle fuel where its characteristics are sub-optimal. CNG is compressed at around 3000psi and has to be stored in large and heavy tanks that for a given packaging volume offer a vehicle range of around a quarter that of the same

volume gasoline or diesel tank [47]. No refuelling infrastructure exists and there is little point investing large amounts into it when its security and cost are only relatively better than oil in the near to mid term and largely based on the expensive extraction of unconventional reserves at an incompletely quantified environmental cost.

2.4.6 Synthetic Liquid Fuels

Synthetic fuels process existing fossil fuels into petroleum substitutes. In the most common process, coal is gasified into synthesis gas, or syngas. The syngas is catalytically converted in the Fischer-Tropsch process to produce liquid fuels. This process is not a new development, having being invented in the 1920's. It allows countries that are rich in coal to independently generate secure supplies of gasoline and diesel.

Synthetic fuels have been used extensively in two regimes that found themselves cut off from sufficient supplies of oil. During World War Two, Japan and Germany developed extensive synthetic fuel plant infrastructure [48]. Germany provided a quarter of their automotive fuels with synthetic oil substitutes. During the period of Apartheid, South Africa was subject to an international oil embargo and used synthetic fuels extensively.

South Africa still has operating synthetic fuel plants but they adequately demonstrate the single major problem with the fuels produced, the environmental cost is vast. Regardless of whether the process is made economic on a wider scale by high oil prices, the process requires large amounts of electrical energy and outputs large amounts of CO₂. The Sasol Synfuels factory in South Africa produces 150,000 barrels of synthetic fuels per day. But it is also one of the worlds largest point sources of CO₂ and accounts for 21% of South Africa's total CO₂ emissions [49]. Capturing, sequestration and storage of carbon dioxide has been proposed in [48, 50, 51] as a solution to this problem but the technology is not yet mature and further increases the price of synthetic fuels. Whilst they may provide some energy security in coal rich countries, synthetic fuels are not a sustainable alternative fuel for world transport and wide spread usage would likely result in an increase of green house gases over the use of petroleum-based gasoline.

2.4.7 Batteries

Pure electric vehicles (PEV) store electricity, typically from the grid, and use it to drive a motor and propel the vehicle. They have many advantages. The ICE generates torque in peaks, generally at several thousand RPM. Low speed torque is low and gearing is used to

ensure grade climbing ability and reasonable acceleration. The electric motor however starts at maximum torque and maintains it through a large portion of its speed range, the PEV is capable of breathtaking performance with a single stage transmission [52].

The battery electric vehicle (BEV) is the classic example of a PEV. The BEV has fewer components, moving parts and ultimately would likely be easier to manufacture and package than existing ICEV. This assumption is predicated on the basis that an electric vehicle essentially features a power source, power converter, electric drive, control system and cooling system. The power train is connected via simple electrical cables, the power source is made from batteries that can be packaged to fit the shape of the vehicle and each component will likely be assembled prior to installation and simply require little more than fixing and the connection of control and power cabling. Compare this to an ICE that has many more components with various types of liquid, gas, electrical and hydraulic connections between them. This technology is mature however and vehicle manufacturers will be required to invest large sums of money in new production techniques and facilities but once that has occurred, the electric vehicle should be simpler to manufacture.

If an ideal battery existed, this thesis could stop here and would probably never have been started in the first place. If there were a 30-50kWh battery that was relatively lightweight and inexpensive, that could be charged in a few minutes and discharged at sustained high currents and cycled thousands of times without failing or degrading the answer to sustainable transport would be simple. Low-carbon nuclear and/or renewably generated electricity would ultimately provide grid power to power an entire fleet of BEVs the world over with vastly reduced levels of CO₂ output, at reasonable cost and our transportation problems could be solved. I'm sure the reader will be relieved to hear that no such battery exists, nor does a survey of experts by Baker et al. suggest it is within technological reach in the next twenty years [53]. Large portions of the technical challenges examined in and faced by this research project are related to compensating for the deficiencies in available electrical power sources [53-57].

Current battery technology ultimately limits the range of BEVs to around 100miles. Re-charging takes several hours and the battery technology is expensive with a 30kWh/100 mile range pack costing £15,000. By 2030 this is predicted to fall to £4,000 [54, 58] but this is still significantly more expensive than a current ICE. Battery lifetime is not currently capable of matching the lifetime of an ICEV [59]. Slow overnight charging of a large fleet of BEVs would need significant investment in charging control or grid reinforcement. The

electricity transmission grid in many developed, let alone developing, countries would not be able to cope with the charging load. Available power would not be a problem though and may better utilise off peak spare capacity and provide useful base load for renewable generation. Should it ever be possible, rapid charging would present significant challenges to both power generation and transmission systems that would require large capital investment to accommodate mass adoption [59-62].

Globally, the ability of the BEV to reduce GHG emissions differs from region to region dependent on the types of power generation used. Although the efficiency of delivering power from the battery to the wheels, or tank-to-wheel (T²W) efficiency is significantly higher than an ICEV, the overall system well-to-wheel (WTW) efficiency and emissions are somewhat closer than may be expected. In countries such as China and India where significant amounts of electricity are generated by coal stations, studies show the BEV WTW GHG emissions are no better or worse than ICEVs powered by gasoline [29, 44, 58, 63, 64]. In Europe where there is more low carbon and renewable generation capacity installed the BEV does reduce GHG emissions and ultimately if all installed generation is renewable the GHG emissions of a BEV are limited to those involved in the manufacture of the BEV and components and emissions from its consumables.

The BEV will have a part to play in sustainable transport, but unless a “silver bullet” can be found to overcome its inherent deficiencies, alone it will not be enough. Affordability, reliability and performance are key consumer requirements [20, 56, 58, 62] and even if the cost reduces in line with current studies expectations, there are doubts as to whether BEV range can ever match that of the ICEV and if not the BEV will probably be limited to short-range commuting vehicles with another solution being necessary to provide longer range vehicles to replace gasoline and diesel ICEV vehicles completely [26, 58, 63, 64].

2.4.8 Hydrogen

Hydrogen is the most abundant element in the universe. It is non-toxic and in its gaseous form it is highly combustible. In the context of this study one of its most important properties is when burned in the presence of oxygen, the only by-products are heat and water. Its combustion generates no GHG or toxic compounds. However there is a major problem. Hydrogen on earth rarely exists in its molecular form as pure hydrogen on Earth. It readily forms covalent compounds with most other elements. In its pure form though hydrogen offers great potential as a fuel. It is not a fuel in the same sense as petroleum

though. Oil is extracted from the earth and is a primary source of energy. Because hydrogen must be generated from a compound that contains it, using energy in the process, hydrogen as a fuel should be considered as a secondary energy carrier in the same way as a battery is a chemical carrier of electricity.

Much of this chapter has compared alternative fuels to gasoline and diesel and in nearly all cases the comparison has been unfavourable in both energy density and ease/cost of production and storage. Hydrogen partially deviates from that trend.

Fuel	Energy / unit mass MJ/kg (LHV ¹)	Energy / unit volume MJ/l (LHV)	CO ₂ Emissions gCO ₂ /MJ	Density kg/m ³ (STP ²)
<i>Gasoline / Petrol</i>	44.15	32.70	70.8	741
<i>Diesel (ULSD³)</i>	42.91	35.94	74.3	837
<i>LPG</i>	46.28	24.67	63.9	533
<i>Hydrogen (gas)</i>	119.95	0.01	0	0.083
<i>Hydrogen (liquid)</i>	119.95	8.87	0	72.4
<i>Natural Gas</i>	45.86	0.04	56.9	0.768
<i>Biodiesel</i>	38.0	33.44	75.0	890
<i>Fischer-Tropsch Diesel</i>	43.60	34.01	71.2	808
<i>E85 Ethanol</i>	26.80	23.10	71.0	787

Table 2.2 - Comparison of Alternative Transport Fuels

Table 2.2 shows a comparison of current and alternative transport fuels and it is clear from it that per unit mass, Hydrogen is nearly three times as energetic as gasoline and diesel [65, 66]. However as also shown in the table, due to its density hydrogen has significantly less energy per unit volume. At standard temperature and pressure, gasoline is 9,000 times as dense as is hydrogen. To be of any use it is clear that hydrogen needs to be pressurised or liquefied, both energy intensive processes with significant manufacture, storage and distribution complications compared to fuels that are naturally liquids at standard temperature and pressure (STP).

Despite these drawbacks, the third column in the table reveals the first of two dimensions that stand hydrogen apart from all alternative fuels (aside from batteries), zero CO₂ emissions. Hydrogen can be utilised in vehicle drive trains in two ways, it can be burnt in a

¹ LHV – Lower heating value.

² STP – Standard temperature and pressure.

³ Ultra-low sulphur diesel.

modified ICE or it can be converted to electricity in a fuel cell to power an EV or HEV. Both these fuel pathways have only two emissions, heat and water vapour. There are no GHG emissions from hydrogen. The second attractive aspect of hydrogen is sustainability and security. Water is returned to the environment as the by-product of hydrogen combustion or conversion and hydrogen can be generated wherever there is water. There is significantly more water easily available on Earth than we need to manufacture sufficient hydrogen to power the entire planet's road transportation fleet [42, 67].

Stored as a compressed gas and used with a fuel cell, hydrogen vehicles have higher ranges than BEVs and in many cases prototype models compare favourably in both range and performance with existing ICEVs. Hydrogen ICEVs have lower ranges for a given volume of gas due to fuel cells typically having twice the efficiency of ICEs.

So, we have found our fuel panacea? Unfortunately as ever things are not so straightforward. It has been said that there are no easy solutions to the problems facing men left to be found, and hydrogen is a prime case in point. It is clean, sustainable and secure, everything petroleum based fuels are not. It encompasses all three of these vectors, where most alternative fuels only provide one or two when compared to petroleum fuels. These considerations make hydrogen the most attractive alternative fuel we have available; the challenges involved in adopting it on large scale though are significant and cannot easily be dismissed.

Currently, most hydrogen is produced for chemical processing needs and nearly all of it is made by steam reforming natural gas. There is neither sufficiently scaled, nor GHG free sustainable generation capacity in place to power a fraction of any single developed nation's vehicle fleet were hydrogen cars to be available, let alone anything approaching a global supply capacity. In the long term, sustainable, GHG free production of hydrogen will likely be generated by using renewable or nuclear generated electricity to electrolyse water [68-73].

In the nuclear sector, the technology is mature and understood though popular opinion is largely opposed and the question of secure long-term waste disposal still largely unresolved. Recent developments in extracting uranium from the oceans suggest that the 4.5 billion metric tonnes that are dissolved in sea water can economically be extracted [74] providing sustainable supplies of nuclear energy far beyond the end of petroleum. Hydrogen can be generated not only by using nuclear power stations' electrical output, but also by utilising

the otherwise wasted thermal output during off peak hours to generate hydrogen by thermally decomposing water [72].

Using renewable energy, hydrogen again offers unique potential. Much of recent investment in renewable electricity in the UK has gone into the wind sector. Wind is an intermittent source whose load profile is often out of sync with demand and at times its output is unused and wasted with no long term way of storing the generated energy. Electrolysis of hydrogen allows energy that would otherwise go to waste to be converted and stored as a fuel [72, 75]. There is of course an efficiency penalty in doing this, but this is energy that would otherwise be wasted and is no different to a hydroelectric-plant using spare off peak capacity to pump water into a storage reservoir. Although on-shore wind has received most of the attention focused on renewables in the UK of late, this is more down to incentives and it being the quickest, cheapest way of installing the amount of renewable energy capacity that the UK needs to meet various environmental treaty commitments. The greatest renewable energy potential lies off the coasts of the UK in the sea in offshore wind and wave energy. One of the many technical challenges of both these technologies is connecting the offshore generation to the onshore grid. With wave energy especially, the optimum sites lay tens or hundreds of miles offshore. Since the discovery of gas and oil in the North Sea, the UK has developed an indigenous offshore industry that leads the world in many areas. With North Sea field reserves dwindling and peak production having been reached, one area where this expertise could be reused and the industry diversified is developing offshore hydrogen generation platforms that bring together huge untapped reserves of renewable electricity and unlimited supplies of water. Existing tanker technology could easily be adapted to transport the hydrogen back to shore and negate the need to connect these sites to the grid to utilise the huge renewable resource they present.

A recent estimate of the potential energy in Earth's oceans suggests that they could yield between 20,000 and 92,000 TWh/year. Current world electricity demand is around 16,000 TWh/year [76].

The how and the why of the so-called 'Hydrogen Economy' are easily understandable, but detractors always centre on cost as its Achilles' heel [46, 52, 77]. In many respects they are correct to do so but there are equally as many proponents [42, 78-80] who argue the cost is worthwhile and necessary. There exists a chicken and egg situation where because hydrogen vehicles require a wholly new fuel infrastructure nobody will invest in it until

there is sufficient demand from the owners of hydrogen vehicles. Yet it is also clear that there will be no mass market take up and nobody will buy a hydrogen vehicle until a refuelling infrastructure exists that enables them to drive in the same way they can drive an ICEV. Government investment will almost certainly be needed and the scale of investment will dwarf the costs of bailing out the financial system in 2008 and run into trillions of dollars. Faced with such a figure it is easy to simply draw the conclusion that the hydrogen economy is a utopian dream that we cannot afford, indeed many studies argue as such but most did so by drawing comparisons with cheap oil, expanding discoveries of oil or in the expectation that battery technology would advance significantly faster than it subsequently has. Hydrogen is energy intensive to produce and distribute, there is no escaping that fact. But if it is the only viable means of capturing and using renewable energy sources then it is paradoxical to view it as a waste of energy. Ultimately if the energy and feedstock are free and the solution provides an alternative to oil that is effectively limitless, efficiency becomes an irrelevant concept.

2.5 A Vision of The Future

It is the considered opinion investigated in this thesis that in the future sustainable transport will be powered by electricity. The path to this has already begun, HEVs are already on the roads and the PHEV will soon introduce grid-generated electricity as a widely used road fuel alongside BEVs that will have a growing importance in short range commuter and utility vehicles. Beyond this transition phase the battle of technology in the all-electric vehicle is between batteries and fuel cells.

Without a currently unexpected step change in battery technology the BEV will not be able to meet all the load profiles of the current vehicle fleet nor can the current renewable electricity generation capacity meet the charging demand of such a fleet. If a battery technology became available to meet all load profiles, vast investment would be required to strengthen the electricity distribution grid to provide charging capacity and unless the current fuel mix of generation changes substantially; in countries that heavily rely on coal and gas fired power stations the CO₂ output of a BEV fleet would be little better and could indeed be worse than the status quo.

Biofuels will in many localities help relieve the pressure on fossil fuel supplies along the pathway, predominantly by being blended with petroleum. Wide scale adoption of biofuels as a complete replacement is unlikely due to the impact on land, forests and food

production. Concerns about air pollution are also not addressed by biofuels and CO₂ emission reduction aside; local health and social impacts of air pollution will remain largely unaffected.

Hydrogen poses the biggest technical and financial challenges, yet offers the most dramatic promise of all alternatives currently on the table. It is the only sustainable solution that can currently provide a vehicle to completely replace the fossil fuel powered ICEV and many of the developments in HEV and PHEV vehicles have applications in hydrogen vehicles and vice versa. Transportation aside, hydrogen also offers one of the only large-scale methods of storing renewable energy and vehicles can carry enough fuel to far exceed the range of a BEV.

From the consumers point of view although the underlying technology of the hydrogen vehicle will be radically different to that of current vehicles, the experience of driving one will be familiar and consistent. The vehicle will be refilled with fuel at a fuelling station in a similar amount of time to a gasoline vehicle and will be able to drive an acceptable distance in-between refuelling. Environmentally conscious and technologically savvy early adopters will likely embrace the hydrogen vehicle as they have with hybrid and electric vehicles but unlike the electric vehicle, the hydrogen vehicle has none of the drawbacks in range or refuelling time that limit the mass market potential of the electric vehicle. The long term advantage of hydrogen as a fuel and the comparable driving experience satisfy both of Everett Rogers key criteria for analysing whether an innovation can diffuse to the mass market.

Key to the sustainability of hydrogen is that water, the raw material required to produce it is plentiful and for all practical purposes, infinite. All the major oil companies show hydrogen fuels in their mid-long term roadmaps. Many governments have active investment programs in hydrogen research and development and most of the major automotive manufacturers have prototype fuel cell vehicles already in production or planned. The world has grown used to change in society being assured, incremental and gradual, evolutionary if you will. Moving to hydrogen however will be a revolutionary step change that requires huge investment and political will. Government funded hydrogen infrastructure will be required before the automotive industry will invest in the production and the consumer will believe in the practicality of hydrogen vehicles but the vision brings with it a secure, clean automotive fuel and energy supply with no resource or environmental limitations or implications.

3 The Hydrogen Vehicle

3.1 Hydrogen Pathways

Hydrogen can be used in motor vehicles in two ways. Standard fossil fuel ICE designs can be modified and re-engineered to run on hydrogen gas or a hydrogen fuel cell can be used to convert hydrogen into electricity and used as the prime energy source in a H₂FCEV.

Both methods are, if not fully “mature”, well understood. Both have technical challenges but the H₂FCEV has a clear theoretical advantage. Combustion of Hydrogen in an H₂ICE has a similar thermal efficiency to fossil fuel ICEs. Converting hydrogen to electricity in a fuel cell has an intrinsic efficiency of around 55-60% at the cell level. When many cells are combined to form a fuel cell stack system that can be used to power a vehicle, ancillary equipment is required to provide reactants to the stack and maintain optimal operating conditions. The overall fuel cell system is around 5-10% less efficient because of the ancillary load and parasitic losses but depending on the load profile of the ICE a typical fuel cell system still is at least twice and sometimes three times as efficient as hydrogen or fossil fuel combustion in an ICE [81].

Hydrogen combustion is the far simpler of the two methods and the most economically viable in the near term as it reuses much of the basic technology involved in current fossil fuel ICEs. The modifications are minimal, as only a new fuel system needs to be installed, the cylinder head has to be modified and the electronic engine management control unit needs to be re-programmed but the rest of the vehicle remains largely the same. In contrast the H₂FCEV is a major change in vehicle technology though from the electric motor and inverter forward they share common components with the BEV. The principle is largely the same as the BEV, using electrical power alone to drive a single motor that propels the vehicle. The electrical characteristics of the fuel cell require additional control and components to produce a usable vehicle.

As detailed in 2.4.8 hydrogen’s density requires it to be stored in a compressed or a liquefied form to be useful. Due to the order of magnitude difference in efficiency between the H₂ICEV and H₂FCEV, for a given size of compressed gas cylinder the H₂FCEV will potentially have a significantly higher range. This chapter will discuss the operating

principles of both types of hydrogen-powered vehicles but the majority of manufacturers research and development programs are, as this thesis is, targeted towards the H₂FCEV.

3.2 Hydrogen Internal Combustion Engines

The hydrogen combustion engine is not a new technology. Literature was found as early as 100 years ago and the first attempt to develop a hydrogen engine was published in 1820 [82, 83]. The attractiveness of hydrogen combustion is that the technology of the H₂ICEV is only a little different from a gasoline ICE. As such, many authors see it as a bridging technology that would allow existing vehicle technology to be used whilst a hydrogen infrastructure was established, easing the capital demands and providing a transitional path rather than necessitating a step change as many H₂ICEVs could be rapidly and cost effectively produced in existing plants [84].

3.2.1 Hydrogen Combustion

Hydrogen combustion is straightforward; air and hydrogen are mixed and fed into a cylinder where upon they are detonated by an ignition source. The chemical properties of hydrogen allow combustion at significantly higher ratios of air to fuel than is possible with gasoline. A high air to fuel ratio is said to be a lean mixture and lean combustion results in lower gas combustion temperatures, higher thermal efficiency and a more efficient low load operation. It also reduces the amount of nitrogen oxides generated during combustion by thermal disassociation of atmospheric nitrogen. NO_x are the only harmful emissions from a H₂ICE and are produced at a vastly reduced rate than a comparable gasoline ICE due to the lower gas combustion temperature [83].

3.2.2 Technical Challenges of the H₂ICE

Although operating on broadly the same principles as gasoline engines, hydrogen combustion is technically more challenging due to the nature of hydrogen itself [83, 84]. The combustion energy of hydrogen is an order of magnitude lower than hydrocarbon fuels. This is advantageous since the spark plug ignition system requires less energy to ignite and detonate a given volume of fuel but troublesome because it makes hydrogen more prone to pre-ignition. Pre-ignition is the combustion of the fuel air mixture in the cylinder before the spark plug has fired and is caused by the hot spots on surfaces, or residual hot exhaust gases from the previous cycle in the engine cylinder. Pre-ignition can cause positive feedback, with the temperature and pressure in the cylinder rising further,

causing more pre-ignition events and eventually, engine failure. The phenomena causes the engine to emit an audible and very disconcerting banging noise. The minimum ignition energy of hydrogen decreases significantly as the fuel to air ratio is increased from lean to rich and thus the power output of the engine is limited by the limits imposed by the phenomena of pre-ignition.

The problem of pre-ignition can be solved by redesign of the cylinder, cooling of the cylinder, and more effective removal of exhaust gases by use of variable valve timing. Direct injection of the fuel into the cylinder, rather than pre-mixing with air also allows pre-ignition to be controlled as the fuel can be injected into the coolest part of the cylinder and timed so that it does not have chance to pre-ignite before the spark ignition [83].

Low ignition energy is also the root cause of another problem that the H_2 ICEV is susceptible to, namely, backfiring. The fuel-air mixture ignites on hot surfaces on intake into the cylinder before the intake valve has closed and causes combustion that detonates back down the inlet pathway. Fortunately, although the ignition energy is quite low, the auto-ignition temperature of hydrogen is higher than gasoline. ‘Knock’ is a problem resulting the ignition of the fuel-air mixture ahead of the flame front caused by the spark plug. It causes an audible knock or banging noise, indistinguishable from that caused by pre-ignition despite the causes being quite different. Since the auto-ignition temperature is higher, the H_2 ICE is less susceptible to knock than a gasoline ICE. The higher temperature makes spark ignition the preferred method of combustion [84].

Direct injection also eliminates backfire entirely as the inlet valve is closed before the fuel is injected into the cylinder. These are all are known technologies used in current gasoline and diesel engines, relatively straightforward to implement and produce a useable H_2 ICE that does not suffer from pre-ignition but the problem still limits the effective output power of the engine. Compared to a gasoline ICE of the same capacity, the power density of the H_2 ICE is reduced by 17-50% [83].

In order to boost the power density, advanced hydrogen engines boost the intake air pressure with a turbocharger or supercharge. Again this is proven technology from the fossil fuel ICE, though some additional precautions need to be taken to avoid exacerbating pre-ignition and knock problems. The intake air is cooled to maintain a lower cylinder temperature and the pressure is monitored so that the compression ratio in the cylinder does not exceed that at which knock begins to occur. Boosting in this way has resulted in

30-35% improvements in H₂ICE output power and the power density of some engines is 115% of gasoline equivalents. The power density is still however less than modern fourth generation common rail turbo diesel engines, though the thermal efficiency is similar and 45% H₂ICE thermal efficiency is expected to be attainable [83, 84].

3.3 Hydrogen Linear Free Piston Engines

Hydrogen can be used as a fuel in some other types of combustion engines. For example, The linear free piston engine (LFPE) differs from the standard internal combustion engine as the motion is linear as opposed to rotational and as the piston is not connected to a crankshaft it's motion within the engine cylinder is not restricted to a set point for each stage of the cycle. The lack of a crankshaft reduces friction losses in the engine and allows a variable stroke length that can yield higher efficiency across a wider range of operating loads. There has been little interest in the free piston engine for the past 50 years, but in common with recent research drives in other areas, the higher potential efficiency of the engine has sparked renewed interest [85, 86]. Like other combustion engines, different fuels can be used with minor changes to the engine.

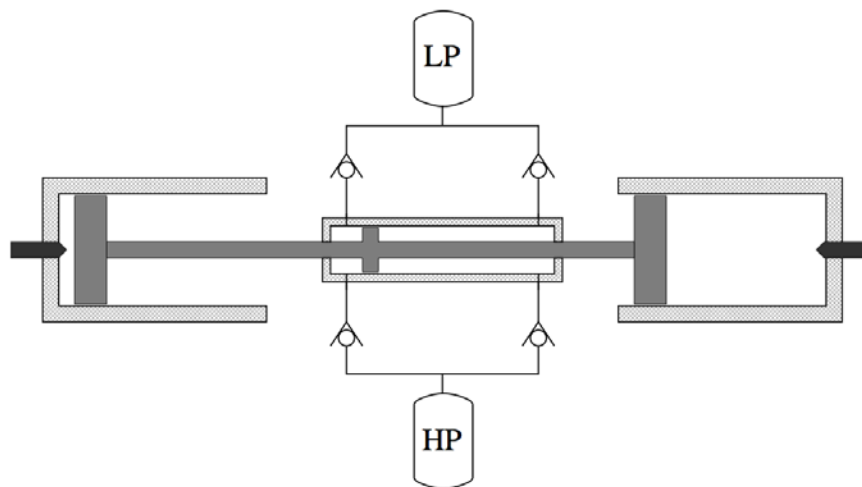


Figure 3.1 - Hydraulic dual piston free-piston engine [85]

Figure 3.1 shows the most common configuration of LFPE, a dual ended piston enclosed in a housing that has a cylinder at each end. This configuration is simple and compact. The expansion cycle of one cylinder also drives the compression cycle of the other cylinder and as a result the engine has a high power to weight ratio. This coupled with the simple design and reduced parts count makes the LFPE cheaper to produce and likely lighter and smaller for a given power density.

The linear motion may appear to be of little use in a vehicle. It is however an advantage, as Figure 3.2 shows the configuration allows for the easy integration of a linear generator in the middle of the engine, allowing the engine and generator of a HEV to be incorporated in a single system with less frictional losses than an ICE driving a rotational generator [85].

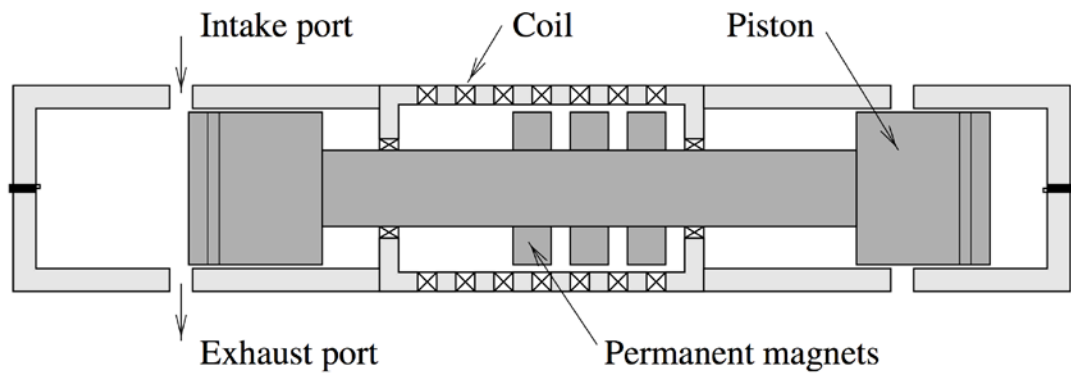


Figure 3.2 - Linear Free Piston Engine Generator [85]

3.3.1 LFPE Advantages

A LFPE generator, fuelled with hydrogen (H_2 LFPEG) has been discussed by van Blarigan [86]. The overall system, generates 40kW with a fuel to electricity efficiency is 50% and because the engine cycle uses a compression ignition strategy that allows very lean fuel mixtures, the NO_x emissions are lower than the H_2 ICE.

3.3.2 LFPE Control Complexity

Harnessing the advantages of the LFPE is dependant upon a suitable control system being feasible. Because the piston position is not fixed about a crank, accurately predicting and controlling the compression ratio is significantly more challenging than in an ICE. Inability to accurately control the compression ratio results in unstable and inefficient operation. Modern microprocessors provide ample computational power to solve the control issue, but this level of control complexity is not necessary in H_2 ICEs.

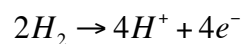
The physical forces on a vehicle chassis from the operation of a single LFPE would be unbalanced and most literature suggests it will be necessary to operate multiple units in parallel to balance the action of these forces.

3.4 Hydrogen Fuel Cells

Analogously with the electric vehicle and the gasoline internal combustion engine, Sir William Grove discovered the hydrogen fuel cell in 1839 nearly twenty years before the first commercial oil well went into production. The fuel cell is an electrochemical energy conversion device that uses a catalytic reaction to combine hydrogen and oxygen to produce electricity, heat and water.

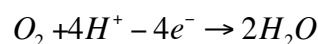
The idea was significantly ahead of its time, so much so that it was not until the 1930's when Francis Thomas Bacon began work and continued development until the 1950's when it was developed into a practical system for a fuel cell using an alkaline electrolyte (AFC). Pratt & Whitney subsequently licensed the patents for AFCs and developed them further into the fuel cell power unit, which was to power all the later NASA Apollo and Space Shuttle spacecraft. General Electric were also working on Fuel Cells during the 1950's and developed the first polymer electrolyte membrane fuel cell which was used in the Gemini spacecraft. The first manned program, Mercury, had used batteries for electrical power. But as the planned mission duration of Gemini was significantly higher than Mercury, NASA turned to fuel cells as they had significantly higher energy density than batteries. This still holds true to this day, with an automotive fuel cell having around ten times the energy density of modern batteries [87, 88] and is the main reason for the automotive interest. Much as NASA turned to the fuel cell when mission duration increased, the automotive industry has turned to fuel cells to increase the range of EVs beyond the limits of the BEV.

All fuel cells operate on the same basic principal. The cell has an anode and a cathode separated by a non-conductive electrolyte. Hydrogen in some form is pumped into the anode region of the cell where it contacts a catalyst and is oxidised. The reaction splits the hydrogen into H^+ protons and H^- electrons:



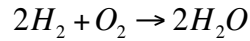
Equation 3.1 – Fuel Cell Anode Reaction

The electrolyte only permits protons to flow between the anode and cathode; the electrons flow via an external circuit to the cathode causing a current to flow. Oxygen is pumped into the cathode region where it is electro-reduced by a catalyst and combines with the hydrogen ions to form water and heat:



Equation 3.2 - Fuel Cell Cathode Reaction

The overall system reaction in the fuel cell can be described as:



Equation 3.3 – Fuel Cell System Reaction

Figure 3.3 shows the basic arrangement of a typical fuel cell. Although there are several different types of cell, that have differing modes of operation and which are constructed from different materials the basic principle remains the same.

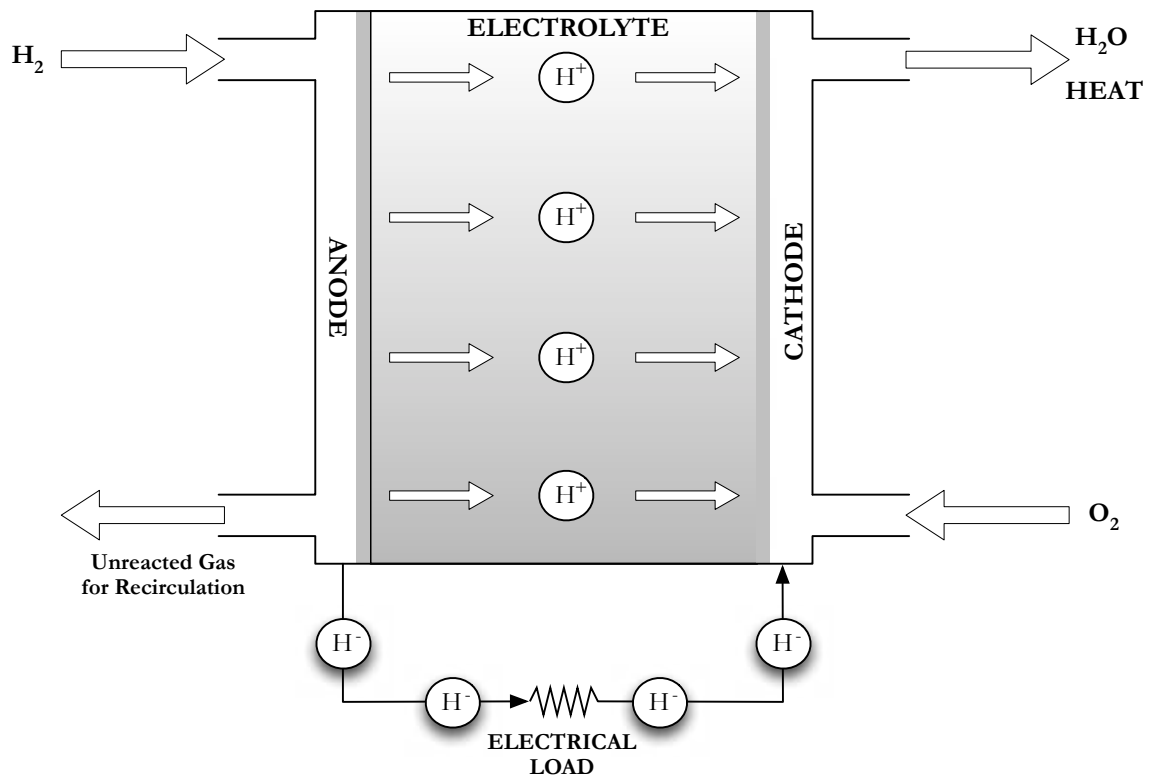


Figure 3.3 – Hydrogen Polymer Electrolyte Membrane Fuel Cell

Cell voltages vary between fuel cell types but are typically around 1V. Consequently multiple cells are connected in a single stack with common reactant flow ducts and each cell is electrically connected in series so that the output voltage of the stack is appropriate for the particular application. Because the output current of the cell is a result of a chemical reaction, changes in output current take a finite time to meet a step response. This time is markedly longer than the time it takes for a battery to respond to a step-change in demand and much slower than a capacitor.

There are six different main types of fuel cell that are currently being examined in “industry” and the literature contains examples for a wide variety of uses. They are defined by the materials used for the electrolyte and catalysts and have a wide range of operating

temperatures, efficiency and suitable applications [88, 89]. The six main types of fuel cell are as follows:

1. Polymer Electrolyte / Proton Exchange Membrane Fuel Cell (PEMFC)
2. Direct Methanol Fuel Cell (DMFC)
3. Alkaline Fuel Cell (AFC)
4. Phosphoric Acid Fuel Cell (PAFC)
5. Molten Carbonate Fuel Cell (MAFC)
6. Solid Oxide Fuel Cell (SOFC)

3.4.1 Polymer Electrolyte / Proton Exchange Membrane Fuel Cell (PEMFC)

The PEMFC uses a polymer material for the cell electrolyte. The main material used is DuPont Nafion. Nafion is a semi-permeable ionomer that is permeable to protons but impermeable to electrons and gases such as hydrogen and oxygen. The material is usually supported on a backbone of a material such as Teflon. The catalyst in the PEMFC is usually platinum which is coated on the anode and cathode material, typically carbon or graphite. The cell construction allows the flow of reactants to the catalytic surfaces and channels for the water to diffuse out of the cell.

The PEMFC is unique in that the electrolyte material is a solid and allows for easy assembly and packaging of the fuel cell stack, low maintenance and no risk of spillage of a hazardous electrolyte. The modern PEMFC has the highest energy density of any fuel cell, can be run on atmospheric oxygen as is unaffected by CO₂, and is capable of self-starting from cold. It is the ideal cell for use in passenger vehicles and all current production and recent prototype vehicles have used the PEMFC.

As has been previously mentioned one of the first commercial applications of fuel cells was in the Gemini space program during the 1960's. The Gemini cell was a PEMFC using polystyrene sulfonate for the proton exchange membrane. Issues with cell durability, high platinum demand, relatively low energy density and lifespan caused NASA to subsequently use the AFCs developed from Francis Bacon's design by Pratt & Whitney in the Apollo spacecraft and the Space Shuttle.

Interest in the PEMFC was renewed in the 1980's and by the early 1990's practical PEMFCs using Nafion were demonstrated. By 2000 the power density had reached the point where fuel cell powered vehicles were both technologically feasible and could

practically be packaged in useful vehicle architectures. Current PEMFC systems, such as that shown in Figure 3.4, suitable for light passenger vehicles generate $\sim 80\text{kW}$, occupy $\sim 200\text{l}$ of space and weigh $\sim 200\text{kg}$, around 50kg heavier than an equivalent internal combustion engine.

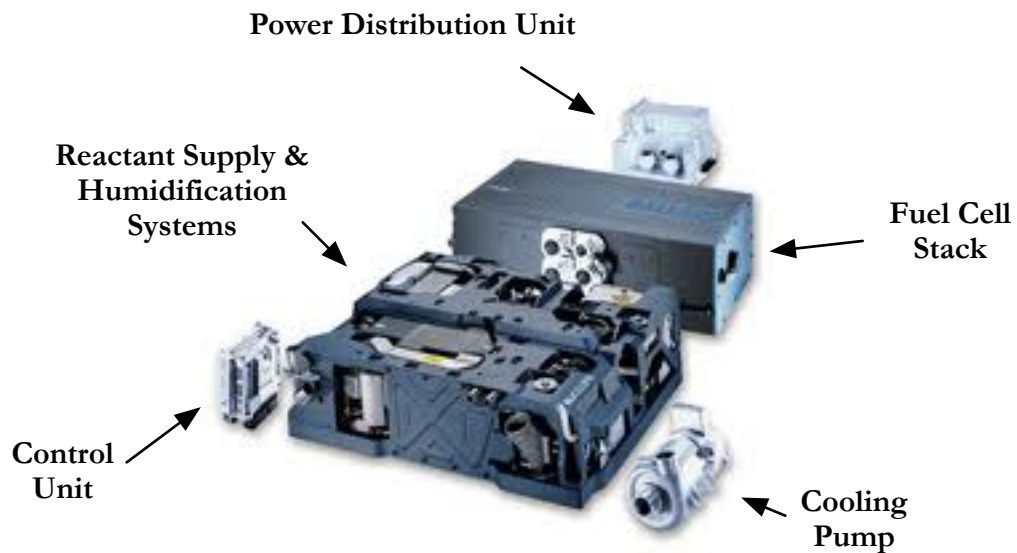


Figure 3.4 - NuCellSys/Ballard HY-80 PEMFC Engine System [90]

The PEMFC operates at a relatively low temperature and is capable of self-starting from cold in a few seconds without external heating, though extreme cold may require defrosting of the cell stack. Appropriately filtered atmospheric air can be used to supply O_2 for the cell and H_2 is supplied via a blower or compressor and humidification system. The humidification is necessary to prevent the Nafion membrane from drying out and degenerating. Constant humidification of the membrane is the main environmental control challenge of the PEMFC. Too little water and the proton transport rate decreases and ultimately the membrane dries and cracks, which allows reactants to combine directly resulting in further heating and the ultimate failure of the cell. If too much water is allowed to accumulate at the electrodes the cell will flood and reactants will be blocked from reaching the catalytic surfaces and the reaction rate decreases.

The reaction between hydrogen and oxygen at the cathode is exothermic and generates significant amounts of heat. The cell must have an effective cooling system to remove this heat. Ethylene-glycol cooling systems, similar to those used in the ICE are used in current production fuel cell systems. The heat in the cooling system can be re-used for heating the vehicle and pre-heating the hydrogen fuel. Either a blower or compressor feeds the hydrogen gas into the cell. Using a compressor achieves a significantly higher power

density in the cell than a blower can, but at a cost in efficiency. Both the compressor and blower are electrically powered devices and they act as a parasitic load on the system that requires a proportion of the PEMFC stack output energy. The compressor consumes an order of magnitude more electrical energy than a blower and this reduces the efficiency of the overall compressor fed system compared to a blower fed, especially at low loads. Because of the larger time lag required to spin the compressor up to pressure compared to increase the flow rate of a blower the step response speed of a compressor fed stack is slower than the blower fed. However, it is an acceptable trade off in automotive applications to attain the higher power densities a compressor enables [91].

The main concerns with the PEMFC are not the system performance but macroeconomic and material technology. The catalyst used in all current production PEMFC stacks is the noble metal platinum and it accounts for ~50% of the fuel cells cost [92]. The rate of oxygen reduction at the cathode is the limiting factor in cell performance and needs a significantly more catalyst than the hydrogen oxidation reaction at the anode. A typical PEMFC has 0.2-0.8mg Platinum/cm². Platinum is one of the scarcest elements on Earth, annual production is limited to a few hundred tonnes and it is traded as a highly valuable commodity. Most production is centred on mines in South Africa and it would be amiss to ignore the insecurity of the supply. A study by the US Department of Energy [93] estimated that 50% market penetration of H₂FCEVs using PEMFCs would cause a 30% increase in the price of platinum and when the penetration reached 80% the demand for platinum would likely exceed supply capability. Sustainable and affordable mass adoption of PEMFCs is restricted by the dependence on platinum.

Platinum catalysts are also vulnerable to carbon monoxide poisoning. CO impurities in the H₂ fuel supply react with and are adsorbed onto the platinum surface, forming a plaque on the platinum that reduces the rate of and could eventually stop the anode reaction.

Whilst other more plentiful materials can be used as catalysts, none are nearly as efficient as platinum. Use of platinum alloys has reduced the amount of platinum needed but much of the research into the PEMFC is focused on further reducing the amount of platinum needed per cell and finding different catalyst materials that do not suffer from CO poisoning. In 2004 Wang et al. [94] described a new method of forming the catalytic surfaces. By depositing finer particles of platinum onto a carbon nanotube structure to form the anode and cathode, rather depositing it on carbon paper, the surface area of platinum is significantly increased and therefore the amount of platinum needed to sustain

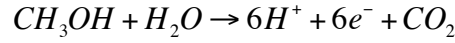
a given reaction rate could potentially be decreased. Seven years later in 2011 and eight years later in 2012 respectively, Wang et al.[95] and Zhang et al. [96] independently described how vertically aligned nitrogen doped carbon nanotubes (VA-NCNTs) can be used as a metal free catalyst that has a reaction rate of 3x that of platinum catalysts and is physical stable. Brouzgou et al. [92] confirms that efforts to reduce the amount of platinum in PEMFC catalysts has already exceeded the targets for 2015 laid down by the US Department of Energy of 0.2g Pt/kW and that the design of platinum free catalysts is yielding positive results.

Membrane durability and cost is another issue associated with the PEMFC with concerns that the PEM may not have a lifespan required of it by standard vehicle life cycles. Chalk et al. [97], Zhang [98] and Cele et al. [99] amongst many other have highlighted progress in composite PEM membranes based on Nafion type materials, new types of membranes based on hydrocarbon materials and advanced manufacturing techniques and suggest that membrane lifespan and durability will be able to meet the demand of future H₂FCEVs.

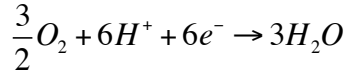
This research can be compared and contrasted with the development of Lithium-Ion batteries in recent years that although progressing forward, has not yielded significant concurrent progress in energy density, power density and safety. If anything the progress in fuel cells has been more marked and although not all the questions have been fully answered and implemented in the technology, there is evidence to suggest the targets will be achieved.

3.4.2 Direct Methanol Fuel Cell

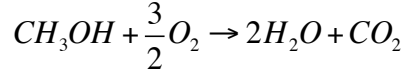
The DMFC is structurally similar to the PEMFC and operates at a similar temperature but uses methanol as a hydrogen carrying fuel rather than being directly fuelled by hydrogen. This is advantageous as methanol is a liquid fuel that can be obtained from petroleum or manufactured as a bio-fuel eliminating the transportation, storage and manufacturer problems associated with hydrogen and enabling the re-use of existing infrastructure and technology. The cell works by oxidation of methanol in the presence of water at the anode to form hydrogen ions and carbon dioxide, the oxygen reduction at the cathode and is the same as for a direct hydrogen cell. The system equations are therefore different to those described at the start of this chapter and are given below in Equation 3.4 for the anode, Equation 3.5 for the cathode and Equation 3.6 for the overall system [100].



Equation 3.4 – DMFC Anode Equation



Equation 3.5 – DMFC Cathode Equation



Equation 3.6 – DMFC System Equation

Though sourcing the fuel for the DMFC is simpler than the direct hydrogen PEMFC the DMFC has its own specific problems that limit power density, speed of response and complicate design, control and packaging.

Essentially because the methanol is mixed with water, the reaction rate is relatively slow compared to a direct hydrogen cell and slow to respond to changes in current demand. This is exacerbated by the need to maintain a weak solution of methanol diffuses through the membrane and causes a direct reaction between methanol and oxygen at the cathode reducing the cell voltage and efficiency [100, 101]. The water to dilute the methanol is recycled from the cathode side of the system though some on-board water storage may be required to compensate for any losses and maintain the solution. The water also requires cooling before being reintroduced into the fuel solution and removal of CO₂ generated at the anode from the solution further complicates and increases the size of the fuel supply system.

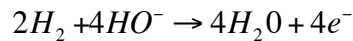
The advantages of methanol over hydrogen as a fuel are clear, but the disadvantages of the current DMFC are highly restrictive and the fuel is also toxic, corrosive and hydrophilic [102]. They do not have the power density to power even small passenger vehicles and the applications of the DMFC are generally limited to small portable power applications where the ease of transport of the fuel is the main factor and the power demand and transient response performance is not so critical such as power devices for portable computers, radios and small mobile utility equipment like electric pallet trucks.

3.4.3 Alkaline Fuel Cell

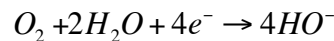
Francis Bacon's AFC is one of the most mature and developed fuel cell technologies available thanks to its extensive use in NASA's manned space programs, Apollo and Space Shuttle programs, replacing the early GE PEMFC design from the Gemini program that could not meet the durability and power density requirements of Apollo. As well as

generating electricity the wastewater output of the cell provided drinking water for the astronauts. The AFC is, compared to other cells, straightforward to construct, operates at modest temperature and is made from readily available materials that have a long lifespan. Nickel is used as a catalyst, which is far cheaper than platinum, carbon and plastic can be used to make the electrodes and the electrolyte is usually a standard potassium hydroxide solution. The cell efficiency is high, typically around 60-70% though the reaction is slightly different to the PEMFC [100, 103].

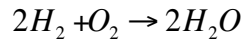
At the anode, 2 hydrogen gas molecules combine with 4 hydroxyl ions to release 4 water molecules and 4 electrons. At the cathode, an oxygen molecule and 2 water molecules absorb 4 electrons that have flowed through the external circuit to form 4 negatively charged hydroxyl ions. The system can be characterised as the anode oxidation reaction of Equation 3.7, the cathode reduction reaction of Equation 3.8 and the overall system as shown in Equation 3.9 and so is ultimately the same reaction as given in Equation 3.3.



Equation 3.7 – AFC Anode Equation



Equation 3.8 – AFC Cathode Equation



Equation 3.9 – AFC System Equation

The main problems with the AFC are its sensitivity to carbon dioxide, the liquid electrolyte and a lower power to weight ratio as compared to the PEMFC. CO₂ reacts with the hydroxyl ions in the electrolyte to form carbonates. In the alkaline solution the carbonates are relatively insoluble and carbonate crystals form, blocking the hydroxyl ion pathways in the electrolyte causing the reaction rate to reduce and ultimately stop. Though methods of reducing the impact are known, such as circulating the electrolyte, the only long-term way to stop this from happening is to scrub CO₂ from the hydrogen and air supply. This was not an issue for the space applications as the AFCs were fed with pure oxygen and hydrogen, but in an automotive air supplied situation, atmospheric CO₂ poisoning of the electrolyte would be a significant problem. The weight of the liquid electrolyte compared to the polymer membrane of the PEMFC lowers the power to weight ratio and complicates packaging a suitably powerful AFC in a vehicle.

3.4.4 Phosphoric Acid Fuel Cell

The PAFC uses phosphoric acid as an electrolyte and the system equations are the same as given in Equation 3.1, Equation 3.2 and Equation 3.3. Due to phosphoric acid being a solid at low temperature, the cells operate at around 200°C and the cell is not capable of self-starting at typical ambient temperatures. Due to this and the relatively low electrical efficiency of 40-50% the PAFC is not considered suitable for use in passenger vehicles. Most applications are in on site stationary power where the waste heat can be captured and the PAFC used in a combined heat and power application. Unlike the AFC, CO₂ does not affect the electrolyte so atmospheric air without filtration can be used to supply oxygen.

3.4.5 Molten Carbonate Fuel Cell

The MCFC uses a molten carbonate salt as the electrolyte and operates at temperatures in excess of 600°C. The MCFC can use a variety of fuels in addition to pure hydrogen, as due to the high temperatures involved it is capable of internally reforming hydrocarbons reducing the cost of the fuel supply and storage system. The efficiency of the MCFC approaches 60% and gives it a significant advantage over the PAFC. The main problem is that the molten carbonate salt is highly corrosive and cell lifespan is limited.

Similarly to the PAFC and SOFC, the MCFC is designed for use in stationary power and co-generation applications, the physical size and weight prohibit use in passenger vehicles.

3.4.6 Solid Oxide Fuel Cell

The SOFC is so named because the electrolyte is a solid oxide or ceramic type material. They differ in operation from the other fuel cells discussed so far in that the electrolyte transports oxygen ions to the anode where they react with hydrogen, rather than transporting hydrogen protons to the cathode.

A high temperature of around 1000°C is needed to support the reaction and the start-up and shutdown times are therefore long. The benefit of the high temperature is that expensive catalysts are not required and plentiful cheap materials can be used instead. The cell is also not poisoned by carbon monoxide though sulphur poisoning is an issue and de-sulphurisation of the air supply is necessary. The SOFC has similar fuel flexibility to the MCFC.

The SOFC is mainly used in CHP applications where low cost, longevity and high system efficiency are more important than size, weight and start-up time. As with the MCFC, the characteristics and operating profile of the SOFC make it completely unsuited to automotive uses.

3.4.7 Hydrogen Fuel Cell Summary

Table 3.1 summarises the characteristics and application of each of the different types of fuel cell that have been discussed in this chapter.

Fuel Cell Type	Electrolyte Material	Operating Temperature	Application	Typical Power Output	Stack Efficiency ¹
<i>PEMFC</i>	Polymer	70-90°C	Portable	High	50-60%
<i>DMFC</i>	Polymer	50-110°C	Portable	Moderate	<40%
<i>AFC</i>	Alkaline Solution	70-100°C	Aerospace	High	70%
<i>PAFC</i>	Phosphoric Acid	200-220°C	Installed Power	Moderate	40%
<i>MCFC</i>	BASE	600-650°C	Installed Power	High	60%
<i>SOFC</i>	Solid Oxide	800-1000°C	Installed Power	Moderate	60%

Table 3.1 - Types of Hydrogen Fuel Cell

¹ Stack efficiency does not include losses due to the parasitic electrical load of the ancillary equipment (compressor, humidifier, control system etc) required to operate the fuel cell system.

3.5 Hydrogen Storage

Storage of hydrogen on-board a vehicle is another area where there is a high level of active research and development that will be of critical importance to the range performance of H₂FCEVs. There are four basic storage systems discussed in the literature and in use:

1. Compressed Hydrogen Tanks
2. Liquid Hydrogen Tanks
3. On-board Reforming of Petroleum or Bio-Fuels
4. Metal Hydrides

The hydrogen storage system used in a vehicle is also likely to be one of the most critical parts of vehicle acceptance amongst the public. The storage system must not only be technically safe, it needs to appear to be safe. Acceptance of compressed gas tanks in vehicles is already relatively common with the usage of LPG vehicles having already been noted in this thesis. Hydrogen however adds an extra dynamic into the situation that makes acceptance of its storage system as safe more difficult if not uncertain.

3.5.1 Hydrogen Safety & Public Perception

As a fuel, hydrogen is easily combusted, but so is gasoline. In contrast to gasoline, hydrogen burns in a controlled, if rapid, manner, usually vertically, and in the absence of an ignition source escapes of gas usually rapidly disperse into air harmlessly and with no risk of explosion. Gasoline burns in an omni-directional manner, for a significantly longer duration and the fuel accumulates and disperses where it has been leaked, remaining highly flammable until cleaned up. Hydrogen is non-toxic and presents no threat to the environment when leaked whilst gasoline is toxic and pollutes groundwater and marine ecosystems.

All this information however is lost or put to one side by the perceptions of people, which can be summarised by one picture. The image shown in Figure 3.5 of the Hindenburg Airship burning in New Jersey in 1937 is a common image associated with furthering the notion that hydrogen is inherently more dangerous than other fuels. The fact that more people have died in helium airship disasters and that a large portion of the fire was due to the heavily doped aircraft skin burning is usually lost or ignored. Moving from the simply misrepresented to the ridiculous, some references also make note of a reported public

perception that hydrogen is synonymous with thermonuclear weapons or 'hydrogen bombs', further enhancing the image of danger that surrounds it [67, 101].



Figure 3.5 - The Hindenburg Disaster, 1937 [104]

Public education and information exercises can correct all this, and the positive economic advantages of hydrogen will likely win over the vast majority of sceptics, but steps must be taken to ensure that the hydrogen storage technologies used in vehicles are as safe as possible as any uncontrolled failures in the early stage of hydrogen vehicle roll-out could spell disaster for the hydrogen vehicle. Most people perhaps forget that petrol is in itself an inherently dangerous fuel. Although it requires no pressurisation it is flammable, toxic and presents an explosive risk. In accidents it has and continues to cause cars fires and people burn to death in vehicles because of its presence. Technology has been developed to prevent this and they are actively used in military vehicles but have never been adopted in passenger cars due to cost and lack of demand. Consequently beyond the additional safety requirements imposed on pressurised storage systems hydrogen does not present any more challenges and may in fact be safer in accident and malfunction situations than petrol.

3.5.2 Hydrogen Storage Systems

The main question surrounding storage is which is the correct choice for vehicle applications. Because of its low molecular weight, Hydrogen is highly diffusive; it causes embrittlement of metals and relative to other gases requires a large amount of energy to compress and liquefy. The most common method seen in literature for storing hydrogen

on-board a H₂ICEV or H₂FCEV is in compressed gas cylinders [97, 102, 105-108]. To adjust for the difficulties in storing hydrogen, H₂ cylinders differ from the standard steel cylinders used to store most gases. To combat the diffusion of hydrogen through materials, joints and interfaces the cylinder is lined with a high-density polymeric material that acts as a gas diffusion barrier. Because of the relatively high pressures (typically 700 bar) required to store enough compressed H₂ to deliver a useable driving range, the cylinders have to be incredibly strong and the low density of hydrogen makes them physically quite large. Using steel for such a vessel would make it prohibitively heavy and therefore carbon fibre is typically used to construct the body of the vessel to make it lighter and stronger. The outside of the vessel needs to ensure protection from impacts and materials such as foam and Kevlar are used to achieve this. A typical fourth generation compressed hydrogen cylinder is shown in Figure 3.6 [109].

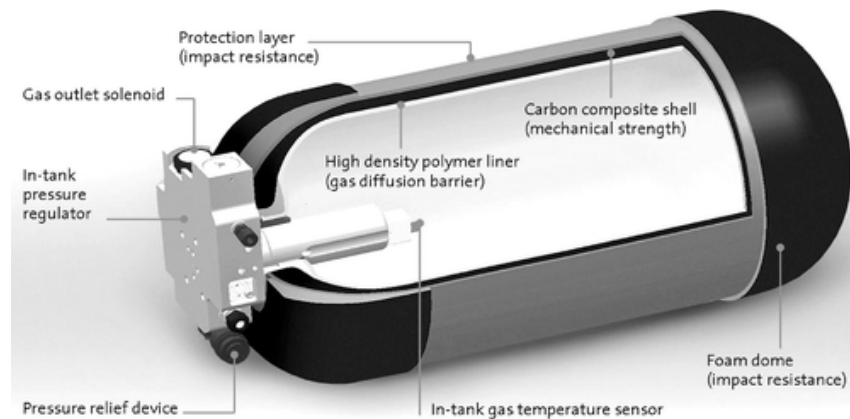


Figure 3.6 - Type IV Compressed H₂ Cylinder [108]

Carbon fibre is the single biggest cost driver of the compressed H₂ cylinder [105] but a significant portion of the current cost is also thought to be due to current low volume assembly costs [107, 108].

On board storage of liquid hydrogen would be the most space efficient method, however it is prohibitively difficult to implement. Hydrogen is a gas down to -235°C. Even with highly insulated containers, a liquid H₂ tank will gain heat from the surrounding environment and the liquid H₂ will boil off into H₂ gas. At a certain point this gas will need to be vented into the atmosphere from the storage device to prevent an explosion. Not only is this wasteful but it means that you could not park a H₂FCEV vehicle at the airport and two weeks later come back and drive it away, the fuel would have literally evaporated into thin air. Cryogenic storage on-board would require a prohibitive amount of electricity to be generated by the fuel cell system simply to maintain the fuel as a liquid. Refuelling a liquid

H₂ tank also takes longer than a compressed H₂ tank as the whole refuelling system needs to be cooled to the liquid point before any sizeable amount of hydrogen will flow. Liquefying hydrogen requires around twice the power of compressing it into a 700 bar tank. Given all these factors liquid H₂ storage is not considered practical for passenger vehicles.

Another option is to use an existing liquid or gaseous petroleum or bio fuel and convert it to hydrogen on board the vehicle in a reformer as detailed by Hauer [110]. This allows existing fuels and infrastructure to be used though adds another system that needs to be powered and packaged into the vehicle. The public perception of safety was noted as important earlier in this section, adding in what is effectively a small piece of chemical plant into a vehicle is a significant step in this regard. In technical aspects it also complicates the control of the vehicle. With a direct H₂ supply, a PEMFC can respond to changes in demand rapidly. If a reforming system is added into the system the transient response time is linked to how fast the reformer can produce hydrogen. System start-up times are also negatively affected by the need of the reformer to warm up to operating temperature before being able to produce any hydrogen and an intermediate compressed storage tank has to be provided to compensate for reformer response time during periods of high demand changes such as hill climbing, adding further weight and volume to the system [102, 106, 111]. As with many chemical processes, even if reforming of existing fuels was considered a sustainable option, doing it on a small scale is inefficient in comparison with large scale reforming plants such as those that generate hydrogen for fertiliser and petroleum production use. The overall system inefficiency, large weight and volume of the reformer system and the financial and environmental cost of putting a reformer system into every fuel cell vehicle makes it a nonsensical choice that this thesis does not consider sustainable or practical.

Metal hydrides are materials that can be heated to absorb hydrogen gas and then can be caused to release it by the application of heat at later point. The application principle would be that hydride canisters would be sold at fuelling stations and the current canister could be removed and replaced with a fresh one and the vehicle could then carry on its way. Sodium aluminium hydride (NaAlH₄) has been the focus of much research though like all hydrides its limiting factor is how much hydrogen it can store as a percentage of its own weight. Currently this is an order of magnitude less than either liquid or compressed hydrogen tanks can provide and given that the hydride needs to be heated at both the absorption and

desorption stage, typically to around 200°C, comparatively inefficient, requiring almost a third of the energy stored in the hydride [107].

	Gasoline Reference	Liquid Hydrogen 235°C	FeTi Hydride (1.2% H ₂)	Compressed H ₂ (70MPa)
<i>BTU</i>	629,500	629,500	629,500	629,500
<i>Fuel Weight (kg)</i>	13.9	4.7	4.7	4.7
<i>Tank Weight (kg)</i>	6.3	18.6	547.5	86
<i>Fuel System Weight (kg)</i>	20.4	23	552	90.5
<i>Volume (l)</i>	18.9	177.9	189.3	227.2

Table 3.2 - Comparison of H₂ Fuel Storage Systems

Table 3.2 [102] summarises the characteristics of the hydrogen fuel systems discussed. Compressed hydrogen gas storage is currently the most viable and promising means of storing hydrogen on-board a vehicle. It requires the least energy of any of the direct hydrogen methods to compress, allows for the fastest refuelling times and the technology already exists to provide tanks of a size sufficient to support long vehicle endurance.

Packaging the cylinders into the vehicle chassis is a non-trivial but not insurmountable problem and various prototype and small-scale production vehicles have managed to achieve this and provide reasonable storage space in the vehicles boot. Initial public education will likely be needed to convey the truth about hydrogen safety and promote consumer acceptance of the fuel amongst early adopters. But ultimately like gasoline vehicles before them, so long as prudent design choices are made the benefits of hydrogen vehicles will likely see the safety aspects accepted by the wider public without major difficulty.

3.6 Hydrogen Vehicles – The State of the Art & Summary

The first commercially produced prototype H₂FCEV is generally accepted to be the 1966 General Motors Electrovan, shown below in Figure 3.7. The Electrovan used 32 alkaline fuel cells and was fuelled with liquid H₂ and liquid O₂. It had a range of 240km, took 30s to go from 0-100kph and weighed ~3500kg[112]. The entire cargo bay was occupied by the system and safety concerns saw the van restricted to operation solely on GM property. Nevertheless it was a valid demonstration that fuel cell technology could power a vehicle.

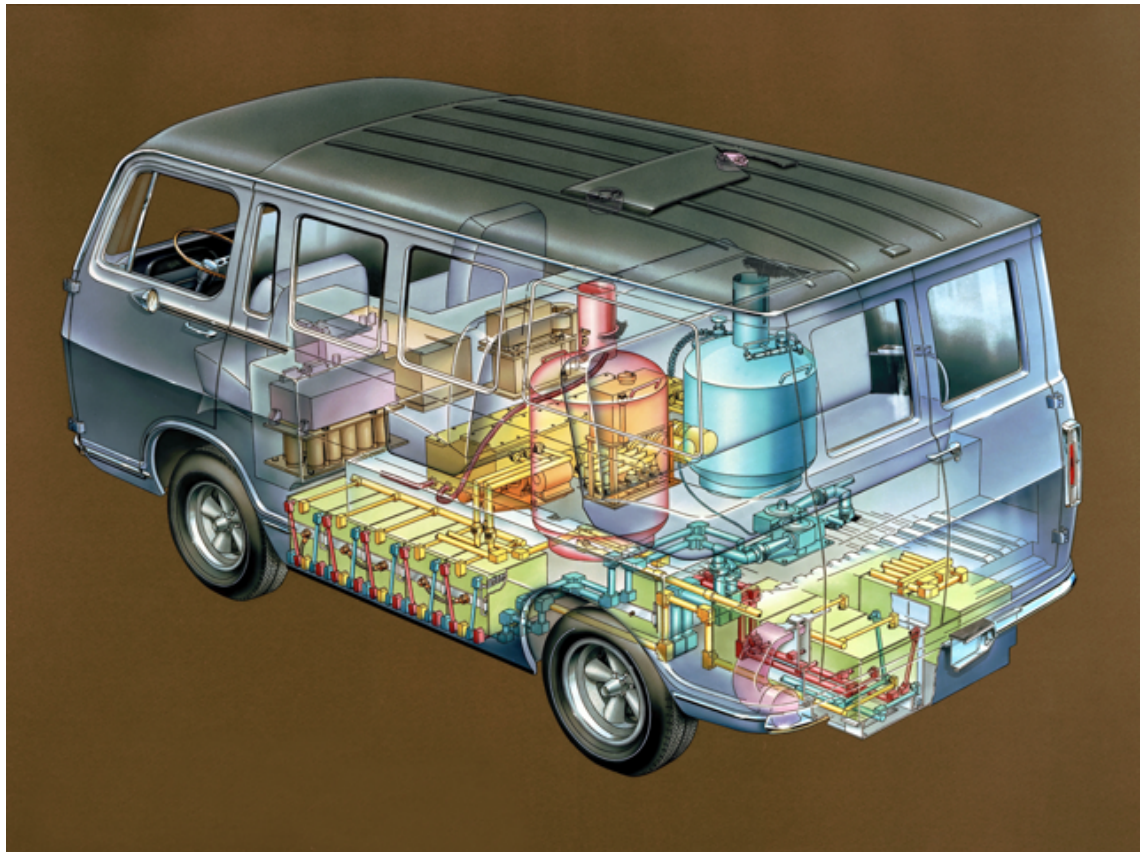


Figure 3.7 - The General Motors Electrovan [112]

Some 45 years later, fuel cell vehicles have progressed substantially. Many major automotive companies have made prototypes and small-scale pre-production models and the H₂FCEV has been one of the major focuses of spending on alternative vehicle technology research and development over the past decade.

A chronological selection of the vehicles produced to date by the major automotive manufacturers is shown in Table 3.3 [108, 113-116].

Vehicle	Year	Drivetrain	Fuel Cell	Fuel	MPG	Speed	Range
<i>Mercedes</i>							
<i>NECAR 1</i> (180 Van)	1994	FCEV ¹	50kW PEM	CH ₂ 30MPa ²	N/A	90km/h	130km
<i>Mercedes</i>							
<i>NECAR 2 V-</i> <i>Class</i>	1996	FCEV	50kW PEM	CH ₂ 25MPa	N/A	110km/h	250km
<i>Toyota RAV4</i>	1996	FCBHEV ³	20kW PEM	Hydride	N/A	100km/h	250km
<i>Mercedes</i>							
<i>NECAR 3 A-</i> <i>Class</i>	1997	FCEV	50kW PEM	Methanol Reformer	N/A	120km/h	400km
<i>Toyota RAV4</i>	1997	FCBHEV	25kW PEM	Methanol Reformer	N/A	125km/h	500km
<i>GM Zafira</i>	1998	FCEV	50kW PEM	Methanol Reformer	80mpg	120km/h	483km
<i>Honda FCX-</i> <i>V2</i>	1999	FCEV	60kW PEM	Methanol Reformer	N/A	130km/h	N/A
<i>Honda FCX-</i> <i>V1</i>	1999	FCBHEV	60kW PEM	Hydride	N/A	130km/h	177km
<i>BMW 7 Series</i>	2000	H ₂ ICEV	N/A	LH ₂	N/A	105km/h	300km
<i>Mercedes</i>							
<i>NECAR 4 A-</i> <i>Class</i>	2000	FCEV	85kW PEM	1.8kg CH ₂ 35MPa	53mpg	145km/h	200km
<i>Mercedes</i>							
<i>NECAR 5 A-</i> <i>Class</i>	2000	FCEV	85kW PEM	Methanol Reformer	N/A	150km/h	450km
<i>Ford Focus</i> <i>FCV</i>	2000	FCEV	85kW PEM	CH ₂ 25MPa	N/A	128km/h	160km
<i>Ford THINK</i> <i>FC5</i>	2000	FCEV	85kW PEM	Methanol Reformer	N/A	128km/h	N/A
<i>VW HyMotion</i>	2000	FCEV	75kW PEM	LH ₂ 60l ⁴	N/A	140km/h	350km
<i>Fiat Seicento</i>	2001	FCBHEV	7kW PEM	CH ₂	N/A	100km/h	140km
<i>Mazda Premacy</i>	2001	FCEV	85kW PEM	Methanol Reformer	N/A	124km/h	N/A
<i>Ford Adv Focus</i> <i>FCV</i>	2002	FCBHEV	85kW PEM	10kg CH ₂ 35MPa	50mpg	N/A	290km
<i>GM Zafira</i>	2002	FCEV	94kW PEM	3.1kg CH ₂ 70MPa	55mpg	160km/h	270km
<i>Honda FCX</i>	2002	FCUHEV ⁵	85kW PEM	CH ₂ 35MPa	50mpg	150km/h	355km

¹ FCEV – Fuel Cell Electric Vehicle

² CH₂ – Compressed Hydrogen Tank

³ FCBHEV – Fuel Cell Battery Hybrid Electric Vehicle

⁴ LH₂ – Liquid Hydrogen Tank

⁵ FCUHEV – Fuel Cell Ultra/Super-Capacitor Hybrid Electric Vehicle

Vehicle	Year	Drivetrain	Fuel Cell	Fuel	MPG	Speed	Range
<i>Nissan X-Trail</i>	2002	FCBHEV	75kW PEM	CH ₂ 35MPa	N/A	150km/h	N/A
<i>VW HyPower</i>	2002	FCUHEV	40kW PEM	CH ₂	N/A	N/A	150km
<i>Fiat Seicento</i>	2003	FCBHEV	7kW PEM	CH ₂	N/A	100km/h	N/A
<i>Audi A2</i>	2004	FCBHEV	66kW PEM	CH ₂	N/A	175km/h	220km
<i>GM Sequel</i>	2005	FCBHEV	73kW PEM	8kg CH ₂ 70MPa	N/A	145km/h	483km
<i>Ford Explorer</i>	2006	FCBHEV	60kW PEM	10kg CH ₂ 70MPa	35mpg	N/A	563km
<i>GM Equinox</i>	2006	FCBHEV	93kW PEM	N/A	39mpg	160km/h	320km
<i>Fiat Panda</i>	2007	FCEV	60kW PEM	CH ₂	N/A	130km/h	200km
<i>Honda FCX Clarity</i>	2007	FCEV	100KW PEM	CH ₂	N/A	160km/h	570km
<i>VW Touran</i>	2007	FCBHEV	80kW PEM	CH ₂ 35MPa	N/A	140km/h	161km
<i>Renault Scenic FCV H2</i>	2008	FCBHEV	80kW	N/A	N/A	161km/h	240km
<i>Toyota FCHV</i>	2008	FCBHEV	N/A	CH ₂ 70MPa	N/A	155km/h	830km
<i>VW Tiguan</i>	2008	FCBHEV	80kW HTFC	3.2kg CH ₂ 70MPa	N/A	140km/h	230km
<i>Mercedes B- Class F-Cell</i>	2009	FCEV	90kW PEM	CH ₂	54mpg	170km/h	385km
<i>Mercedes Blue Zero F-Cell</i>	2009	FCBHEV	N/A	N/A	81mpg	N/A	400km
<i>Audi Q5</i>	2010	FCBHEV	98kW PEM	CH ₂ 70MPa	N/A	N/A	N/A

Table 3.3 - Existing Fuel Cell Vehicles

Further analysis of the material summarised in Table 3.3 reveals several significant trends:

- Compressed hydrogen storage is the only storage system now used; reformers, liquid hydrogen and hydrides have been tried and discontinued.
- The trend in compressed hydrogen storage is towards the use of high-pressure 70Mpa composite fuel tanks.
- Most recent fuel cell vehicles are hybridised with a nickel metal hydride (NiMH) or lithium ion/polymer (Li-Ion/LiPo) battery pack.
- Ballard was the pre-eminent supplier of fuel cell stacks though today Toyota, General Motors, Honda and VW now produce their own stacks.
- Significant amounts of data about the existing prototype vehicles is not publically disclosed and what is, often has to be collated from multiple sources.
- Though performance figures are given, little information exists about the conditions under which they were measured.

Reviewing these trends, a) and b) are in line with this study. c) is a direct result of the slow reaction rate of the fuel cell discussed in 3.4. The fuel cell system can not instantaneously meet the power demands of acceleration and the response times seen in the literature vary between 1s and 10s depending on both the fuel cell and size of the power demand change as a percentage of the cells power rating. To avoid a sluggish response, poor performance and negative driving experience an additional power source is needed to hybridise the power drive train and provide the transient power to fill the gap between the power demand and the actual fuel cell output. Three methods exist in the literature for doing this, batteries, ultra/super-capacitors and flywheels. The predominant approach is to use batteries as although ultra-capacitors have significantly higher power density than batteries they also have significantly lower energy density and can be exhausted before the fuel cell has caught up with demand. Batteries can also capture more energy from regenerative braking and in certain configurations provide all electric range (AER), usually in a fuel cell plug-in hybrid electric vehicle (FCPHEV).

The lack of data highlighted in e) and f) is the single largest driving force behind this study. In order to evaluate and develop the FCHEV power drivetrain it is critical that the existing approaches can be analysed in detail both qualitatively and quantitatively. Even on the qualitative side this is incredibly difficult and starkly highlights the difference and conflict between academic research and commercial research and development. Quite prudently and understandably, manufacturers gloss over research failures and rigorously protect the intellectual property and patents their R&D investment yields. Breakthroughs in fuel cell membranes, catalysts, power converters, drive train control strategies, gas cylinders or any of the other critical components in the fuel cell vehicle could ultimately be worth billions of pounds. With these potential windfalls and due to the substantial sums invested, published information is often incomplete, cursory or too high level to be of any real scientific use.

Take two vehicles for instance, the published information tells us that both drive trains are fuel cell battery hybrid drive trains, and that the rating of the fuel cell and battery is identical in each. The performance figures however, are completely different. We know nothing about the energy management strategy of each vehicle, the power converters used, whether they both use the same motor or whether one is including all electric range on remaining charge in the battery as part of the range once the hydrogen fuel has been expended or a host of other necessary parameters we need to perform proper critical

analysis. In many cases the vehicles are tested against different benchmarks yet the headline efficiency figures are published in a manner that suggests equivalence.

From an academic point of view, it is impossible to completely describe or quantify the current state of the art without significant caveats that all but make the comparison useless for anything other than establishing what is currently said to be possible. Different methods of arranging the same components may yield gains or losses. Configurations may be suited to one type of driving or automotive market more than another, a fuel cell system may be better suited to a different vehicle or a highly efficient drive train may be let down by the type of motor being used. The constraints that commercial research places on companies, often using single chassis types, component sets and following a single development pathway targeted towards their existing markets, prohibits this useful and direct comparison. The costs involved would be significant and in the current economic climate it is unlikely that such projects will be funded. Yet this sort of research is vital to achieving the step developments needed to realise advanced alternative fuel vehicles in the near term. Incremental change will be useful, but it is not in itself a guarantee that vehicles can become sustainable or that they will be available before substantial adverse economic impacts arise from increasing oil prices.

There is a wealth of information in peer-reviewed publications about the fuel cell power drive trains, subsystems, control and associated subjects. A small fraction relates to the development programs of major automotive manufacturers but the overwhelming majority is academic research aimed at developing various aspects of the drive train. Comparison between much of this literature is also very difficult as different aspects of subsystems are often analysed which makes drawing conclusions about the overall system difficult. Where similarities exist or where whole systems are analysed, different tests and metrics are applied.

In order to fully establish the performance of current fuel cell vehicle drive train systems a detailed study of existing drive trains that can be qualitatively and quantitatively studied is needed. An extensive search of the literature revealed that some limited studies have been carried out but a comprehensive review and analysis of all current and proposed topologies did not exist and the decision was therefore taken to undertake one. Building on the methodologies discovered in the literature a multi-stage review process was developed and the results used to highlight the most optimal systems and possibly identify opportunities

to further develop and optimise systems into more efficient, higher performance, less complex and cheaper drive trains.

4 A Review of FCEV Drive Trains

4.1 Introduction

The need for a review of existing fuel cell vehicle drive trains has been established. The aim of this review is to provide data that can be used to determine the best vehicle drive train architectures. The power drive train is the heart of the vehicle, everything else aside, such as the chassis, vehicle body, fittings and ancillary equipment have easily quantifiable effects on vehicle performance and are little different from the effect they have on existing ICEVs.

An extensive literature search was conducted to identify all known drive train configurations. Data was obtained from scientific journals and conference proceedings, manufacturers' data, automotive industry publications, media articles and the Internet. Consideration was also given to relevant material from outside the automotive field where deemed prudent. Fuel cells have many applications and research and production work going on in different fields may have benefits to the automotive use of fuel cell technology. The largest problem identified with existing research is the lack of commonality in the systems, metrics and components. This prohibits like for like analysis. The difficulty of physically building multiple permutations of complete fuel cell vehicles has also been discussed. Given that it is beyond the financial means of some of the worlds largest automotive companies, it goes without saying that it would be an impossible aim for a PhD research project.

Computer simulation however, provides a solution. Software and computer hardware costs aside, a simple investment of time and diligence has allowed multiple different power drive train models to be designed using a common vehicle chassis, power drive train components and control system. These vehicle models were then tested against a range of common driving cycles that represent single modes of driving, or single world automotive markets. The selection of cycles in the existing literature was often narrow. This review deliberately used a wide range of cycles to represent the majority of driving modes seen across the world. By appropriate model design, choice of simulation software and adequately rated computer hardware these models could iterate through the driving cycles many times faster than real time.

Certain compromises in the modelling process were necessary to produce models that could be solved in a realistic timeframe. Empirical data was extensively used to minimise any adverse impact these compromises had on the validity of the results. The results of the modelling process were used to draw comparisons between the various power drive train configurations in a way that existing information did not allow. This analysis was then used to determine avenues for further work in the design of drive train components, the arrangement of components in the drive train topology and the power management control within the drive train system.

This chapter will set out the power drive train topologies found in the literature, review and discuss them and chose suitable candidate systems for detailed modelling and simulation based analysis.

4.2 System Architecture

The literature review identified that there are currently three main ways implementing a fuel cell powered passenger vehicle:

1. Fuel Cell Electric Vehicle.
2. Fuel Cell Battery Hybrid Electric Vehicle.
3. Fuel Cell Super-Capacitor Hybrid Electric Vehicle.

The overwhelming majority of topologies that were studied have been hybrid designs. This was by necessity rather than desire and is due to the inherent deficiencies in current fuel cells response to transient demand. An additional power source is therefore essential to ensure acceptable performance. An additional power source is also essential to provide the capacity for instant drive power. All vehicle users are used to getting into a vehicle, starting the engine and driving off without any delay. In contrast, some fuel cell power units can take around 10 minutes to be ready for use, imposing such a penalty on the driver that would be a serious barrier to market acceptance and so the additional power source provides both power to start the fuel cell and also motive power to the vehicle while the fuel cell reaches operational readiness.

However, hybrid design introduces extra control overheads, weight, cost and further imperfect technologies into a vehicle. Using batteries or super capacitors for power assist

and traction in vehicles introduces more complexity and lifecycle issues, but without significant advances in fuel cell technology, it is a necessary evil.

It is important to note that a hydrogen fuel cell hybrid electric vehicle (H₂FCHEV) differs from the now well-established concept of a petrol or diesel hybrid electric vehicle. In the fossil fuel engine hybrid, the battery is typically used to replace part of the engine capacity, whereas in most current H₂FCHEVs it is used to supplement it.

4.2.1 Hybrid Power Source

Although near universal agreement can be found in the references that the hybrid approach is necessary, agreement on the additional power source is lacking. The published studies fall into two main camps. One advocates the use of batteries, the other, the use of super capacitors (also known as ultra capacitors). Typically, batteries are considered energy dense and super capacitors power dense.

In this thesis batteries were chosen to provide the power assist energy source over super capacitors for several reasons:

- Greater energy storage capacity.
- Charge retention time is significantly longer.
- Lower volume for a given power rating.

However such “qualities” of batteries are not without their comparative disadvantages and these include:

- Lower peak power.
- Increased weight.
- Increased charging time.
- Shorter operational lifespan.

But these disadvantages are outweighed by the benefits of using battery as the power assist source in the H₂FCHEV. One of the main disadvantages of the super-capacitor approach is that a pack can potentially discharge in a shorter time than the fuel cell can respond to transient demand, thus resulting in a sudden loss of power to the drive train. During normal driving this would result in an unpredictable and frustrating driving experience and

if this situation occurred midway during an overtaking manoeuvre on a two-lane road whilst there was oncoming traffic there could be serious safety consequences.

The primary disadvantage though is that with super capacitors, the vehicle cannot be driven away the moment the driver turns the vehicle on and it cannot be left parked for a long period of time and retain its stored charge. Left charged, super capacitors will self-discharge in a relatively short space of time (hours) and they do not contain sufficient energy even when full to power the entire vehicle whilst the fuel cell is starting up. The fuel cell needs its compressor, heating and humidification systems powering during start-up and further energy is required to provide instant drive away capability. Without a hybrid power source that can meet both these demands the fuel cell vehicle would have an unacceptable wait for the driver during start-up before they can drive away. That is not a feature of ICEVs or EVs and fails one of the key criteria for the diffusion of innovations. The battery is the only energy source that can

Both technologies include control “overheads” to manage and protect the individual battery cells or capacitors but the differences between the amount of control and electronic hardware needed for cell balancing a battery pack compared to an super capacitor pack are negligible and do not really affect the choice.

Some of the topologies found in the literature and used in this study were published using super capacitor packs. These packs were removed and supplanted by a battery pack for the purposes of this study, as the overall topology schema is unchanged.

4.2.2 Drive Selection

The two prime considerations when selecting a drive for use in an electric vehicle are the maximum speed the machine needs to run at and the maximum torque that the machine has to generate [117]. Ideally the machine will be able to operate through a single speed transmission and thus enable the elimination of a multi-gear, manual or automatic transmission from the vehicle, removing a point of failure, weight, cost and assembly complexity. Consequentially a suitable machine should be able to generate high torque over a wide range of operating speeds. Existing drive trains were found to use one of four motor technologies as the prime mover in the drive train. They were:

- Brushed DC Permanent Magnet Motor

- Brushless DC Permanent Magnet Motor (BDCM)
- Switched Reluctance Motor (SRM)
- Induction Motor (IM)

Brushed DC motors were discounted many years ago due to the poor efficiency, short life cycle, high weight and reliability problems associated with the mechanical commutation used in such devices all of which are considered to be significant problems [118].

Permanent magnet brushless DC motors (BDCM) are currently the motor of choice in most combustion engine-electric hybrid vehicles. They have high efficiency and generate high torques for a low machine weight [117-120]. Advances in digital signal processing have made their control relatively straightforward and they have a higher power density than other drives. However they are typically limited to low speed operation and require intensive liquid cooling. The cost of the permanent magnets, most made from rare-earth materials is very high. Manufacturing large PM machines in any volume is expensive and complex [119, 120]. They offer promise for direct drive applications where the operational speed is low but significant development is needed before they can compete with induction machines or switch reluctance motors as the prime mover in an all electric vehicle [121].

Switched reluctance motors are an area of growing research interest and capability. They can operate through a much greater range of field weakening operation when compared to PM machines and thus can operate efficiently at high speeds [122]. They can also operate from conventional inverter drives and are simple to manufacture, with scale production yielding substantial cost savings when compared to BDCM drives [121]. For a given torque capability they are smaller and lighter than induction machines, can operate at higher speeds and are more efficient [118]. When this project started, SRM machines were considered immature and not ready for production usage in electric vehicles. The high torque ripple compared to induction machines and severe acoustic problems were considered to risk producing a poor driving experience and consumer rejection [102]. Development since however has seen them emerge as one of the pre-eminent choices for electric vehicle applications [123]. Because the SRM has many discrete windings they are also fault tolerant. The motor can continue to operate, albeit at reduced performance, should one or a few windings fail. It also has less risk of a shoot through fault in the windings than an IM or BDCM drives.

Induction motors are relatively inefficient when compared to SRM and BDCM drives however at high speeds they are capable of operating far more efficiently than BDCM topologies. The technology is mature and IM drives are very reliable and cheap to manufacture and have a very low torque ripple [118] and unlike BDCM drives, IM drives can be air cooled. Even though a BDCM of a given power rating may be physically smaller a similarly rated IM drive can generate a higher peak torque though the torque at speed is limited because of the requirement to operate a field weakening control strategy at high speeds. Advances in power semiconductor devices over recent years have resulted in once prohibitively expensive inverter drives now being mass manufactured commodity items. Similar advances in microprocessor technology have meant that sensor-less control is now achievable with relatively cheap hardware.

The IM drive is larger than a similar SRM or BDCM but for this application its torque speed characteristic, high reliability, manufacturing simplicity and low cost make it the ideal choice. The majority of electric vehicles up until the mid-2000s were made using IM drives for traction and the drive used in this project was a Siemens IM drive. The drive had a rated speed of 0 – 10,000 rpm and a peak torque of 260Nm. This meant a single reduction gear could be used and eliminated a multi-gear transmission from the vehicle. A reverse gear is also not needed as the motor can simply be turned in the opposite direction by the inverter.

4.3 Drive Train Topology Architecture Overview

This review of existing topologies covered numerous different architectures, not all of which were fuel cell hybrid vehicles. By covering different applications of electric vehicle and hybrid drive trains it was thought that any ideas found to have beneficial effects in other areas may be found and potentially applied to enhance a fuel cell vehicle. From the published roadmaps it is clear that the automotive industry intends that the first production H₂FCEV will follow on from ICE hybrid vehicles and that the fuel cell will be used to replace the internal combustion engine.

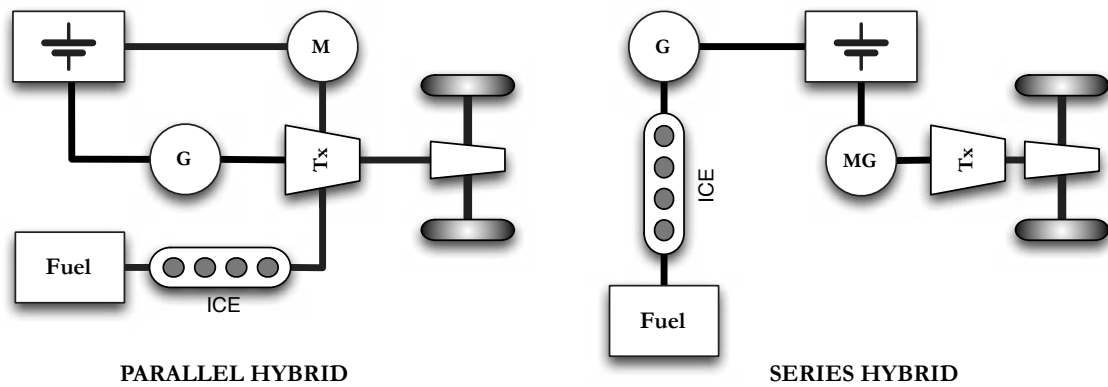


Figure 4.1 - HEV Drivetrains

Whilst the series-parallel mechanically coupled hybrid shown in Figure 4.1 currently used in vehicles like the Toyota Prius makes the most sense for passenger vehicles using an internal combustion engine, it does not necessarily follow that the ideal H_2 FCEV is created by directly substituting the ICE with a fuel cell system. Although it would be possible to replace the ICE with a fuel cell, inverter and motor and then couple the output of the fuel cell motor and battery motor mechanically, the system would be needlessly large and inefficient when compared to combining the two power sources electrically and then driving a single, higher rated motor. Most of the fuel cell topologies in literature use this arrangement.

The large number of topologies found upon an initial comprehensive search of the literature necessitated a two-stage approach to assessment. It was clear that not all the topologies could or should be fully developed into simulation systems and appraised by computer modelling. Some were ruled out after a simple qualitative evaluation, others were taken forward for a high level quantitative analysis and from this the topologies that would ultimately be simulated in this study were chosen.

Because of the problems discovered when trying to compare the data from different systems contained in the myriad of literature found, the topologies found have been reformed from a common set of components. The arrangement of the topology typically dictates the overall system performance and by using a common set of comparison the different topologies could be compared against a common baseline with no need for ratios or fudge factors to account for differing component sizing. This allowed a quantitative analysis approach using generalised figures for efficiency, weight and power rating to be applied to each and every topology. Although sizing of the system components is

important, at this nascent stage drawing comparable initial conclusions about the relative merits of each topology was the objective.

Table 4.1 shows the component parts used to build the drivetrain topologies in this study. Nominal steady state efficiency values for each of the components are given as used to carry out the initial quantitative analysis.

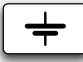
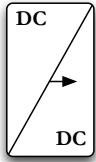
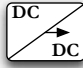
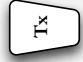
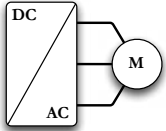
Component	Nominal Efficiency	Weight	Symbol
85kW H ₂ PEMFC	0.56	200kg	
4.5kWh (45kW Peak Power) Li-Ion Battery [124]	0.88 (Charge) 0.94 (Discharge)	45kg ¹	
80kW Uni-Directional DC-DC Converter [125]	0.95	37.5kg ²	
45kW Bi-Directional DC-DC Converter[125]	0.93	28.5kg ³	
80kW Bi-Directional DC-DC Converter [125]	0.91	43kg	
4.5kW Uni-Directional DC-DC Converter	0.97	2.25kg	
Power Diode	0.99	0.2kg	
9.81:1 Fixed Ratio Transmission	0.97	n/a	
75kW (Peak Power) 3-Phase Drive & Induction Motor [126]	0.86	110kg ⁴	

Table 4.1 - Power Drive Train Topology Components

¹ Pack weight of Kokam Li-Ion cells.

² Weight based on 2kW/kg for uni-directional DC-DC converter.

³ Weight based on 1.75kW/kg for bi-directional DC-DC converter.

⁴ Weight of DC-AC inverter and AC induction motor includes fixed ratio transmission.

4.3.1 Traditional Electric Vehicles

To start the review we begin by considering the traditional topology of a BEV, as shown in Figure 4.2. This consists of a battery electrical power source connected to an inverter drive and motor. Acceleration demand from the vehicle driver increases the amount of power drawn from the source and delivered to the motor.

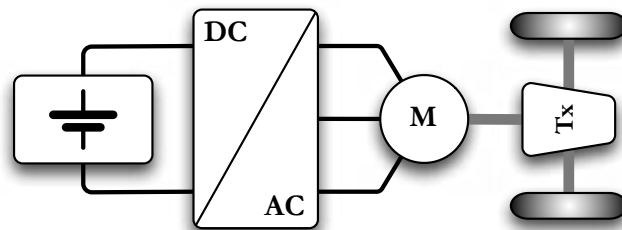


Figure 4.2 - BEV

This system is a simple architecture that is the optimal method of designing an electrical vehicle. The current drawbacks and limited expected advancement of batteries discussed in 2.4.7 make it highly unlikely that the BEV can entirely replace the ICEV in the near-mid term future.

4.3.2 Adding the Fuel Cell

The most simplistic approach to powering an electric vehicle with a fuel cell was to replace the battery with a fuel cell as shown in Figure 4.3 [127]. A power diode is included to prevent power flowing back into the fuel cell stack that can reverse the polarity of the cells and irreversibly damage the proton exchange membrane [128].

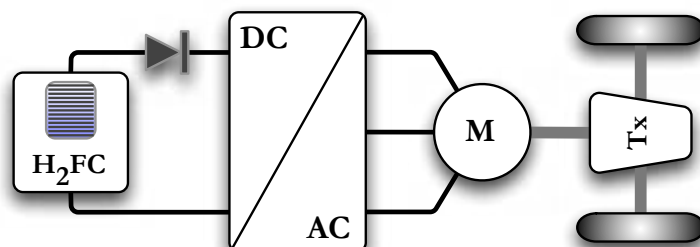


Figure 4.3 – Basic H₂FCEV Drivetrain

Unfortunately this is not currently a viable approach to building a fuel cell powered electric vehicle because of one major problem alluded to previously, of the lack of power in the

early start up of the fuel cell. The characteristics of the currently available automotive fuel cell power systems require an additional power source to drive away and start up the fuel cell system and compensate for the slow dynamic response of the fuel cell to transient power demands during acceleration. The simplest way of doing this is by adding a battery or capacitor across the fuel cell output [102, 129-136] as shown below in Figure 4.4.

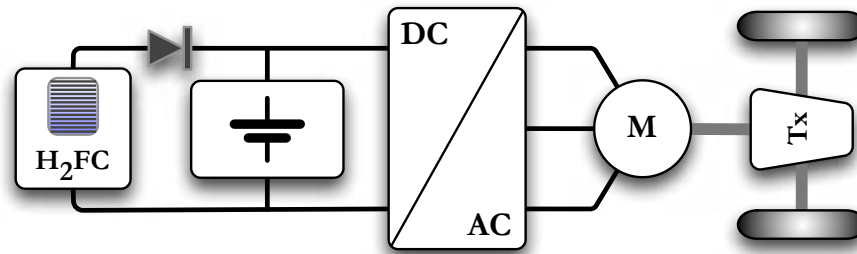


Figure 4.4 – Basic H₂FC Battery Hybrid Drivetrain

This arrangement is only possible if the characteristics of the fuel cell and battery are carefully matched. The two power sources will share the load and by controlling the flow of hydrogen gas into the fuel cell stack it is possible to control the amount of power provided by the battery and the amount of power provided by the fuel cell [102].

Immediately on analysis of such suggestions there are several clear problems with this system. Matching the fuel cell and the battery, whilst possible, normally compromises the specification of one or both of the components and results in a non-optimal system. Given that the fuel cell voltage fluctuates as a function of its current, the battery pack is also required to tolerate variations in terminal voltage. Although some battery technologies will, some can be damaged, most will have a shortened lifespan and all will be run at inefficient points of operation for long periods. There is also no protection against deep discharging or overcharging. The fuel cell takes time to respond to changes in load and during the intervening period the system will try to meet the power deficit by drawing it from the battery, regardless of its state of charge, and there is no way of isolating the battery from the system. Using Lithium Ion batteries in such a system is not ideal and could be potentially dangerous as over discharging can lead to cells exploding and potentially catching fire.

Ultra/Super capacitors are used in some systems though since they are significantly less energy dense than batteries they provide no drive away capability whilst the fuel cell system is starting up, and also yield negligible range when driving on the power from the ultra

capacitor system alone (all-electric range). They are however more capable of delivering large transient power demands and the components are physically more tolerant to the effects of such demands than batteries and have a longer service life.

4.3.3 Controlling the DC Power

Given the problems in matching the characteristics of a battery and fuel cell together so that they can be arranged on a common bus most systems use power converters to interface the output of either the battery or the fuel cell to the DC bus that supplies the motor. This is a similar approach to that of the series hybrid shown in, although the addition of power in DC format, rather than AC, is the most common approach found in the literature, primarily because both the battery and fuel cell are DC power sources.

The addition of the converter into the system allows complete control over both power sources and allows each source to be optimally designed. The addition of a converter introduces cost, weight and loss into the system but the distinct advantages of having it there outweigh the losses.

Figure 4.5 shows one implementation of this architecture. A bi-directional DC-DC converter is placed between the output of the battery pack and the DC bus [137-140]. Using the components that will be used to form the system in this study the topology will require a 50kW bi-directional DC-DC converter.

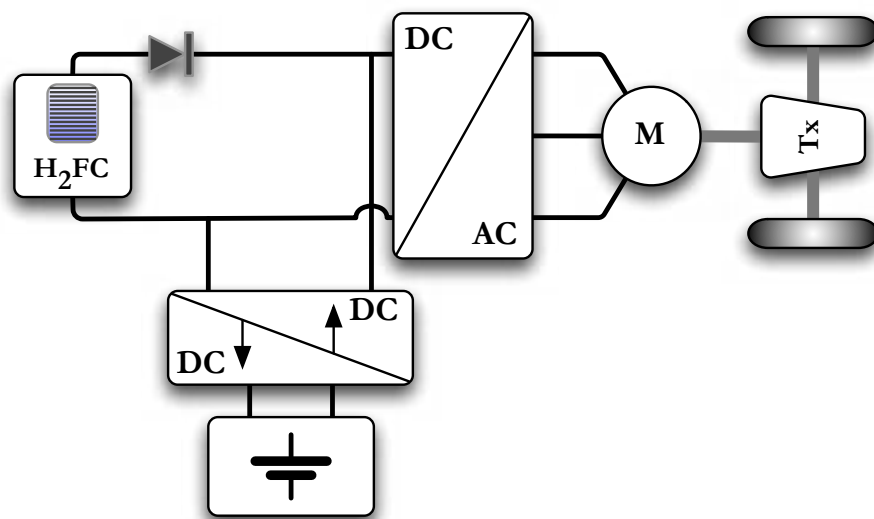


Figure 4.5 – Fuel Cell Determined DC Bus System

The converter operates so as to match the output voltage of the battery system to the fuel cell stack voltage. This introduces a control overhead on the system as this requires the DC bus to be constantly monitored. Consequently, there will be points of operation where the converter is operating in relatively inefficient regions due to the poor input to output voltage ratio of the converter. These points of operation will either be due to heavy load on the fuel cell reducing the bus voltage, or a period of heavy transient load where the fuel cell voltage will be high and the battery voltage will be low.

Power flow from the fuel cell to the drive is very efficient in this system, nominally being around 0.83 with the only loss in the power path being the power diode. Power transfer from the battery to the drive is slightly less efficient due to the power converter, typically around 0.79. Battery charging has an efficiency of 0.80 and regenerative braking energy capture efficiency is 0.69.

In order to protect the battery pack the system monitors the battery SOC and controls the DC-DC converter to prevent power being drawn from the battery pack when the SOC is too low and prevent charging once the SOC has reached its optimal maximum. This allows the vehicle to maximise the life of the battery pack.

The DC-DC converter also allows re-generative braking energy to be utilised effectively. In the system shown in Figure 4.4 the whole of the regenerative braking energy would be presented at battery terminals and the battery can only be switched in or out of circuit by the battery management system. Much like the problems with charging the battery in the system, under certain circumstances the regenerative energy could be of a magnitude or duration whereby it would act to charge the battery in an inefficient, detrimental or unsafe manner. The DC-DC converter can act to control charging the battery with the regenerative energy and ensure that it does not damage the battery or present a risk to the system.

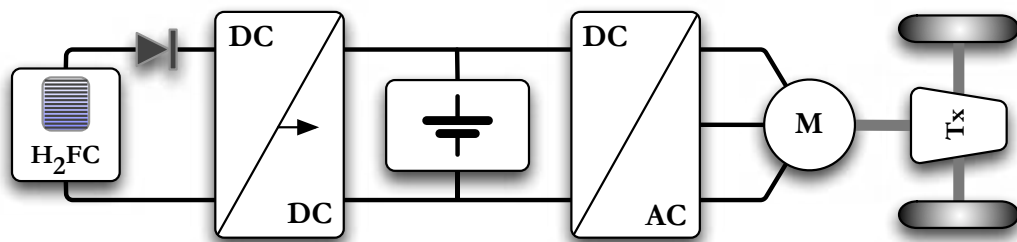


Figure 4.6 – Battery Determined DC Bus System

Figure 4.6 shows by far the most prevalent approach to controlled power addition in a fuel cell drive train with 25 direct references found in literature [57, 89, 108, 133, 134, 140-160]. In this system the bus voltage is dictated by the terminal potential of the battery pack and the DC-DC converter at the output of the fuel cell either steps up or steps down the fuel cell voltage to match this level.

The converter used in this system is rated at 75kW, larger than that of the previous units used but it is a uni-directional converter, which simplifies the design and reduces the cost, typically using half the number of switching devices of a bi-directional converter. The introduction of the converter does incur a performance penalty with the efficiency of the power path from the fuel cell to the drive being 0.80. Though in circumstances where the battery is heavily loaded and the fuel cell stack voltage is relatively high, this efficiency can drop as low as 0.70 due to the input to output voltage ratio of the DC-DC converter negatively impacting on the efficiency. As is clear from the layout of the system, power transfer from the battery is more efficient being nominally 0.85.

Whilst charging the battery pack is as controlled and safe as the previous system, the recapture of regenerative braking is not, with the battery directly exposed to all reverse power coming from the drive and the battery management system only having on/off control of charging. Although a more efficient path for regenerative power it could lead to over charging or otherwise expose the battery pack to non-optimal charging conditions that can reduce life cycle or potentially damage the battery.

4.3.4 Performance Optimisation

The topologies detailed so far have all had one common feature. The DC bus voltage at the input to the inverter drive for the motor varies with load and time. This is dictated by the response of the fuel cell and the battery pack. As shown in Figure 4.7 and Figure 4.8, the output of both sources varies with load current and so regardless of whether the DC bus level is dictated by the fuel cell or battery pack, it will vary with load.

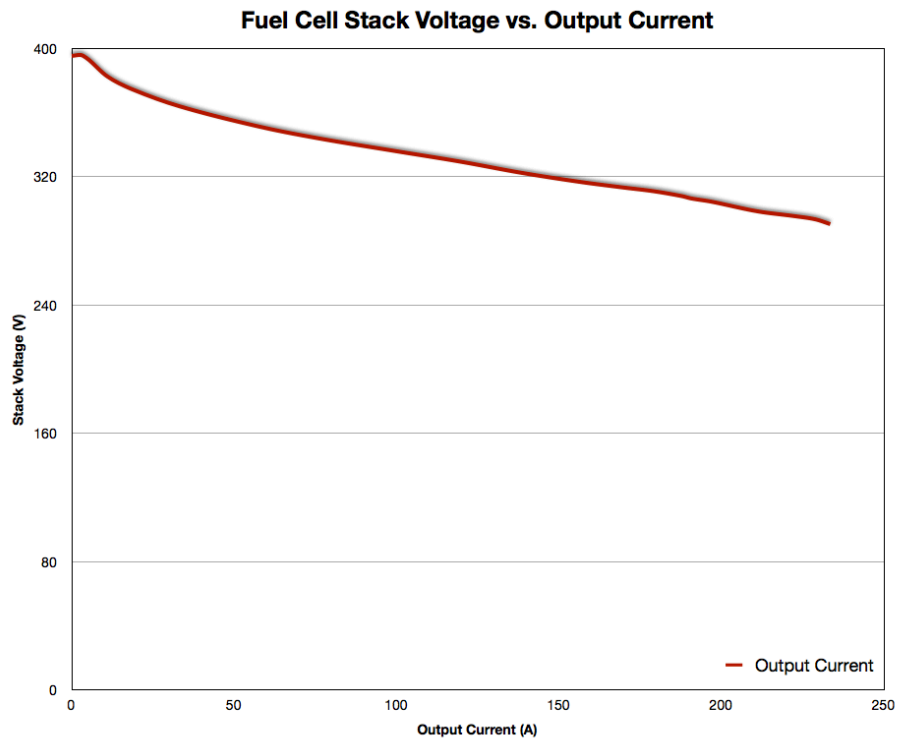


Figure 4.7 - Fuel Cell Output Voltage vs. Current

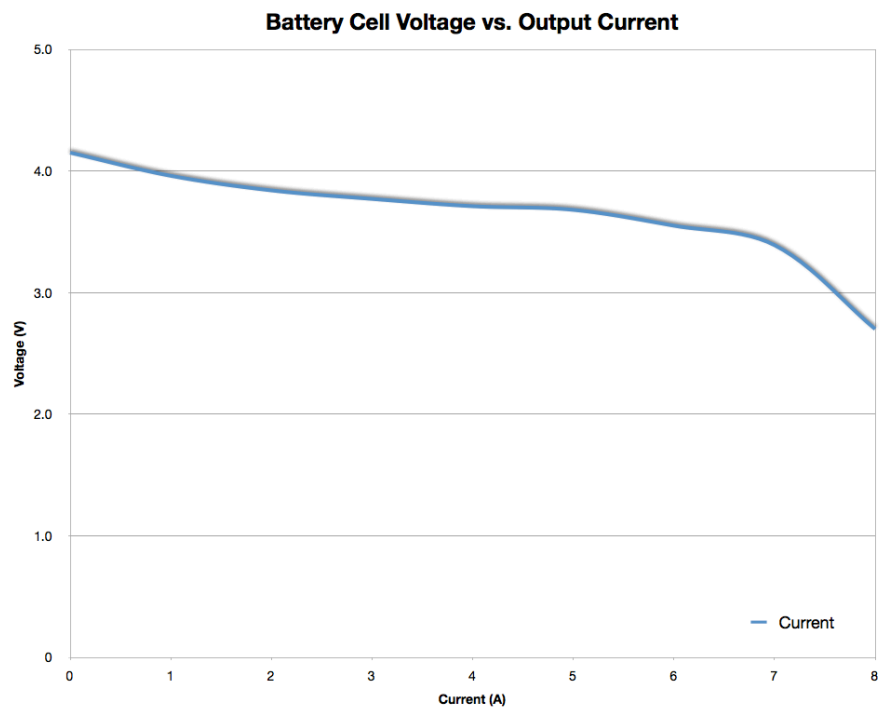


Figure 4.8 - Battery Cell Output Voltage vs. Current

The fluctuation of DC link voltage has one main impact and that is to decrease performance. Both the fuel cell and battery voltages can vary by up to 100V over their rated range. If the bus voltage is fixed by the terminal voltage of the battery pack the

maximum voltage is 369V and the minimum voltage is 270V. If fixed by the fuel cell the maximum voltage is 395V and the minimum is 285V.

The output of both sources decreases under load and increases as the load is removed, as is typical of electric power sources. However in the application that creates a self-compounding problem that negatively affects vehicle performance. When acceleration is demanded by the driver the power consumed by the motor increases too and consequently the DC bus voltage decreases. Figure 4.9 shows the torque speed curves for the motor at four different DC bus voltages. As the voltage decreases, the maximum torque available at a given speed decreases. Therefore, at a point where the driver demands maximum torque, the load placed on the electrical system may act to decrease the maximum torque available.

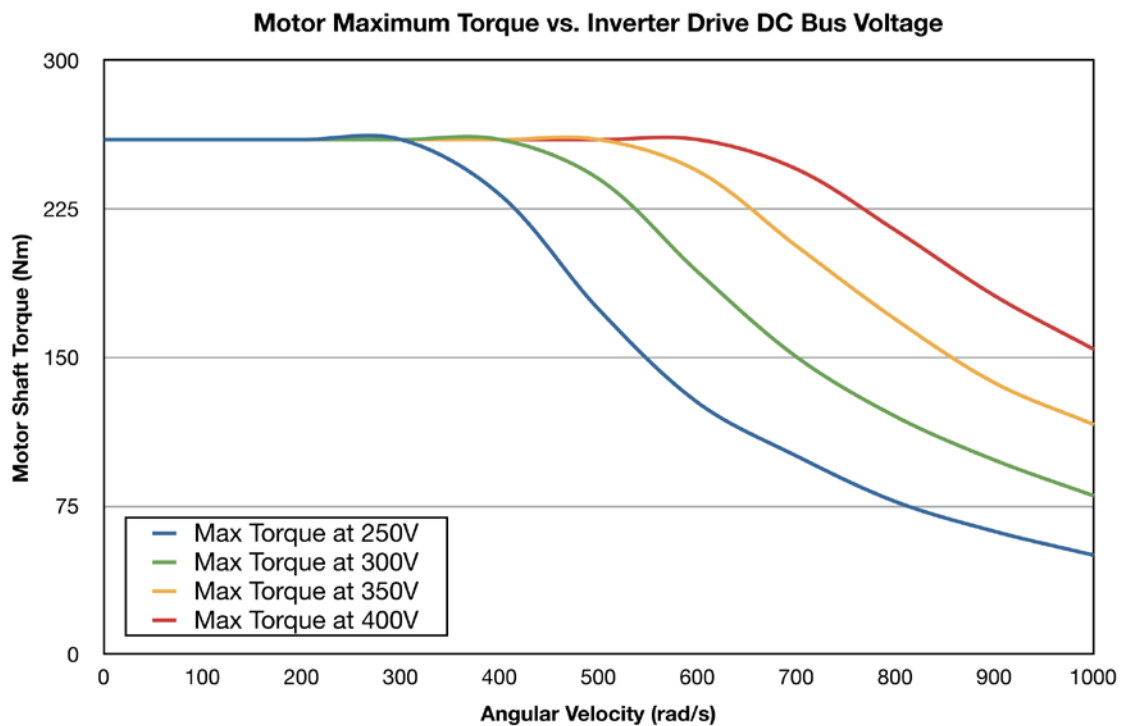


Figure 4.9 - Torque Speed Curves for 75kW Induction Motor & Drive

The solution to this performance limitation is to fix the DC bus voltage at the optimal point. Both power sources must be interfaced to the bus with DC-DC converters, reducing the overall efficiency of all the power flow paths in the system but ultimately should ensure that sustained high acceleration is possible. This architecture also allows controlled charging and optimal bus voltage is presented in Figure 4.10 [136, 161-166].

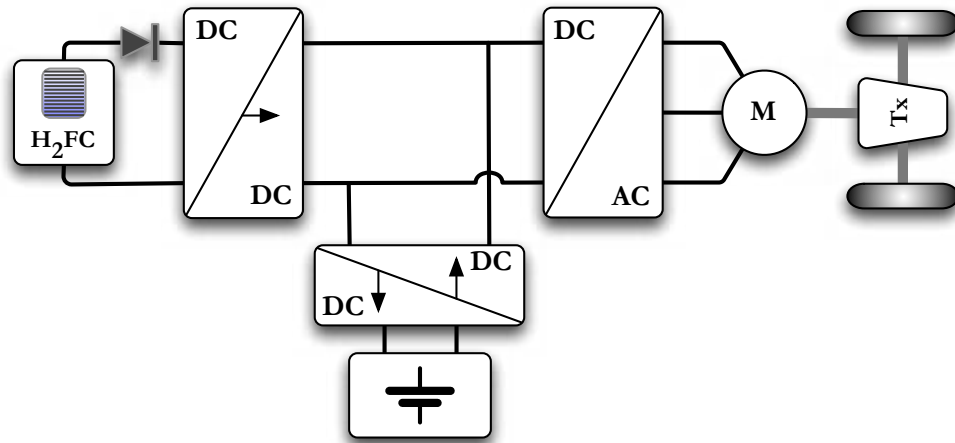


Figure 4.10 - Fixed DC Bus Voltage System

An evolution of this architecture is presented in [167, 168] and shown in Figure 4.11. The authors suggested that the charging losses involved in charging the battery from the fuel cell were significant and used a separate, significantly smaller ($\sim 5\text{kW}$) uni-directional DC-DC converter to optimise the efficiency of charging. This is similar to the use of a separate generator for battery charging in the Toyota Prius HEV rather than using a single motor drive as the traction motor and generator.

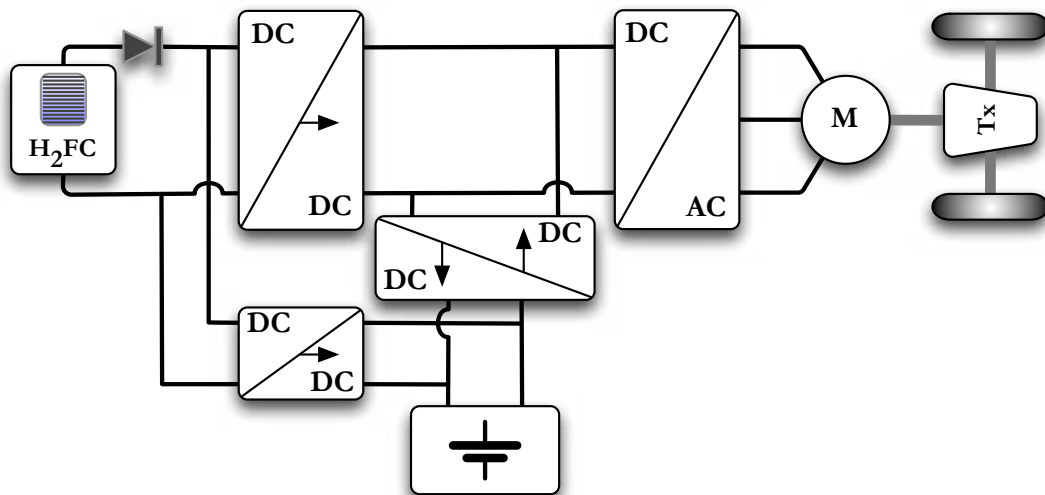


Figure 4.11 – Charge Efficiency Optimised Fixed DC Bus Voltage System

4.3.5 AC Power Control

So far, the topologies discussed have combined power on a DC bus and then used a DC-AC inverter drive to power a 3-phase AC induction motor. However some systems combined the power on an AC bus, to which the motor was directly connected. The first method of doing this is shown in Figure 4.12. This system uses two grid connected DC-AC

inverters connected to each of the sources. The outputs of each of the inverters are coupled using 3-phase line inductors.

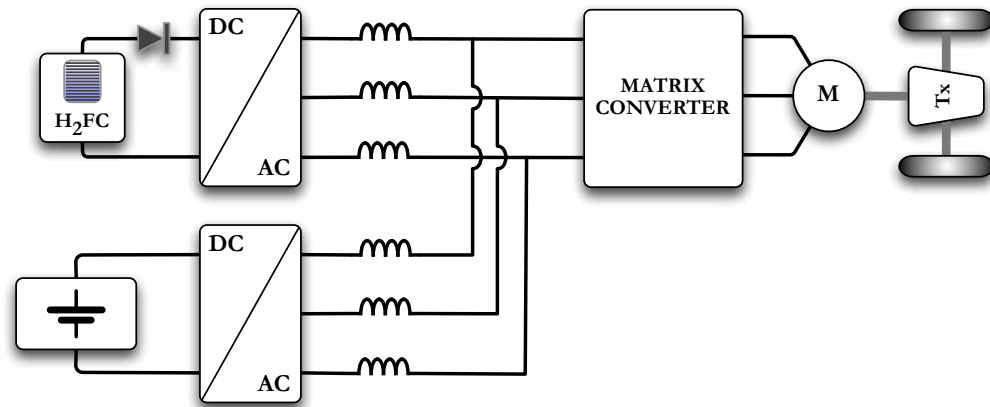


Figure 4.12 – AC Bus Drivetrain System with Matrix Converter Motor Drive

The immediate problem with such a system is one of control. If the inverters had identical power sources, control would be relatively simple with the power demand being split equally between each. In this application however the sources are not identical in any sense. They have different power capabilities, different IV characteristics and different response times. Whilst theoretically possible to split the power demand across the two inverters, it would require very computationally intensive control and the control algorithm would be complex to develop.

Aside from the software problems there are also several hardware problems inherent with such a system. The inductors required are large and heavy and not eminently suitable for use in a vehicle. The number of switching devices and associated driver circuits required for two DC-AC converters is greater than for a single DC-AC converter and a DC-DC converter, further increasing cost, weight and cooling requirements. Even using half bridge converters the number of switching devices required for a 3 phase inverter is 3 times that of a bi-directional DC-DC converter.

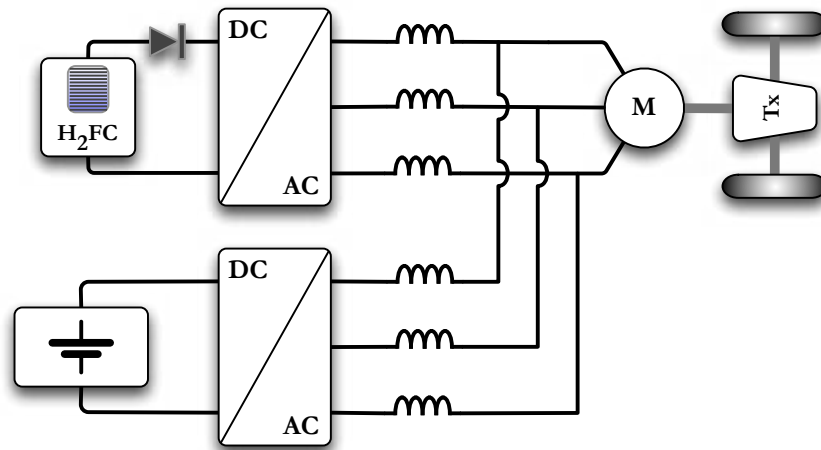


Figure 4.13 – Dual DC-AC Inverter AC Bus Drivetrain System

Another system based on an AC bus is shown in Figure 4.13. This is an evolution of the ICE hybrid drive train shown in Figure 4.14 [169].

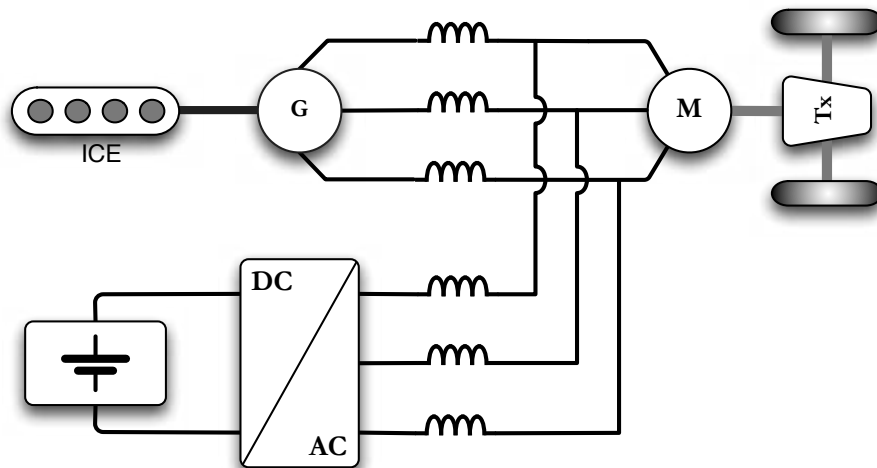


Figure 4.14 - AC Bus ICE HEV Drivetrain

However, the fuel cell vehicle lacks an AC source and as such creating an AC bus requires a DC-AC conversion step. In this system there is also a Matrix converter before the motor. The matrix converter is a relatively new type of AC-AC converter, used because it requires no inductors, and relatively small capacitors. However it cannot boost the voltage and needs a large amount of switching devices. Control of the converter is computationally intensive and complex to understand. These are all safety concerns given that many of its failure modes will short circuit the input to the output with no way of isolation.

Both these DC-AC and AC-AC conversion steps introduce efficiency losses, weight, control and component increases onto the system. Given this it is clear that a DC bus is

most suitable system choice for a fuel cell vehicle or indeed any electric vehicle where the primary power source is DC.

One application where the AC bus architecture would potentially make sense is in a vehicle that required multiple distributed drives, such as that shown in Figure 4.15. Applications such as these are normally limited to large vehicles or electric vehicles fed by an AC supply, such as electric trains. It should be noted that there is no overall control of each motor in this configuration and its practical applications in road transport are consequently limited.

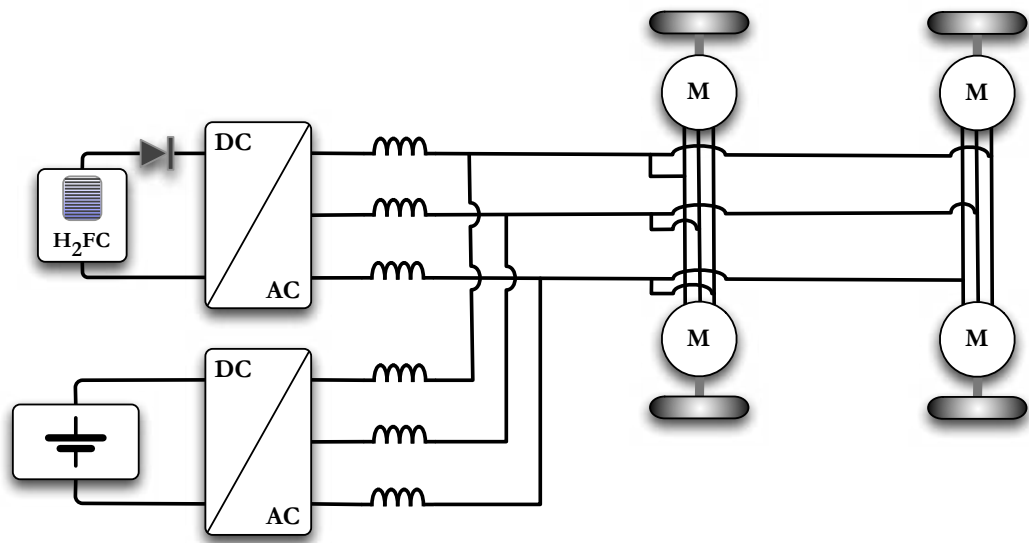


Figure 4.15 - Multiple Drive AC Bus Drivetrain

4.4 Detailed Topology Analysis

Using the data set out in Table 4.1, each of the topologies identified in the literature were analysed and the efficiency of the main power flows in the drive trains quantitatively described using headline efficiency figures for each of the components. Aside from giving a general overview of the efficiency of the drivetrain, issues with control complexity, packaging, manufacture and servicing, and the driver experience are also discussed. The weight and volume of the drivetrain have also been described where possible. Several non fuel cell drive trains have been included as they provide a useful reference and comparison to existing BEV and HEV technologies

This section was written to provide a concise reference to all available drive train topologies and for ease of reference each of the topologies set out in this chapter will be titled with a letter of the alphabet. These references will be used going forward throughout this study.

4.4.1 Topology A

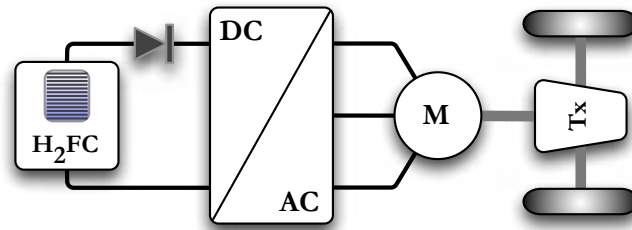


Figure 4.16 - Topology A

Power Flow Analysis

Power Flow Path	Efficiency Calculation	Efficiency η
<i>Fuel Cell to Wheel</i>	$0.56 \times 0.99 \times 0.86 \times 0.97$	0.462

Table 4.2 - Topology A Power Flow Analysis

Control and Performance Pros & Cons

Pro	Con	Feature
✓		Simple control
✓		Low subsystem count reduces weight
	✗	Floating DC bus voltage limits performance at speed

Table 4.3 - Topology A Control & Performance Characteristics

Driver Experience Pros & Cons

Pro	Con	Feature
	✗	Poor acceleration and hill climbing performance
	✗	Driver has to wait for fuel cell system start-up to complete before drive away

Table 4.4 - Topology A Driver Experience Characteristics

Manufacture and Packaging Pros & Cons

Pro	Con	Feature
✓		Simple, low subsystem and component count power train.

Table 4.5 - Topology A Manufacture & Packaging Characteristics

Topology A Summary

This topology [128] represents a pure fuel cell electric vehicle and is not a hybrid vehicle. The system is straightforward to implement, the acceleration pedal simply controls the rate of flow of reactants to the fuel cell stack. Due to limitations in fuel cell response times this vehicle cannot respond to all acceleration or electrical system demands instantly and therefore has a poor driving performance. Significant and currently “unforeseen” developments in fuel cell technology are required before it alone can be used to power a vehicle that has acceptable performance.

Known Variants

Adding a DC-DC converter [170] on the output of the fuel cell ensures that the DC bus voltage is fixed and thus drive performance at speed is not restricted though is still ultimately limited by the response time of the fuel cell. This does however reduce the overall efficiency of the drive train.

Known Production & Prototype Implementations

1. GM Hy-Wire
2. Ford Focus FCV
3. Mazda Premacy FC-EV

4.4.2 Topology B

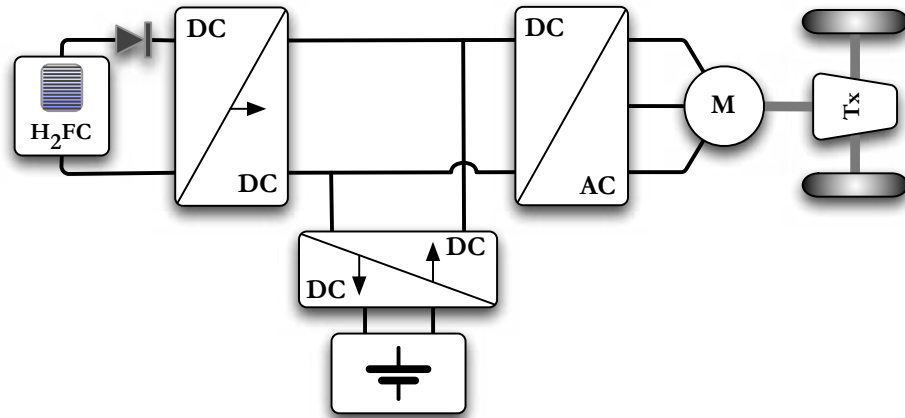


Figure 4.17 - Topology B

Power Flow Analysis

Power Flow Path	Efficiency Calculation	Efficiency η
<i>Fuel Cell to Wheel</i>	$0.56 \times 0.99 \times 0.95 \times 0.86 \times 0.97$	0.439
<i>Battery to Wheel</i>	$0.94 \times 0.93 \times 0.86 \times 0.97$	0.729
<i>Fuel Cell to Battery (Charging)</i>	$0.56 \times 0.99 \times 0.95 \times 0.93 \times 0.88$	0.431
<i>Regenerative Braking</i>	$0.97 \times 0.86 \times 0.93 \times 0.88$	0.683
<i>Fuel Cell to Battery to Wheel</i>	0.431×0.729	0.314

Table 4.6 - Topology B Power Flow Analysis

Control and Performance Pros & Cons

Pro	Con	Feature
✓		DC bus voltage is fixed. Torque speed characteristic operates at a fixed point of high performance and drive control is straightforward.
✓		Fully controlled regenerative braking energy capture enables full utilisation without adversely affecting the battery.
✓		DC-DC allows the operation of the fuel cell system at a single high efficiency steady state independent of power demand.
	✗	Operating the DC bus at a constant fixed high voltage via DC-DC converters may not always be the most efficient method, especially during low speed driving where there is no demand for a high voltage to ensure high performance.

Table 4.7 - Topology B Control & Performance Characteristics

Driver Experience Pros & Cons

Pro	Con	Feature
✓		High acceleration performance
✓		Instant drive away capability at start-up (also a feature of all topologies hereafter)

Table 4.8 - Topology B Driver Experience Characteristics

Manufacture and Packaging Pros & Cons

Pro	Con	Feature
✓		Modular design allows converters and sources to be packaged around the vehicle utilising space better than a single large converter.
	✗	Separate converters increase the semiconductor, capacitor and inductor component count in the system.

Table 4.9 - Topology B Manufacture & Packaging Characteristics

Topology B Summary

This arrangement [88, 130, 171-174] is based around a common DC bus that is defined as having has a constant voltage, normally of a magnitude that is the same as the maximum input voltage to the DC-AC inverter drive. By fixing this voltage at maximum, the motor is operated at the highest point on its torque speed curve, allowing the motor to generate the highest possible torque across its speed range and as such this is a very high performance system. The penalty for the performance is that each source has to interface to the bus via a power converter that carries an inherent power loss and therefore decreases the overall system efficiency.

Known Variants

An evolution of this topology was also found in several pieces of literature whereby the three power converters are integrated into a single block that claims to improve the overall system efficiency [174-179].

Topology I, to be introduced in due course, utilised a separate converter for battery charging to increase the efficiency of power flowing from the fuel cell to the drive via the battery.

Known Production & Prototype Implementations

None

4.4.3 Topology C

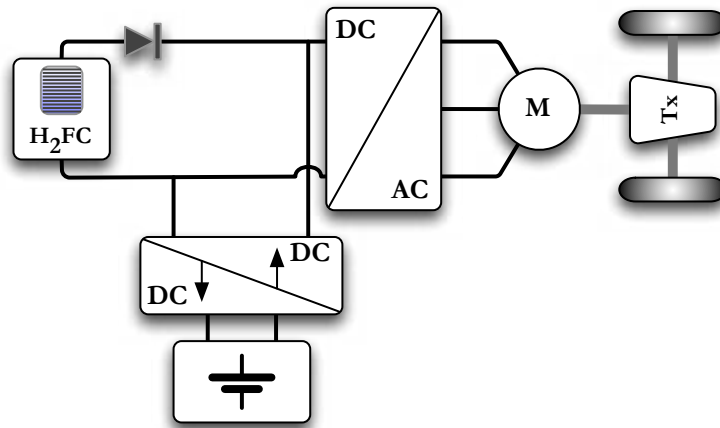


Figure 4.18 - Topology C

Power Flow Analysis

Power Flow Path	Efficiency Calculation	Efficiency η
<i>Fuel Cell to Wheel</i>	$0.56 \times 0.99 \times 0.86 \times 0.97$	0.463
<i>Battery to Wheel</i>	$0.94 \times 0.93 \times 0.86 \times 0.97$	0.725
<i>Fuel Cell to Battery (Charging)</i>	$0.56 \times 0.99 \times 0.93 \times 0.88$	0.454
<i>Regenerative Braking</i>	$0.97 \times 0.86 \times 0.93 \times 0.88$	0.683
<i>Fuel Cell to Battery to Wheel</i>	0.454×0.725	0.329

Table 4.10 - Topology C Power Flow Analysis

Control and Performance Pros & Cons

Pro	Con	Feature
✓		Efficient transfer of power to drive and battery.
✓		Controlled regenerative braking
	✗	Floating DC bus voltage limits maximum motor torque, acceleration and performance during high demand.

Table 4.11 - Topology C Control & Performance Characteristics

Driver Experience Pros & Cons

Pro	Con	Feature
	✗	Floating DC bus voltage reduces acceleration performance under circumstances where the driver requires extra acceleration.

Table 4.12 - Topology C Driver Experience Characteristics

Manufacture and Packaging Pros & Cons

Pro	Con	Feature
✓		Smallest possible power converter requirement whilst retaining full control over battery utilisation and power management.

Table 4.13 - Topology C Manufacture & Packaging Characteristics

Topology C Summary

One of the most common methods of providing a power assist to the fuel cell system is to interface a battery to the fuel cell DC output bus with a DC-DC converter [130, 131, 137-140, 173, 180]. The battery provides a power assist through its DC-DC converter whilst tracking the bus voltage that is dictated by the fuel cell stack current. The battery DC-DC converter, though bi-directional, is lower-rated and thus smaller and lighter than a DC-DC converter for the fuel cell would be. The converter also enables optimal and safe charging of the battery system from both regenerative braking energy and the fuel cell.

Known Variants

Topology D will add an additional DC-DC converter before the input to the inverter drive to fix the bus voltage and increase performance. Topology E effectively reverses the energy source that has the DC-DC converter connected to it

Known Production & Prototype Implementations

1. Toyota FCHV.
2. Honda FCX (Li-Ion Model)

4.4.4 Topology D

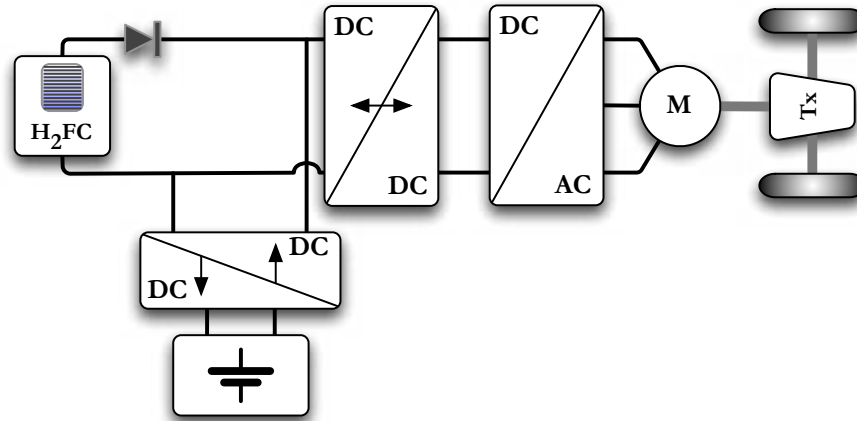


Figure 4.19 - Topology D

Power Flow Analysis

Power Flow Path	Efficiency Calculation	Efficiency η
<i>Fuel Cell to Wheel</i>	$0.56 \times 0.99 \times 0.91 \times 0.86 \times 0.97$	0.421
<i>Battery to Wheel</i>	$0.94 \times 0.93 \times 0.91 \times 0.86 \times 0.97$	0.663
<i>Fuel Cell to Battery (Charging)</i>	$0.56 \times 0.99 \times 0.93 \times 0.88$	0.453
<i>Regenerative Braking</i>	$0.97 \times 0.86 \times 0.91 \times 0.93 \times 0.88$	0.621
<i>Fuel Cell to Battery to Wheel</i>	0.454×0.663	0.301

Table 4.14 - Topology D Power Flow Analysis

Control and Performance Pros & Cons

Pro	Con	Feature
✓		DC bus voltage is fixed. Torque speed characteristic operates at a fixed point of high performance and drive control is straightforward.
	✗	During high load the ratio of V_{in}/V_{out} of the bus DC-DC converter is dictated by the fuel cell voltage and diverges significantly from unity, resulting in lower efficiency.
	✗	Regenerative braking energy has to flow through two power converters, reducing the amount of energy that can be recaptured.

Table 4.15 - Topology D Control & Performance Characteristics

Driver Experience Pros & Cons

Pro	Con	Feature
✓		High acceleration performance
	✗	Extra converter between inverter and DC bus may increase acceleration response reaction time and introduce a lag between demand and acceleration response.

Table 4.16 - Topology D Driver Experience Characteristics

Manufacture and Packaging Pros & Cons

Pro	Con	Feature
	X	The system requires a large 75kW bi-directional DC-DC converter increasing cost, packaging and cooling requirements.

Table 4.17 - Topology D Manufacture & Packaging Characteristics

Topology D Summary

Topology D is deficient in that the DC bus voltage is dictated by the output of the fuel cell. At high output the fuel cell voltage decreases, reducing the input voltage to the drive and limiting available torque and performance. Topology D [181] overcomes this by adding an additional power converter to the DC bus the voltage can be stepped up to the maximum permissible level to ensure maximum torque is available at all times and thus increasing the performance of the vehicle. In order to continue to capture regenerative braking energy the additional power converter must be bi-directional. This incurs system efficiency, cost, weight, volume and packaging penalties that must be balanced with any increase in performance gained.

The inverter drive control overheads are also reduced if the DC bus voltage is a fixed and known quantity. This eliminates the need to monitor the input voltage and alter the inverter switching strategy to cope with changes in the DC bus.

Known Variants

None.

Known Production & Prototype Implementations

None.

4.4.5 Topology E

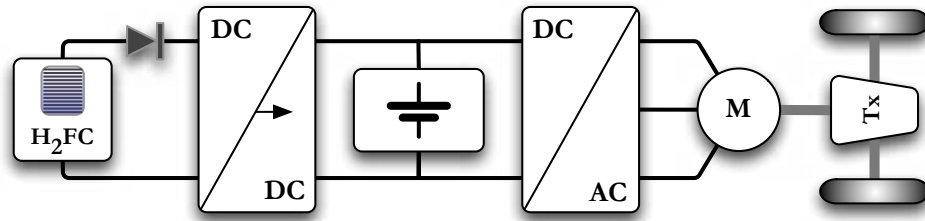


Figure 4.20 - Topology E

Power Flow Analysis

Power Flow Path	Efficiency Calculation	Efficiency η
<i>Fuel Cell to Wheel</i>	$0.56 \times 0.99 \times 0.86 \times 0.97$	0.463
<i>Battery to Wheel</i>	$0.94 \times 0.86 \times 0.97$	0.784
<i>Fuel Cell to Battery (Charging)</i>	$0.56 \times 0.99 \times 0.88$	0.489
<i>Regenerative Braking</i>	$0.97 \times 0.86 \times 0.88$	0.734
<i>Fuel Cell to Battery to Wheel</i>	0.784×0.489	0.383

Table 4.18 - Topology E Power Flow Analysis

Control and Performance Pros & Cons

Pro	Con	Feature
	X	Non-optimal charging and potentially uncontrolled application of regenerative braking energy to the battery terminals could shorten battery life and cause potential safety hazards.
	X	No protection from exceeding battery safe state of charge/discharge threshold.
	X	Even unloaded, the battery and DC bus voltage is typically lower than the fuel cell stack voltage, resulting in lower drive performance than topologies where the bus voltage follows the fuel cell. To avoid this the battery pack needs more cells in series to increase the voltage.
✓		DC-DC allows the operation of the fuel cell system at a single high efficiency steady state independent of power demand.
	X	Floating DC bus voltage limits maximum motor torque, acceleration and performance during high demand.

Table 4.19 - Topology E Control & Performance Characteristics

Driver Experience Pros & Cons

Pro	Con	Feature
	X	High acceleration performance
		Extra converter between inverter and DC bus may increase acceleration response reaction time and introduce a lag between demand and acceleration response.

Table 4.20 - Topology E Driver Experience Characteristics

Manufacture and Packaging Pros & Cons

Pro	Con	Feature
✓		Single uni-directional DC-DC converter required, low switching component count.
	✗	Careful consideration of battery protection necessary. Packaging and cooling that can cope with any excess thermal energy will be required.

Table 4.21 - Topology E Manufacture & Packaging Characteristics

Topology E Summary

Topology E is by far the most common topology in the literature [57, 89, 102, 108, 128, 130, 131, 133, 134, 140-160, 182-184]. The battery acts as a power source and power sink on the DC bus whereby power deficits are drawn from it and any excess power is sunk into it. Most current implementations have used NiMH batteries that are more tolerant than Li-Ion to the effects of the fluctuating bus voltage.

Li-Ion batteries need a significantly higher level of power conditioning and control and topology C is a better arrangement when using a single DC-DC converter and Li-Ion battery technology.

Known Variants

Topology F, detailed next, controls the voltage of the DC link to match the battery pack, before subsequently boosting the voltage with a second DC-DC converter before the inverter drive. This circumvents some of the problems with this topology, but not all.

Known Production & Prototype Implementations

1. Ford Focus FCV Hybrid
2. Nissan X-Trail FCV
3. Renault Laguna FEVER
4. Mercedes A Class F-Cell
5. Mercedes B Class F-Cell
6. VW Bora HyMotion
7. VW Tiguan HyMotion

4.4.6 Topology F

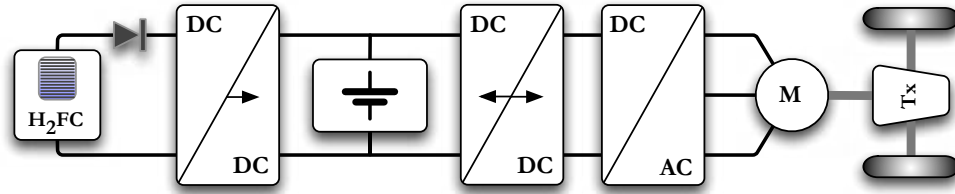


Figure 4.21 - Topology F

Power Flow Analysis

Power Flow Path	Efficiency Calculation	Efficiency η
<i>Fuel Cell to Wheel</i>	$0.56 \times 0.99 \times 0.91 \times 0.86 \times 0.97$	0.421
<i>Battery to Wheel</i>	$0.94 \times 0.86 \times 0.91 \times 0.97$	0.713
<i>Fuel Cell to Battery (Charging)</i>	$0.56 \times 0.99 \times 0.88$	0.489
<i>Regenerative Braking</i>	$0.97 \times 0.86 \times 0.91 \times 0.88$	0.668
<i>Fuel Cell to Battery to Wheel</i>	0.489×0.713	0.349

Table 4.22 - Topology F Power Flow Analysis

Control and Performance Pros & Cons

Pro	Con	Feature
✓		Additional DC-DC allows efficient operation of intermediate battery DC bus at lower voltage.
✓		DC-DC allows the operation of the fuel cell system at a single high efficiency steady state independent of power demand.
	✗	During high load the ratio of V_{in}/V_{out} of the bus DC-DC converter is dictated by the battery voltage and diverges significantly from unity, resulting in lower efficiency.
✓		Additional DC-DC converter enables controlled re-generative braking energy capture.
	✗	Additional large bi-directional DC-DC converter decreases the efficiency of the entire drive train and increase the component count, cooling, volume, weight and vehicle packaging complexity.
	✗	No protection from exceeding battery safe state of charge/discharge threshold

Table 4.23 - Topology F Control & Performance Characteristics

Driver Experience Pros & Cons

Pro	Con	Feature
✓		High acceleration performance.
	✗	Extra DC-DC converter may introduce lag into acceleration response.

Table 4.24 - Topology F Driver Experience Characteristics

Manufacture and Packaging Pros & Cons

Pro	Con	Feature
	✗	Two large DC-DC converters required, increasing component count, cost and converter volume.
	✗	Careful consideration of battery protection necessary. Packaging and cooling that can cope with any excess thermal energy will be required.

Table 4.25 - Topology F Manufacture & Packaging Characteristics

Topology F Summary

Topology F [185, 186] is a simple evolution of Topology E in the same way that Topology D is an evolution of Topology C. An additional DC-DC converter is again used to boost the bus voltage and increase the performance of the vehicle with the same intrinsic system penalties.

Known Variants & Known Production & Prototype Implementations

None

4.4.7 Topology G

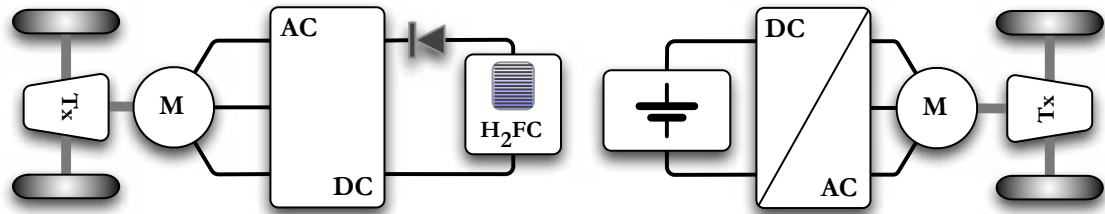


Figure 4.22 - Topology G

Power Flow Analysis

Power Flow Path	Efficiency Calculation	Efficiency η
<i>Fuel Cell to Wheel</i>	$0.56 \times 0.99 \times 0.86 \times 0.97$	0.463
<i>Battery to Wheel</i>	$0.94 \times 0.86 \times 0.97$	0.784
<i>Fuel Cell to Battery (Charging)¹</i>	$0.56 \times 0.97 \times 0.86 \times 0.80 \times 0.97 \times 0.86 \times 0.88$	0.274
<i>Regenerative Braking</i>	$0.97 \times 0.86 \times 0.88$	0.734
<i>Fuel Cell to Battery to Wheel</i>	0.274×0.784	0.215

Table 4.26 - Topology G Power Flow Analysis

Control and Performance Pros & Cons

Pro	Con	Feature
✓		Efficient power path from fuel cell to road in constant load situations.
	✗	Battery charging through the road is incredibly inefficient.
	✗	Complicated control of power split between twin axle drive.
✓		Fault tolerance – vehicle can withstand a failure to either of the drives and still provide motive power.

Table 4.27 - Topology G Control & Performance Characteristics

Driver Experience Pros & Cons

Pro	Con	Feature
✓		4-wheel drive design gives high grip, increased vehicle adverse weather capability and potentially improved acceleration performance.
	✗	Potential driving quality problems with the twin axle drive if control not optimally designed.

Table 4.28 - Topology G Driver Experience Characteristics

Manufacture and Packaging Pros & Cons

Pro	Con	Feature
✓		Mechanical power addition removes need for DC-DC power converters.
	✗	Cost, weight and system size increase due to dual inverters, motors and transmissions.
	✗	Not possible to package the larger drivetrain system in all vehicle body types.

Table 4.29 - Topology G Manufacture & Packaging Characteristics

¹ The efficiency of transferring power through the front to rear transmission through the wheels and road is taken as 0.8

Topology G Summary

Instead of driving a single axle in a two wheel drive arrangement Topology G uses a two axle drive [187, 188] in a drive train configuration known as ‘through-the-road’ (TtR). The system is a 4-wheel drive, mechanically coupled parallel H₂FCBHEV. The front axle is designed to take the bulk of the slow transient driving load and is powered by the fuel cell. The rear axle is designed to provide power during periods of acceleration and is driven by the battery. The battery can also be charged through the road by increasing the power to the front axle and then running the rear axle motor as a generator.

This configuration is more suited when a mechanical and electrical power source are being combined, as in a typical HEV or PHEV. When both power sources are electrical to begin with its advantages are less obvious.

Early implementations of the system showed significant driving quality and control issues with combining the power sources through the road. Real time monitoring of road surface conditions needs to be implemented to achieve optimal power combination through the road. More recent HEV/PHEV TtR systems have overcome these issues. TtR vehicles tend to be large chassis estate, MPV or SUV type vehicles, the increased size of the drivetrain would be difficult to package into compact, mini and super-mini type cars.

Known Variants

Topology H improves on this topology by including an electrical charging link between the two systems, increasing the charging efficiency to practical levels.

Known Production & Prototype Implementations

None – see Topology H.

4.4.8 Topology H

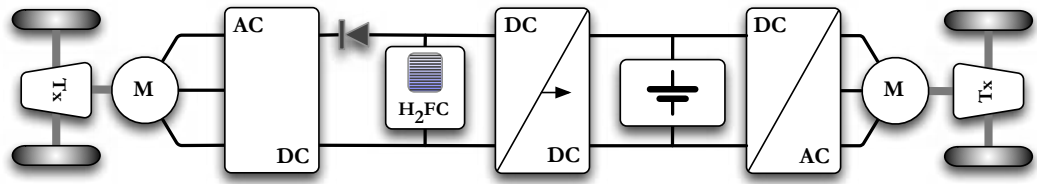


Figure 4.23 - Topology H

Power Flow Analysis

Power Flow Path	Efficiency Calculation	Efficiency η
<i>Fuel Cell to Wheel</i>	$0.56 \times 0.99 \times 0.86 \times 0.97$	0.463
<i>Battery to Wheel</i>	$0.94 \times 0.86 \times 0.97$	0.784
<i>Fuel Cell to Battery (Charging)</i>	$0.56 \times 0.97 \times 0.88$	0.478
<i>Regenerative Braking</i>	$0.97 \times 0.86 \times 0.88$	0.749
<i>Fuel Cell to Battery to Wheel</i>	0.478×0.784	0.375

Table 4.30 - Topology H Power Flow Analysis

Control and Performance Pros & Cons

Pro	Con	Feature
✓		Significantly increased battery charging efficiency over Topology G.
✓		Efficient power path from fuel cell to road in constant load situations.
	✗	Battery charging through the road is incredibly inefficient.
	✗	Complicated control of power split between twin axle drive.
✓		Fault tolerance – vehicle can withstand a failure to either of the drives and still provide motive power.

Table 4.31 - Topology H Control & Performance Characteristics

Driver Experience Pros & Cons

Pro	Con	Feature
✓		4-wheel drive design gives high grip, increased vehicle adverse weather capability and potentially improved acceleration performance.
	✗	Potential driving quality problems with the twin axle drive if control not optimally designed.
✓		Fault tolerance, car can continue to be driven (with reduced performance) with one power source or drive having failed.

Table 4.32 - Topology H Driver Experience Characteristics

Manufacture and Packaging Pros & Cons

Pro	Con	Feature
	✗	DC-DC power converters required in addition to twin drive system.
	✗	Cost, weight and system size increase due to dual inverters, motors and transmissions.
	✗	Not possible to package the larger drivetrain system in all vehicle body types.

Table 4.33 - Topology H Manufacture & Packaging Characteristics

Topology H Summary

This is a variation on Topology G, as the addition of a small 4.5kW uni-directional DC-DC converter allows the direct charging of the battery from the fuel cell rather than charging the battery by transferring power between the transmission, wheels and the road.

Known Variants

The Honda Sport Hybrid All Wheel Drive system uses three motors, one on the front axle and one each on the rear wheels to eliminate the need for a rear differential.

Known Production & Prototype Implementations

1. Volvo V60 Diesel PHEV
2. Peugeot 3008 HYbrid4 Diesel HEV
3. Vauxhall Vivaro TtRHEV

4.4.9 Topology I

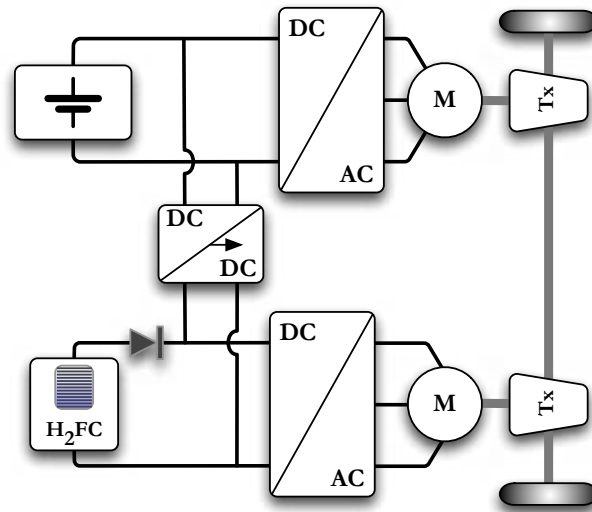


Figure 4.24 - Topology I

Power Flow Analysis

Power Flow Path	Efficiency Calculation	Efficiency η
<i>Fuel Cell to Wheel</i>	$0.56 \times 0.99 \times 0.86 \times 0.97$	0.462
<i>Battery to Wheel</i>	$0.94 \times 0.86 \times 0.97$	0.784
<i>Fuel Cell to Battery (Charging)</i>	$0.56 \times 0.99 \times 0.97 \times 0.88$	0.473
<i>Regenerative Braking</i>	$0.97 \times 0.86 \times 0.88$	0.734
<i>Fuel Cell to Battery to Wheel</i>	0.473×0.784	0.371

Table 4.34 - Topology I Power Flow Analysis

Control and Performance Pros & Cons

Pro	Con	Feature
✓		Highly efficient battery charging.
✓		Fault tolerance – vehicle can withstand a failure to either of the drives and still provide motive power
	✗	With only one power source active, the other idle drive will introduce a frictional loss into the system unless a clutch is included to isolate it.

Table 4.35 - Topology I Control & Performance Characteristics

Driver Experience Pros & Cons

Pro	Con	Feature
✓		Fault tolerance, car can continue to be driven (with reduced performance) with one power source or drive having failed.

Table 4.36 – Topology I Driver Experience Characteristics

Manufacture and Packaging Pros & Cons

Pro	Con	Feature
	X	Cost, weight and system size increase due to dual inverters, motors and transmissions. Not possible to package the larger drivetrain system in all vehicle body types.

Table 4.37 - Topology I Manufacture & Packaging Characteristics

Topology I Summary

Instead of two motors driving separate axels as in Topologies G & H, this system uses two separate motors to drive the same axle and is a 2-wheel drive mechanical parallel fuel cell H₂FCBHEV configuration. The same principal of using the fuel motor to provide the base relatively un-transient drive load and the battery to provide fast transient power is used. In some systems the overall size of each of the motors is decreased such that the drive trains overall power output remains the same. So for a vehicle that would traditionally have a single 75kW drive two motors are used, normally in a 1 to 1/3 power split whereby the fuel cell drives the 75kW drive and the battery a 25kW drive. Different splits can be chosen and tailored specifically to the mode of driving the vehicle is designed for. This in turn can allow for drives smaller and slightly more efficient in their own right, though combining the power output of the two motors incurs an efficiency penalty in each of the separate transmissions. Other systems do not downsize the fuel cell drive as to do so would limit the efficiency of the system at high steady state power levels where the battery drive would have to contribute to the total system power output despite its power flow path being significantly less efficient

Known Variants

This topology has been proposed in either front wheel drive or rear wheel drive configuration.

Known Production & Prototype Implementations

None.

4.4.10 Topology J

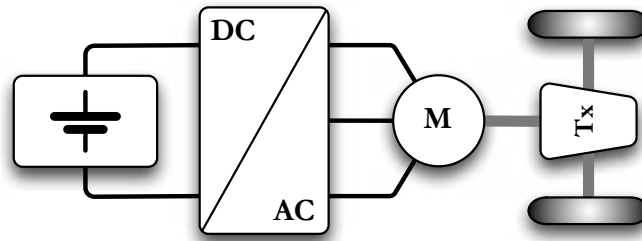


Figure 4.25 - Topology J

Power Flow Analysis

Power Flow Path	Efficiency Calculation	Efficiency η
<i>Battery to Wheel</i>	$0.94 \times 0.86 \times 0.97$	0.784
<i>Regenerative Braking</i>	$0.97 \times 0.86 \times 0.88$	0.734

Table 4.38 - Topology J Power Flow Analysis

Control and Performance Pros & Cons

Pro	Con	Feature
✓		Simple architecture, considerably cheaper than fuel cell vehicle.
✓		High performance if battery suitably specified.
	✗	Mass companding effect of increasing vehicle range by increasing size of battery pack.
✓		Cuts out use of Hydrogen as intermediate energy carrier. Significantly higher efficiency of converting renewably generated electricity to motive power.

Table 4.39 - Topology J Control & Performance Characteristics

Driver Experience Pros & Cons

Pro	Con	Feature
✓		High performance.
	✗	Limited range and long battery recharge time (several hours).
	✗	Batteries need to be replaced during vehicle lifetime.

Table 4.40 - Topology J Driver Experience Characteristics

Manufacture and Packaging Pros & Cons

Pro	Con	Feature
✓		Simple architecture, no DC-DC power converters.
✓		Drive train has far fewer components than ICEV and H ₂ FCEV.
	✗	Uses significantly more, costly, batteries than H ₂ FCEV or HEV.

Table 4.41 - Topology J Manufacture & Packaging Characteristics

Topology J Summary

This is a classic battery electric vehicle [127] power drive train that has been included in this review to compare the performance of a H₂FCHEV to that of a BEV. As previously discussed the BEV is the most efficient way of using renewable electricity to drive a vehicle but its range limitations and significant recharge times limit the types of driving modes it can be used for. Even if cost was not an issue, simply increasing the size of the battery can not solve this alone. Beyond a certain size the mass of the structural components required to support a larger and larger battery becomes an increasingly negative factor on vehicle efficiency.

Known Variants

Topology K.

Known Production & Prototype Implementations

1. General Motors EV1
2. Nissan Leaf
3. Tesla Roadster
4. Mitsubishi iMiEV
5. Ford Focus Electric
6. Renault Zoe
7. Toyota RAV4 EV
8. BMW Mini E

4.4.11 Topology K

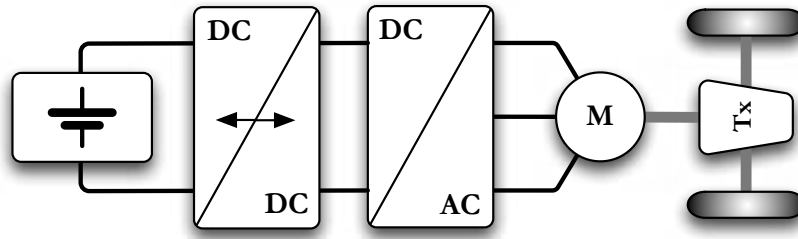


Figure 4.26 - Topology K

Power Flow Analysis

Power Flow Path	Efficiency Calculation	Efficiency η
<i>Battery to Wheel</i>	$0.94 \times 0.91 \times 0.86 \times 0.97$	0.713
<i>Regenerative Braking</i>	$0.97 \times 0.91 \times 0.86 \times 0.88$	0.667

Table 4.42 - Topology K Power Flow Analysis

Control and Performance Pros & Cons

Pro	Con	Feature
✓		Very high performance. Simplified control and tracking of motor torque.
	✗	Reduced system efficiency.

Table 4.43 - Topology K Control & Performance Characteristics

Driver Experience Pros & Cons

Pro	Con	Feature
✓		Very high acceleration performance.
	✗	Further reduction in vehicle range.

Table 4.44 - Topology K Driver Experience Characteristics

Manufacture and Packaging Pros & Cons

Pro	Con	Feature
	✗	Extra power converter complicates drive train and increases cost, weight and volume.
	✗	More battery cells required to achieve same range.

Table 4.45 - Topology K Manufacture & Packaging Characteristics

Topology K Summary

By adding a DC-DC converter into the drive train of Topology J the DC bus voltage can be maintained at the highest possible inverter input voltage, thus ensuring maximised performance over the entire speed range of the motor. The weight of the converter and power loss in the system both act to reduce the range of the vehicle.

Known Variants

None.

Known Production & Prototype Implementations

None.

4.4.12 Topology L

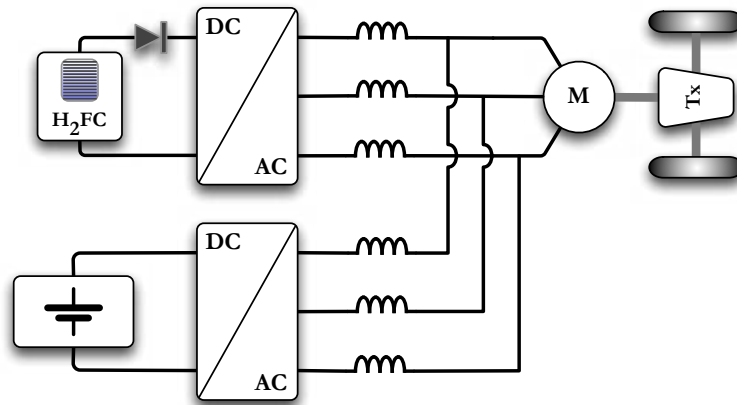


Figure 4.27 - Topology L

Power Flow Analysis

Power Flow Path	Efficiency Calculation	Efficiency η
<i>Fuel Cell to Wheel</i>	$0.56 \times 0.99 \times 0.86 \times 0.99^1 \times 0.97$	0.458
<i>Battery to Wheel</i>	$0.94 \times 0.86 \times 0.99 \times 0.97$	0.776
<i>Fuel Cell to Battery (Charging)</i>	$0.56 \times 0.99 \times 0.86 \times 0.99 \times 0.99 \times 0.86 \times 0.88$	0.354
<i>Regenerative Braking</i>	$0.97 \times 0.99 \times 0.86 \times 0.88$	0.727
<i>Fuel Cell to Battery to Wheel</i>	0.776×0.354	0.275

Table 4.46 - Topology L Power Flow Analysis

Control and Performance Pros & Cons

Pro	Con	Feature
✓		No DC-DC converters required.
		Both converters are grid connected and therefore must have the same output voltage and frequency. Therefore maximum output voltage is determined by the magnitude of the converter that has the lowest output.
	✗	Voltage cannot be stepped up and the maximum output voltage is less than the maximum DC input voltage to the DC-AC inverter. This will lead to low torque capability at speed and low performance.
	✗	The allowable range of modulation indices will limit the range of power split control between the two power sources.
	✗	Careful control of the inverters will be necessary to ensure frequency and voltage synchronisation and to also prevent circulating currents in the system.
		Low battery charging efficiency.

Table 4.47 - Topology L Control & Performance Characteristics

¹ Losses in coupling inductor set, L_c , are taken to be 1% for R_L of 0.05Ω . Weight of each 3 phase inductor set = 60kg.

Driver Experience Pros & Cons

Pro	Con	Feature
	X	Limited acceleration performance.
	X	Acoustic noise and mechanical vibration from ripple and circulating currents.

Table 4.48 - Topology L Driver Experience Characteristics

Manufacture and Packaging Pros & Cons

Pro	Con	Feature
	X	Coupling inductors and additional DC-AC converter ¹ add additional weight, power loss and cost into the system.

Table 4.49 - Topology L Manufacture & Packaging Characteristics

Topology L Summary

This topology draws on the idea of grid-connected inverter systems, usually found in renewable power generation systems to supply power from the two sources to an electric motor. In most of the other systems detailed, the power from both sources is joined on a DC bus, in this arrangement the power is joined on the AC bus that is then directly connected to the motor.

The fundamental limitation of this arrangement is the relationship between the power provided by each power source. In a controlled DC bus system such as Topology B, each source can contribute as small or large a fraction of the total demand as required. In this system there is a limit imposed by the modulation index of the DC-AC converter. Unwanted harmonics, non-linear, circulating currents and square wave outputs are all consequences of running the converter outside of a certain range which would likely limit the degree to which the battery can assist the fuel cell in responding to transient power demands. The inductors used to couple the outputs of the converters are also large, heavy and with the escalating price of copper expensive additional components in the drive train.

Known Variants

Instead of using independent inductors to couple the two AC busses, one variant of this topology uses the coils of the motor as the coupling inductor. Although in this arrangement the power flows in the motor become quite complicated and only a single energy source can be used at any given instant. This application is normally limited to a system where there are multiple identical power sources.

¹ DC-AC converter weight = 40kg

Known Production & Prototype Implementations

None.

4.4.13 Topology M

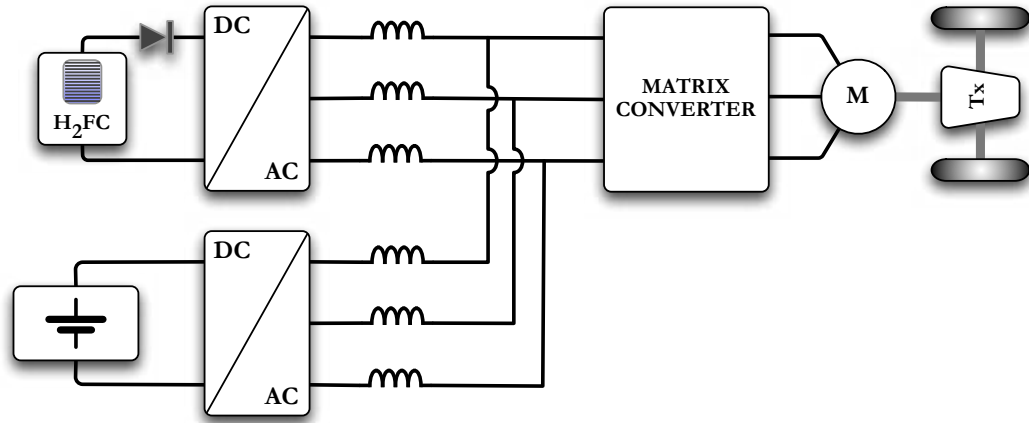


Figure 4.28 - Topology M

Power Flow Analysis

Power Flow Path	Efficiency Calculation	Efficiency η
<i>Fuel Cell to Wheel</i>	$0.56 \times 0.99 \times 0.86 \times 0.99 \times 0.98^1 \times 0.97$	0.449
<i>Battery to Wheel</i>	$0.94 \times 0.86 \times 0.99 \times 0.98 \times 0.97$	0.760
<i>Fuel Cell to Battery (Charging)</i>	$0.56 \times 0.99 \times 0.86 \times 0.99 \times 0.99 \times 0.86 \times 0.88$	0.354
<i>Regenerative Braking</i>	$0.97 \times 0.98 \times 0.99 \times 0.86 \times 0.88$	0.712
<i>Fuel Cell to Battery to Wheel</i>	0.354×0.760	0.269

Table 4.50 - Topology M Power Flow Analysis

Control and Performance Pros & Cons

Pro	Con	Feature
✓		Relatively high efficiency converter.
	✗	Matrix converter output voltage is equivalent to $0.88 \times$ the AC bus voltage level, whilst higher than the series connected inverter system is still less than most DC power addition systems and limits drive performance.
	✗	More suited to systems where the source is AC, eg. Electric trains.

Table 4.51 – Topology M Control & Performance Characteristics

Driver Experience Pros & Cons

Pro	Con	Feature
	✗	Matrix converter can have significant resonant acoustic noise issues associated with it.
	✗	Matrix converter can fail closed, presenting a safety hazard.

Table 4.52 - Topology M Driver Experience Characteristics

¹ Losses in coupling inductor set, L_c , are taken to be 1% for R_L of 0.05Ω . Weight of each 3 phase inductor set = 60kg.

Manufacture and Packaging Pros & Cons

Pro	Con	Feature
✓		Matrix converter requires no inductor or magnetic components so is therefore smaller and lighter for a given power rating.
✓		Filter capacitor size of matrix converter significantly smaller than a standard DC-AC inverter.
	✗	Matrix converter ¹ has 50% more switching components than a traditional inverter; this can outweigh any cost, packaging volume or assembly benefits yielded by lack of inductors, power diodes and smaller capacitors.
	✗	Matrix converter can fail closed, presenting a safety hazard and requiring additional safety devices to isolate power from the drive in the event of such a fault.
	✗	Coupling inductors add additional weight and cost into system.

Table 4.53 - Topology M Manufacture & Packaging Characteristics

Topology M Summary

Continuing with the AC bus systems, this topology uses a three-phase forced-commutated AC-AC cycloconverter (matrix converter) as the final drive to the motor [169]. The matrix converter has fewer components compared to traditional DC-AC converters reducing cost, weight and assembly complexity. The output voltage is also higher for a given input voltage and appropriate control schema [189].

Known Variants

None.

Known Production & Prototype Implementations

None.

¹ Matrix converter weight = 80kg.

4.4.14 Topology N

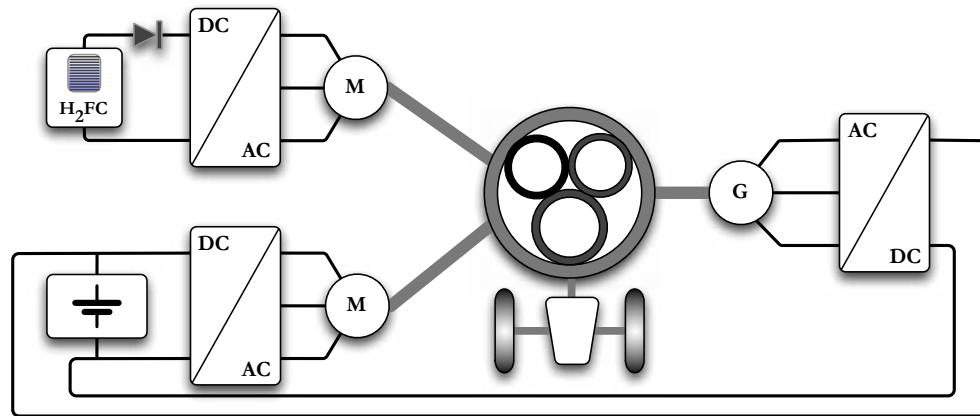


Figure 4.29 - Topology N

Power Flow Analysis

Power Flow Path	Efficiency Calculation	Efficiency η
<i>Fuel Cell to Wheel¹</i>	$0.56 \times 0.99 \times 0.86 \times 0.92$	0.439
<i>Battery to Wheel</i>	$0.94 \times 0.86 \times 0.92$	0.744
<i>Fuel Cell to Battery (Charging)</i>	$0.56 \times 0.99 \times 0.86 \times 0.92 \times 0.86$	0.377
<i>Regenerative Braking</i>	$0.92 \times 0.86 \times 0.88$	0.696
<i>Fuel Cell to Battery to Wheel</i>	0.377×0.744	0.280

Table 4.54 - Topology N Power Flow Analysis

Control and Performance Pros & Cons

Pro	Con	Feature
	X	Inefficient method of combining electrical power.
	X	Inefficient battery charging.

Table 4.55 - Topology N Control & Performance Characteristics

Driver Experience Pros & Cons

Pro	Con	Feature
	X	Inefficiency compared to fully electric power train type H ₂ FCEV will reduce range.

Table 4.56 - Topology N Driver Experience Characteristics

Manufacture and Packaging Pros & Cons

Pro	Con	Feature
✓		Provides linear, incremental development step with component and platform reuse from HEV to H ₂ FCEV
	X	Planetary gear system is comparatively expensive, mechanically complex and bulky when compared to single speed fixed ratio transmission.

Table 4.57 - Topology N Manufacture & Packaging Characteristics

¹ Power loss of each stage of planetary gear set taken to be 8%

Topology N Summary

This arrangement is based on the current parallel hybrid drivetrain found in vehicles such as the Toyota Prius. The ICE in the Prius type drivetrain is replaced with fuel cell, inverter and motor [190].

Whilst this configuration makes sense when dealing with a mechanical engine, it does not when dealing with an all-electric drive system. The power from the two sources is summed mechanically in this system through the planetary gear system power split device. The efficiency penalty imposed by doing this instead of combining the power electrically is significant, and is a big enough barrier in itself to not use this method. Proponents of the system would argue that in an evolutionary path, it is the path of least cost for manufacturers, who over time can develop petrol hybrid cars and then drop in a replacement for the engine.

However another problem is the use of a generator to charge the battery, meaning power from the fuel cell has to be converted to mechanical power, transferred through a lossy transmission and be converted back from mechanical to electrical power before it can charge the battery. Not only is such a system highly inefficient, it is unnecessarily over complicated and substantially increases the number of electro-mechanical and power electronic elements in the topology. From a usability perspective, the servicing and failure potential of this electromechanical system is significantly higher than a simple power converter and far more difficult to replace if it does fail.

Known Variants

None.

Known Production & Prototype Implementations

1. Toyota Prius HEV (using Toyota Hybrid Synergy Drive)
2. BMW 3 Series Active Hybrid HEV (using Global Hybrid Corporation system)
3. Chevrolet Volt EV / ER-EV¹

¹ ER-EV – Extended range electric vehicle. ICE in power train used to generate electricity to charge the battery only.

4.4.15 Topology O

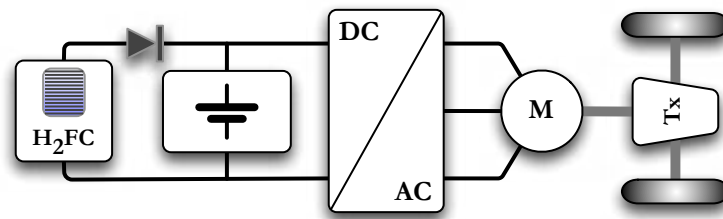


Figure 4.30 - Topology O

Power Flow Analysis

Power Flow Path	Efficiency Calculation	Efficiency η
<i>Fuel Cell to Wheel</i>	$0.56 \times 0.99 \times 0.86 \times 0.97$	0.463
<i>Battery to Wheel</i>	$0.94 \times 0.86 \times 0.97$	0.784
<i>Fuel Cell to Battery (Charging)</i>	$0.56 \times 0.99 \times 0.88$	0.488
<i>Regenerative Braking</i>	$0.97 \times 0.86 \times 0.88$	0.734
<i>Fuel Cell to Battery to Wheel</i>	0.784×0.488	0.383

Table 4.58 - Topology O Power Flow Analysis

Control and Performance Pros & Cons

Pro	Con	Feature
✓		No control of power flows required.
	✗	Floating DC bus voltage limits performance at speed.
	✗	Non-optimal charging and potentially uncontrolled application of regenerative braking energy to the battery terminals could shorten battery life and cause potential safety hazards.
	✗	No protection from exceeding battery safe state of charge/discharge threshold.

Table 4.59 - Topology O Control & Performance Characteristics

Driver Experience Pros & Cons

Pro	Con	Feature
	✗	Low acceleration performance
	✗	Potential safety hazard from uncontrolled battery charge and discharge.

Table 4.60 - Topology O Driver Experience Characteristics

Manufacture and Packaging Pros & Cons

Pro	Con	Feature
✓		Low cost, simple arrangement - no DC-DC converters.
	✗	Careful consideration of battery protection necessary. Packaging and cooling that can cope with any excess thermal energy will be required.

Table 4.61 - Topology O Manufacture & Packaging Characteristics

Topology O Summary

This is an example of early implementations of H₂FCBHEV [102, 129-136]. The battery is used as a “dumb energy buffer” in the system, following the fuel cell voltage responding to transient demand and absorbing spare power. Essentially the battery acts as a capacitor would on the rail of a DC power supply.

With modern lithium ion and to a lesser extent nickel metal hydride batteries this system would not be practical as there would be no control of over-charge and over discharge of the battery cells or under and over voltage conditions at the terminal of the battery pack. Lead acid packs and super-capacitors are far more tolerant of such conditions.

Known Variants

Topology P.

Known Production & Prototype Implementations

Honda FCX 2005 (Ultra-capacitor Model)

4.4.16 Topology P

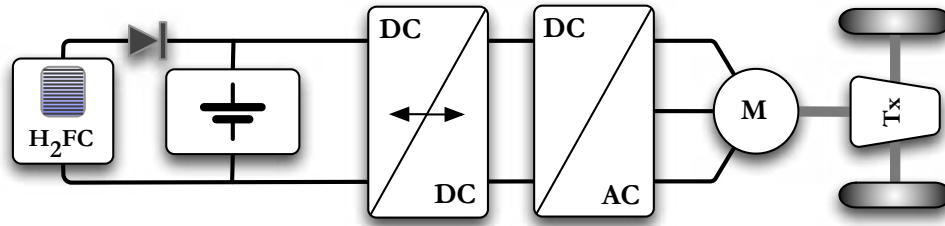


Figure 4.31 - Topology P

Power Flow Analysis

Power Flow Path	Efficiency Calculation	Efficiency η
<i>Fuel Cell to Wheel</i>	$0.56 \times 0.99 \times 0.91 \times 0.86 \times 0.97$	0.420
<i>Battery to Wheel</i>	$0.94 \times 0.86 \times 0.91 \times 0.97$	0.713
<i>Fuel Cell to Battery (Charging)</i>	$0.56 \times 0.99 \times 0.88$	0.488
<i>Regenerative Braking</i>	$0.97 \times 0.91 \times 0.86 \times 0.88$	0.668
<i>Fuel Cell to Battery to Wheel</i>	0.713×0.488	0.348

Table 4.62 - Topology P Power Flow Analysis

Control and Performance Pros & Cons

Pro	Con	Feature
✓		Increased Performance (vs. Topology O).
✓		Controllable regenerative braking.
	✗	Reduced system efficiency.

Table 4.63 - Topology P Control & Performance Characteristics

Driver Experience Pros & Cons

Pro	Con	Feature
✓		Improved acceleration performance.

Table 4.64 - Topology P Driver Experience Characteristics

Manufacture and Packaging Pros & Cons

Pro	Con	Feature
	✗	Large, costly bi-directional DC-DC converter increases component count, cost, system volume and cooling capacity.

Table 4.65 - Topology P Manufacture & Packaging Characteristics

Topology P Summary

Topology P [129] shown in Figure 4.31 adds a bi-directional DC-DC converter to the DC bus to boost the bus voltage to ensure the vehicle has maximum torque capability and therefore increases the performance of the system. As ever, this approach reduces the

efficiency of the system, increases the cost and adds another large subsystem that requires packaging and cooling.

Known Variants

None.

Known Production & Prototype Implementations

None.

4.4.17 Topology Q

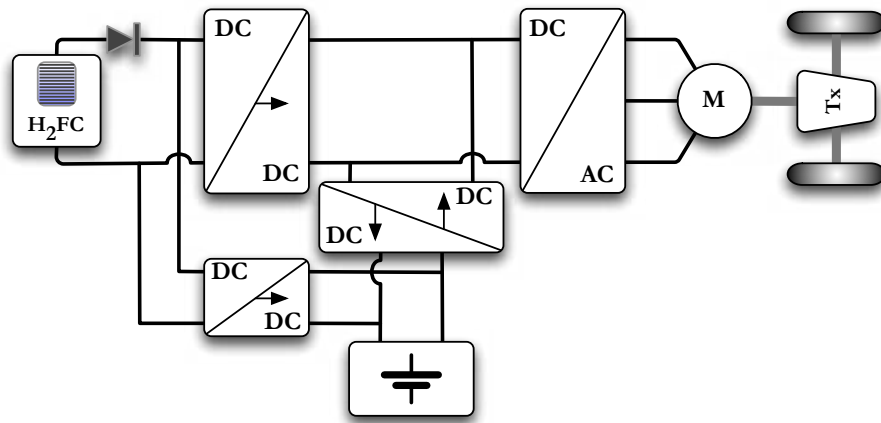


Figure 4.32 - Topology Q

Power Flow Analysis

Power Flow Path	Efficiency Calculation	Efficiency η
<i>Fuel Cell to Wheel</i>	$0.56 \times 0.99 \times 0.95 \times 0.86 \times 0.97$	0.439
<i>Battery to Wheel</i>	$0.94 \times 0.93 \times 0.86 \times 0.97$	0.729
<i>Fuel Cell to Battery (Charging)</i>	$0.56 \times 0.99 \times 0.95 \times 0.93 \times 0.88$	0.431
<i>Regenerative Braking</i>	$0.97 \times 0.86 \times 0.93 \times 0.88$	0.683
<i>Fuel Cell to Battery to Wheel</i>	0.431×0.729	0.314

Table 4.66 - Topology Q Power Flow Analysis

Control and Performance Pros & Cons

Pro	Con	Feature
✓		Efficient battery charging.
✓		Battery can be charged whilst traction portion of drive train system is shut down.
✓		High performance fixed bus voltage architecture.
	✗	In-efficient architecture for low power driving modes.
✓		Optimally sized power converters.

Table 4.67 - Topology Q Control & Performance Characteristics

Driver Experience Pros & Cons

Pro	Con	Feature
✓		High acceleration performance.

Table 4.68 - Topology Q Driver Experience Characteristics

Manufacture and Packaging Pros & Cons

Pro	Con	Feature
	✗	Large number of power converters, high cost, high component count and large system volume.

Table 4.69 - Topology Q Manufacture & Packaging Characteristics

Topology Q Summary

Topology Q [167, 168] is essentially Topology B but with a separate, small and highly efficiency uni-directional DC-DC converter for battery charging. Although the addition of another converter into the system incurs material, weight, volume and packaging costs, it can improve the efficiency of battery charging by around 4-8% depending upon the type of converter used.

The figure quoted in Table 4.66 is for a hard-switched converter. The charging system could also be run independently of the main drive train and potentially be used whilst the vehicle is parked without the overhead of running the power, control and cooling. The sizing of the converter is highly dependant on the battery pack used.

Known Variants

None.

Known Production & Prototype Implementations

None.

4.5 Topology Review Summary

The simple overview of the topologies reveals three prominent trends.

1. Performance and efficiency are inversely correlated.
2. Fully controllable and safe systems generally have more power train components.
3. Mechanical summation of power in an all-electric drive train is highly inefficient.

Topology	FCtW η^1	BtW η^2	FCtB η^3	FCtBtW η^4	Regen η^5	Bus Type ⁶	Vehicle Mass
Topology A	0.462	N/A	N/A	N/A	N/A	Variable	1214.0kg
Topology B	0.439	0.729	0.431	0.314	0.683	Fixed	1280.0kg
Topology C	0.463	0.725	0.454	0.329	0.683	Variable	1242.5kg
Topology D	0.421	<u>0.663</u>	0.453	0.301	<u>0.621</u>	Fixed	1285.5kg
Topology E	0.463	0.784	0.489	0.383	0.734	Variable	1251.5kg
Topology F	0.421	0.713	0.489	0.349	0.668	Fixed	1294.5kg
Topology G*	0.463	0.784	<u>0.274</u>	<u>0.215</u>	0.734	Variable	1324.0kg
Topology H*	0.463	0.784	0.478	0.375	0.734	Variable	1329.0kg
Topology I**	0.462	0.784	0.473	0.371	0.734	Variable	1349.0kg
Topology J***	N/A	0.784	N/A	N/A	0.734	Variable	1469.0kg
Topology K***	N/A	0.713	N/A	N/A	0.667	Fixed	1506.5kg
Topology L	0.458	0.776	0.354	0.275	0.727	Variable	1394.0kg
Topology M	0.449	0.760	0.354	0.269	0.712	Variable	1454.0kg
Topology N	0.439	0.744	0.386	0.280	0.696	Variable	<u>1509.0kg</u>
Topology O	0.463	0.784	0.488	0.383	0.734	Variable	1241.0kg
Topology P	<u>0.420</u>	0.713	0.488	0.348	0.668	Fixed	1257.0kg
Topology Q	0.439	0.729	0.431	0.314	0.683	Fixed	1285.0kg

Table 4.70 - Topology Simple Power Flow Analysis Summary Table

Table 4.70 shows that with the applied simple power flow analysis. The best values are highlighted in bold, whilst the worst are underlined. It is apparent that topology E is the most efficient in all comparisons, though several other systems feature one or more equivalent ratings. No single system has all of the worst efficiency ratings though the systems that use mechanical power summation, either through-the-road or with a planetary

¹ Fuel Cell to Wheel Efficiency

² Battery to Wheel Efficiency (Battery Charging)

³ Fuel Cell to Battery Efficiency (Battery Driving)

⁴ Fuel Cell to Battery to Wheel Efficiency (Total Battery Charge & Battery Driving)

⁵ Regenerative Braking Efficiency

⁶ Bus Type – Fixed DC Bus Voltage (High Performance) or Variable (Reduced Performance)

* Through-the-Road Mechanically Power Coupled Topology

** Twin Motor Mechanically Power Coupled Topology

*** BEV Topology

gear system show clearly marked losses due to the drive trains when power is being drawn from the battery.

At this stage it is possible to narrow the focus of the study and identify the drive train topologies to be taken forward for full simulation. Several topologies will be discarded. Firstly the AC bus systems, the large magnetic components incur significant cost, performance and packaging penalties that make their use in a passenger vehicle impractical. The simple overview has shown that the planetary gear system in Topology N is clearly an inefficient method of combining the power and developing a full simulation model of the planetary transmission is beyond the scope of this study.

Topologies O and P are not practical or safe when lithium ion battery technology is used and so will also not be considered. Despite using mechanical power combination, Topologies G, H and I seemingly offer high single pathway fuel cell to wheel or battery to wheel efficiencies and will be simulated to see if this steady state efficiency is replicated during variable speed driving. Topology J, a BEV will be simulated so that BEV and H₂FCHEV drive trains based on the same vehicle chassis and battery and motor components can be directly compared.

5 Simulation Model Design

5.1 Choice of Simulation Software

Whilst carrying out background reading and literature research it became evident that a multitude of simulation software packages were currently in use within the fuel cell vehicle industry, the wider automotive industry and other fields of science and engineering related to the development of fuel cell, hybrid and electric vehicles.

Along with integrated simulation packages some studies designed simulation models from the ground up in programming languages such as Assembly, C/C++, FORTRAN and Java [191]. This approach was not considered for this study, firstly because much time and effort would be focused on programming discrete mathematical functions that already exist as ready made building blocks in other systems and second and perhaps most importantly, validating the output of the program would be significantly more challenging. One benefit of this method is the execution speed of compiled code is typically several orders of magnitude faster than using a GUI simulation environment such as MATLAB Simulink. Some simple, high-level simulation studies ran as a series of numerical calculations in Microsoft Excel spread sheets but Excel could not be used to model the system at a sufficient level of detail for this study.

The choice of software was driven by both suitability and economics. Support was a key issue as this was the first study to design a complete vehicle simulation tool within the department. The University had existing licenses for MATLAB Simulink so a review of the other packages was undertaken in order to find out if it was worth using and investing in new software.

After an initial period of consideration three software packages became possible choices for use in this study. These are detailed in the forthcoming parts of this section. Table 5.1 details the other pieces of software that were also evaluated, but discarded from further investigation for a variety of reasons but predominantly due to a lack of data and information about them which precluded being able to fully evaluate them. Finding basic information about some of the packages was difficult enough; information about support, existing users and implemented projects was practically none-existent. Several packages

were also unsuitable due to inflexibility. They had been designed with a library of fixed and specific drive train systems and limited simulation variation to changing the parameters and sizing of those systems.

Software Package	Reason(s) for Discarding from Further Consideration
<i>ADVISOR</i>	ADVISOR is a dedicated virtual vehicle analysis program built atop MATLAB Simulink that was created as an open source project between various research establishments and automotive manufacturers. However the package was sold for commercial licensing in 2003 to AVL. Although subsequently released under open source license again in 2012 between 2003 and 2012 it was not available.
<i>AVTE</i>	UC Davis provide little information on the package designed for advanced vehicle technology evaluation.
<i>ELVIS</i>	Southwest Research Institute has no current information available about the ELVIS project, the last point of mention in any documents is dated 2001. ELVIS was built for MATLAB Simulink and LabVIEW. Limited to set library of drive train topologies, mainly of electric and hybrid-electric vehicles
<i>FCVSim</i>	FCVSim was one of the most developed simulation systems found in literature it was developed in MATLAB Simulink. FCVSim could not be obtained for evaluation.
<i>Hyzem</i>	Now being developed by MSC Software and Boeing as a (very expensive) commercially sold package called 'Easy5'.
<i>PSAT</i>	PSAT is a program that integrates its models with the simulation runtime engine of MATLAB Simulink.
<i>Path</i>	Berkeley states Path's main purpose as that in the area of research into intelligent vehicle projects rather than fuel cell vehicles.
<i>Simplev</i>	Simplev is a DOS based program written in QBASIC. The last known revision is version 3.1 which at the time ran on DOS 5 and DOS 6 based machines. Models are designed via text based files and speed and flexibility of design are limited as a consequence. It is out of date and requires an operating system that is no longer easily available though can be run in a Virtual Machine environment under a hypervisor such as Xen or VMWare.
<i>VSP</i>	Built in the LabVIEW

Table 5.1 - Simulation Software Not Considered For Use

5.1.1 PSpice

Orcad PSpice is an electronic circuit simulation package that has libraries full of component models, including power electronic devices. Indeed most major semiconductor manufacturers provide free PSpice models for the majority of their devices. It provides detailed and accurate simulations of circuits however it is limited in the complexity of control structures that it can simulate. Control circuits normally have to be constructed from discrete components such as ideal op-amps and as such the size and complexity of anything but the most basic control systems becomes prohibitive. Creating control systems similar to those that would be provided by embedded microcontrollers in a real system is practically impossible especially when compared to how easy it is to implement such control functions in MATLAB.

5.1.2 Modelica

Modelica is a European open source project that was created to provide a freely available modelling language for complex physical systems. It provides a simulation environment similar to that of MATLAB Simulink in that objects are taken from a library, placed in a model and connected together to form a complete system in an intuitive manner. However the objects that make up Modelica's libraries are unlike MATLAB Simulink. Simulink's libraries are mainly made up of discrete control elements whereas Modelica has physical entities and devices, actual building blocks of real systems that can be brought into a simulation and used straight away [192].

Modelica also has a large library of electrical and electronic devices. The models for these devices are much more comprehensive than MATLAB Simulink's and are based on PSpice models. This provides a more realistic simulation of power electronic subsystems.

For that reason, Modelica appears to have been embraced by a large cross-section of the engineering world for modelling large systems. Interest and activity has been especially high in the automotive industry which has designed and contributed many libraries to the Modelica community for components of vehicles, including hybrid-electric and fuel cell vehicles.

To utilise the Modelica language and its libraries it is necessary to use one of the available Modelica simulation environments. Although Modelica itself and its libraries are provided free, the simulation runtime environments are commercial packages. Of the two available

runtime packages – Dymola and MathModelica, Dymola is the most widely used. Dymola not only provides a full graphical Modelica simulation environment complete with all the Modelica libraries but also an interface to MATLAB Simulink, allowing Modelica models to be imported into Simulink. This link is provided so that Modelica users can take advantage of MATLAB's advanced data processing and analysis tools.

Aside from the cost implications of using Modelica (~£1500), using it for this study was ruled out due to other drawbacks. The software was very 'bleeding edge' and as such little support was available for it and it was not used within the University. Its libraries were also provided 'as is' with no warranty or guarantee for use and came with no inherent validation. Although they are submitted in good faith by establish developers who have used them for their own development there is no independent auditing or checking of the libraries by a central body to a set of defined standards. This could possibly open results derived from Modelica to be challenged as inaccurate, flawed or invalid and it may be subsequently hard to defend the data given that the code behind the system has no recognised guarantee of quality.

5.1.3 MATLAB Simulink

MATLAB Simulink provides a very intuitive graphical based modelling system and is a standard throughout many areas of the engineering world. It offers an ideal environment to provide a topological simulation of a fuel cell vehicle and its subsystems. There is comprehensive and in depth support available via the MATLAB website and numerous third party websites and the design of complex control structures is straightforward since they can be coded in script files and then inserted into simulation blocks.

The main limitation of Simulink is the way it simulates electronic devices. Native support is limited to representing a few basic electronic components and power semiconductors are only modelled as basic on-off switches ignoring the effects of turn-on or turn off times, on-state resistance, leakage currents, parasitic capacitances and temperature effects. However although all of these are relevant to the operation of the electronic power conversion systems in a fuel cell vehicle they will be common across all topologies. Simulink can therefore be used to simulate vehicles and provide valid comparison between different topologies even though it cannot model the exact behaviour of the power devices. The use of empirical data in look up table based simulation models can be used to compensate for this.

If more accurate data were required, a common approach found in published literature was to take power flow information generated by the MATLAB Simulink simulation and feed this into a PSpice simulation model of the electronic circuits and then analysing the specific behaviour of the electrical devices. Alternatively, a separately purchasable toolbox, SIMPowerSystems could be used to provide more comprehensive and detailed simulation of power electronic circuits [152]. For comparing the performance of vehicle topologies it was decided that the simulation did not need this low-level power electronic detail.

5.1.4 Choice of Simulation Software

Several of the simulation packages in use in research and industry; FCVSim [126], ADVISOR [184, 188, 193-195], ELVIS and PSAT are built atop of MATLAB and/or Simulink and the majority of simulation systems found in literature have been built in MATLAB Simulink [140, 142, 152, 155, 196-198] or the very similar LabVIEW environment [199]. MATLAB Simulink appears to be the pre-eminent choice of software for designing simulation systems and given that it was already available and widely supported throughout the University with a large user and knowledge base available within the department it seemed the ideal choice of simulation tool for use in this study.

5.2 Simulation Model Construction

All of the simulation models are based on a common vehicle chassis and drive, common power conversion elements and common power sources as detailed in Table 4.1. The variation between the simulation models was predominantly in how the selected components were arranged and controlling the flow of data signals between the various elements. Using these components and rearranging them for the different topologies enabled the simulation models to be designed quickly and efficiently.

The subsystem models for the fuel cell, motor, power converters and battery pack were based on validated empirical data rather than being complete discrete simulation models. Complete modelling of the power electronic subsystems was also limited because of the lack of the SimPowerSystems toolbox. Complete dynamic modelling of the electro chemical processes occurring in the fuel cell would have been a substantial undertaking in its own right, likewise modelling the electromagnetics at work in the motor drive. The computational requirements of simulating these systems entirely would also have been prohibitive. In any event the data required to design such models was not available from the manufacturers of these components. The current level of confidentiality surrounding hybrid and electric vehicles cannot be understated [184] and whilst understandable, proved a substantial hindrance in the development of the simulation model. Data from the Laboratory tests of the fuel cell, power converters and motor was obtained from various sources. The datasets contained sufficient data points to enable lookup table based performance map models to be used represent the internal operation of the components. Sufficient data exists such that intervening data points could be extrapolated linearly using MATLAB Simulink's built in 2D and 3D lookup tables. This is a common and accepted method of abstracting and decreasing the computational complexity of many engineering models [200]. The validity of these datasets has where possible also been established and double-checked against models of the same hardware in other published studies and commercial research projects. The published information was used to check the models once they had been constructed. The battery subsystem was constructed as a dynamic model using data that in contrast to the other components was easily available from the battery manufacturer.

Each of the subsystems in the drive train was designed separately and fully tested before being integrated into a full vehicle model. This model was then itself tested before the full suite of drive train topologies was designed.

5.2.1 Simulation Model Subsystems

Once broken down into separate modules, each topologies simulation system comprises of a combination of some or all of the following components:

- a. 1100kg 5 Door Saloon Vehicle Chassis
- b. 75kW (Peak Mechanical Power) Motor & Integrated DC-AC Inverter Drive
- c. 75kW H₂PEMFC
- d. 4.5kWhr/45kW Peak Power Battery & Battery Controller
- e. Bi-directional 45kW DC-DC Converter
- f. Bi-directional 80kW DC-DC Converter
- g. Uni-directional 80kW DC-DC Converter
- h. Uni-Directional 4.5kW DC-DC Converter
- i. Vehicle Management & Control System
- j. Driving Cycle Controlled Driver Emulation System

This section will describe in detail how each of the subsystem models was constructed, tested and finally controlled and integrated into the overall models of the range of vehicle drive trains.

5.2.2 Subsystem Component Sizing

One active area of research highlighted by the literature review was that the choice of relative sizing of each of the subsystems could have significant impact on the performance and efficiency of the drive train. Some studies even focused solely on finding the optimal size of components as the method of improving the efficiency [160].

The sizing of the components in this simulation model was fixed so that the different configurations could be compared on a like for like basis. The size of the components was largely pre-determined by the currently available systems and this was further restricted by which of those systems data could be obtained for. For passenger vehicles the chassis' of typical European mid-size compact vehicles are all relatively similar. Fuel cell systems for passenger vehicles were largely rated at 75kW peak power, to power a motor drive that has

a similar power output to a 1.6l petrol or 1.9l diesel ICE. The battery pack needed to provide the entire power capability of the fuel cell to maintain vehicle performance during fuel cell start-up phase and transient response periods. Its output voltage needed to be of a similar magnitude to the fuel cell to maintain an efficient ratio between the two. With the power requirements and output voltage set the configuration of the cells in the battery pack was then determined by the available Li-Ion cells and once again, which battery cells full data was available for.

5.3 Vehicle Chassis & Vehicle Dynamics Model

The vehicle chassis model takes drive torque from the motor shaft, passes it through the transmission and calculates the actual speed of the vehicle, considering all the forces that act on the vehicle. The chassis model is limited in that it models the straight-line dynamic behaviour of the vehicle on flat surfaces and gradients. Cornering, suspension dynamics, skid behaviour, lateral forces such as roll and pitch and advanced interaction forces and transient effects are not modelled as they are beyond the scope of this study. Although they occur in real vehicles, they had little effect on the metrics that this study sought to measure and would only serve to unnecessarily complicate the model and increase the simulation runtime. The model used provides a sufficiently accurate representation of the vehicle so as to be sure the data generated by the simulations is accurate.

The model is based on data from a European production 5-door saloon car that has an unladen weight of 1137kg in the production ICEV version. Removing the 1.6L 16V ICE (150kg), fuel system (65kg), lead-acid battery (14.5kg) and 5 speed manual gearbox (48.5kg) leaves a chassis of 859kg to which the mass of various H₂FCEV components is added for each topology to give a net weight for that particular drive train. Each topology had a separate configuration file where its weight was defined.

The drive train operated by calculating the angular acceleration of the vehicle based on the torque applied to the wheels by the output of the transmission, the torque applied to the vehicle by retarding forces and brakes and dividing that by the inertia of the transmission and wheels. The angular acceleration was then integrated to obtain the angular velocity of the vehicle that is then multiplied by the tyre radius to obtain the linear velocity.

5.3.1 Forces Acting On the Vehicle

The following retarding forces that acted on the vehicle were considered in this study:

1. Rolling Resistance
2. Wind Resistance
3. Grade Resistance
4. Applied Braking Force
5. Inertial Resistance

The vehicle was considered to have a centre of mass exactly half way between the two axles and that the traction force was applied to the front wheels only. The braking force is only applied when the brakes are applied. Although in reality disc brakes pads are always in contact with the disc and thus causing retarding friction, the magnitude of the force is small and varies according to many variables and consideration of this force is therefore outside the scope of the study. Figure 5.1 shows the retarding forces acting on a vehicle whilst on a flat surface and Figure 5.2 shows how a gradient affects the weight vector of the vehicle.

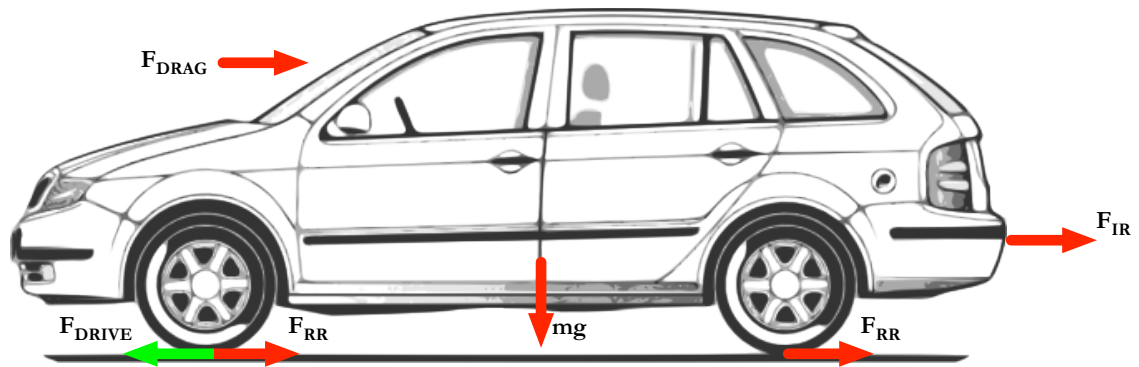


Figure 5.1 - Forces Acting on Vehicle on Level Ground

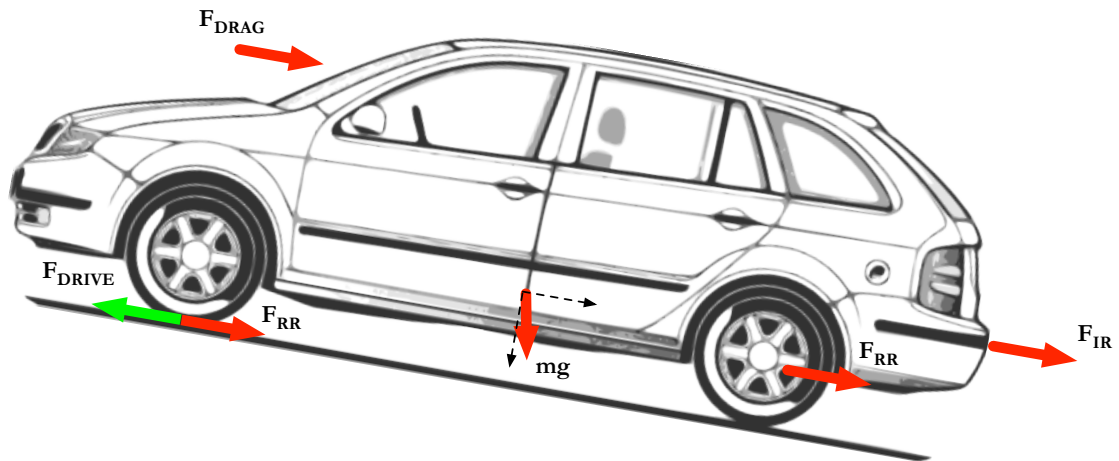


Figure 5.2 - Forces Acting on Vehicle on Incline

5.3.2 Wind Resistance

The wind resistance or aerodynamic drag of the vehicle can be expressed as [201]:

$$F_{DRAG} = v^2 \left(\frac{1}{2} \cdot \rho_{air} \cdot C_d \cdot A_{vehicle} \right)$$

Equation 5.1 - Wind Resistance Force

Where:

ρ_{air} = Density of air

C_d = Coefficient of aerodynamic drag

$A_{vehicle}$ = Cross sectional frontal area of vehicle

v = Speed of vehicle

From data supplied by the vehicle manufacturer:

$$C_d = 0.30$$

$$A_{vehicle} = 2.11m^2$$

5.3.3 Rolling Resistance

The resistance of a vehicle to rolling is a function of its weight and the coefficient of friction of the tires. The rolling resistance can be expressed as:

$$F_{RR} = \mu \cdot m \cdot g$$

Equation 5.2 - Rolling Resistance Force

Where:

μ = tyre coefficient of friction

m = vehicle mass (kg)

g = gravitational constant

The tyre used in the simulation is a Michelin 195/85 R15 and the co-efficient of friction data was obtained from the manufacturer and is shown below in Figure 5.3. The tyre and wheel combined have a weight of 16.71kg.

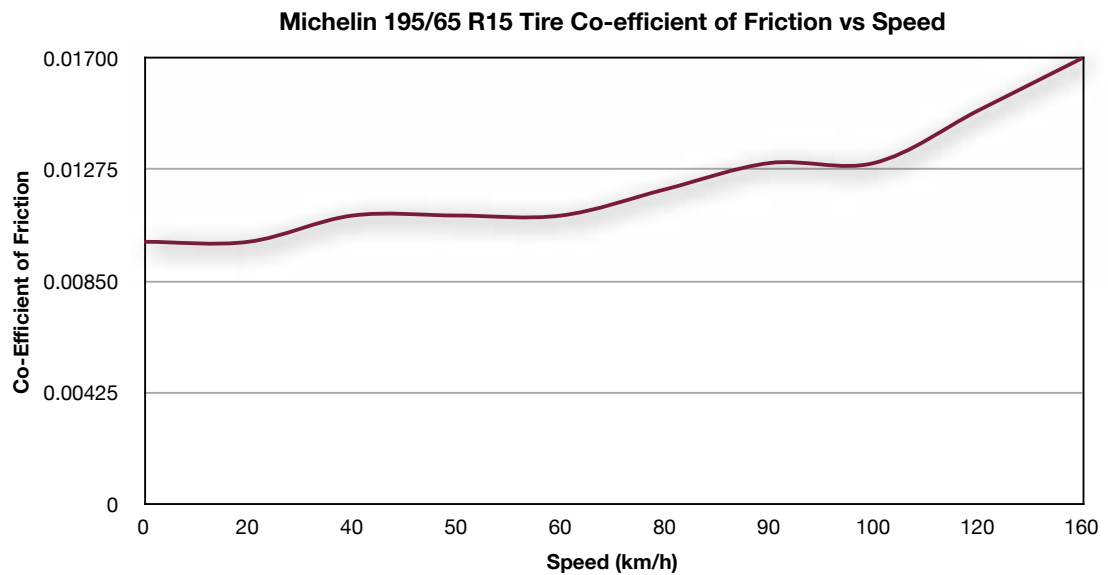


Figure 5.3 - Michelin 195/65 R15 Tyre Co-efficient of Friction Data

5.3.4 Grade Resistance

The grade or slope of the road the vehicle is on affects the force necessary to accelerate or decelerate the vehicle. If the vehicle is going uphill the grade resistance will be positive and act to resist the motion of the car up the hill. If the vehicle is going down hill the grade resistance will be negative and will act as an acceleratory force on the vehicle.

$$F_{GRADE} = m \cdot g \cdot \sin\left(\tan^{-1}\left(\frac{Grade_{\%}}{100}\right)\right)$$

Equation 5.3 - Grade Resistance Force

Where:

$$Grade_{\%} = \text{percentage value of slope incline (0\% - 100\%)}$$

It is therefore clear that on a flat surface (grade = 0) there is no grade resistance. On an uphill gradient the force acts against the direction of motion and decelerates the vehicle and on a downhill gradient the force acts in the direction of motion and accelerates the vehicle. None of the driving cycles used other than the AMS cycle had gradient data associated with them.

5.3.5 Braking Force

The driver simulation subsystem generates a brake demand signal between 0 and 1. This demand is multiplied by the maximum braking force to calculate how much braking torque is applied to the wheels. The maximum braking force is defined as:

$$F_{BRAKE[MAX]} = \frac{3}{5}(m \cdot g)$$

Equation 5.4 - Vehicle Braking Force

The actual braking force at any instant, F_{br} is calculated as:

$$F_{BR} = Brake_{DEMAND[0>1]} \cdot F_{BRAKE[MAX]}$$

Equation 5.5 - Braking Force Calculation

5.3.6 Inertial Resistance

The inertial resistance force of a vehicle is the resistance to a change in the vehicles velocity by the inertial components of the vehicle. Namely the angular inertia of the motive parts in the power drive train and the linear inertia of the vehicle. The linear force can be expressed as:

$$F_{IR[LINEAR]} = m_{VEHICLE} \cdot a$$

Equation 5.6 - Linear Inertial Resistance Force

To consider the angular inertia, it can be seen from Figure 5.4 that there are three main rotating components in the drive train, the motor, the gearbox transmission and the wheels. The axles and transfer shafts are also included in the calculation but are minor actors in determining the angular inertia. The inertia of these components is known from empirical data.

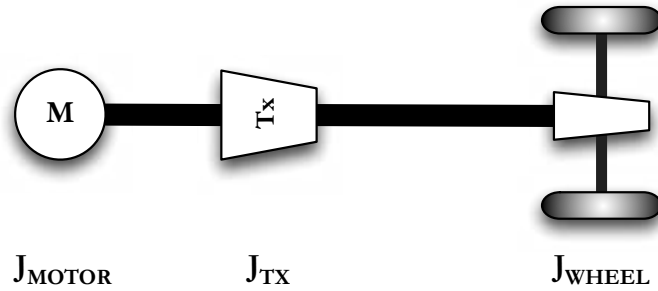


Figure 5.4 - Rotating Components in Power Drive Train

Knowing the inertia for each of these components, an equivalent mass m_{EQ} can be calculated for the rotating system as a whole [202, 203] so that Equation 5.6 can be modified and F_{IR} calculated as:

$$F_{IR} = (m_{VEHICLE} + m_{EQ}) \cdot a$$

Equation 5.7 - Inertial Resistance Force

Looking from the wheel, each inertial force can be expressed as an equivalent mass and then summed together to derive m_{EQ} :

$$m_{EQ} = 4 \left(J_{WHEEL} \left(\frac{1}{r_{WHEEL}} \right)^2 \right) + J_{TX} \cdot \eta_{TX} \left(\frac{R_{TX}}{r_{WHEEL}} \right)^2 + J_{MOTOR} \cdot \eta_{TX} \left(\frac{R_{TX}}{r_{WHEEL}} \right)^2$$

Equation 5.8 - Equivalent Mass of Rotating Components

Where:

J_{WHEEL} = Inertia of the wheel and tyre ($kg \cdot m^2$).

J_{MOTOR} = Inertia of the motor rotor shaft ($kg \cdot m^2$).

J_{TX} = Inertia of transmission including axel ($kg \cdot m^2$).

$r_{WHEEL} = \text{Radius of tyre (m)}$

$\eta_{TX} = \text{Efficiency of transmission.}$

$R_{TX} = \text{Gear ratio of transmission.}$

5.3.7 Total Resistance Forces

The total resistance forces, F_{RES} , for the vehicle can therefore be expressed for all cases as follows.

For a stationary vehicle on a flat surface:

$$F_{RES} = F_{RR}$$

Equation 5.9 - Total Resistance Forces at Rest

For an accelerating or decelerating vehicle on a flat surface:

$$F_{RES} = F_{RR} + F_{DRAG} + F_{IR}$$

Equation 5.10 - Total Resistance Forces During Acceleration

For a vehicle at constant velocity on a flat surface:

$$F_{RES} = F_{RR} + F_{DRAG}$$

Equation 5.11 - Total Resistance Forces at Constant Velocity

For an accelerating or decelerating vehicle on a gradient:

$$F_{RES} = F_{RR} + F_{DRAG} + F_{IR} + F_{GRADE}$$

Equation 5.12 - Total Resistance Forces During Acceleration on a Gradient

For a vehicle at constant velocity on a gradient:

$$F_{RES} = F_{RR} + F_{DRAG} + F_{GRADE}$$

Equation 5.13 - Total Resistance Forces at Constant Velocity on a Gradient

5.3.8 Calculating Vehicle Linear Acceleration & Velocity

The transmission delivers a known torque, T_{DRIVE} to the vehicle wheels. The angular acceleration of the vehicle at any given instant can be calculated using the rotational adaption of Newton's second law of motion:

$$\alpha = \frac{T_{DRIVE}}{J}$$

Equation 5.14 - Vehicle Angular Acceleration

Where:

$J = \text{Total moment of inertia of motor rotor, transmission, wheels, shafts and axles (kg } m^2 \text{)}.$

Integrating α yields the angular velocity, ω :

$$\omega = \int \alpha$$

Equation 5.15 - Vehicle Angular Velocity

Converting both properties to linear measurements is simply a matter of multiplying by the radius of the vehicles tyre:

$$a = \alpha \cdot r_{WHEEL}$$

Equation 5.16 - Vehicle Linear Acceleration

$$v = \omega \cdot r_{WHEEL}$$

Equation 5.17 - Vehicle Linear Velocity

5.3.9 Vehicle Dynamics Assumptions

The model of vehicle dynamics makes several key assumptions:

1. The vehicle is driven in a straight line on a dry road surface of uniform construction and zero camber.
2. There is no atmospheric wind and it is not raining.
3. The air is at standard temperature and pressure.
4. The vehicles centre of mass is in the middle of the vehicle.
5. The weight distribution of the vehicle over the front and rear axels is 50%.
6. There is no weight transfer during breaking or acceleration.
7. The wheels do not slip.
8. The tires do not deform and maintain a constant radius.

5.4 Motor & Inverter Drive

The traction motor is a model based on laboratory test data from a commercially produced electric vehicle motor with integrated DC-AC PWM drive [125, 126, 204]. The motor is a 3-phase AC induction motor capable of generating 260Nm of torque and operating at speeds of up to 10,000rpm, generating 75kW of mechanical power (peak). The 3-Phase DC-AC inverter operates with a DC supply rating of 250-400V.

The model of the motor is principally based on three lookup tables created from empirical data supplied by the motor drive manufacturer:

1. 2D Lookup Table A. Inputs: Speed, DC Bus Voltage. Output: Maximum Torque
2. 3D Lookup Table A. Inputs: Speed, Torque, DC Bus Voltage. Output: Power Loss
3. 3D Lookup Table B. Inputs: Speed, Motor Power, DC Bus Voltage. Output: Torque

Using these three tables it is possible to accurately calculate and describe all the required properties of the motor and drive without the computational overhead of calculating the discrete electrical, electromagnetic and mechanical events occurring within the drive.

5.4.1 Maximum Torque Control Data

A two-dimensional lookup table is used to calculate the maximum torque the motor can generate for a given DC bus voltage and motor speed. Four sets of data are used for $V_{DC} = 250V, 300V, 350V \text{ \& } 400V$ and the Simulink lookup table block interpolates between them when the bus voltage is fluctuating. The data used is shown below in Figure 5.5.

The vehicle controller uses the maximum torque, T_{MAX} , to generate the demand signals for acceleration and braking. These signals are values of 0-1 used to emulate a drive actuating the accelerator and brake from off to fully depressed position. The maximum available braking torque is fixed as per Equation 5.4

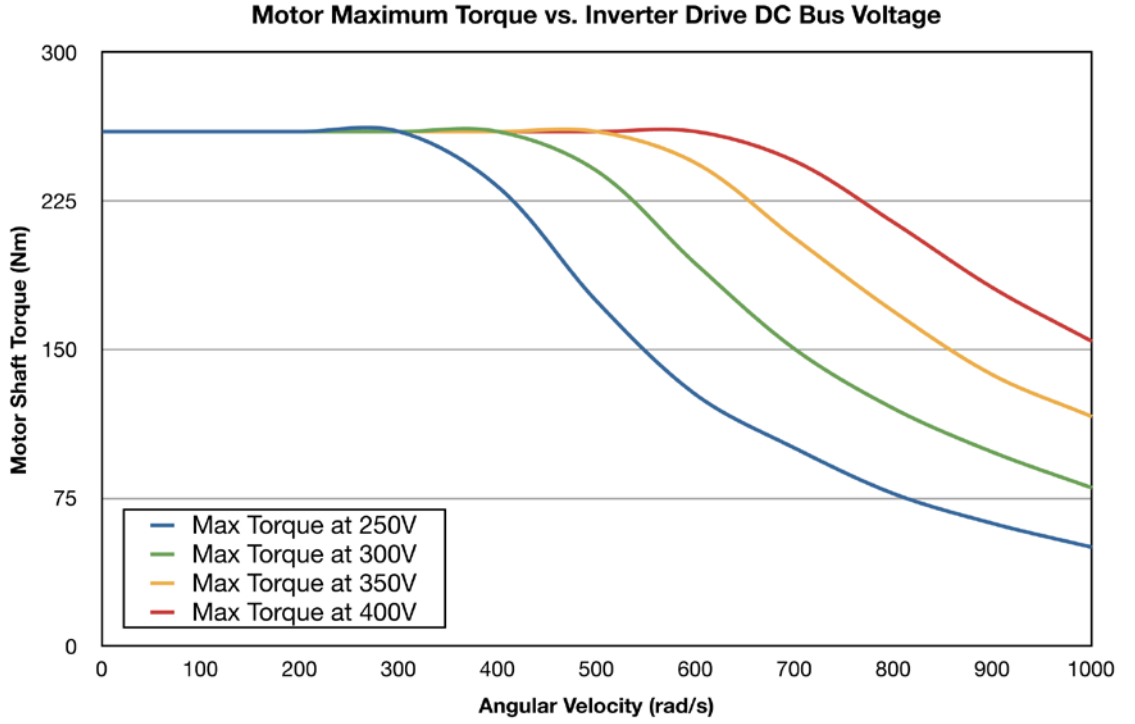


Figure 5.5 - Maximum Motor Torque vs DC Bus Voltage

5.4.2 Motor Power

The first of the 3D lookup tables calculates the power lost, P_{LOSS} , by the motor and inverter drive for any given combination of speed, torque and DC bus voltage. Taking an empirical dataset measured for values of Torque (T_{MOTOR} in Nm) and Speed (ω_{MOTOR} in rad/s) at four different bus voltages ($V_{DC} = 250V, 300V, 350V$ & $400V$) the power lost by the system can be calculated for any valid set point of the system, with the Simulink 3D lookup table linearly interpolating points between the datasets.

The mechanical power of the motor is calculated from the inputs to the motor, taking into account the fixed gear ratio of the transmission, such that the total power of the motor and inverter drive system can be characterised as:

$$\begin{aligned}
 P_{MOTOR} &= P_{LOSS} + P_{MECHANICAL} \\
 P_{MOTOR} &= P_{LOSS} + \left(\frac{T_{DRIVE}}{R \cdot \eta_{TX}} \right) (\omega_{DRIVE} \cdot R) \\
 P_{MOTOR} &= P_{LOSS} + \frac{T_{DRIVE} \cdot \omega_{DRIVE}}{\eta_{TX}}
 \end{aligned}$$

Equation 5.18 - Motor Power

Where:

$R = \text{Gear Ratio}$

$\eta_{TX} = \text{Mechanical efficiency of the gearbox.}$

Given the DC bus voltage, V_{DC} , calculating the electrical input current, I_{MOTOR} required by the motor at that instant is straightforward:

$$I_{MOTOR} = \left(\frac{P_{LOSS} + \left(\frac{T_{DRIVE} \cdot \omega_{DRIVE}}{\eta_{TX}} \right)}{V_{DC}} \right)$$

Equation 5.19 - Motor Input Current

The efficiency of the system can be calculated as:

$$\eta_{MOTOR} = \frac{T_{DRIVE} \cdot \omega_{DRIVE}}{P_{LOSS} + \left(\frac{T_{DRIVE} \cdot \omega_{DRIVE}}{\eta_{TX}} \right)}$$

Equation 5.20 - Motor Efficiency Calculation

An overview of how this subsystem was implemented in Simulink is shown below in Figure 5.6.

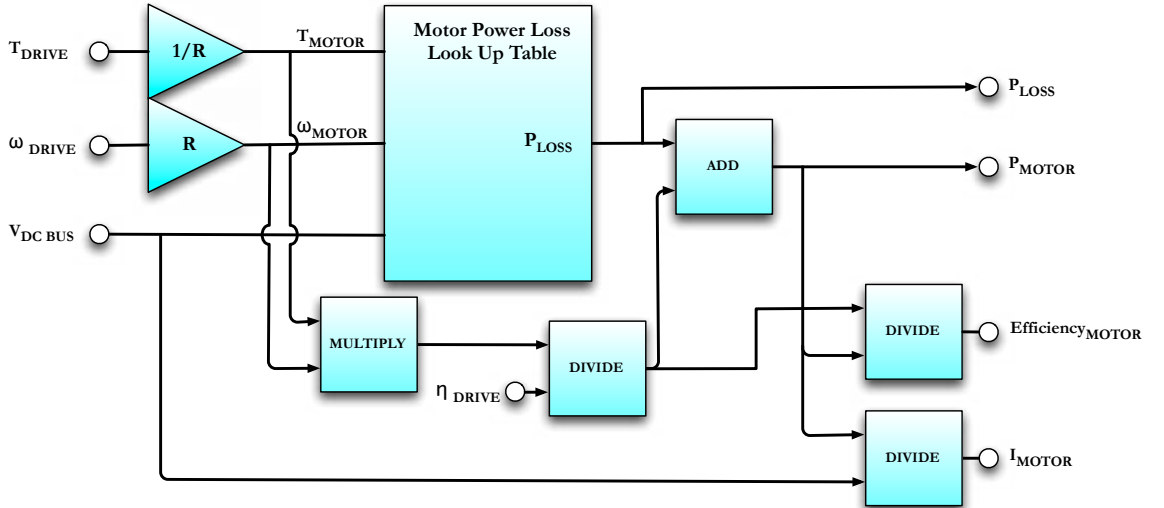


Figure 5.6 - Motor Power Loss Calculating Simulation Model

5.4.3 Motor Torque

The method of simulation will be discussed in more detail later in this chapter but the model of the motor just described is a backwards-looking model. It takes a known state of

the system and calculates how much power is required to achieve that state. Due to the nature of the power sources being used, the simulation system required both this type of motor model, and a forward-looking model.

At certain points the combination of fuel cell and battery output currents may not be sufficient to meet the request demand current to attain a given torque at a certain speed. Therefore a second motor block is needed that takes the speed, DC bus voltage and input current as inputs and generates torque as an output. The system can then accurately calculate the speed of the vehicle using the actual output torque of the motor that is attainable with the available power in the system. 3D lookup tables were once again used to achieve this. The forward-looking model is shown below in Figure 5.7.

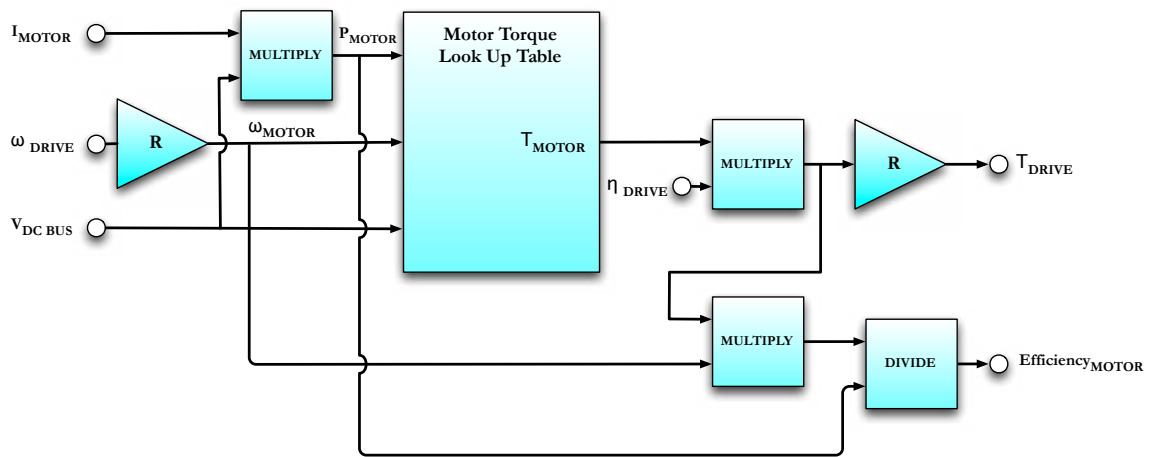


Figure 5.7 - Motor Torque Output Calculating Simulation Model

5.4.4 Regenerative Braking

Regenerative braking was one of the final parts of the motor model to be considered, however its implementation placed an additional computational load on the simulation model and in an effort to optimise the simulation the decision was made to not implement regenerative braking in the model.

The regenerative braking model is computationally intensive for several reasons. At the simplest level, the braking torque available from the motor could provide the force required to decelerate the vehicle when the driver presses the brake pedal. If the available braking torque from the motor does not meet the demanded braking torque, the friction brakes could be applied to make up the deficit. The amount of regenerative energy

available to charge the battery can then be calculated from the motor speed, torque and efficiency of the inverter in converting the energy from AC to DC.

Things are not so straightforward though as the implementation of regenerative braking would need to have a control strategy that could be adapted to the differing topology arrangements as each has specific requirements to ensure the battery is protected from over voltage and over charge. Optimal control of the braking force split between the friction brakes and regenerative braking so as to recuperate the maximum amount of power possible is the topic of several studies as a subject in its own right [205-208]. Furthermore the different driving cycles have variable opportunities to use regenerative braking and different regenerative strategies can be adopted for each cycle to optimise the recovered energy.

This study involved a significant scale of simulation with multiple topologies tested against many driving cycles. Due to the combined forward and backwards looking approach used in the model, the simulation was computationally intensive. The model was optimised where possible and the simulation step sized increased to the maximum possible size that still allowed the model to be solved. Despite this, the limitations of the available computation resources at the time were prohibitive and the simulations took a significant amount of time. Depending on the driving cycle length and the particular topology being simulated, simulations took anywhere between 2 and 12 hours to complete. A high performance computer was used but 32 bit hardware allowed a maximum of 3.5GB of RAM, running at a relatively low memory bus speed on a dual core CPU that was connected to an enterprise grade, but by today's standards relatively slow, hard disk drive. No affordable high speed solid state storage was yet available and as a result virtual memory operations where the system swapped data to disk as it ran out of available RAM had a significant time cost.

Implementation of regenerative braking in the model would have necessitated another combined forwards and backwards looking model as the control of regeneration would have to factor in battery SOC, drive speed and torque and the performance of any DC-DC converters in the electrical path between the drive and the battery. A test model was developed on a single topology but the overall computation time was increased significantly. Additionally, as the control model would have to be modified for each topology, the time required to develop, test, modify and test the model before the actual vehicle simulations were undertaken would also have been significantly increased. The

decision was therefore taken to exclude regenerative braking from the simulation model. Data existed that allowed the amount of energy available for recapture to be estimated and several of the driving cycles have limited or no opportunity to recapture any regenerative energy thus allowing direct comparison with models that do implement regenerative braking.

5.4.5 Idle & Braking Losses

The standby overhead power losses of the inverter and drive are a constant value of 20W. The friction brakes are assumed to be actuated by an electrically power hydraulic actuator. Typically much of the braking in an electric vehicle is done through using the motor in reverse as a generator and drawing power from it to charge the battery whilst slowing down the vehicle. The friction brakes are typically used for less than a third of the braking they would be in an ICEV. Since regenerative braking is not part of this studies scope and no data could be obtained for an electrically actuated friction brake it is assumed that the net-power balance required to operate the brakes would be zero or positive and therefore no loss due to braking is factored into the model.

5.4.6 Motor Protection

The motor and inverter drive need to be protected from several operating states that could cause damage to the real system. Over speed of the rotor can cause the centrifugal force acting on the rotor to exceed its design limits and cause it to fail. The motor bearings can also fail and the increased thermal energy generated in the motor can cause the windings to fail. The system is protected from this by an absolute speed limit at 100% of the motor rating being placed in the control path the motor cannot be driven in excess of this speed and any erroneous command to do so will be adjusted to the limit value. It is assumed that the vehicle cooling system maintains the motor at a safe, constant operating temperature so thermal risks during normal operation and electrical parameter variations due to temperature are ignored.

5.4.7 Motor Characterisation

Whilst validating the model against the empirical data several visualisations of the combined motor drive were created to aid the process that also serve to illustrate the drives performance.

The efficiency of the motor and drive through the entire range of operating points at a DC link voltage of 400V is shown in Figure 5.8.

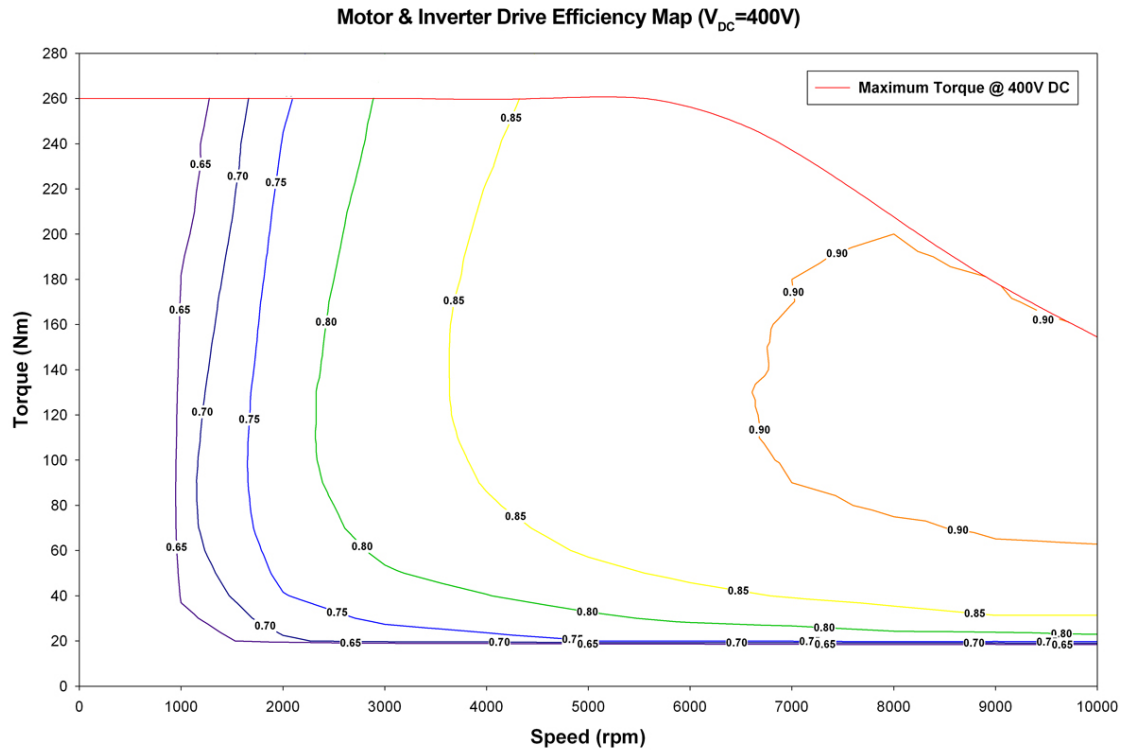
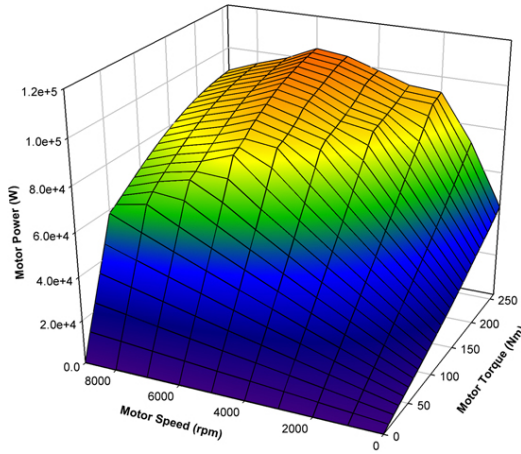


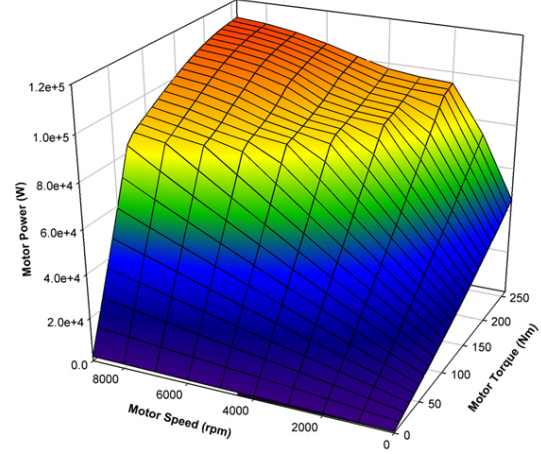
Figure 5.8 - Motor & Inverter Drive Efficiency Map

Figure 5.9 illustrates the total electrical power consumed by the motor and drive across the entire range of operating set points permissible during safe operation. The power limitations of running at lower DC link voltages can be clearly seen at 250V whilst the larger flatter plateau at high torque and speed levels shown whilst operating at 400V shows that the drive is more efficient at these points when operated with a higher DC link voltage resulting in lower losses in the converter and motor in addition to the benefits of higher performance.

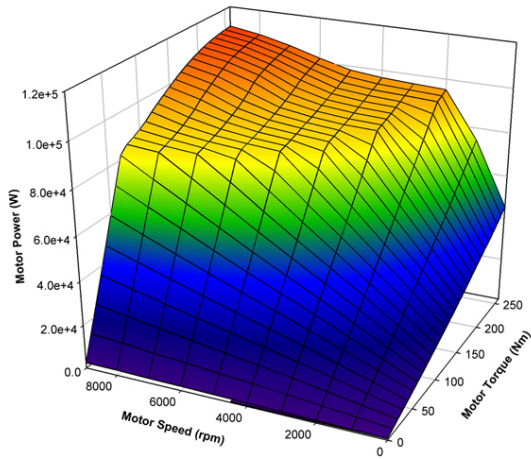
Motor & Inverter Drive Power Consumption ($V_{DC}=250V$)



Motor & Inverter Drive Power Consumption ($V_{DC}=300V$)



Motor & Inverter Drive Power Consumption ($V_{DC}=350V$)



Motor & Inverter Drive Power Consumption ($V_{DC}=400V$)

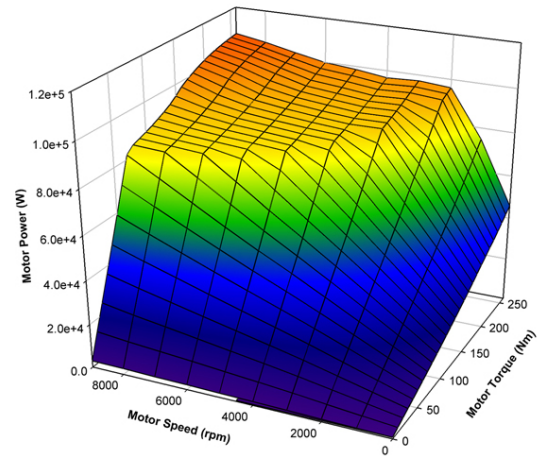


Figure 5.9 - Total Motor Power Consumption at all Operating Points and DC-Link Voltages

5.5 Transmission

The gearbox used in all simulations is a fixed ratio transmission of 1:9.81. With a maximum permissible motor torque, T_{MOTOR} , of 260Nm and maximum motor speed, N_{MOTOR} , of 10,000rpm the gearbox reduces the speed and increases the torque such that:

$$T_{\text{DRIVE}[\text{MAX}]} = 2550.60 \text{ Nm}$$

$$N_{\text{DRIVE}[\text{MAX}]} = 1019.37 \text{ rpm}$$

Equation 5.21 - Maximum Drive Speed & Torque

As mentioned in 5.4.5, it is important to note that the maximum speed of the vehicle needs to be carefully monitored to prevent damaging the motor by over speeding. Since the radius of the tyre is 0.358m (15”) and the maximum permissible speed of the motor is 10,000rpm (1047.2 rad/s) the maximum speed of the vehicle can be calculated.

$$v_{\text{MAX}} = 2\pi \cdot r_{\text{WHEEL}} \left(\frac{\text{rpm}_{\text{MAX}}}{60} \right)$$

$$v_{\text{MAX}} = 38.21 \text{ ms}^{-1}$$

$$v_{\text{MAX}} = 137.56 \text{ kph}$$

Equation 5.22 - Maximum Vehicle Speed

Under certain downhill road conditions this top speed could be exceeded, therefore the vehicle speed is monitored constantly and the maximum speed enforced by the control system which will actuate the vehicle brakes if necessary to protect the motor from over speeding. The efficiency of the transmission is considered as a fixed efficiency of 0.97.

5.6 Direct Hydrogen PEM Fuel Cell

The fuel cell model used in this study is based on empirical data from a production model 75kW (net power) direct hydrogen polymer exchange membrane fuel cell (PEMFC). Fully modelling the system would require a postgraduate level education in chemical engineering, so in order to abstract the system whilst retaining a sufficient level of accuracy and validity in the model a variety of look up tables are used to characterise the operation of the fuel cell system. These tables are based on empirical data derived from lab testing of the actual fuel cell system.

The fuel cell system consists of three key components:

1. PEMFC Stack
2. Compressed H₂ 70MPa Storage Tank
3. Reactant Management System & Air Compressor

In the actual system varying the rate of flow of reactants into the cell changes the electrical output of the cell. Air is fed into the system by a turbo compressor and the hydrogen by an electrically controlled and actuated valve system. The main purpose of the model is to treat the fuel cell as a voltage source and calculate the fuel cell output voltage and hydrogen gas consumption rate for any given instantaneous current load. Unlike the power electronic systems in the simulation model, the response time of the fuel cell to a change in the flow of these reactants does not last less than one simulation cycle and so the model takes into account the transient response of the system. The losses in the fuel cell are also modelled so as to calculate the overall efficiency of the fuel cell stack system.

From a current demand value, $I_{FC[DEMAND]}$, the model is used to calculate the following outputs:

1. Gas Flow Rate \dot{m}_{FC} / H₂ Fuel Consumption
2. Output Voltage, V_{FC}
3. Output Current, I_{FC}
4. Net Electrical Output Power, P_{FC}
5. Gross Stack Power, P_{STACK}
6. Efficiency, η_{FC}

Figure 5.10 shows how an overview of how the fuel cell system was implemented in MATLAB Simulink.

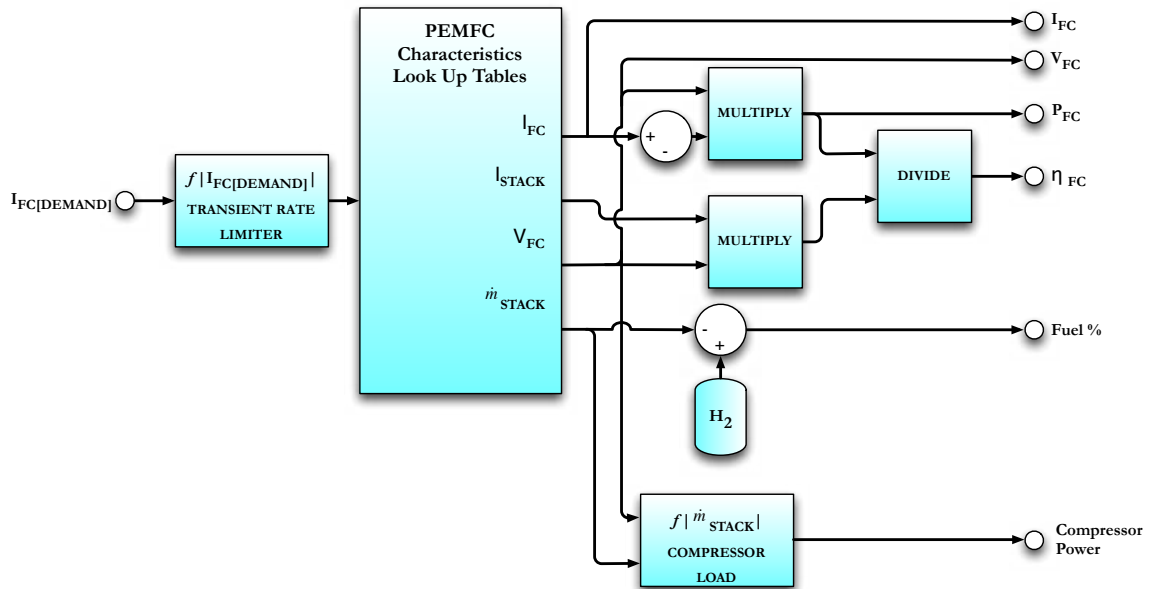


Figure 5.10 - Fuel Cell System Model Overview

5.6.1 Fuel Storage

The fuel tank is modelled as an ideal representation of a 5kg 70MPa 4th generation carbon fibre composite compressed hydrogen tank [209, 210]. Although in reality these tanks are very complex systems in themselves and none have yet completely eliminated hydrogen wastage through leaking, the affects of gas leakage over time were not considered in the simulation, as the affect on fuel used is only detrimental when the vehicles performance is assessed over a period of days.

5.6.2 Stack Losses & Stack IV Characteristic

The relationship between the stack voltage and the current is not entirely linear. There are three dominant methods of loss in the fuel cell stack that affect cell potential under load, a) Activation losses, b) Ohmic losses and c) Mass transport losses.

Activation losses occur because of the force required to initiate the reaction, forcing hydrogen to split on the catalyst, forcing protons through the membrane to combine with oxygen and cause electrons to flow in the external circuit. They account for the initial rapid drop in cell potential. Ohmic losses in a fuel cell are no different to Ohmic losses in any other electrical circuit and occur due to the resistance of the electrode plates in the cell, the

potential loss is proportional to the current density and as such the IV characteristic is linear during this area of operation. Mass transport losses occur when the reactant concentration at the reaction surface reduces due to the reactants being consumed faster than the fuel delivery system can supply them. The stack efficiency drops sharply at this point and cell temperature can also increase so the stack is not normally operated in this region. These three loss regions are highlighted in Figure 5.11.

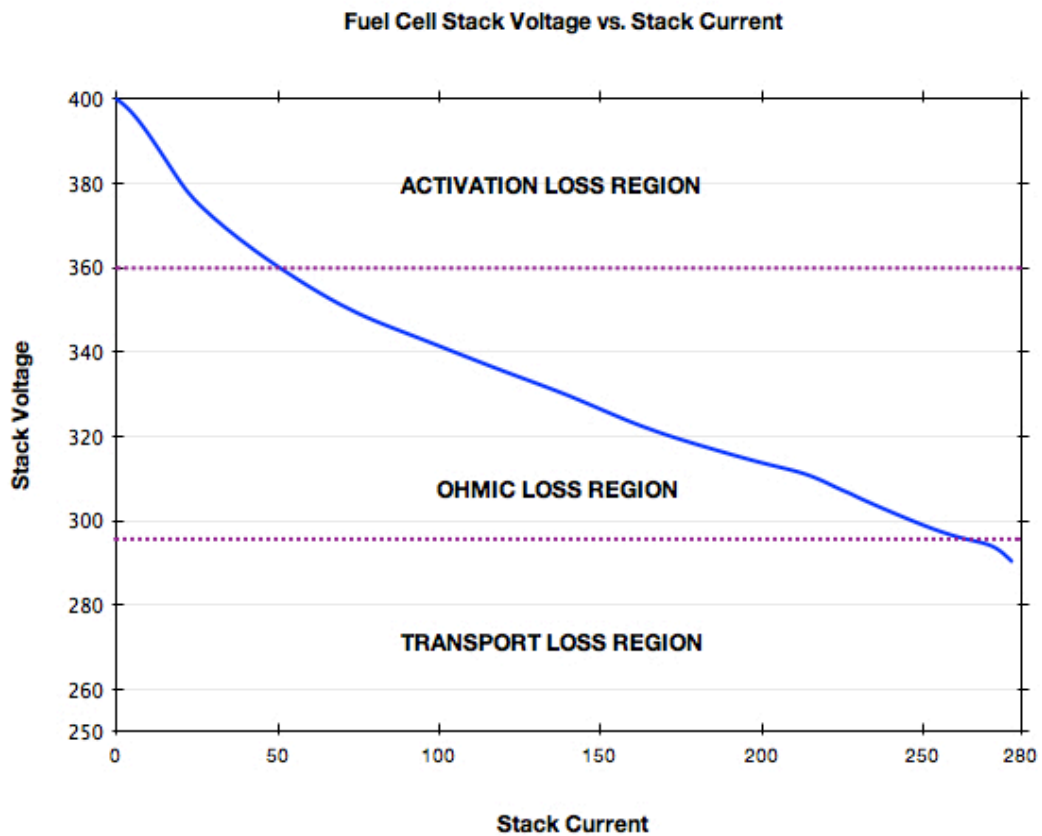


Figure 5.11 - Fuel Cell Stack Loss Regions

Together these losses are represented in the model as parasitic losses within the fuel cell stack. For a given electrical output current the manufacturer measured this parasitic loss and the information was entered into a lookup table in the model. The sum of the output current and parasitic current represents is the total stack current for that operating point. The system current is the electrical output current supplied to the vehicle and its relationship to the stack voltage is shown in the systems IV characteristic graph in Figure 5.12.

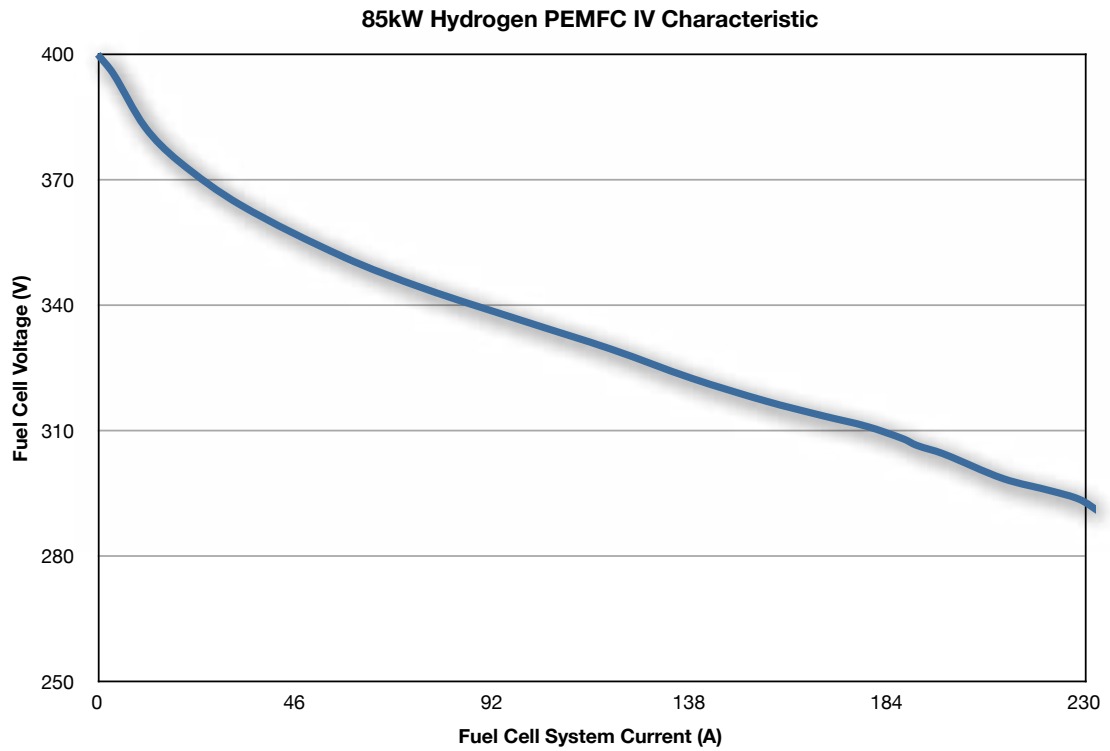


Figure 5.12 - Fuel Cell System IV Characteristic

5.6.3 Transient Response

The response of a fuel cell to a step change in demand is inherently non-linear however due to the lack of available data or mathematical functions to describe the response, reproducing it analytically is impossible. In common with most similar studies the fuel cell transient response rate has been simulated as a linear response. Typically the time taken to change from 10% to 90% is around 1-2s [91, 211]. This was easily implemented using a rate of change limiting function and it transpired the net power output during the response using this approximation is not dramatically different to the actual responses described in the literature, the main difference is the shape of the response for V_{FC} and I_{FC} . Since the interest of this study was power, modelling the exact response of the fuel cell to transient demand was deemed unnecessary.

The rate limiter block in Simulink is such that the limit of rate of change R , can be defined as:

$$R = \frac{y_{(i)} - y_{(i-1)}}{\Delta t}$$

Equation 5.23 - Fuel Cell Transient Response Limit Factor

In this simulation the transient response to a step demand of 10% of rated current to 23A. 90% of rated current (23A - 207A) is 2s and is shown in Figure 5.13.

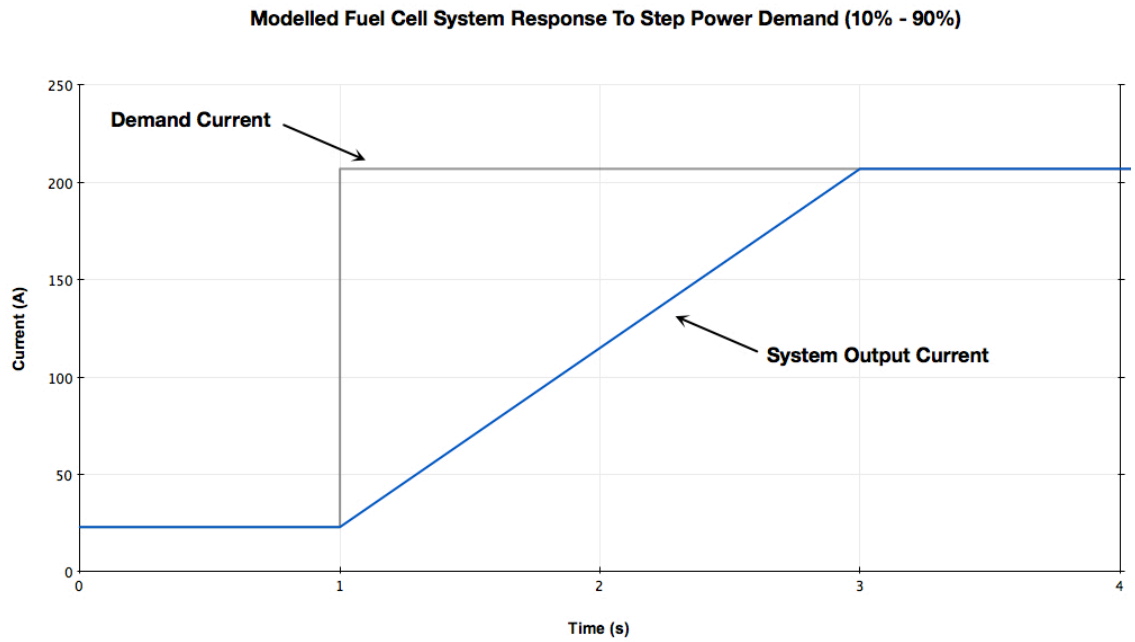


Figure 5.13 - Fuel Cell System Output Current Step Response

5.6.4 System Losses & Efficiency

Figure 5.14 shows how the efficiency of the fuel cell system varies across the rated system output power range.

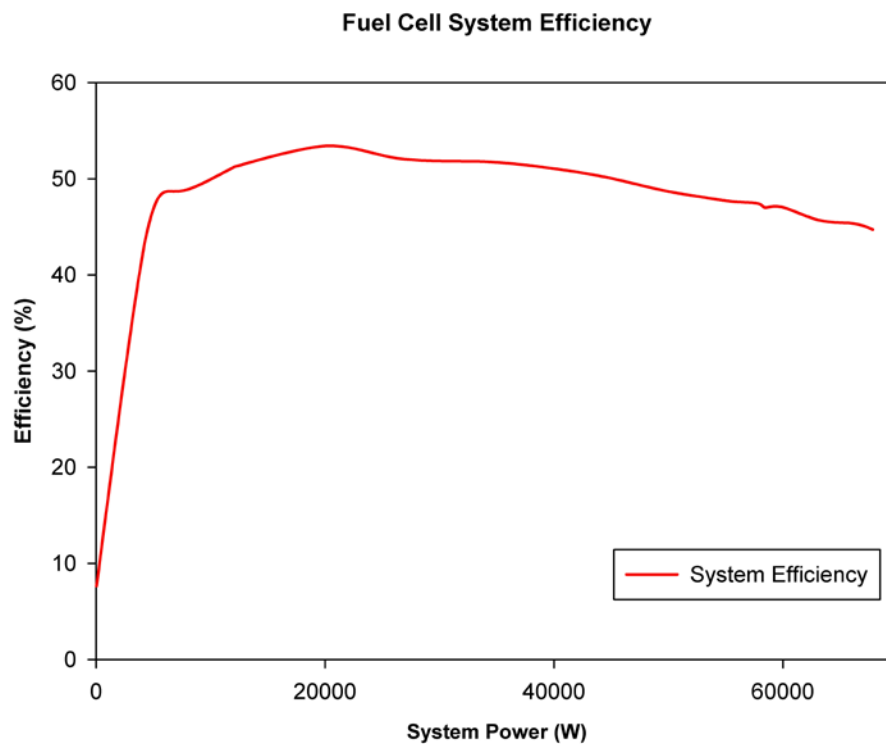


Figure 5.14 - Fuel Cell System Efficiency

The dominant source of loss at the low end of the power range is the auxiliary load of the fuel cell system that maintain the operation of the fuel cell once it is started. The auxiliary load comprises a) turbo compressor, b) reactant humidification system, c) hydrogen flow control valve and d) fuel cell heating/cooling system. Together with the fuel cell stack and hydrogen tank these components make up the complete fuel cell system, sometimes referred to in the press and literature as the fuel cell engine and shown earlier in Figure 3.4.

Current limitations in materials technology limit the lifespan of the fuel cell stack. One key limitation is the finite number of times the fuel cell stack can be started up and shut down. For current fuel cells this is in the order of 4000 start-up and shutdown cycles and so once the system has been started on a journey it must remain on. The stack cannot be shut down during the journey like an ICE can be turned on and off in a stop-start mild hybrid. The fuel cell stack also takes considerably longer to start than an ICE, typically around a minute though the exact time varies with ambient temperature e.g. in cold conditions the stack must be warmed before the fuel cell can be started to prevent damage to the membrane from frozen water vapour that was not completely purged from the stack at the end of the last operating period.

The auxiliary load is therefore an additional parasitic load on the fuel cell system and present for the entire duration of operation and is modelled as such. The main source of loss within this auxiliary load is the air compressor [91, 193]. To provide the volume of air sufficient to sustain the reaction rate required ambient air must be pressurised and fed into the stack. This can be done with a blower or turbo compressor however as previously discussed using a turbo compressor results in a significantly higher power density in the cell. Most automotive fuel cell systems require the maximum possible power density for a given system volume and all employ turbo compressors to pressurise the air supply.

Humidification is one of the key control processes in the fuel cell system. If the membrane is allowed to become too dry the reaction rate decreases and the cell internal resistance increases, decrease the efficiency of the reaction. Hot spots can also occur on the membrane that can ultimately cause it to break down and degenerate. If there is too much water in the cell it can block the gas channels and slow down the reaction, again decreasing the efficiency of the stack [212, 213]. The reactant humidification system therefore carries out three processes key to ensure the efficient and safe operation of the stack a) Humidification of the reactants to prevent the membranes drying out b) Heating of the

reactants to ensure the stack operates at an optimum temperature c) Removal of waste heat and water vapour from exhaust gases.

The integration of the turbo compressor and humidifier into the reactant delivery system is shown below in Figure 5.15. The hydrogen control valve is presumed to be ideal and can deliver the exact flow rate of gas required in an ideal laminar flow upon demand.

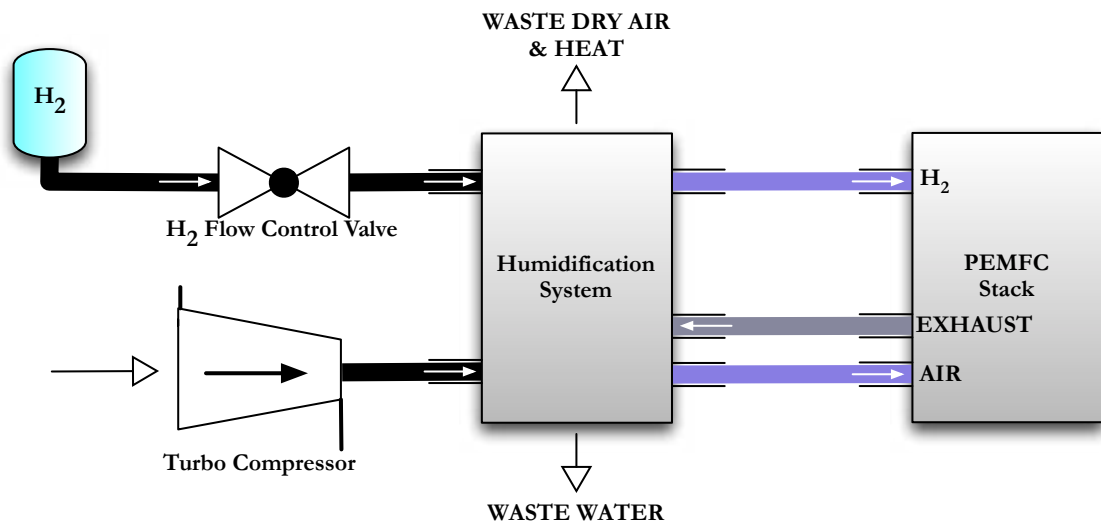


Figure 5.15 - Fuel Cell Reactant Delivery System

Some studies model the turbo compressor loss as a fixed value, Ogburn et al, for instance measured a power loss to the system of 3.65kW at full load and to reduce the simulation complexity used this value for the entire range of stack loads[193]. The turbo compressor however requires careful consideration. The stoichiometric ratio of air to hydrogen is not constant throughout the full range of operation and therefore the amount of air the compressor supplies in the real system changes. Since the turbo compressor is the dominant source of loss in the fuel cell system auxiliary load ensuring that the losses associated with it are represented accurately is vital. Otherwise if a fixed value of full compressor load power is used the losses may be far higher or lower at any given point than they are in reality, devaluing the fuel cell model and compromising the whole analysis.

The power consumed by the turbo compressor can be related to the gas flow rate of the system, which in turn can be related to the system current demand. The power map of the auxiliary load related to system demand current was obtained from the manufacturer and the electrical power consumed by the auxiliary systems relative to the fuel cell output power is shown in Figure 5.16. The power at low loads is dominated by the very low efficiency of the turbo compressor at low mass flow rates [214].

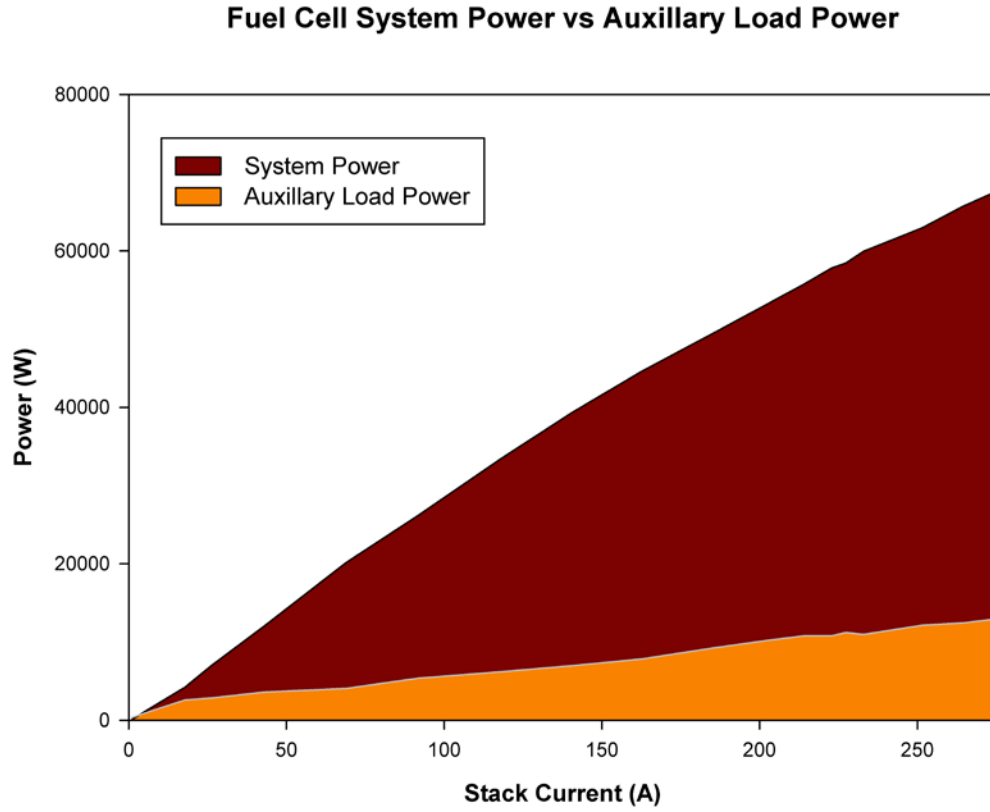


Figure 5.16 - Fuel Cell System Output Power vs. Auxillary Load Power Loss

The final characteristic determined by the fuel cell model is the mass flow rate of oxygen and hydrogen in the cell. The rate of oxygen then determines the mass flow rate of air that the turbo compressor must supply to the stack. The manufacturer measured the mass flow rates across the full range of system demand currents (as shown in Figure 5.17) and a linear constant derived for each to relate the flow of gases to the system current:

$$\dot{m}_{Hydrogen} = K_{Hydrogen} I_{FC}$$

$$\dot{m}_{Air} = \left(K_{Oxygen} I_{FC} \right)^{100/21}$$

Equation 5.24 - Reactant Mass Flow Rates

Where:

$\dot{m}_{Hydrogen}$ = Mass flow rate of hydrogen gas in kg/h

\dot{m}_{Air} = Mass flow rate of atmospheric air in kg/h

$K_{Hydrogen}$ = Hydrogen flow rate constant

K_{Oxygen} = Oxygen flow rate constant

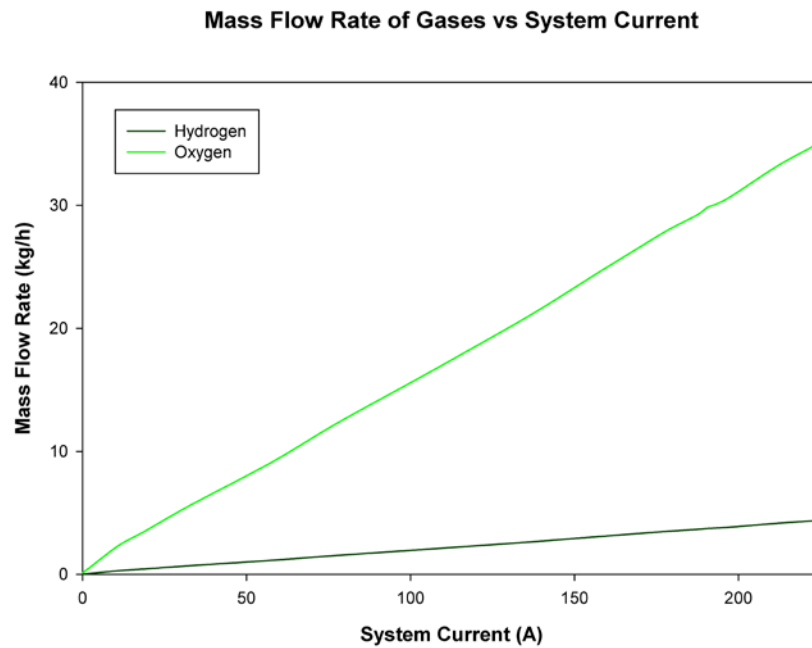


Figure 5.17 - Gas Mass Flow Rate vs System Current

Using the hydrogen flow rate and the lower heating value of hydrogen it is possible to calculate the total power consumed by the hydrogen stack. The relationship of the stack efficiency to the overall fuel cell system efficiency can therefore be calculated. Figure 5.16 showed how large a fraction of system power the auxiliary power demand was at low load. However the resulting efficiency penalty is more dramatically illustrated below in Figure 5.18.

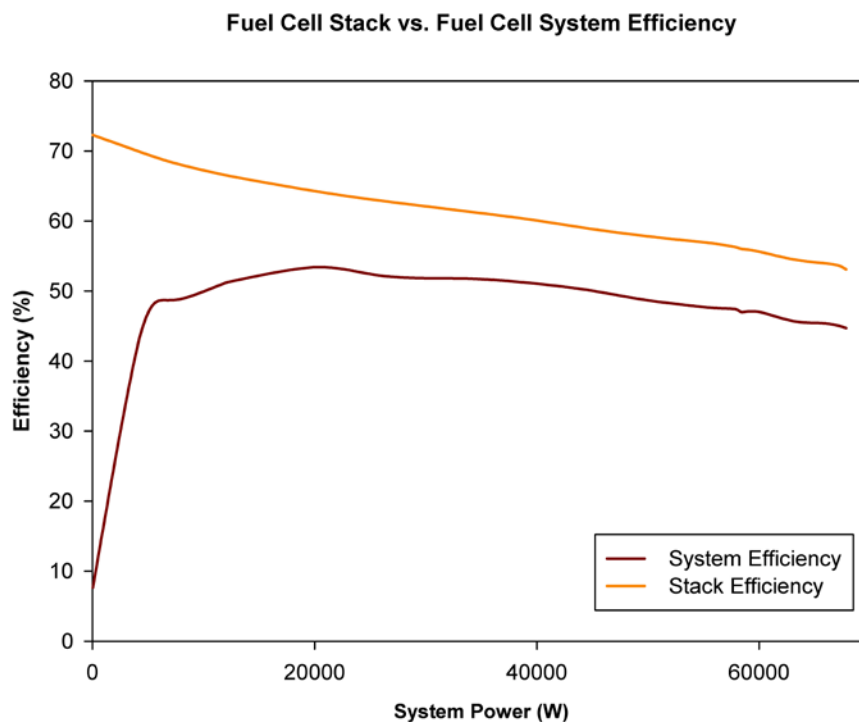


Figure 5.18 - Stack vs. System Efficiency of PEMFC System

5.6.5 Fuel Cell System Assumptions & Limitations

Several assumptions are made in the model of the fuel cell system:

1. All gases behave ideally and are distributed uniformly through the whole fuel cell stack.
2. No poisoning of the membranes by contaminated reactants occurs.
3. The reactants and cell membranes are kept at a constant humidity by the humidification system that is represented by a constant electrical load on the system.
4. Temperature variations across the stack are neglected and the temperature of the stack is constant at the value that the empirical data was measured at.
5. The stack cooling system maintains the stack at this temperature throughout the simulation.
6. Cold start of the fuel cell is not considered beyond ensuring the battery pack is designed and sufficiently rated so that it could power both the fuel cell system and the vehicle during this phase.
7. The vehicle is freshly fuelled to 100% of the tank capacity at the start of each simulation. The effects of fuel leaking from the cylinder are not considered, as the leak rate during the period of any of the cycles is inconsequential [155].
8. No losses are incurred from purging the fuel system at the end of the simulation. The amount of hydrogen lost would depend on the volumetric capacity of the system, which isn't known and in any case the amount lost is thought to be insignificant and would be the same for each driving cycle and each different topology so the validity of the relative performance comparison between the systems is not impacted.
9. Oxygen constitutes 21% of atmospheric air.

5.7 Battery Pack

The battery pack provides the vehicle with an energy storage system (ESS). The ESS has three functions in a H₂FCHEV:

1. Power the vehicle during start-up and shutdown of the fuel cell system.
2. To capture and store energy recovered by regenerative braking.
3. To meet the fuel cell output power shortfall relative to demand during transient periods of demand.

The ESS also provides a backup power system in the event of the fuel cell system failing. With careful management and limitation on vehicle power even a battery pack designed largely for handling transient power peaks can provide a few km of all electric driving to get the vehicle and passengers to help and/or their destination. This can potentially be seen as an advantage over ICEVs and is used in marketing current PHEVs.

5.7.1 Requirements & Sizing

There are several criteria that dictate the sizing of the ESS. The most important are a) that it is sized so that it can provide sufficient power to operate the vehicle b) that its operation is transparent to the driver in c) it is rated such that its output voltage matches the fuel cell relatively closely and maintains efficient voltage ratios across the DC-DC converters and c) it is sufficiently small and light enough to package into the vehicle without adversely impacting on the vehicles performance. Given those criteria, the sizing was then largely dictated by the battery technology chosen.

5.7.2 Battery Technology

From the requirements it is clear that the battery pack had to be capable of meeting high transient power demands, potentially for sustained periods whilst the application also demanded the battery pack to be as low weight as possible, therefore a battery pack with a high power and energy density was needed. There were four possible battery technologies available to use in the battery pack.

1. Lead Acid
2. Nickel Cadmium (NiCd)

3. Nickel Metal Hydride (NiMH)
4. Lithium Ion

Lead acid batteries have been used as the starting battery in internal combustion engine vehicles for decades and are also used to recapture energy in mild-hybrids. However they are very heavy and intolerant to deep discharging. The energy density is $\sim 35\text{Wh/kg}$.

Nickel cadmium batteries have a higher energy density than lead acid and can be deep discharged. However they contain toxic materials and can develop a 'memory effect' after incomplete charge or discharge cycles that can effectively reduce the capacity of the battery whilst it is installed in a system. Given the likely usage of transient power demand followed by recharging during periods of surplus power and regenerative braking the memory effect makes NiCd impractical in this application. The energy density is $\sim 50\text{Wh/kg}$.

Nickel metal hydride batteries have been used in many current and past electric vehicles. They are not susceptible to the memory effect that Nickel Cadmium batteries are and can withstand repeated incomplete charge and discharge cycles. The energy density is 70Wh/kg .

Lithium batteries of varying compositions such as Lithium Ion, Lithium Iron, Lithium Cobalt, are a relatively new, high performance battery technology. They have double the energy density of NiMH but can provide very high output power levels for short periods of time. They operate across a wide temperature range from -20°C to 60°C and are capable of being recharged in a few hours [215]. They are the battery of choice in mobile devices such as laptops, cell phones and tablet computers. There are however several drawbacks to using Lithium batteries. The types of batteries used in EV applications are still a developing and new technology and are comparatively expensive compared to NiMH. The battery chemistry dictates careful and complex monitoring and control during operation to protect the cell. Due to the organic electrolyte used in the cell, if pushed beyond its safe operating limits the cell can explode, catch fire and leak toxic gas. The control used in the battery pack must a) ensure charge balance between cells in any battery pack b) ensure that high discharge rates are not sustained for long periods, c) that periods of high discharge are not repeated within a certain timeframe to allow the battery to maintain a safe thermal operating point, d) that the charge current is controlled to the manufacturers specification and e) the cell voltage is not allowed to drop below specified limits. The lifespan of Lithium ion cells is also currently not as long as other battery technologies but they can

provide an adequate operating life with careful management. The energy density of a typical lithium battery is 150Wh/kg.

Although high cost and high complexity, the energy density of Lithium ion batteries makes them the obvious choice for use in the battery pack in this study. Since most of the problems belong to the physical implementation of the technology, a simulation using a Lithium ion based battery system would only be complicated by some extra control algorithm overheads to replicate these physical restraints. It also seems reasonable to assume that in due course as the applications for the technology become wider and the technology improves, that the cost and control complexity will decrease and the lifespan of the cells will increase. Already, the now widespread usage of Lithium ion batteries in portable computers and mobile phones has seen the price drop quite substantially in the past few years.

5.7.3 Lithium Ion Cell Characteristics

Kokam SLPB75106100 lithium ion polymer cells were chosen to construct the battery pack. The cell specifications are summarised below in Table 5.2 and the cell IV characteristic is illustrated in Figure 5.19 [124]. The C rate is an expression of the rate of discharge related to the 1-hour capacity of the battery. For example, discharging a battery rated 10Ah at a rate of 10A would be a discharge rate of 1C. Discharging at 50A would be 5C.

Characteristic	Value
<i>Cell Voltage (Nominal)</i>	3.7V
<i>Rated Capacity</i>	8.0Ah
<i>1C Rate</i>	7.5A
<i>Maximum Discharge Rate (Constant)</i>	37.5A (5C)
<i>Maximum Discharge Rate (Pulse)</i>	60A (8C)
<i>Charge Current & Voltage</i>	8A @ 4.2V
<i>Cell Cut-off Voltage</i>	2.7V
<i>Operating Temperature</i>	Charge: 0°C - 45°C Discharge: -20°C - 60°C
<i>Weight</i>	150g
<i>Dimensions</i>	Length: 103mm Width: 107mm Thickness: 7.9mm

Table 5.2 - Kokam SLPB75106100 Lithium Ion Polymer Cell Specification

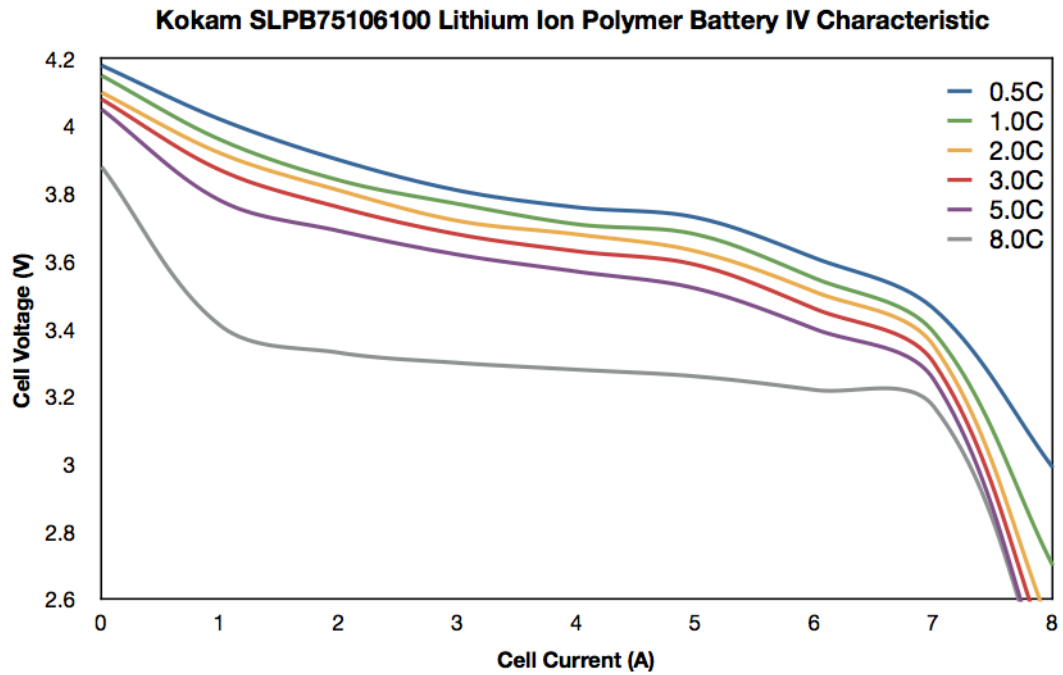


Figure 5.19 - Kokam SLPB75106100 Cell IV Characteristic

Kokam cells were chosen due to their established use in several electric and hybrid electric vehicles, relatively high capacity of the cells compared to the rest of the market but also significantly on the wide range of characteristic data available for their products. A123 Systems, Panasonic, Saft, Altairnano and Yuasa all also manufacture lithium batteries for electric vehicles. Some manufacturer cells with equivalent specifications to the Kokam cells but none of those that do provided anything beyond basic specifications that were not sufficient to characterise the cells and generate the simulation model. Attempts to obtain the data from several of these manufacturers were unsuccessful.

5.7.4 Battery Pack Design

The sizing of the battery pack can be determined by two main factors, the size and the electrical output characteristics. During a large step change in the fuel cell system current, the battery pack could be expected to meet nearly 2/3 of the motors rated power (50kW) during the period whilst the fuel cell responds. Yet under sedate driving conditions where the transient demand rate does not exceed the fuel cells response rate the battery pack may be barely utilised at all and act as nothing more than a dead weight in the vehicle. This poses a design problem but also reinforces the choice of lithium ion for the battery pack as it can provide the currently highest available energy density and also provide relatively large output power for short periods of time by burst discharging.

The DC-DC converters in the drive train are most efficient when operating at close input to output voltage ratios. The battery pack size in drive trains found in the literature was around 50kg, allowing 5% for mechanical and electronic overheads this left 45kg available for battery cells. At 150g per cell this allows for 300 battery cells. The most suitable configuration of the available cells was found to be 100 series sets of 3 cells in parallel.

The overall battery pack design is illustrated in Figure 5.20. The charge balancers ensure an equal charge in each cell and the battery management system ensures the battery is operated within safe boundaries of operation.

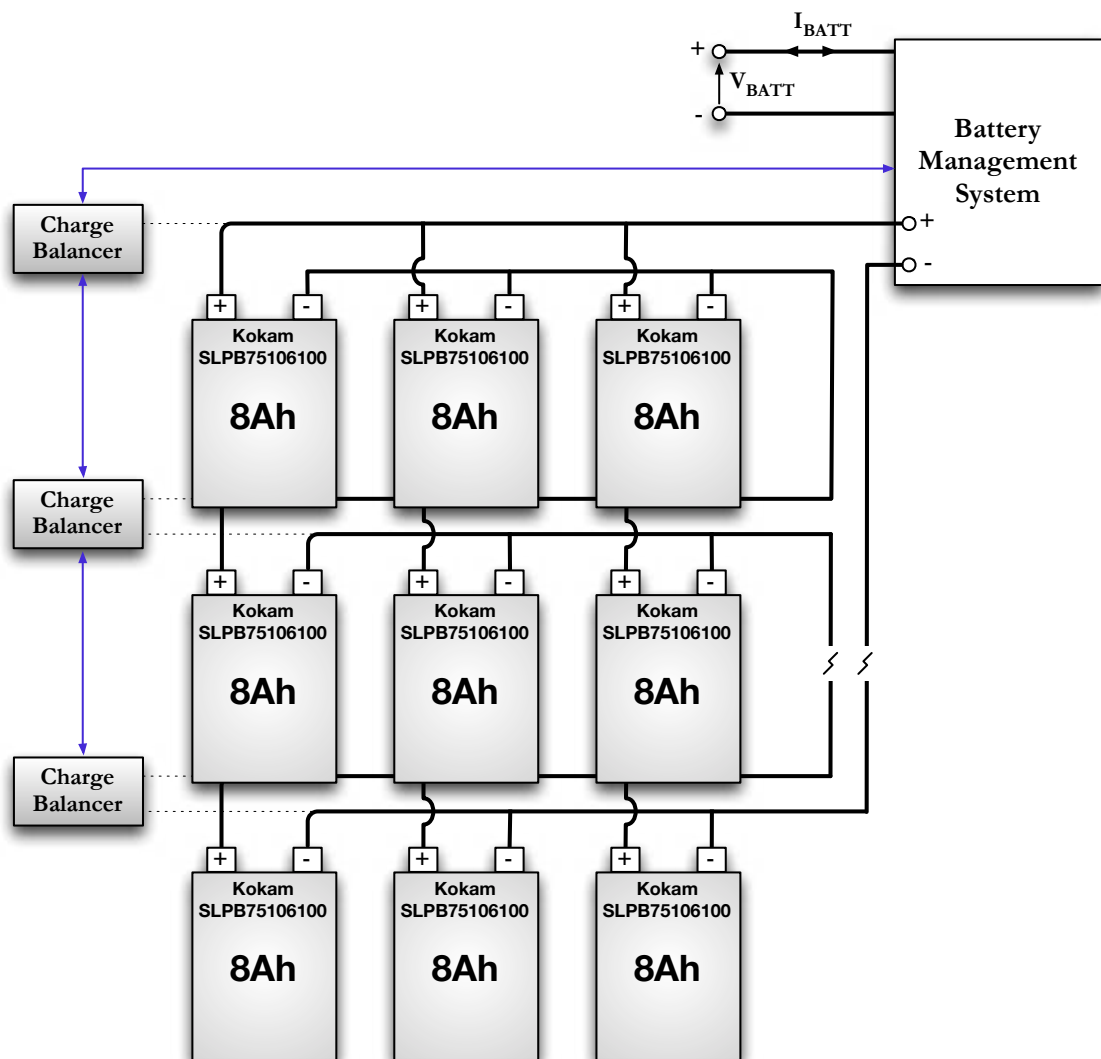


Figure 5.20 - Battery Pack Design

This configuration results in the battery system described below in Table 5.34. The VI characteristic of the completed battery system is shown in the rated capacity is quoted for the different C rates that the battery can support in continuous operation. Taking 0.5C as the nominal operating point for the system extends both battery lifespan and capacity.

Characteristic	Value
<i>Number of Cells</i>	300
<i>Cell Weight</i>	45kg
<i>Voltage, Nominal</i>	370V
<i>Voltage, Maximum</i>	420V
<i>Voltage, Minimum</i>	270V
<i>Rated Capacity, 0.5C</i>	11.25Ah ¹
<i>Rated Capacity, 1.0C</i>	22.50Ah
<i>Rated Capacity, 5.0C</i>	112.50Ah
<i>Power, Rated²</i>	4.2kWh
<i>Power, Nominal Discharge</i>	4.2kW
<i>Power, Peak Power</i>	48.6kW
<i>Discharge Rate, Continuous (5C)</i>	112.5A
<i>Discharge Rate, Peak (8C)</i>	180.0A
<i>Dimensions (l x w x d)</i>	350mm x 1000mm x 150mm
<i>Volume</i>	0.05m ³
<i>Total System Weight</i>	50kg

Table 5.3 - Battery System Specification

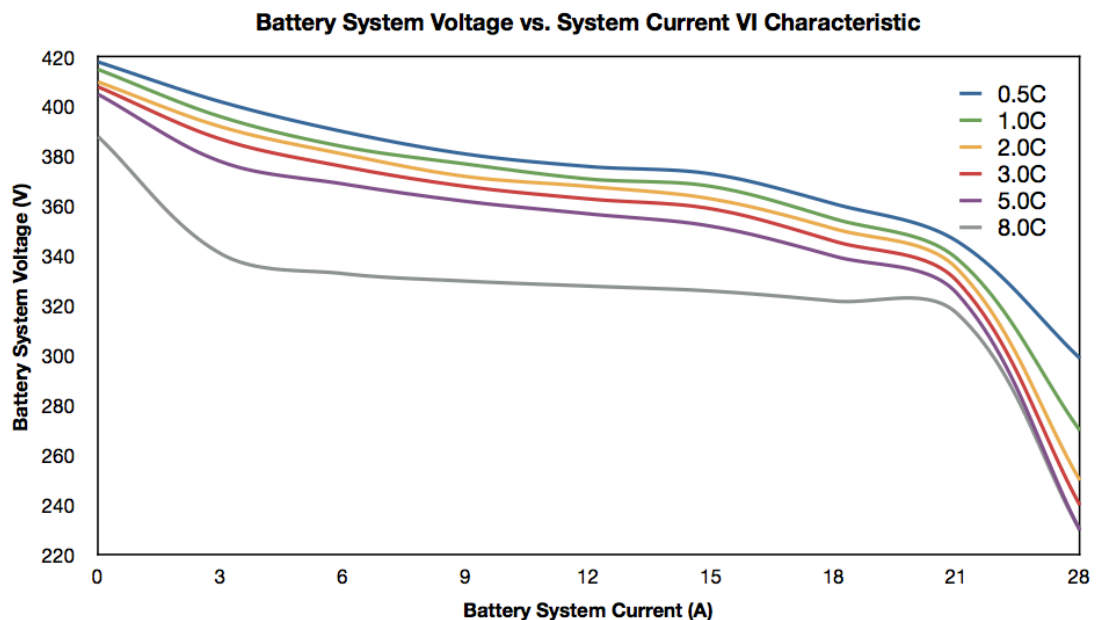


Figure 5.21 - Battery System VI Characteristic

¹ Although cells are rated at 8Ah, discharge rates calculated at 7.5Ah which is maximum current obtainable before cut off voltage is reached under high load.

² Nominal power is based on cell discharge rate of 0.5C

In some respects the battery pack may seem oversized. The fuel cell response time of 2s is five times smaller than the maximum burst duration of the battery cells. It is important to note though that the capacity of the battery is quoted as the total stored energy but as with all lithium battery based systems, the battery pack is only used in a small window of operation to protect the battery and extend its lifespan. In this study the state of charge of the battery is maintained between 60% and 80% at all times. Subject to repeated step changes in power demand the battery could be forced to operate outside of this safe region if sized incorrectly.

5.7.5 Model Operation

Simplistically, the MATLAB Simulink model of the battery pack takes a current demand and produces a system current and voltage output magnitude, efficiency and state of charge value. The pack also takes account of negative input demands as charging currents from the fuel cell or regenerative braking, though regenerative braking is not implemented in the vehicle model. When the battery is tied to the DC bus directly, the fuel cell DC-DC converter is used to charge the battery to ensure it is charged at the correct voltage. Were regenerative braking to be included, a further DC-DC converter would be needed to ensure a regulated charge.

The model has a battery management system (BMS) integrated into it by way of a MATLAB Simulink S Function. The S function controls the demand current to protect the battery from unsafe operating conditions. The system current and voltage can be described thus:

$$\begin{aligned}
 I_{BATT} &= f|I_{DEMAND}| \\
 I_{CELL} &= \frac{I_{BATT}}{3} \\
 V_{BATT} &= f\left|I_{CELL} \frac{I_{CELL}}{I_{1C}}\right| \cdot \left(\frac{N_{CELLS}}{3}\right) \\
 P_{BATT} &= V_{BATT} I_{BATT}
 \end{aligned}$$

Equation 5.25 - Battery System Characterisation

Where:

N_{CELLS} = Number of battery cells in pack (300)

I_{1C} = 1C Discharge Current (7.5A)

I_{CELL} = Current flowing in each battery cell

The non-linear functions $f|I_{DEMAND}|$ and $I_{CELL} \frac{I_{CELL}}{I_{1C}}$ represent a) the BMS and b) lookup table that relates cell current to cell voltage respectively. The BMS takes the current demand from the overall vehicle controller and regulates the output of the battery, it also manages the charging of the battery, its operation is summarised in Figure 5.22.

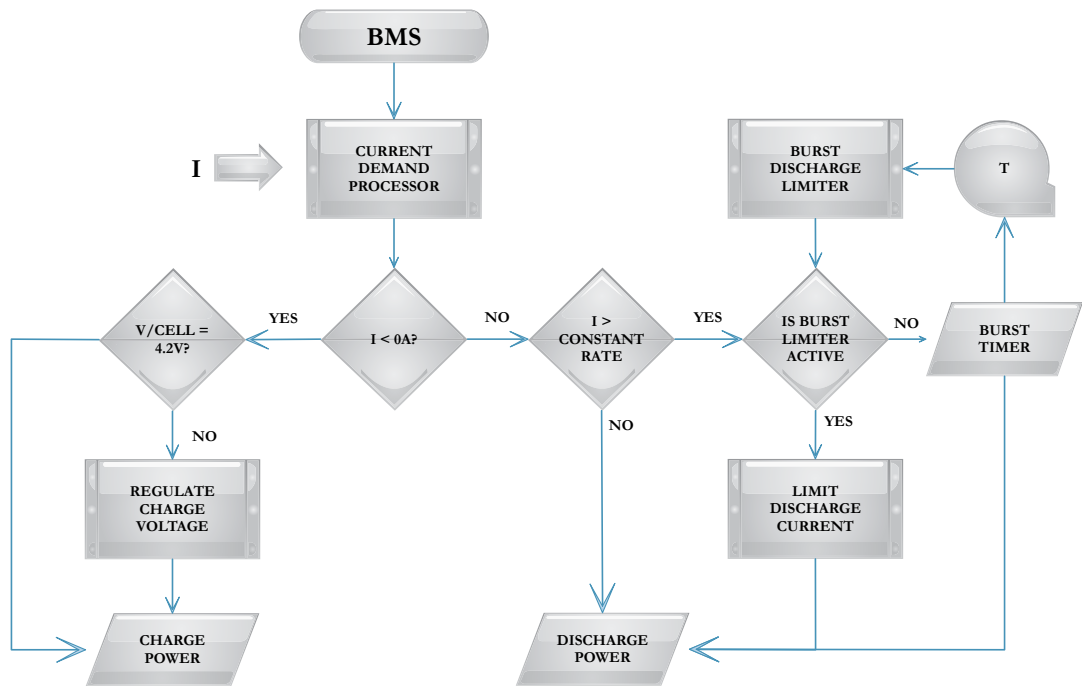


Figure 5.22 – Battery Management System

Each period of pulse discharge must be followed by a period of rest to allow the battery to cool. The maximum length of pulse discharge is 10s and a proportional rest period of up to 20s is enforced between all pulse discharges by the burst limiter [216, 217]. During this period the maximum current any cell can deliver is 0.5C.

Once the battery current is calculated, dividing it by three yields the individual cell current. A two-dimensional lookup table takes this current and the C ratio at that instant and puts the values into a lookup table. The lookup table generates the cell voltage, multiplying this by the number of battery strings in series gives the battery system voltage.

The internal losses are calculated based on the manufacturers data for the internal resistance of each cell, the cell voltage and the current drawn. The efficiency of the battery is then calculated. Figure 5.23 shows the schema of the MATLAB Simulink model for the battery pack.

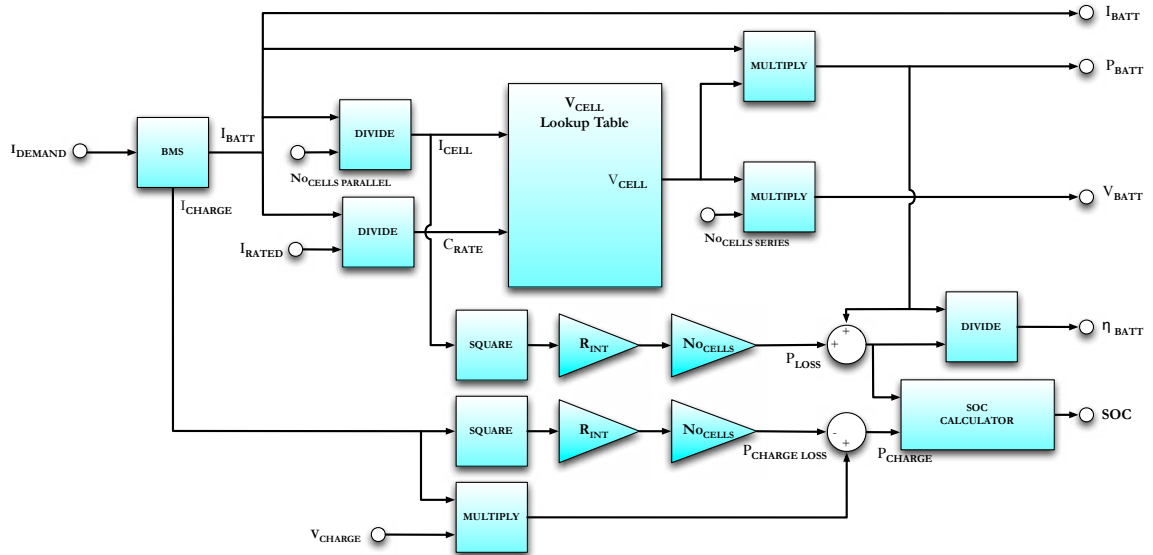


Figure 5.23 - MATLAB Simulink Battery Model Subsystem

5.7.6 State of Charge Calculation

The state of charge of a battery is an indicator of how much charge the battery has left and serves the same purpose as a fuel gauge for the hydrogen tank. It is typically quoted, as a value between 0 & 1 or 0% & 100% where 0 is empty and 1 is full. To calculate the current SOC, the amount of charge used during a simulation step is calculated and then subtracted from the state of charge at the previous simulation step [150].

$$SOC_{[t]} = SOC_{[t-1]} - \frac{P_{BATT} \cdot \Delta t}{3600 \cdot P_{FULL}}$$

Equation 5.26 - SOC Calculation

Where:

$SOC_{[t-1]}$ = SOC at previous simulation step

P_{FULL} = Full charge power of battery pack

P_{BATT} = Power consumed during simulation step

Δt = Simulation step length

This characterisation of SOC is however only truly valid for a constant discharge rate. When the cell is discharged at a variable rate, the batteries nominal capacity must be adjusted as if it were to be discharged at a high rate for long periods, the batteries capacity will be less than quoted by the manufacturer. Peukert's law expresses the capacity of a battery in relation to the rate of discharge. It does not sufficiently describe the remaining capacity of lithium ion batteries, as it does not take into account the temperature of the cell which influences the remaining capacity [218]. However since this study assumes that the battery is held at constant temperature Peukert's law was used to improve the accuracy of the SOC calculation as follows:

$$C_{ACTUAL} = C_{RATED} \left(\frac{C_{RATED}}{I_{AVG} H} \right)^{K_{PC}-1}$$

Equation 5.27 - Peukert Battery Capacity Calculation

Where:

C_{ACTUAL} = Actual capacity (Ah)

C_{RATED} = Rated capacity (Ah)

H = Time capacity rated over (hours)

I_{AVG} = Average Discharge Current (A)

K_{PC} = Peukert Constant (1.02)

The SOC calculation can now be expressed as:

$$SOC_{[t]} = SOC_{[t-1]} - \frac{P_{BATT} \Delta t}{3600 H (C_{ACTUAL} \cdot V_{NOMINAL})}$$

Equation 5.28 - Peukert Modified SOC Calculation

To ensure prolonged battery life and prevent thermal problems the SOC is maintained between 0.6 and 0.8 at all times [53, 54, 134, 219]. It can never exceed 0.8 though if transient power demand is necessary and the SOC is at 0.6 the system controller will allow it to drop further to 0.4.

To ensure efficient charging of the battery the fuel cell will only recharge it when its operating efficiency exceeds 51%. The total fuel cell output power range for this efficiency is 12kW – 40kW. This rule can be breached if the SOC reaches 0.4. If this occurs the controller will then regardless of the fuel cell operating point start to recharge the battery.

5.7.7 Internal Losses

Providing the simulation time step is small enough (<10ms), the losses in the battery cells can be considered to be purely Ohmic and calculated from the data provided by the manufacturer.

$$P_{LOSS} = N_{CELLS} (I_{CELL}^2 R_{INT})$$

Equation 5.29 - Battery Losses

Where:

N_{CELLS} = Number of cells in battery system

R_{INT} = Internal resistance of battery cell

5.7.8 Battery Pack Safety

The safety of lithium batteries has been brought sharply into focus recently by the widely reported problems on the Boeing 787 'Dreamliner'. In 2007, Toyota came to the conclusion that lithium battery technology was not ready for market and it wasn't until 2012 that they first deployed lithium batteries in the Prius PHEV. In 2011 a Chevrolet Volt EV burst into flames while parked. Fires in laptops and mobile phones using lithium batteries have occurred with regularity since they were first introduced to the market around the turn of the century. A shipment of lithium batteries being carried by a UPS Airlines 747 cargo flight was also held responsible for causing the plane to crash and killing both its crew when the batteries caught fire and could not be extinguished with the fire fighting equipment available on board.

The high energy density of lithium batteries means there is much more stored energy in the battery and unlike other battery technologies, lithium batteries use a solid electrolyte that is typically bound with a highly inflammable solvent. If a cell exceeds thermal limitations due to over discharge this solvent can vaporise and ignite, the resulting fire can burn at 2,000°F and the gas is toxic. The degeneration of one cell in a pack will tend to spread to the cells surrounding it and the entire pack can thermally runaway creating a significant fire and the rapid release of stored energy.



Figure 5.24 – Boeing 787 APU Lithium Ion Battery

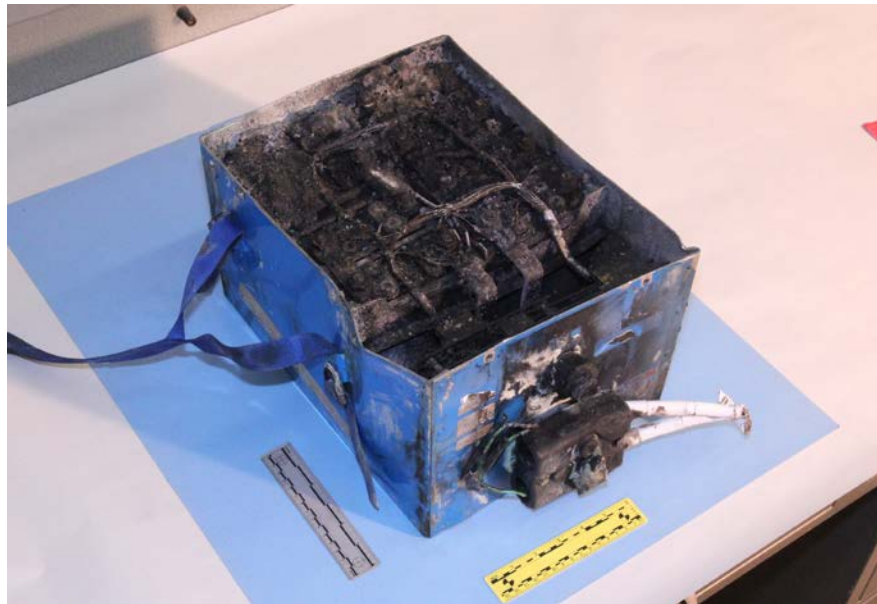


Figure 5.25 - Failed Boeing 787 APU Lithium Ion Battery

Similarly to hydrogen, public perception of the safety of the battery pack in a H₂FCEV will play a large part in market acceptance of the vehicles. Images such as Figure 5.24 and Figure 5.25 can't be ignored and although this study is simulation based, due consideration was given to including the appropriate aspects of protection systems that are designed to prevent thermal runaway of lithium ion batteries in the simulation.

The main three safety precautions are a) control of relative charge between each cell, b) control of the charge and c) control of discharge of the battery. Control these aspects within certain parameters and thermal management of the battery can be achieved. If the

battery is thermally controlled, cell expansion and ultimate degeneration of the electrolyte can be prevented.

Balancing the charge between each cell is necessary because lithium ion batteries, unlike NiMh, NiCd and Lead Acid batteries have no natural charge balancing. If unmonitored, cells in a parallel string can have differing states of charge that over time will deviate from each other. If the state of charge of one of these batteries is such that its cell voltage is below the cut-off voltage, its temperature can start to rise when it is forced to operate below the cut-off voltage because the cells around it give the appearance that the parallel string of batteries has sufficient state of charge to operate safely [220, 221]. There are various methods for balancing the charge between lithium ion batteries and the operation of the charge balancing circuit within this study is assumed to maintain a constant charge amongst all cells in the pack and is not directly simulated. Typical methods of balancing are discussed in detail in [220, 222, 223].

Management of the charge and discharge voltage is also of critical importance. The potential required to breakdown the electrolyte is, alarmingly, within a few tenths of a volt of the maximum cell voltage [220]. Ensuring a correct charge voltage is achieved with control of the DC-DC converter that interfaces the battery to the DC bus, or in cases where the battery is directly connected to the DC bus, the fuel cell DC-DC converter regulates its output to the required voltage. In topologies where the battery is connected to the fuel cell directly, charging is via a small fixed DC-DC converter. To prevent operation below the cut off voltage, the battery is isolated from the system if the terminal voltage drops below the cut off voltage though the state of charge management should prevent this from ever being necessary.

5.7.9 Battery Pack Model Assumptions & Limitations

1. Effects such as transfer reactions and chemical diffusion are be ignored, the small simulation step size means all losses are considered to be purely Ohmic.
2. Each cell is electrically, chemically and physically identical
3. Thermal degeneration of the battery cells from manufacturing contamination with metal that causes internal short circuits is ignored. It is presumed all cells have been manufactured correctly and will perform as specified.
4. Cell balancing operation is assumed to be a background operation that occurs during periods of zero load.

5. The affect of aging on the battery cells is ignored. The physical and chemical properties are assumed constant throughout all simulations.
6. Charge balancing is assumed to operate on an equal number of over charged and undercharged cells. The charge in the overcharged cells is redistributed to the undercharged cells with a sufficient net balance to power the charge balancing circuitry.
7. Temperature rises due to I^2R losses in the battery are cooled by the battery cooling system and the battery is maintained at a constant safe operating temperature. The cooling system acts on all cells equally.

5.7.10 Battery Pack Notes

During the course of this study the battery was changed due to a newer model being available that was both more efficient and had more data available to improve the accuracy of the simulation model. The previous cell, the Kokam DL6750140SP, had a rated capacity of 4Ah and a rated lifespan of 600 cycles. The rated continuous discharge rate was 1C and pulse discharge rate was 10C. Using the newer cell, the Kokam SLPB75106100 [124], rated at 8Ah and 1600 cycles, the number of cells in the battery pack could be reduced by 25% whilst increasing the peak and continuous output power. This allowed the battery to be operated at lower duty ratios, increasing the cell voltage under load and increasing battery capacity for the same battery pack weight. It was also more representative of contemporary battery packs.

5.7.11 BEV Simulation Model

The BEV model used in Topology J, uses the same basic battery pack design and model but instead of 3 cells in parallel, it uses 13. This gives a battery with a nominal rated power of 36kWh, similar to existing EV battery packs.

5.8 DC-DC Converters

Power converters are perhaps the most challenging aspects of electrical engineering in any all-electric vehicle drive train. Whilst fuel cells are still relatively nascent, they have now had many years of sustained development. It is true that technology behind DC-DC power converters is far more established and applied in many more fields and everyday commodity goods than fuel cells are. But the practice of designing and creating the high power converters for H₂FCEVs is still relatively new [224-226].

The DC-DC power converter is necessary to interface the different power sources and sinks in the drive train, all of which have unmatched impedances, VI characteristics and safe operating boundaries and need de-coupling from each other to enable full control of the drive train [227]. As discussed previously boosting the voltage of the DC-DC bus also increases the maximum available motor torque and therefore being able to control the DC-DC bus voltage has performance benefits.

The electrical system in ICEVs is still predominantly 12V negative earth with a lead-acid battery and mechanically driven alternator generating DC current. Though some vehicles are moving to 48V in search of higher efficiency. There is little electrical power technology that is transferrable from current production vehicles to the H₂FCEV. HEV and PHEV share more in common, with the Prius being the only real established vehicle but with the design of its drive train still a closely guarded secret there is little information about how much commonality there will be between them.

Looking at the areas where high power electrical drives are currently used to provide motive power highlights the key difficulty with applying the technology in a vehicle. The London Underground runs at around 600V DC, but has the luxury of large areas of space between the bogeys of the train carriages to install power converters, spaces that are also conveniently cooled by the airflow around the train when it is moving. The fuel cell passenger bus schemes that have successfully been trialled in several countries had large buses with power converters installed on the large available roof space, again well sited to utilise free air-cooling. Whilst the efficiency of the converter is a key parameter in any application, existing large power DC-DC converters and DC-AC motor drives are typically found in large installed or mobile industrial applications where size, weight and to some extent cost are not the primary concerns. In the H₂FCEV a power converter needs to be

small, highly efficient, thermally stable, lightweight and as cost effective as possible. The ripple current drawn from the fuel cell or battery also needs to be low to minimise transient losses. It also needs to be quieter in operation. The high-pitched whine of a power converter during a short journey on a rapid transit system is acceptable and probably beyond the perception and concern of most passengers, people have never known the system without the associated noise. Modern cars, especially at the premium end of the market are remarkably quiet. With the engine and transmission sat behind metal, a firewall and significant amounts of plastic and acoustic insulation drivers and passengers have become accustomed to vehicle interiors that are relatively comfortable environments. To aid adoption electric vehicles will by necessity have to spread the components around the vehicle and the power converters must be designed so that switching noise, noise due to harmonic distortion and heat losses are minimised.

Existing non-automotive fuel cell systems have all had relatively low voltage power buses that matched the output of the stack, for instance $28V_{DC}$ on the Space Shuttle and Apollo spacecraft and large installed residential fuel cell generators use a DC-AC grid connected inverter to interface with the normal electricity supply.

The EV and HEV sector requirement for high power, lightweight, compact, liquid cooled, cost effective and efficient power converters is unique and in large part only possible due to the rapid developments in high power semi-conductors and microprocessor based digital control algorithms. There are several research active threads on the best type of converter to use in the EV application and no real consensus yet on the best approach. The choice of converter topology used in this study is based on reviews of existing research and once again, the availability of data.

5.8.1 DC-DC Power Converter Topology

In its most simplified form, a DC-DC converter takes an unregulated or regulated input voltage and converts it to a regulated output voltage of differing magnitude. The converters are constructed of several key components, switching devices, diodes, inductors, transformers and capacitors. The input and output of converters can be none-isolated or isolated by using a transformer in the circuit though this increases the size, cost and control complexity of the converter. There are none-isolated DC-DC converters designed to reduce the voltage (Buck), increase the voltage (Boost) or both (Buck-Boost, Cuk) in one (uni-directional) or both directions (bi-directional). Isolated converters used a high-

frequency transformer to de-couple the input of the converter from the output. Half-bridge, push-pull, forward and fly-back isolated converters can all be used as bi-directional converters. In none isolated converters the maximum ratio of input to output voltage is around 4:1. In isolated converters the transformer allows very high voltage ratios to be achieved [228].

There are two main methods of controlling DC-DC converters:

1. Hard switched converters.
2. Soft switched converters.

Hard switching involves turning the switching devices on and off at moderate frequency (10kHz - 100kHz) whilst the circuit is carrying current. The high voltage (dV/dt) and current (di/dt) transients cause stress on the switching devices and additional losses beyond the on-state conduction and gate charge losses. EMI is also high and wiring and printed circuit boards must be carefully designed to avoid any stray capacitance and/or inductance causing further losses.

Soft switching switches the converter at instants where the current or voltage is zero. Zero voltage switching (ZVS) or zero current switching (ZCS). Soft switching allows the converter to operate at much higher frequencies (100kHz – 1MHz). Operating at higher frequency is attractive as it reduces the size, cost and weight of the inductive and capacitive components. Smaller inductors result in lower iron losses in the inductor core and lower I^2R conduction losses through the inductor. ZVS or ZCS also reduces the dV/dt or di/dt losses but as the switching frequency increases the conduction losses increase so there is a balance to be found. Accurately controlling and producing a stable output with soft switching is also more challenging than with hard switching.

At the power levels required 80kW peak the range of switching devices that can be used is generally limited to IGBT devices. Power MOSFET transistors do not exist with sufficiently high enough current and voltage ratings to match the capability of IGBT devices though if the voltage level is low enough multiple MOSFET devices can be connected in parallel to achieve the required rating. IGBTs have an upper switching frequency limit of around 100kHz but are usually operated around 25kHz [229]. Hard switching losses and transients can be mitigated with the use of active clamping and snubber circuits [230, 231] and typically the difference in efficiency between hard switched and soft-switched converters is around 1-2% [226].

5.8.2 DC-DC Power Converter Design

The type and design of the DC-DC power converters used in this study was dictated by the power sources and the requirements of fitting the power converter into the vehicle chassis. The maximum difference between the voltages in the system is around 2:1, well within the limits for none isolated converters. The maximum DC bus voltage, $V_{DC\text{ BUS}}$, is 400V and the maximum system current, I_{MAX} , is around 290A, these parameters dictate the use of IGBT switching devices. The topologies chosen were none-isolated half-bridge and full bridge, uni and bi-directional Buck-Boost hard-switched converters shown in Figure 5.27 and Figure 5.27 [232].

The simulation models for both were developed using characterisation data detailed by Hauer et al. in [110, 125, 126, 204], this was by far the most detailed dataset available in the literature and no manufacturers responded to requests for data about commercially available systems. A traditional two-switch Buck-Boost converter could be used but has the drawback that when V_2 is the input and V_1 is the output the voltage is negative with respect to ground. Using a four switch full bridge enables the voltage to be positive regardless of which side is the input

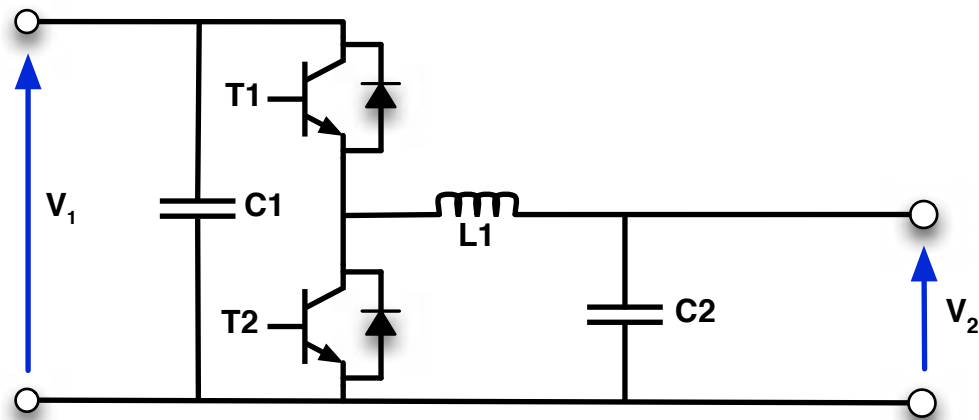


Figure 5.26 - Uni-Directional DC-DC Converter

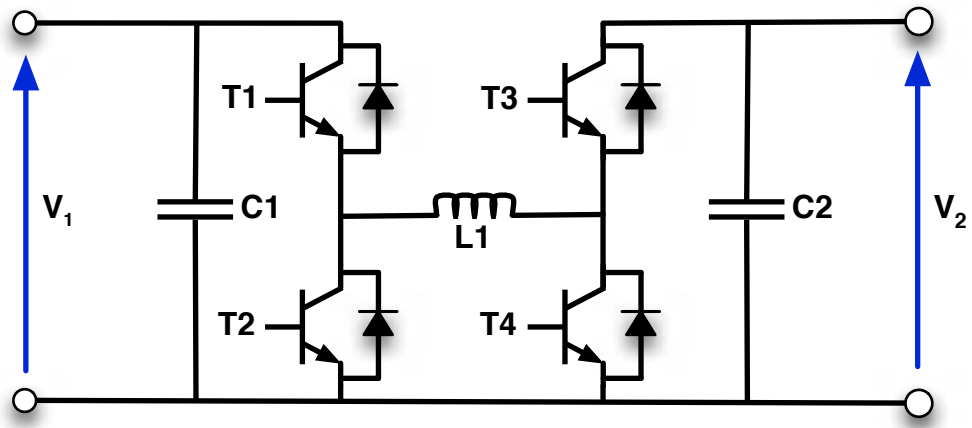


Figure 5.27 - Bi-Directional DC-DC Converter

One issue highlighted in some studies regarding none-isolated DC-DC converters is safety. They cite that the transformer decouples the input from the output and offers a degree of protection in the event of component failure whereas the none-isolated converter provides none. Given the additional losses, devices, cost and weight associated with the extra switching devices and transformer of an isolated component there is a much simpler solution to achieve an equal or better degree of protection. To control the DC-DC converters and the DC-AC inverter drive of the motor, current-sensing devices will be connected to microprocessors. Detecting fault currents and short circuits and then using control signals to open relays or activate crowbar circuitry to blow fuses and isolate the power sources is a much simpler solution all round. There are very minimal losses associated with both approaches and they achieve complete electrical isolation, not just the galvanic isolation offered by a transformer.

5.8.3 DC-DC Power Converter Model Construction

As previously highlighted, MATLAB Simulink does not have the ability to accurately model the discrete operation of the DC-DC converters, nor was any information able to accurately describe the power converters mathematically and allow an analytical approach to simulation. Given the scale of the complete vehicle model there were concerns regarding the availability of computational resources that may in any event have made analytical simulation impossible. Using the data from Hauer et al [204], models of the converters were constructed using the empirical data to create a two dimensional look up table to determine efficiency of the DC-DC converter for a given operating point through different ratios of V_{IN} to V_{OUT} .

Knowing the input voltage, output voltage and current flowing into the converter, the efficiency is determined from the lookup table and the power output, power loss and output current calculated.

$$\eta_{DC-DC} = f \left[\frac{V_{OUT}}{V_{IN}}, P_{DC-DC} \right]$$

Equation 5.30 - DC-DC Converter Efficiency Calculation

Having calculated the efficiency of the converter for a given operating point, calculating its output power is performed with simple arithmetic.

$$P_{OUT} = \eta_{DC-DC} (V_{IN} I_{IN})$$

Equation 5.31 - DC-DC Converter Power Output

A high level overview of the simulation model is shown in Figure 5.28 and visualisations of the datasets used for the look-up table are shown in Figure 5.29 for the unidirectional converter and Figure 5.30 for the bidirectional converter.

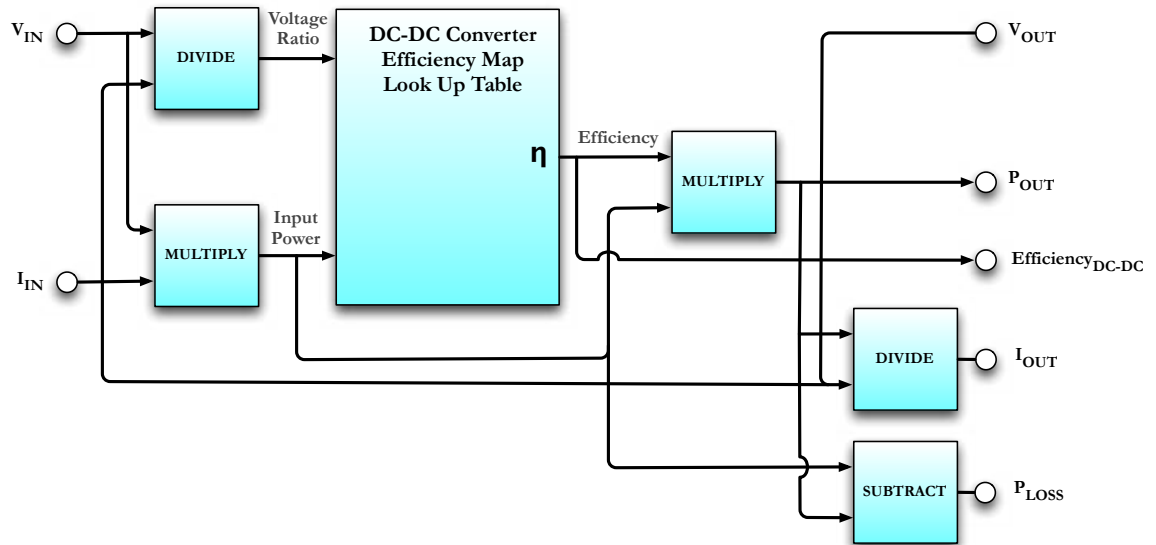


Figure 5.28 - DC-DC Converter Simulation Model

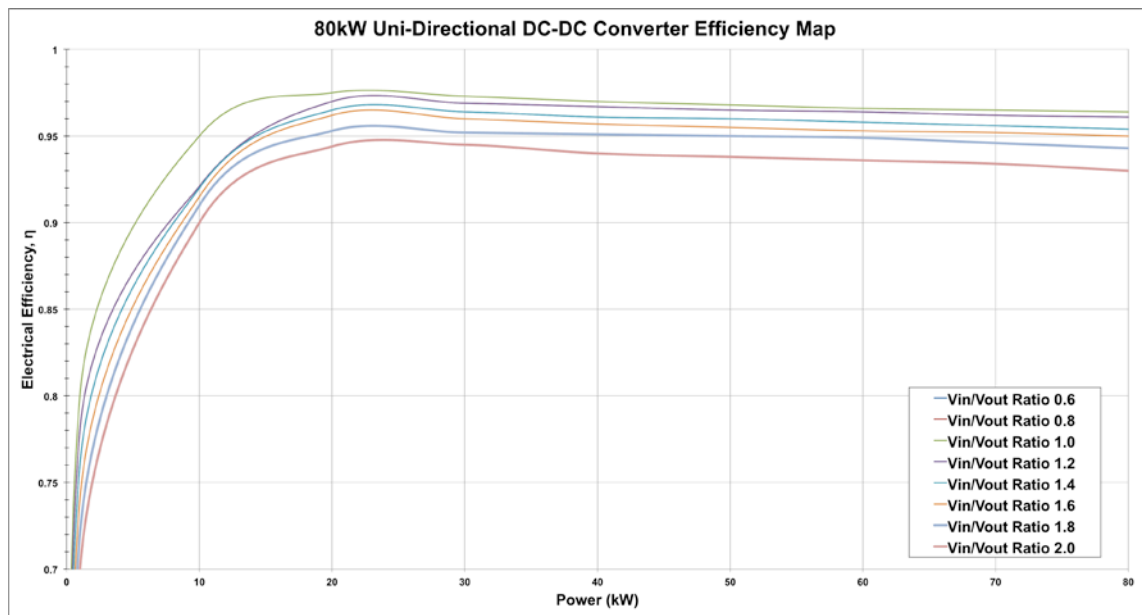


Figure 5.29 - 80kW Uni-Directional DC-DC Converter Efficiency Map

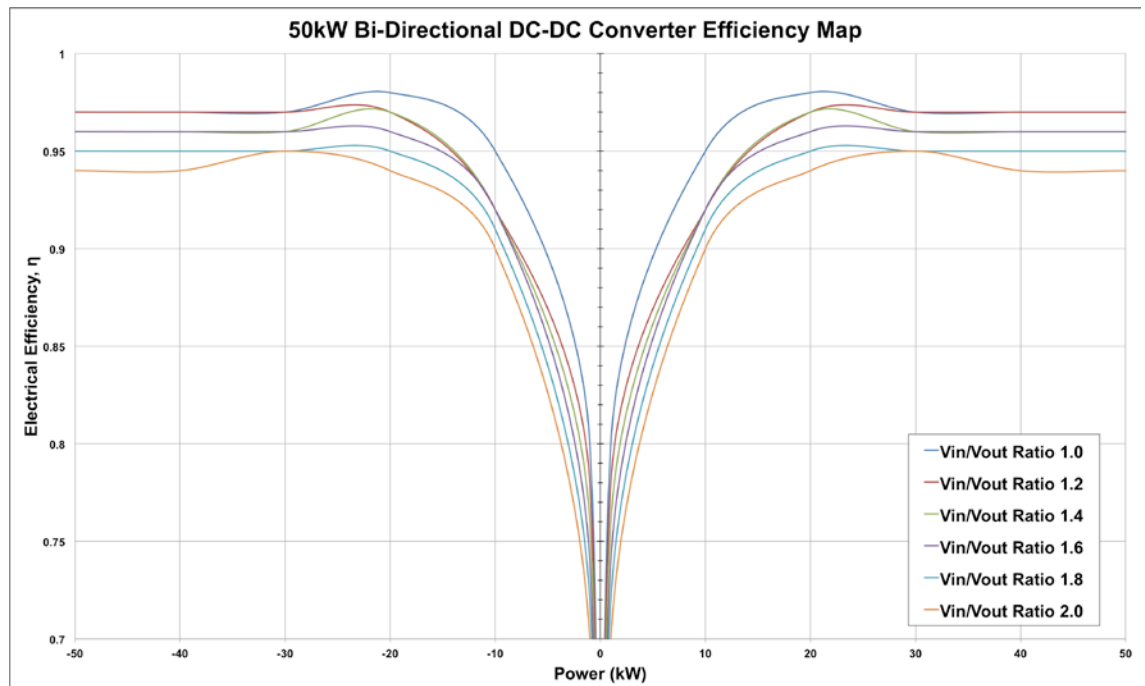


Figure 5.30 - 50kW Bi-Directional DC-DC Converter Efficiency Map

5.8.4 DC-DC Power Converter Model Assumptions

Several assumptions and implications are made about the DC-DC converter system during simulation.

1. The converter temperature is constant and within safe operating margins.
 - Transient effects of temperature on converter efficiency are ignored.
 - The switching devices are operating at their optimal temperature point.
 - The cooling system maintains this temperature.

- Cold start conditions are ignored.
- 2. The safety isolation circuit has zero loss during normal operation.
- 3. Cooling and control overhead are defined as a fixed electrical load.
- 4. The control system will prevent overload conditions at all times and restrict the output to 100% of the rated power if such an output is demanded by the control inputs.

5.9 Driving Cycles

In order to test the simulation models in multiple different modes of driving, a range of driving cycles were used. Standard cycles for urban, combined urban and extra-urban/highway and extra-urban/highway driving were used from the three main automotive markets in the world, the United States, Europe and Japan. The cycles were fed into the simulation models as time-speed data sets and used by the driver simulation subsystem to generate the brake and acceleration demand signals fed to the motor and brakes.

5.9.1 Driving Cycle Summary

Broadly speaking the driving cycles fall into two categories, simple stylised speed time modal profiles of differing journey types and speed time profiles based on real world driving conditions. The table below gives a summary of the driving cycles used in the simulation and graphs of speed versus time for each of the cycles are shown over the following pages in Figure 5.31 - Figure 5.45.

Driving Cycle	Length (s)	Distance (km)	Avg Speed (km/h)	Max Speed (km/h)	Max Accel. (m/s ²)	Type
<i>US06 Cycle</i>	600	12.81	76.75	128.48	3.73	Aggressive
<i>New European Driving Cycle (NEDC)</i>	1180	10.93	33.35	120.00	1.06	Combined
<i>Elementary Urban Cycle (ECE)</i>	195	0.99	18.26	50.00	0.89	Urban
<i>Extra Urban Driving Cycle (EUDC)</i>	400	6.95	62.44	120.00	0.83	Extra-Urban
<i>Japanese 10-15 Mode Cycle</i>	892	6.34	25.58	70.00	0.81	Combined
<i>Japanese 10 Mode Cycle</i>	135	0.66	17.57	40.00	0.81	Urban
<i>Japanese 15 Mode Cycle</i>	231	2.17	33.74	70.00	0.78	Extra Urban
<i>US Highway Cycle</i>	765	16.41	77.13	95.84	1.42	Highway
<i>New York City Cycle</i>	598	2.67	11.34	44.32	2.67	Urban
<i>Hyzem Urban Cycle</i>	559	3.47	57.20	22.31	2.19	Urban
<i>Hyzem Road Cycle</i>	842	11.22	47.93	47.93	2.42	Extra Urban
<i>Hyzem Motorway Cycle</i>	1803	46.20	92.20	138.10	3.19	Highway
<i>Hyzem Combined Cycle</i>	3206	60.90	68.36	138.10	3.19	Real-world
<i>AMS Cycle</i>	4913	71.02	53.60	99.90	6.44	Real-world
<i>Urban Dynamometer Driving Schedule</i>	1369	7.45	19.58	56.70	0.92	Urban
<i>US Federal Test Procedure (FTP-75)</i>	1874	17.67	33.92	90.72	1.47	Combined
<i>Artemis Urban</i>	993	4.87	17.64	57.70	2.86	Urban
<i>Artemis Road</i>	1082	17.27	57.42	111.60	2.36	Extra Urban
<i>Artemis Highway</i>	1082	29.55	99.50	150.40	1.92	Highway

Table 5.4 - Driving Cycle Summary

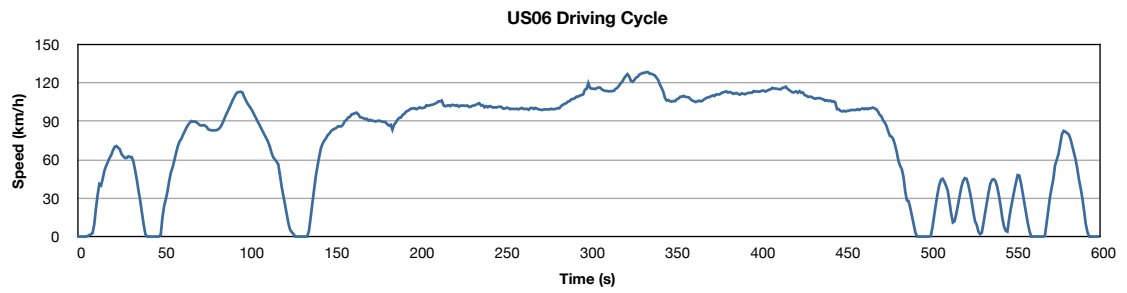


Figure 5.31- US06 Driving Cycle

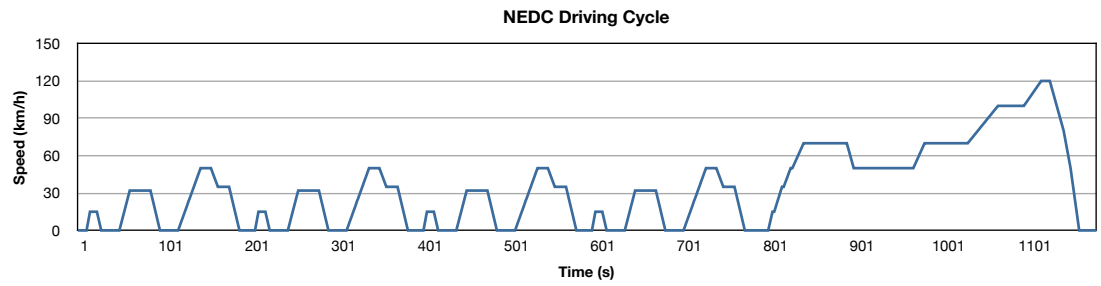


Figure 5.32 - NEDC Driving Cycle

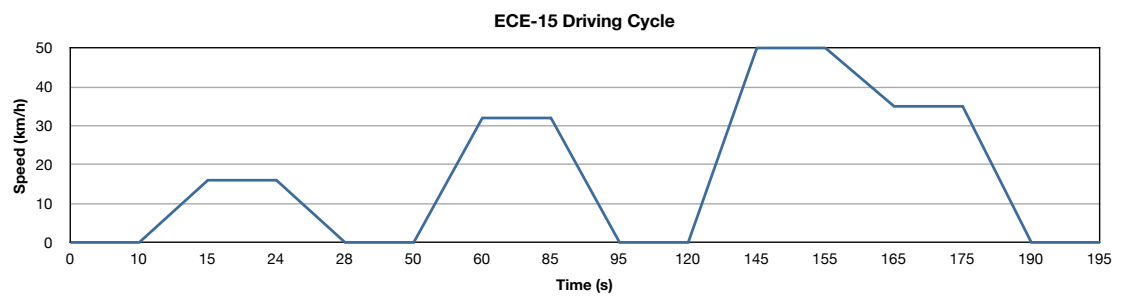


Figure 5.33 - ECE-15 Driving Cycle

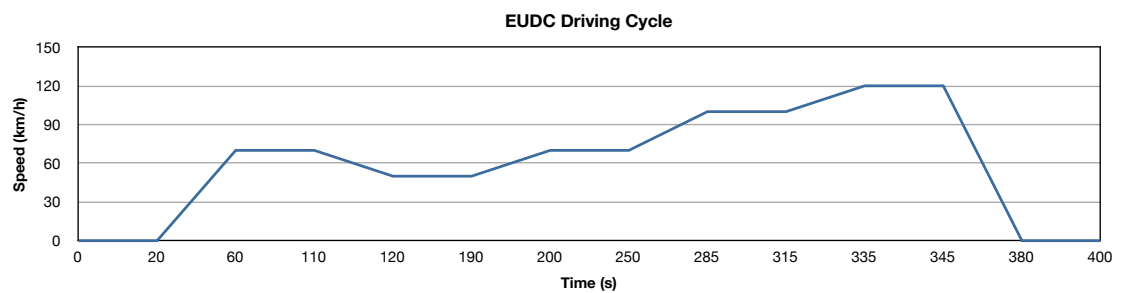


Figure 5.34 - EUDC Driving Cycle

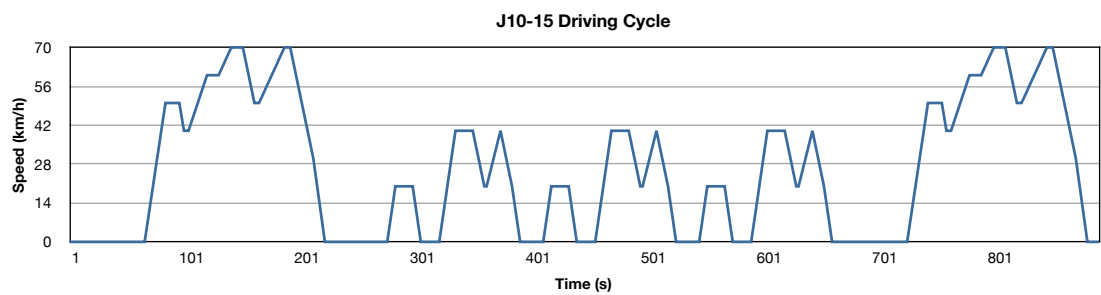
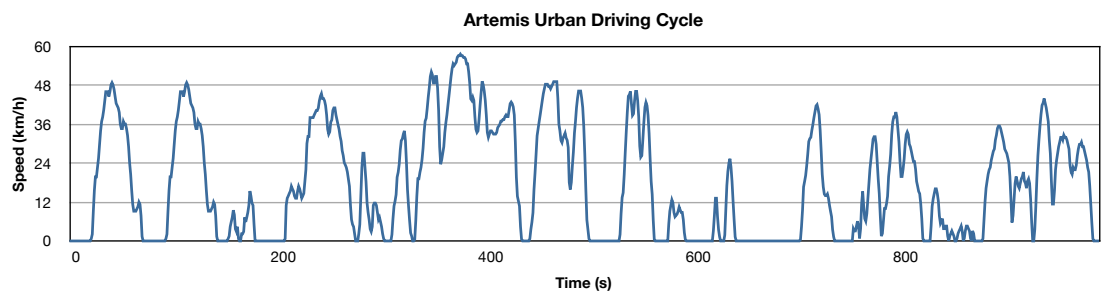
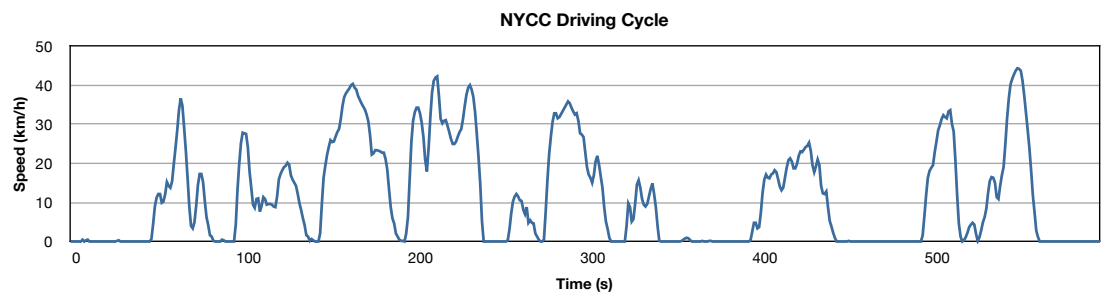
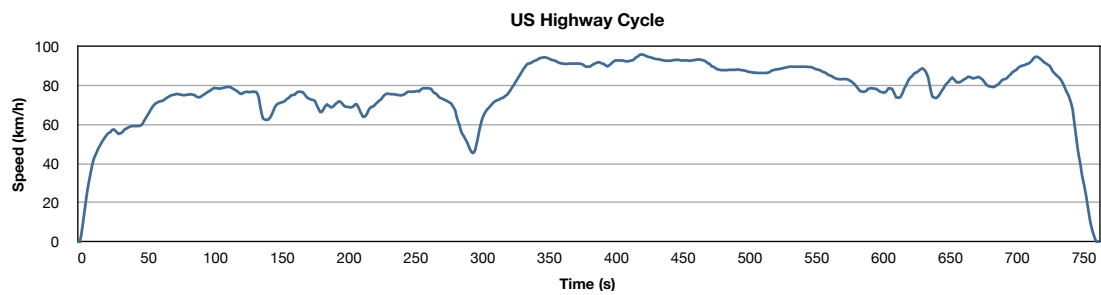
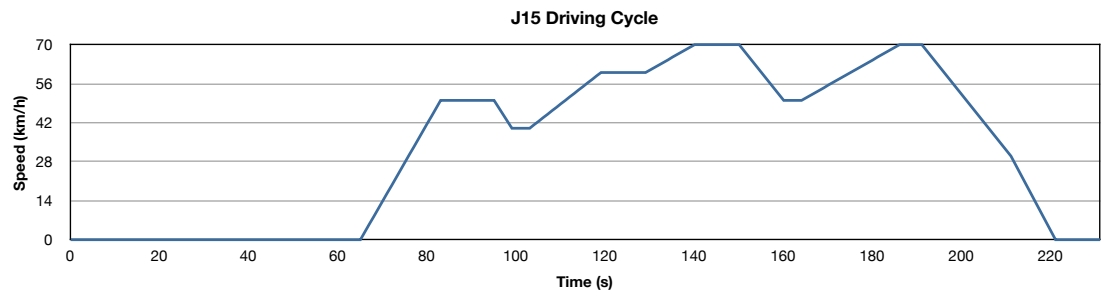
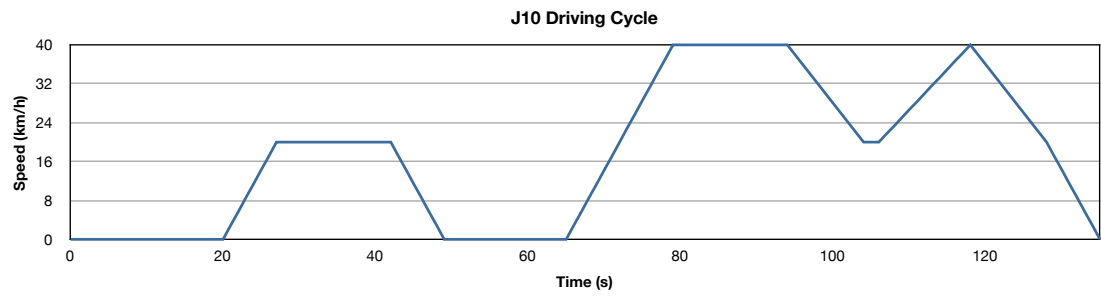


Figure 5.35 - J10-15 Mode Driving Cycle



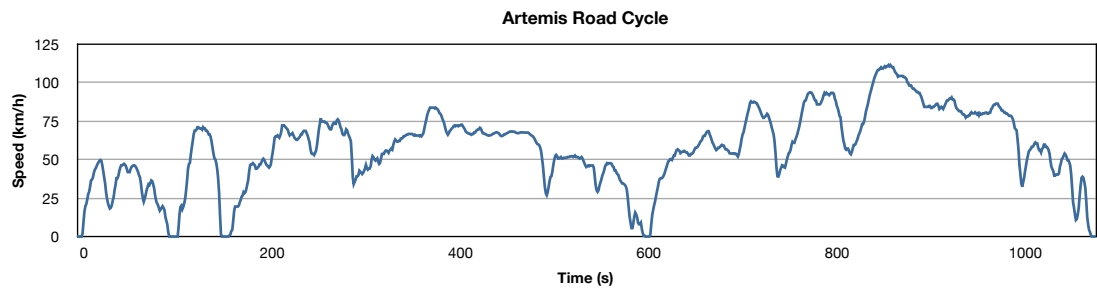


Figure 5.41 - Artemis Road Driving Cycle

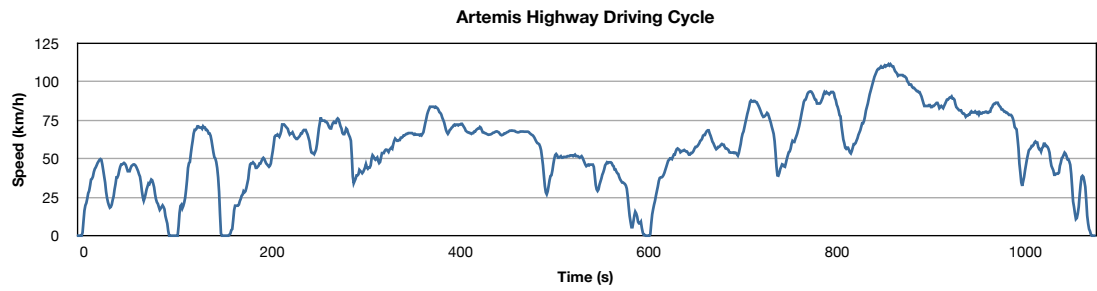


Figure 5.42 - Hyzem Motorway Driving Cycle

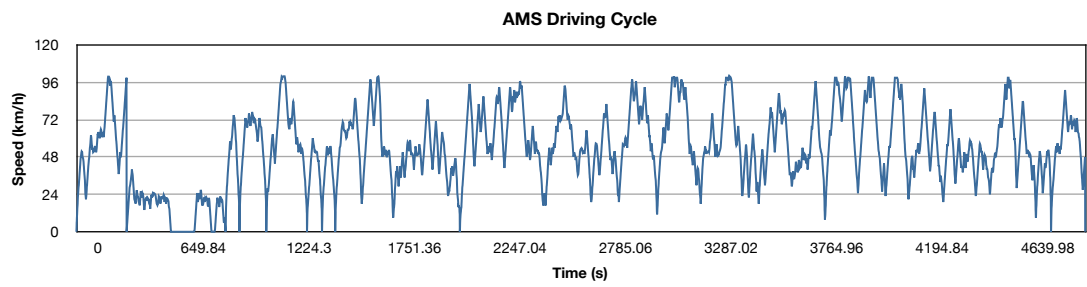


Figure 5.43 - AMS Driving Cycle

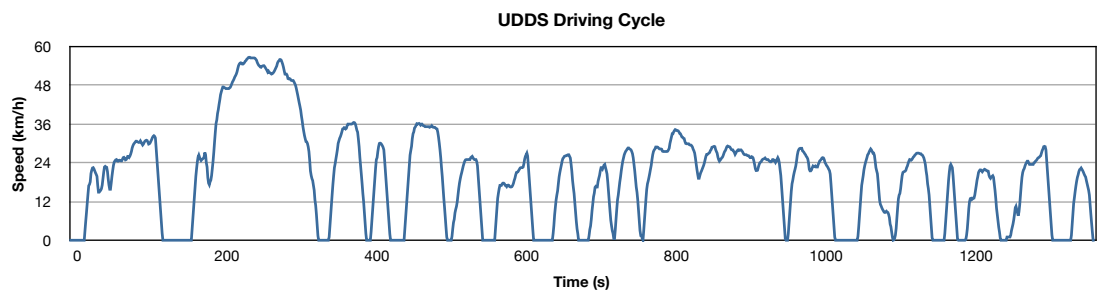


Figure 5.44 - UDDS Driving Cycle

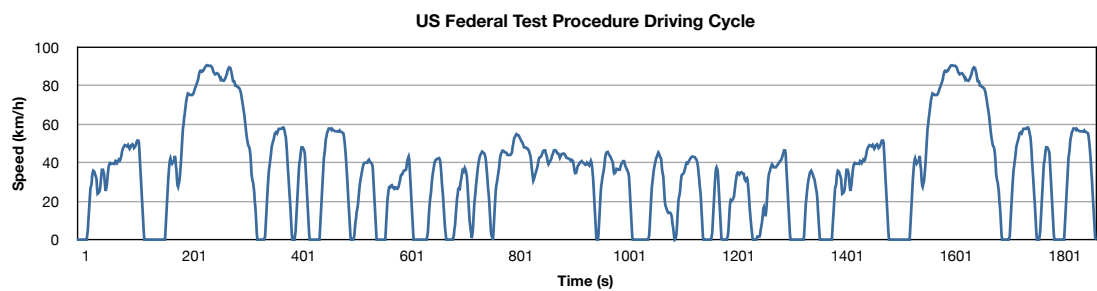


Figure 5.45 - US FTP-75 Driving Cycle

5.9.2 Driving Cycle Classification

From the graphs shown above the stark difference between the real world and simple stylised modal cycles is obvious. The stylised cycles are not representative of real world driving but they are used in legislative tests and are the basis of fuel economy figures quoted by manufacturers of production ICEV and HEV and it is therefore necessary to use them in the simulations to draw direct comparisons between the H₂FCEV drive trains in this study and existing production vehicles.

The published legislative cycles originate from three distinct geographic areas, Europe [233, 234], America [235] and Japan [233]. For each of these areas this study has used cycles representing urban, extra-urban/rural and motorway driving. The European and Japanese cycles for these modes of driving are modal stylised cycles whereas the American cycles incorporate transient features are more representative of real world driving conditions [234, 236]. The American test procedures also incorporate an additional aggressive motorway cycle that has no direct peer in the European and Japanese test cycle sets. Concerns have been expressed that the current European cycles are deficient because they do not represent real world driving and the efficiency and emissions data they are used to generate could be misleadingly positive as a result. In response to these concerns research projects have aimed to develop more realistic cycles. The result of one such research project is the MODEM Hyzem set of driving cycles that are a statistical representation of real world driving and were specifically developed for testing HEVs using extensive empirical data from actual journeys [234].

5.9.3 Driving Cycle Assessment

One potential pitfall of driving cycle analysis alone, especially with modal cycles, is that they don't test all the potential real world operating points of a drive train system and in missing these points critical set points are not evaluated and the results. It was essential to ensure that the collective set of test cycles would test a broad range of operating points. Consideration of the number of variations in speed time profile alone was not sufficient, the acceleration at each point in the driving cycle also needed to be taken into account to properly account for the power required by the drive train at each speed/torque operating point. The variation in operating points from a selection of cycles was visualised with two methods. The first used simple 2D scatter plots to show the operating points. A selection

of these that serve to illustrate the stark differences between modal and transient/real world based cycles are shown below in Figure 5.46 - Figure 5.49.

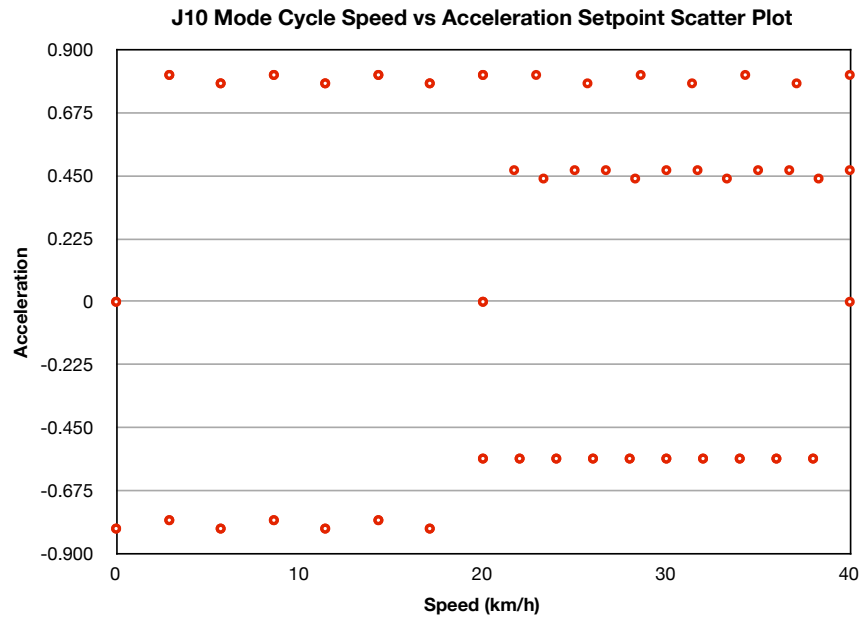


Figure 5.46 - J10 Driving Cycle Setpoint Scatter Plot

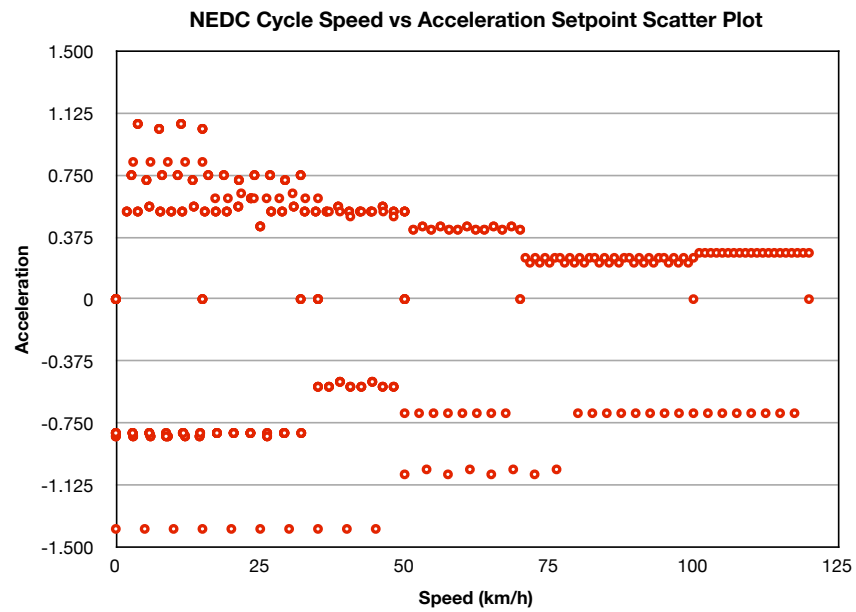


Figure 5.47 - NEDC Driving Cycle Setpoint Scatter Plot

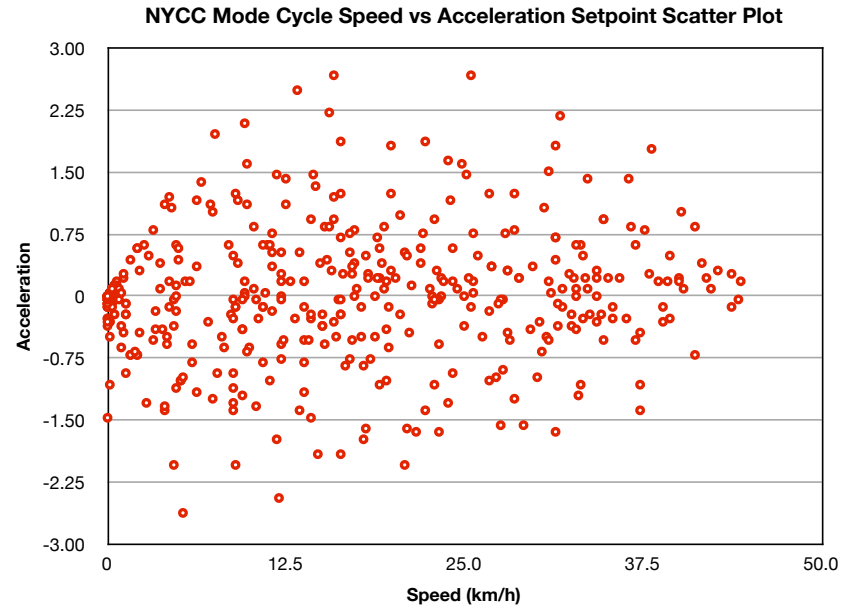


Figure 5.48 - NYCC Driving Cycle Setpoint Scatter Plot

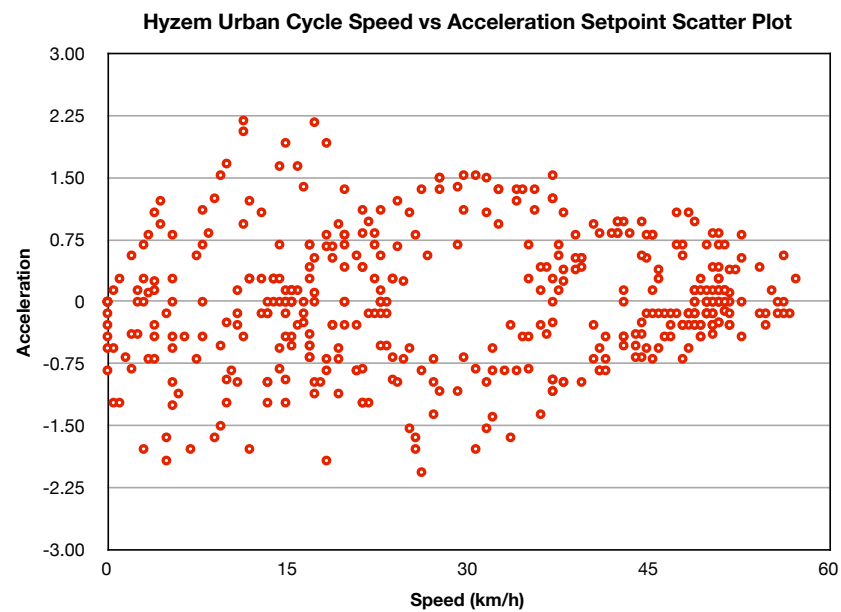


Figure 5.49 - Hyzem Urban Driving Cycle Setpoint Scatter Plot

Secondly, a software tool was written to take the driving cycle datasets and calculate a frequency distribution plot for each of them. This created a XYZ dataset for each cycle that was used to plot a 3D visualisation of the cycle. The 2D scatter plots illustrated that the modal cycles have a limited set of operating points when compared to the transient and real world cycles. The 3D frequency distribution plots of Figure 5.50 - Figure 5.53 clearly demonstrate that just a few of these limited points are the highly dominant points of operation during modal cycles. Transient and real world cycles show a much wider spread

of operating points in the 2D plots and 3D plots where there are substantially more peaks of significantly lower frequency.

The range of driving cycles selected for this study represents both the necessary modal cycles to ensure the results of the simulation can be compared to existing benchmarks and transient real world cycles to adequately test all the possible operating points of the drive train as possible. Some authors such as Schaltz & Rasmussen, recorded their own real world cycles with data loggers [227] and there are some important questions to be asked regarding the suitability of modal cycles for the realistic testing for all types of vehicle but their current use for benchmarking production vehicles and the need to draw comparisons with them makes their use mandatory and the point moot.

J10 Mode Driving Cycle Frequency Distribution Plot

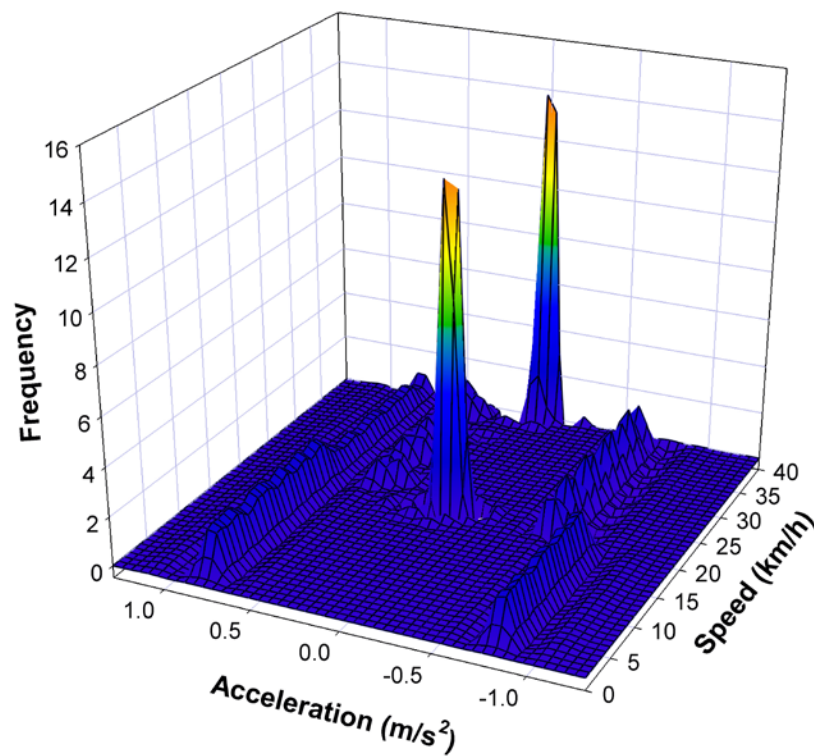


Figure 5.50 - J10 Driving Cycle Frequency Distribution Plot

NEDC Driving Cycle Frequency Distribution Plot

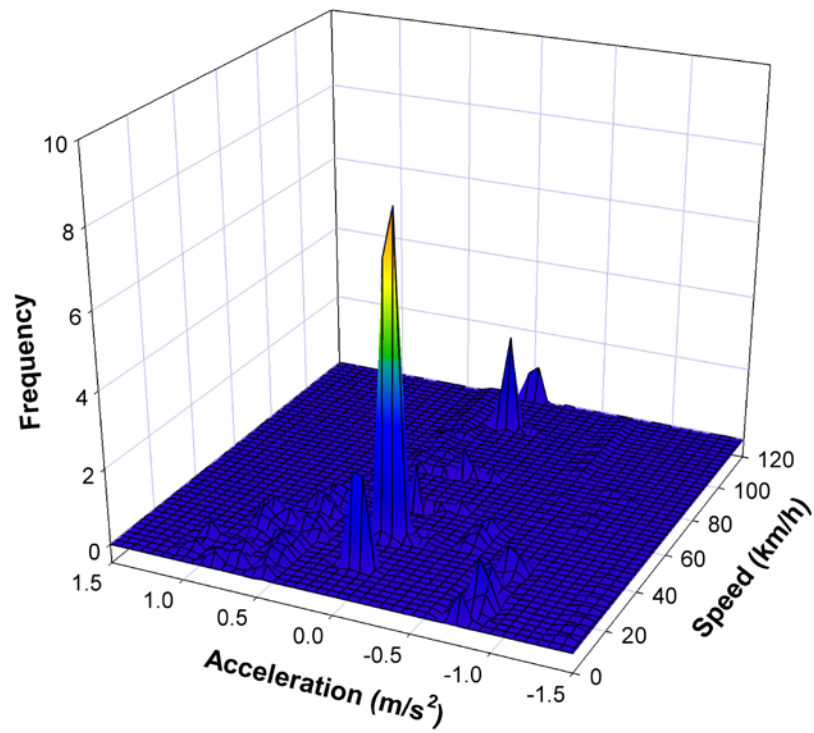


Figure 5.51 - NEDC Driving Cycle Frequency Distribution Plot

Hyzem Urban Driving Cycle Frequency Distribution Plot

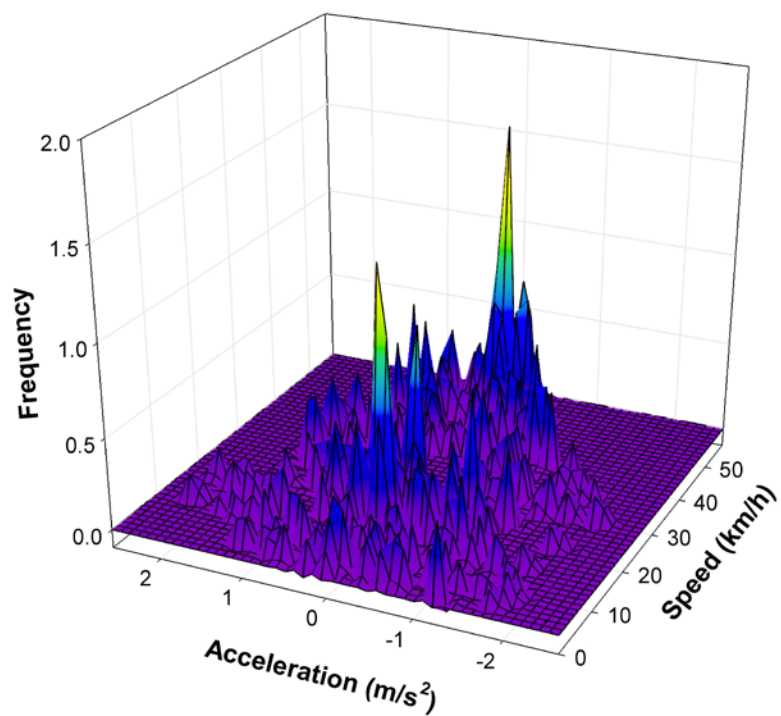


Figure 5.52 - Hyzem Urban Driving Cycle Frequency Distribution Plot

NYCC Driving Cycle Frequency Distribution Plot

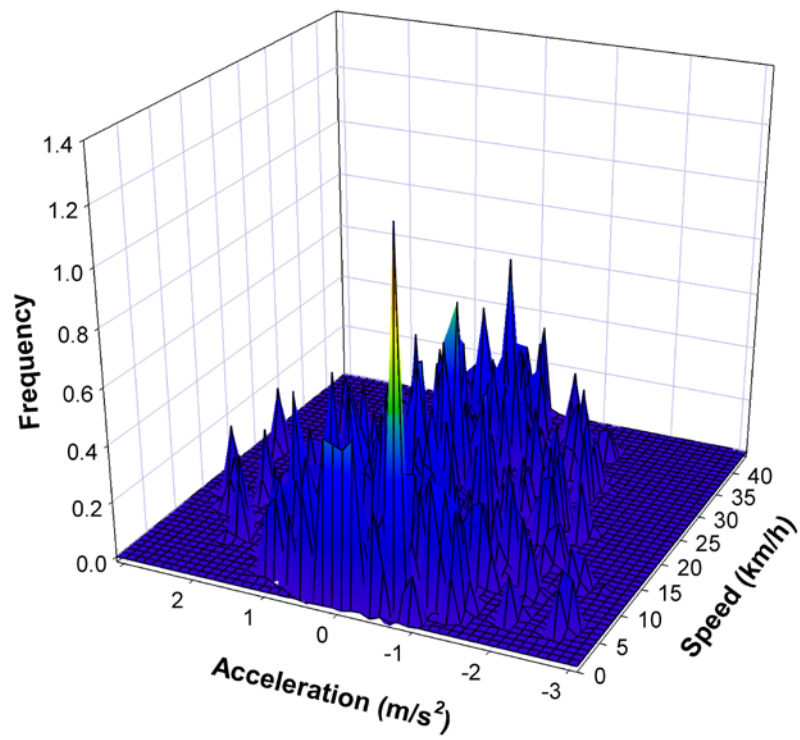


Figure 5.53 - NYCC Driving Cycle Frequency Distribution Plot

5.10 Simulation Operation & Control

The interconnection and overall control of the complete vehicle simulation model was relatively straightforward and aided by the common I/O parameters of the separate components. To aid comprehension, it is best described in two levels of abstraction. The highest-level model of the simulation operation is shown in Figure 5.54. The simulation creates a speed demand from a driving cycle and then compares it to the current vehicle speed. A PID controller takes the error signal and acts on the vehicle to equalise the actual and demanded speeds.

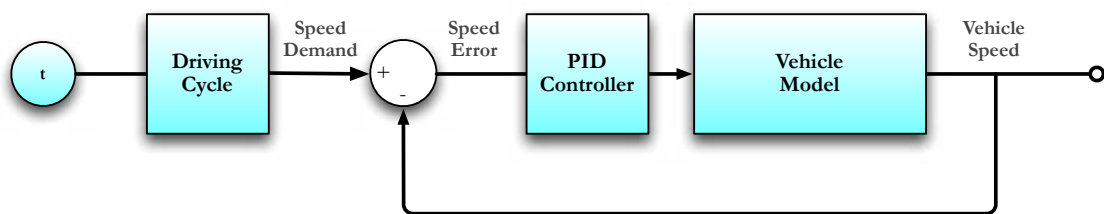


Figure 5.54 - High Level Simulation System Abstraction

Each component within the vehicle model has its characteristics and parameters determined at each simulation step. A positive speed error results in the motor accelerating the vehicle, drawing current from the fuel cell and battery system. A negative speed error causes the vehicle to engage its braking system and decelerate the vehicle.

Breaking down into the more detailed view of the model Figure 5.55 shows the arrangement of the different modules and the various signal flows in the model. The overall operation can be summarised in five steps:

1. The speed error is calculated and a torque demand signal is produced.
2. The torque demand signal is passed to the motor model. It calculates the power required.
3. The power demand is passed to the fuel cell. It calculates the actual fuel cell output and requests additional power from the battery if it cannot meet demand.
4. The total power on the DC bus is summed and passed to the motor model which calculates the actual output torque.
5. The vehicle dynamics model calculates the acceleration, speed and distance travelled.

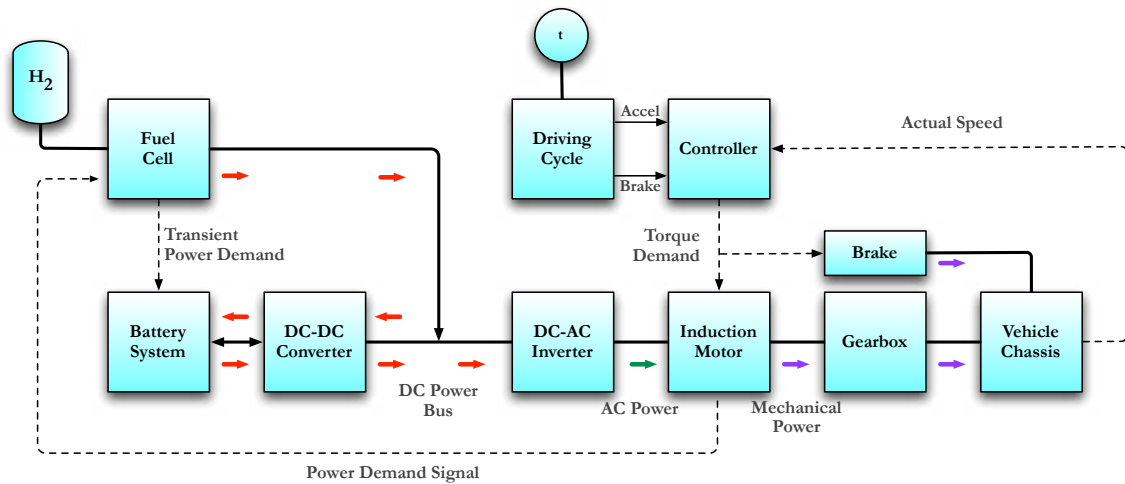


Figure 5.55 - Detailed Vehicle Simulation System Overview

5.10.1 Forward Looking vs. Backward Looking Operation

Simulation methodologies are generally grouped into two categories, 1) forward-looking and 2) backward-looking. The forward approach takes an input signal, in this case the driver accelerating or braking, and calculates the dynamic effect of the input through the model to calculate the simulation output values. The backwards approach takes a pre-determined fixed output, the vehicle velocity, and statically calculates what the input states within the model need to be to achieve that output.

Both approaches have merit but to properly represent dynamic effects within a system the forward-looking approach has to be used [126, 140, 188]. The forward-looking method also allows the development of a system that can subsequently be easily transferred to hardware testing as every aspect of the real system is simulated. The backwards method does not represent the driver and is not easily reproduced in a hardware test system.

There is however a penalty to the forward approach, it is computationally far more intensive [188]. Placing a PID control loop around the entire system proved to be very difficult to stabilise and the simulation runtime was initially in the order of 72s of computation for every 1s of input data. The traditional approach to stabilisation would be to analytically describe the system and solve the system equation. This was not possible, as large pieces of the simulation have been characterised with empirical data. Though the transfer function of the vehicle dynamics could have been derived, it alone would have been useless as the transfer functions for the fuel cell system, motor and battery are unknown and not derivable from the available data. To solve this problem, the simulation model was developed using a combination of forward looking and backward looking

methods. Similar approaches to designing the simulation were commonly seen in the literature and described as a quasi-static model [142, 188, 193, 237].

The outer loop between the driver acceleration/braking input and the vehicle speed is forward looking. The point at which the model deviates is in the motor drive model, which is a forward looking and backward looking model in one. The driver demand signals drive the backward looking element of the motor. It calculates the power required to achieve the given demand.

This power demand is then fed to the main vehicle controller. It requests the power level from the fuel cell, another quasi-static model. Any difference between the demand and actual output is passed to the battery system. The output of these two systems is summed together and then passed back to the motor drive block and put through the forward motor model that generates an actual torque for the power being supplied to the motor. This allows the simulation model to accurately simulate situations where the demanded power exceeds the output capability and/or transient response capacity of the power sources.

The motor output torque is passed to the vehicle dynamics model that then calculates the actual vehicle output speed which is passed back to the driver block ready for the simulation loop to repeat itself. This approach speeds up the computation and stability of the simulation model significantly with no discernible difference in the accuracy of the output. The vehicle still follows the driving cycle accurately with no deviation. The effective simulation signal flow is shown below in Figure 5.56.

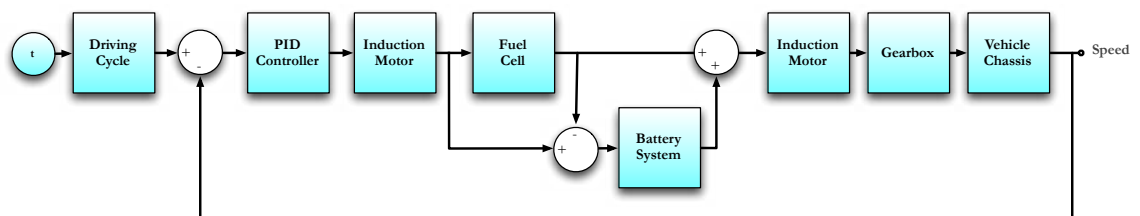


Figure 5.56 - Quasi-Static Simulation Methodology

The control loop was at first designed by construction a PID control from discrete elements in MATLABSimulink. No derivative term was used and the PI controller was initially manually tuned by trial and error. Once values that produced a reasonably accurate system response were found, the MATLAB Simulink PID controller block was used. This

pre-defined function has an auto-tune feature which allowed automatic refinement of the control parameters.

5.10.2 Hybridisation & Power Split Control

How to control the power sources in an electric drive train and the relative size of the ESS to the fuel cell are the subject of many studies as topics in there own right alongside considering the implications as part of a simulation system design [134, 145, 155, 188, 198, 237, 238]. In this study, the ESS was designed to match the electrical requirements of the system with a rated capacity of 4.5kWh, it is of comparable size to ESS seen in other studies. The question of whether it is ideally sized is perhaps an important one for further study, the fact it was constant across all the topologies is the primary consideration in this study. The hybridisation ratio, X_{HYBRID} , of a drive train is defined as [239]:

$$X_{HYBRID} = \frac{P_{BATTERY}}{\left(P_{FC} + P_{BATTERY} \right)}$$

$$X_{HYBRID} = 34.6\%$$

Equation 5.32 - Hybridisation Ratio

Biurrun et al [239] came to the conclusion that the ideal hybridisation ratio was 30% and with consideration given to existing prototype H₂FCHEVs it was concluded that the hybridisation in this studies system was appropriate and the results would not suffer distortion from a badly specified ESS.

Controlling how the power sources interact with each other is another area of active research with many differing strategies proposed and developed in the literature. Because many of the more highly developed control strategies are specific to the topology and not directly applicable to all the different drive trains simulated this study uses a simple strategy that uses the ESS to cope with transient demand only and regulates when the ESS can be recharged by the fuel cell to maximise the charging efficiency.

The main vehicle controller therefore monitors the power demanded by the motor and the vehicles auxiliary systems (air conditioning, in car entertainment, lighting etc). It requests this power from the fuel cell and uses the ESS to provide any transient demand that the

fuel cell isn't capable of providing at any given simulation step. The power in the system can be described as:

$$P_{[t]} = P_{MOTOR[t]} + P_{AUX[t]} = P_{FC[t]} + P_{BATTERY[t]}$$

$$P_{BATTERY[t]} = P_{[t]} - P_{FC[t]}$$

Equation 5.33 - Power Split

In certain cases where the battery burst discharge limiter is operating to protect the battery from repeatedly bursting, large transient demands could cause $P_{[t]}$ to be less than demanded by the controller. The quasi-static motor model will ensure that the actual available power is properly iterated through the model in these cases.

When the battery SOC falls below 0.8 and the ESS is idle, either during steady state driving or idling, the battery can be recharged from the fuel cell. To ensure maximum charging efficiency, a control rule is enforced such that charging is only enabled when $P_{FC[t]}$ is between 12kW and 40kW and operating in the region shown below in Figure 5.57. This rule is ignored if the SOC drops below 0.4 to prevent over discharge of the ESS.

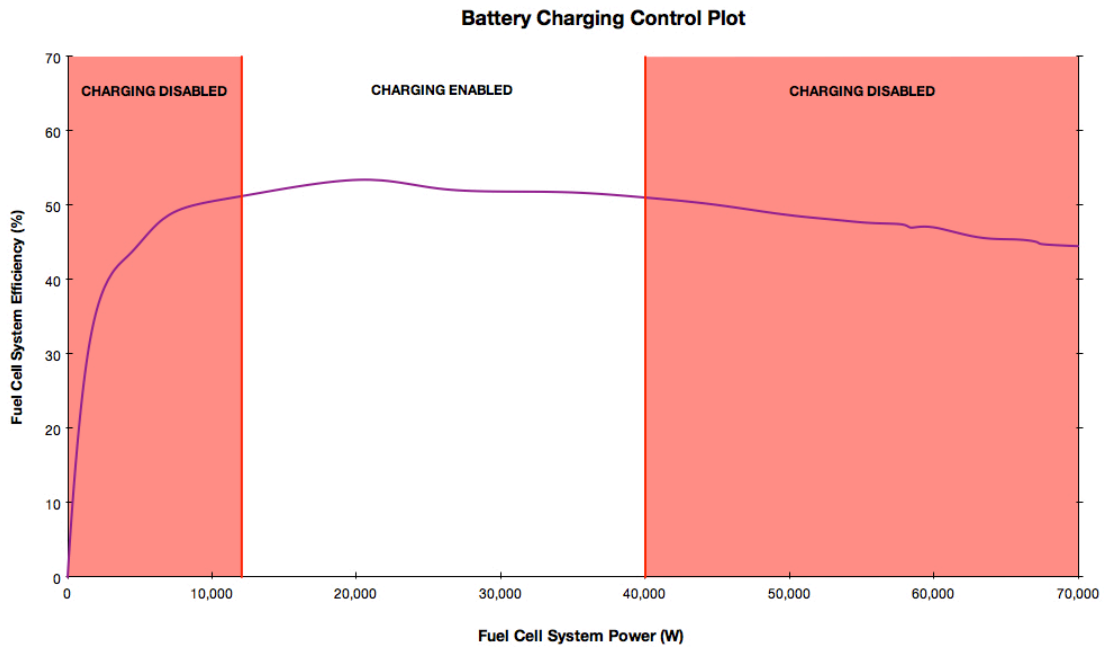


Figure 5.57 - Battery Charging Rule

5.10.3 Driver Simulation

It should be acknowledged that ultimately a human driver would drive the vehicle and that implies certain behaviour that would modify the model that accelerates and breaks the

vehicle. Human drivers would struggle to accurately drive according to a driving cycle and it would be almost impossible for that human driver to replicate the journey in the same way multiple times. A valid model of a human driver would have to include delays for reaction times and randomly varying over and undershoot of the speed time profile the driver was attempting to follow according to some normal distribution based on real world driver observations. Hauer built some of these feature into his simulation system [125]. After some thought it was decided not to replicate the drivers behaviour and that the control system would follow the speed time profile of the driving cycle without modification, within the capabilities of a digital control system. This study seeks results that are directly comparable. Introducing pseudo-random behaviour into the system, however small an affect it would have, would make each simulation different and partially invalidate the results by default. What is of interest is the electrical and mechanical power flows in the system, not how driver behaviour might discretely modify those for each and every journey.

5.10.4 Computational Requirements

When initially developed, the model was run under MATLAB Simulink 6.5 running on Windows XP 32 bit on a Pentium 4 computer with 512MB of RAM. It was established, similarly to [125], that the simulation model would have to be run with the ODE1 Euler fixed step solver. In addition to several of the calculations being related to fixed discrete time intervals, the variable step solvers generally crashed or encountered unsolvable algebraic loops. The largest step size that did not cause MATLAB to generate errors whilst running in fixed step mode was 0.005s and this step size was used for all of the simulations.

Since this study was started, desktop computing has advanced significantly. The collapse in the price of RAM, move from 32 bit to 64 bit operating systems and the advent of solid state memory hard drives (SSDs) have changed the modelling speed quite significantly. The original computer used to take up to 70s for every 1s of simulation times. Running an NEDC driving cycle could take nearly 24 hours. The cause of this problem was principally limited RAM causing MATLAB to have to arduously swap virtual memory to disc once it ran out of physical memory and the speed of the physical memory being 1/3 of what it now is. The system now runs on a twin processor, dual core Intel Xeon X5000 based machine running Windows 7 64 bit with 16GB of RAM and a 6Gbps SSD system drive. Some of the less complicated driving cycles now simulate up to five times faster than real time. The computational power now available on the desktop probably permits further

development beyond this study such that it could feature thermal effects and discrete power electronic simulation.

5.10.5 Telemetry

To aid analysis, almost every important parameter is stored at each simulation step. Around 50 variables are stored, in the extreme case at the end of an AMS cycle this can result in ~50 million data points. The results section will detail the critical points but needless to say tabulating and printing every measured data point would serve little purpose and be practically impossible.

5.10.6 Simulation Method Summary

The following paragraph provides a simplistic overview of how the model operates once the simulation is underway.

1. Speed demand generated by driving cycle based on a time clock signal.
2. Actual vehicle speed subtracted from speed demand to give a speed error signal.
3. PI controller generates a torque demand value based on speed error.
4. Torque demand value and actual speed passed through motor module power loss look up table.
5. Electrical power loss from the motor is summed with the mechanical power to generate the total electrical traction power demand.
6. Power demand is passed to fuel cell module.
7. Fuel cell output changes to meet demand.
8. Battery pack monitors the difference between demanded power and fuel cell output power and provides the difference during the time it takes the fuel cell to respond to the demand.
9. Actual electrical output power passed to motor.
10. Actual torque generated.
11. Torque passed through gearbox to vehicle chassis module.
12. Vehicle accelerates/decelerates according to the torque input.
13. Vehicle speed decreases/increases.

This closed loop repeats until the end of the driving cycle. For the avoidance of doubt, in the case of a negative speed difference (i.e. the vehicle is required to brake) the motor module is replaced in the loop by the brake system module. A procedural flow diagram of

this process is shown in Figure 5.58 and an example of the overall system for one of the topologies created in MATLAB Simulink is shown in

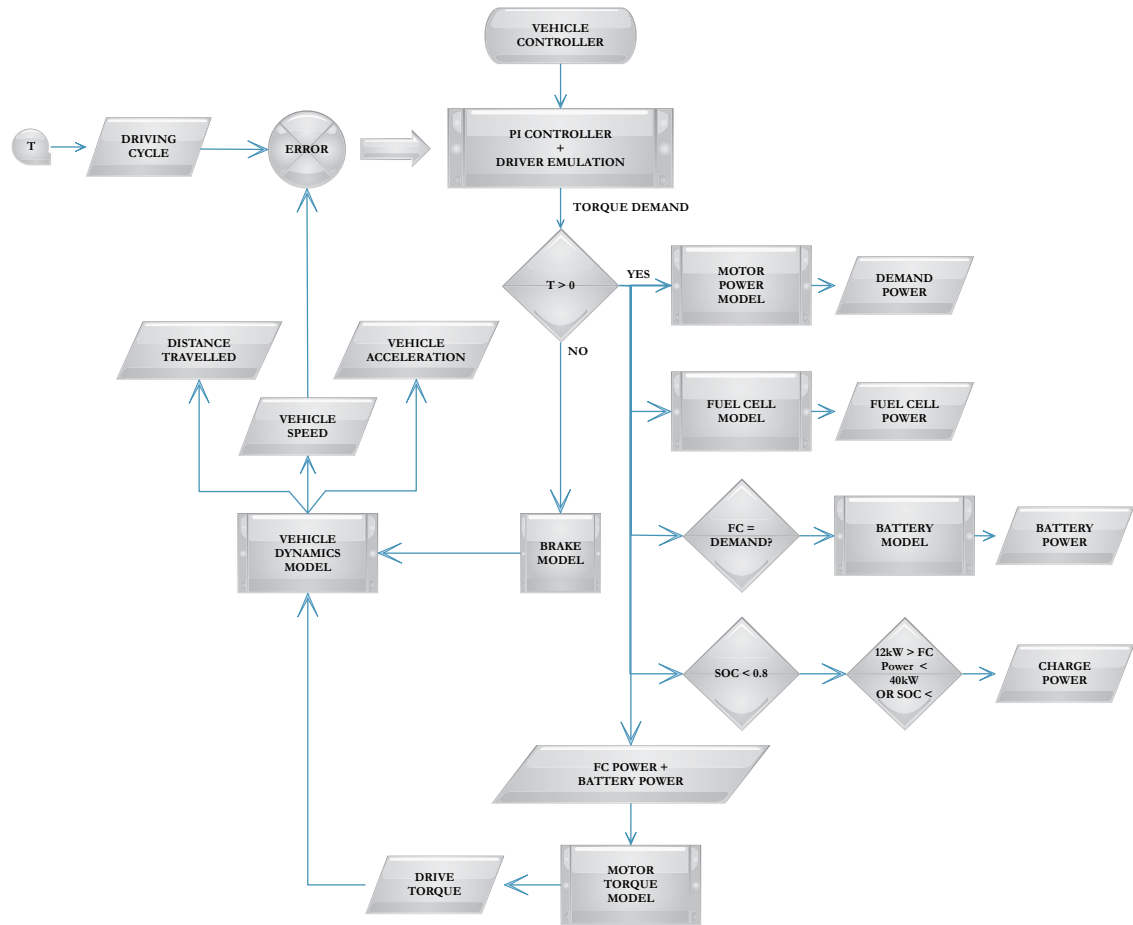


Figure 5.58 - Simulation Operation Flow Diagram

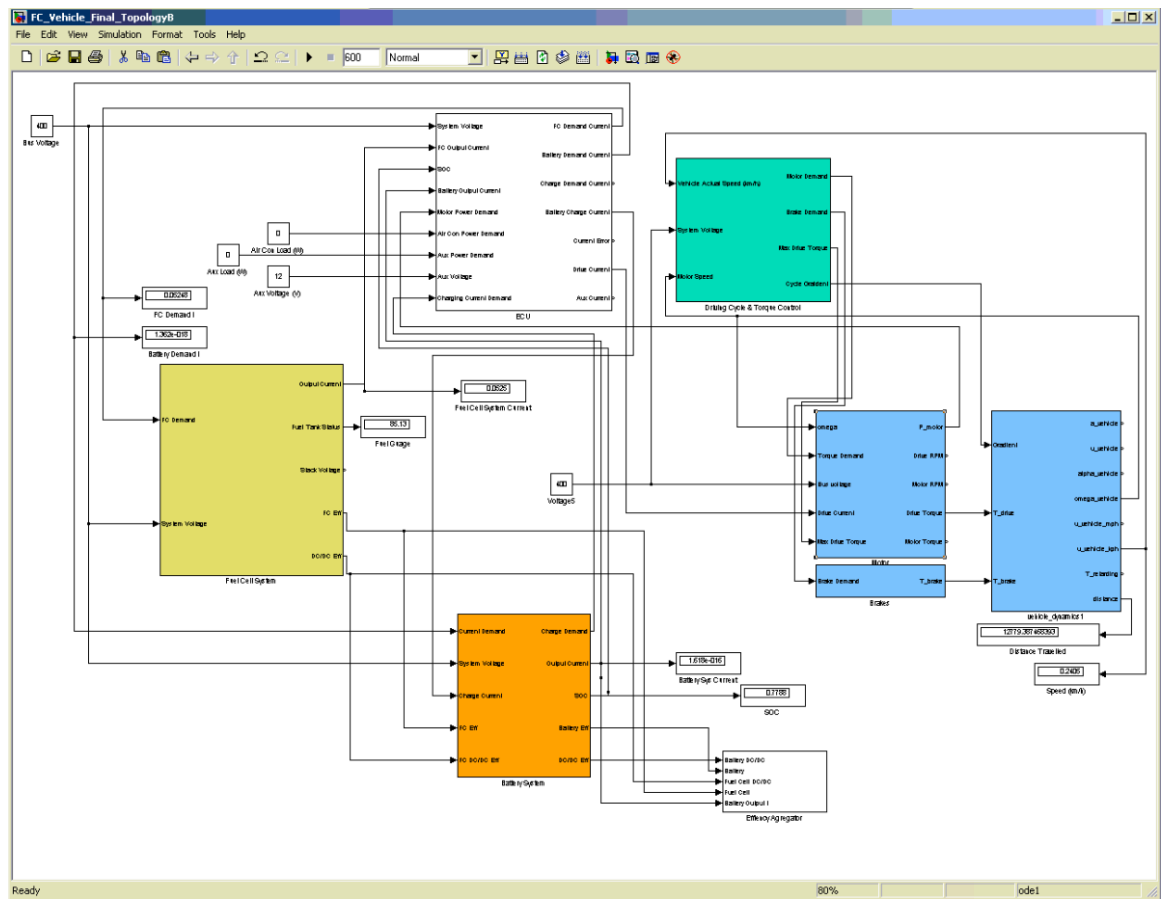


Figure 5.59 - MATLAB Simulink Simulation Model

5.11 Simulation Model Test Procedures

Once assembled, each topology was subject to a range of test procedures to ascertain its performance and efficiency in addition to being tested with each of the driving cycles. From these tests the following metrics were established for each topology.

5.11.1 Driving Cycle Testing

Each topology is tested with each of the driving cycles described in 5.9. Each cycle is run five times and the distance travelled and fuel consumed averaged across the runs and recorded.

5.11.2 System Efficiency Analysis

In each simulation model the efficiency of the system elements is logged as a telemetry parameter at every simulation step for all of the driving cycles. The average efficiency of each component across the whole cycle is calculated at the end of each simulation.

5.11.3 Vehicle Range

The total range of the vehicle is measured for every driving cycle simulated. The percentage of the fuel consumed is used to calculate the distance that could be travelled on a complete tank of fuel for the current mode of driving as follows:

$$Range_{Vehicle} = \frac{s_{vehicle}}{Fuel_{[t=0]} - Fuel_{[t=end]}}$$

Equation 5.34 - Vehicle Range

Where:

$Range_{Vehicle}$ = Maximum range of vehicle when driving current cycle (km).

$Fuel_{[t=0]}$ = Fuel at start of simulation (100% of tank capacity, 5kg)

$Fuel_{[t=end]}$ = Fuel at end of simulation (%)

$s_{vehicle}$ = Distance travelled by vehicle during simulation (km)

Aggregate ranges for urban, extra-urban and motorway modes of driving were based on the average range for each class of driving cycle. An overall average efficiency for every driving cycle was also calculated.

The vehicle range is only calculated on the amount of hydrogen in the tank, it does not consider how much further could be driven using the remaining charge in the battery as a reserve fuel source as this is not a normal driving mode.

5.11.4 Motive Efficiency

In order to draw useful comparisons to current internal combustion engine vehicles, the motive efficiency of the fuel cell vehicle simulations are presented in one H₂FCEV specific measure and two metrics which are analogous with the standards that are currently used to quote the efficiency of ICEVs and HEVs. Due to the anachronism of Great Britain being a metric nation but still measuring transport with imperial units both metric and imperial values are calculated for certain quantities.

1. Miles and Kilometres per kg of H₂ (M/kgH₂, km/kgH₂)
2. Kilograms of H₂ per 100km (kgH₂/100km)
3. Miles Per Gallon, Gasoline Equivalent (MPGe)

The first is easily calculated as follows:

$$M / \text{kgH}_2 = \frac{\text{Range}_{\text{VEHICLE}}}{\text{Fuel}_{\text{CAPACITY}}}$$

Equation 5.35 - Miles per kg of Hydrogen

Where:

$$\text{Fuel}_{\text{CAPACITY}} = \text{Total capacity of fuel tank (kg)}$$

The second is derived from the vehicle range:

$$\text{kgH}_2 / 100\text{km} = 100 \left(\frac{1}{\text{Range}_{\text{VEHICLE}} / \text{Fuel}_{\text{CAPACITY}}} \right)$$

Equation 5.36 - kg Hydrogen per 100km

Using the lower heating value, H₂ contains 119.93MJ/kg of energy. Petrol contains 44.72MJ/kg [66]. Petrol weighs 0.773 kg/l and an imperial gallon of petrol is 4.54609l. Using the LHV of 95RON fuel, 1 gallon of petrol contains 157.15MJ of energy. Therefore, imperial MPGe can be calculated using the M/kgH₂ data:

$$MPGe_{IMPERIAL} = \frac{M / kgH_2}{1.31}$$

Equation 5.37 - MPGe

The 5kg hydrogen tank used in this study contains the same amount of energy as 3.81 gallons of 95RON petrol, starkly illustrating the technical limitations of fuel capacity in a typical H₂FCEV when compared to a standard midsize passenger ICEV that carries a 60l/13.2gallon petrol tank.

5.11.5 Acceleration Tests

Two driving cycles were developed to test the acceleration performance of the vehicle.

1. Acceleration test 0-60mph (0-96kph)
2. Overtaking test 50-70mph (80-112kph)

Neither of these cycles was meant to be followed precisely as was the case with the other test cycles; step changes in speeds of such magnitude are clearly impossible.

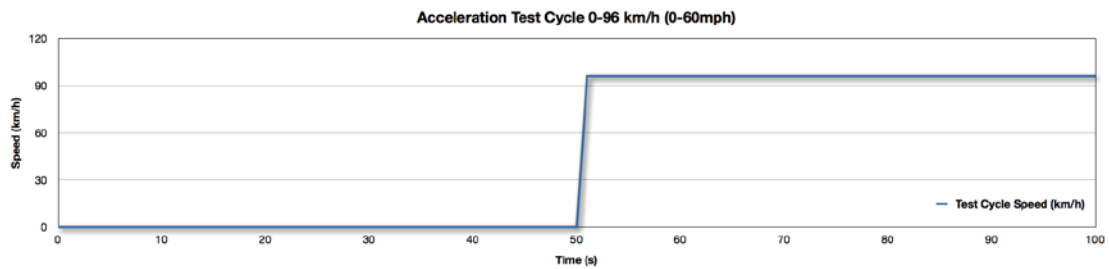


Figure 5.60 - 0-60mph Acceleration Test Cycle

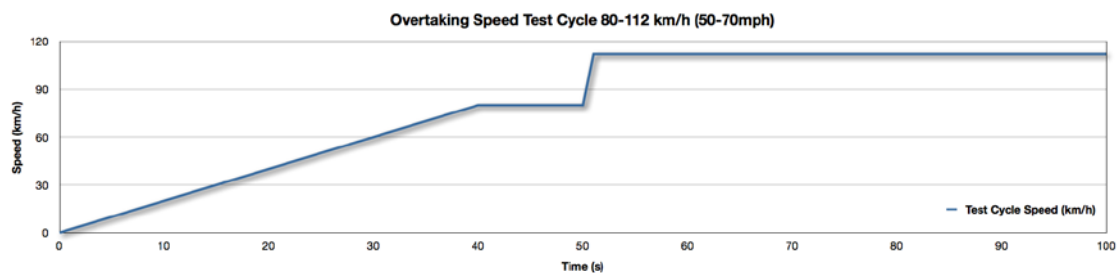


Figure 5.61 - 50-70mph Overtaking Test Cycle

5.11.6 Gradeability

The vehicle is idled for 50s at which point the speed demand is set to 5 km/h. The driver model accelerates the car to 5km/h and holds the speed steady. At 70s the grade of the road the vehicle is travelling on is increased by 1% steadily at 10s intervals. The grade ability of the vehicle is defined as the maximum grade at which the car is capable of

maintaining its initial velocity. Electric Vehicles should be capable of gradeability in excess of 25% [240].

6.1 Introduction

This chapter will present a selection of the significant data gathered from the vehicle simulations. The key criteria for evaluating the vehicle topologies were:

1. Driving Range.
2. Vehicle Performance.
3. Power Drivetrain Efficiency.
4. Electrical Performance.
5. Control Performance.

Since this work has been based on computer simulation, the results needed validating externally from the simulation model. The validation methods used are discussed at the end of this chapter and a selected set of validations shown.

6.2 Vehicle Driving Range

One of the benchmarks usually highlighted in electrical vehicles is range. The limited range of a BEVs is their single largest drawback given how long it takes to recharge them. The phrase “range anxiety” has often been mentioned when discussion of how the limited range of BEVs limits their potential applications.

The principle stated advantage of the H₂FCHEV is not that it is more efficient than the BEV. We know this not to be true without the need to simulate anything. But that it overcomes the problem of limited range in two ways, firstly that a H₂FCHEV can travel further on a single tank of fuel than any BEV and secondly that it can be refilled, not in hours, but in a few minutes.

In a BEV, the range is easily equated to the power demands placed on the vehicle. The higher the demand, the quicker the battery will be depleted. Things are not so straightforward in the H₂FCEV however and the characteristics of the fuel cell and driving mode have additional influences that affect the range. Since driving modes vary throughout

the world the vehicle range was measured with cycles of various modes from different geographic areas.

The tables that follow in this section show the range in km and miles. The optimal topology in each table is highlighted in bold for clarity and the tables also show the relative percentage difference in range between each topology and the topology that is highlighted as optimal in each case.

6.2.1 Urban Driving

Urban driving range is calculated by averaging the vehicle range of each topology during the ECE, J10, NYCC, UDDS and Artemis Urban driving cycles. Topology

Topology	Drivetrain Type	Range (km)	Range (miles)	Relative Range ¹
<i>A</i>	H ₂ FCEV	367.96	229.98	+1.82%
<i>B</i>	H ₂ FCEV	325.54	203.46	-9.92%
<i>C</i>	H₂FCEV	361.40	225.88	-
<i>D</i>	H ₂ FCEV	322.29	201.43	-10.82%
<i>E</i>	H ₂ FCEV	330.74	206.71	-8.48%
<i>F</i>	H ₂ FCEV	303.60	189.75	-15.99%
<i>I</i>	H ₂ FCEV	349.11	218.19	-3.40%
<i>J</i>	BEV	157.46	98.41	-56.43%
<i>Q</i>	H ₂ FCEV	325.07	203.17	-10.05%

Table 6.1 - Urban Driving Range

6.2.2 Extra-Urban Driving

Extra-urban driving range was calculated by averaging the vehicle range of each topology during the EUDC, J15 and Artemis Road driving cycles.

Topology	Drivetrain Type	Range (km)	Range (miles)	Relative Range
<i>A</i>	H ₂ FCEV	507.44	229.98	+2.00%
<i>B</i>	H ₂ FCEV	456.16	203.46	-8.30%
<i>C</i>	H₂FCEV	497.47	225.88	-
<i>D</i>	H ₂ FCEV	450.43	201.43	-9.46%
<i>E</i>	H ₂ FCEV	453.36	206.71	-8.87%

¹ The relative range is the range of the topology relative to the most efficient H₂FCEV topology, Topology C.

<i>F</i>	H ₂ FCHEV	432.09	189.75	-13.14%
<i>I</i>	H ₂ FCHEV	492.16	218.19	-1.07%
<i>J</i>	BEV	216.61	98.41	-56.46%
<i>Q</i>	H ₂ FCHEV	454.56	203.17	-8.62%

Table 6.2 - Extra-Urban Driving Range

6.2.3 Motorway/Highway Driving

Motorway driving range is calculated by averaging the vehicle range of each topology during the US06, US Highway and Artemis Highway driving cycles.

Topology	Drivetrain Type	Range (km)	Range (miles)	Relative Range
<i>A</i>	H ₂ FCEV	524.50	327.82	1.33%
<i>B</i>	H ₂ FCHEV	480.45	300.28	-7.18%
<i>C</i>	H₂FCHEV	517.61	323.51	-
<i>D</i>	H ₂ FCHEV	476.92	298.08	-7.86%
<i>E</i>	H ₂ FCHEV	487.86	304.91	-5.75%
<i>F</i>	H ₂ FCHEV	462.15	288.84	-10.72%
<i>I</i>	H ₂ FCHEV	499.49	312.18	-3.50%
<i>J</i>	BEV	228.08	142.55	-55.94%
<i>Q</i>	H ₂ FCHEV	480.19	300.12	-7.23%

Table 6.3 - Highway Driving Range

6.2.4 Real World Driving

Real world driving range was calculated by averaging the vehicle range of each topology during the Artemis set of real world driving cycles, the Artemis Urban, Road and Highway driving cycles.

Topology	Drivetrain Type	Range (km)	Range (miles)	Relative Range
<i>A</i>	H ₂ FCEV	363.87	227.42	1.74%
<i>B</i>	H ₂ FCHEV	330.79	206.75	-7.51%
<i>C</i>	H₂FCHEV	357.64	223.52	-
<i>D</i>	H ₂ FCHEV	326.10	203.82	-8.82%
<i>E</i>	H ₂ FCHEV	339.36	212.10	-5.11%
<i>F</i>	H ₂ FCHEV	317.45	198.40	-11.24%
<i>I</i>	H ₂ FCHEV	342.94	214.34	-4.11%
<i>J</i>	BEV	160.95	100.60	-55.00%
<i>Q</i>	H ₂ FCHEV	330.52	206.58	-7.58%

Table 6.4 - Real World Driving Range

6.2.5 Combined Driving

Combined driving range was calculated by averaging the vehicle range of each topology during the NEDC, J10-15 and FTP-75 combined driving cycles.

Topology	Drivetrain Type	Range (km)	Range (miles)	Relative Range
<i>A</i>	H ₂ FCEV	472.27	295.17	2.21%
<i>B</i>	H ₂ FCHEV	422.12	263.83	-8.65%
<i>C</i>	H₂FCHEV	462.08	288.80	-
<i>D</i>	H ₂ FCHEV	417.14	260.71	-9.73%
<i>E</i>	H ₂ FCHEV	427.01	266.88	-7.59%
<i>F</i>	H ₂ FCHEV	397.52	248.45	-13.97%
<i>I</i>	H ₂ FCHEV	425.10	265.69	-8.00%
<i>J</i>	BEV	197.41	123.38	-57.28%
<i>Q</i>	H ₂ FCHEV	419.76	262.35	-9.16%

Table 6.5 - Combined Driving Range

6.2.6 European Market

The European market driving range was calculated by averaging the vehicle range of each topology during the ECE, EUDC and NEDC driving cycles.

Topology	Drivetrain Type	Range (km)	Range (miles)	Relative Range
<i>A</i>	H ₂ FCEV	528.83	330.52	2.23%
<i>B</i>	H ₂ FCHEV	469.41	293.38	-9.26%
<i>C</i>	H₂FCHEV	517.28	323.30	-
<i>D</i>	H ₂ FCHEV	464.26	290.16	-10.25%
<i>E</i>	H ₂ FCHEV	474.45	296.53	-8.28%
<i>F</i>	H ₂ FCHEV	439.76	274.85	-14.99%
<i>I</i>	H ₂ FCHEV	496.72	310.45	-3.97%
<i>J</i>	BEV	223.25	139.53	-56.84%
<i>Q</i>	H ₂ FCHEV	468.95	293.10	-9.34%

Table 6.6 - European Market Driving Range

6.2.7 North American Market

The North American market driving range was calculated by averaging the vehicle range of each topology during the NYCC, UDDS, US Highway, FTP-75 and US06 driving cycles.

Topology	Drivetrain Type	Range (km)	Range (miles)	Relative Range
<i>A</i>	H ₂ FCEV	471.53	294.71	1.44%
<i>B</i>	H ₂ FCHEV	424.74	265.46	-8.63%
<i>C</i>	H₂FCHEV	464.83	290.52	-
<i>D</i>	H ₂ FCHEV	420.96	263.10	-9.44%
<i>E</i>	H ₂ FCHEV	430.48	269.05	-7.39%
<i>F</i>	H ₂ FCHEV	401.85	251.16	-13.55%
<i>I</i>	H ₂ FCHEV	434.88	271.80	-6.44%
<i>J</i>	BEV	202.74	126.71	-56.38%
<i>Q</i>	H ₂ FCHEV	423.08	264.43	-8.98%

Table 6.7 - North American Market Driving Range

6.2.8 Japanese Market

The Japanese market driving range was calculated by averaging the vehicle range of each topology during the J10, J15 and J10-15 driving cycles.

Topology	Drivetrain Type	Range (km)	Range (miles)	Relative Range
<i>A</i>	H ₂ FCEV	438.91	274.32	2.10%
<i>B</i>	H ₂ FCHEV	393.20	245.75	-8.53%
<i>C</i>	H₂FCHEV	429.87	268.67	-
<i>D</i>	H ₂ FCHEV	389.68	243.55	-9.35%
<i>E</i>	H ₂ FCHEV	388.19	242.62	-9.70%
<i>F</i>	H ₂ FCHEV	370.79	231.74	-13.74%
<i>I</i>	H ₂ FCHEV	434.12	271.33	0.99%
<i>J</i>	BEV	182.42	114.01	-57.57%
<i>Q</i>	H ₂ FCHEV	391.70	244.81	-8.88%

Table 6.8 - Japanese Market Driving Range

6.2.9 Vehicle Driving Range Results Summary

Topology C had the highest driving range of any H₂FCHEV in all modes of driving. Topology A, the only non-hybridised H₂FCEV topology, was marginally higher but due to poor performance it could not follow and maintain the speed profile of many of the driving cycles accurately and was excluded from further comparison. During very low performance cycles, such as the ECE or J10, the battery is used very little, if at all as the acceleration and the rate of change in power demand is low. Effectively during these

periods Topology C is using the same power pathway as Topology A, not using its battery and carrying round the battery and power converter as dead weight.

It is abundantly clear from all the results that the vehicle exceeds the range of the BEV simulation model, more than doubling the range in all cases.

6.2.10 Driving Mode Summary

Plotting the ranges for each driving mode reveals a slightly surprising trend. It was expected that highway driving would be more efficient and thus yield longer ranges than extra urban driving and the real world driving cycles since the modal highway cycles tend to have large periods of relatively constant high speeds. Figure 6.1 shows this not to be the case.

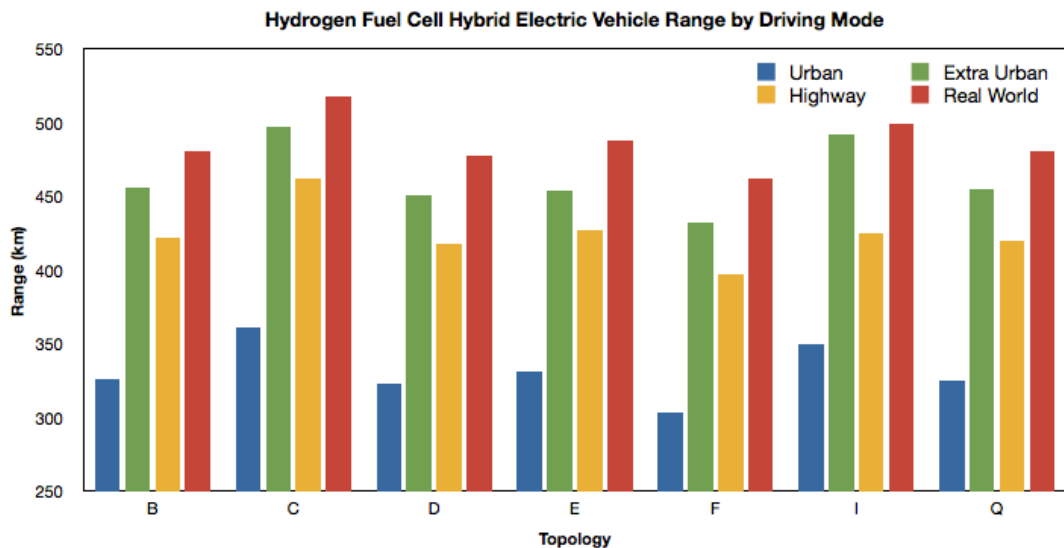


Figure 6.1 - H₂FCHEV Range by Driving Mode¹

After further analysis it became clear that the aggressive US06 driving cycle was having an adverse impact on the entire highway range dataset and distorting the graph. The US06 cycle has frequent periods of extreme acceleration. The maximum acceleration of the cycle is 3.73 m/s², more than double the 1.42m/s² of the US Highway Cycle.

The data was therefore re-plotted, excluding the US06 cycle from the highway range dataset. The results are shown overleaf in Figure 6.2. The average increase in highway driving range was 147km, an extra 32% for a given quantity of fuel. This significant difference demonstrates the sensitivity of the H₂FCHEV to driving style and furthermore

¹ Note the Y-axis origin has been shifted to aid clear visualisation of the differences between the topologies.

the BEV does not exhibit the same high variance between the different highway cycles. This is because of the penalty incurred by having to recharge the hybrid power storage device after discharge.

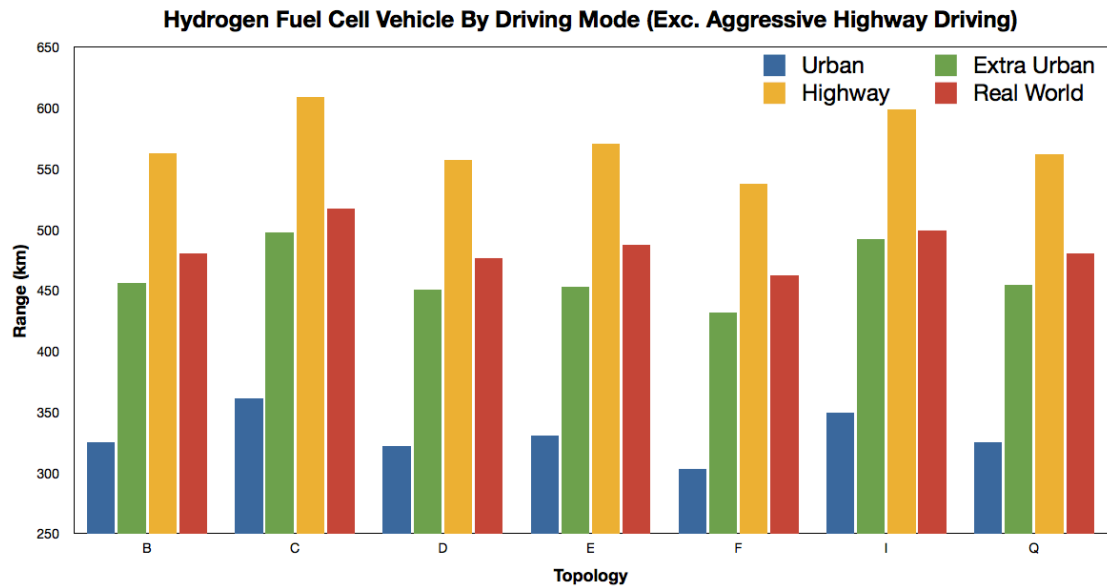


Figure 6.2 - H2FCHEV Range by Driving Mode (Excluding Aggressive Highway Driving)¹

6.2.11 World Market Summary

When each world market simulated is analysed side by side the results are quite striking and highlight one of the key observations of this thesis. The general pre-conception about world automotive markets, at least from a UK point of view is that North America loves its big cars with high displacement, low efficiency engines. The Far East, with much more densely populated metropolitan area prefers predominantly smaller city cars with small, high efficiency engines and that Europe lies somewhere between the two. None of these pre-conceptions however influence production of vehicles to an extent that stops manufacturers importing into different markets. A city car ICEV manufactured in Japan will perform perfectly adequately in any European or US city.

As illustrated in Figure 6.3 overleaf, the simulations show that according to the legislative driving cycles of each region, within each vehicle topology there is a significant variation in vehicle range in the different world market areas and that typically the European range is higher than the US range which is higher than the Japanese range.

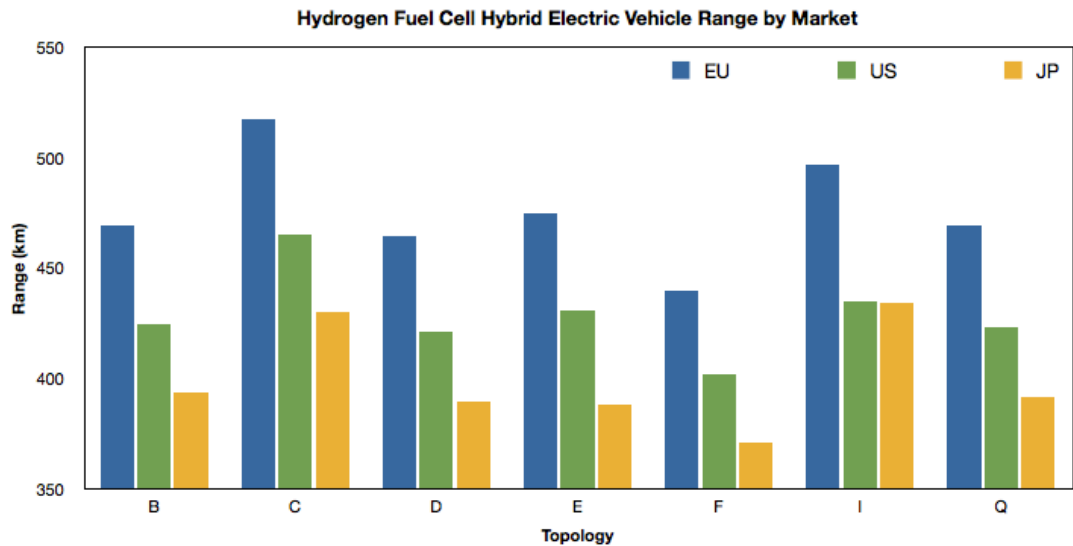


Figure 6.3 - H₂FCHEV Range by Market¹

6.3 Vehicle Performance

Vehicle performance is another important aspect of analysing any passenger vehicle that will ultimately be targeted at consumers. Even though the majority of vehicles sold are done so primarily on the basis of utility or economy, the market for performance models of these vehicles or dedicated sports and performance models is significant and in many cases is where the highest margins for manufacturers lies.

Beyond the raw figures, there is also a psychological aspect of motoring that manufacturers lean heavily on when marketing their vehicles. Though the reality of most driving is mundane trips on over crowded roads to work or the shops, many people also buy into the idea that at the first sign of open road they can open the throttle and glide round the corners at speed. A quick examination of automotive TV advertising reveals premium variants of any given marque being driven through perfectly surfaced; empty Alpine passes in glorious sunshine.

This is where the ideals of renewable energy clash with the reality of selling cars. Performance and efficiency are diametrically opposed and high performance comes at a cost. It is clear from the sales of Golf GTI, Astra VXR, BMW M Sport models and the like that there is an established market though and we need to ensure that we know where the

¹ Note the Y-axis origin has been shifted to aid clear visualisation of the differences between the topologies.

performance of fuel cell vehicles lies and how it can be improved if necessary to ensure topologies can be designed to meet all corners of the market.

6.3.1 0-60mph (0-96km/h) Acceleration Test

The 0-60mph-acceleration test is oft quoted as the defining factor in a vehicles performance. Whilst the truest indicator of flat out acceleration ability, there are few situations in real world driving where it is either necessary or safe and beyond marketing materials and track days its use is questionable. Nevertheless it is needed for comparison.

Topology	Drivetrain Type	0-60mph (s)	Relative 0-60mph Time ¹
<i>A</i>	H ₂ FCEV	18.48	+34.8%
<i>B</i>	H₂FCHEV	13.71	-
<i>C</i>	H ₂ FCHEV	15.27	+11.4%
<i>D</i>	H ₂ FCHEV	14.88	+8.5%
<i>E</i>	H ₂ FCHEV	15.27	+11.4%
<i>F</i>	H ₂ FCHEV	13.96	+1.8%
<i>I</i>	H ₂ FCHEV	19.13	+39%
<i>J</i>	BEV	12.73	-7.2%
<i>Q</i>	H₂FCHEV	13.71	-
<i>1.6l Ref</i> ²	ICEV	11.60	-15.4%

Table 6.9 – 0-60mph Acceleration Test Results

6.3.2 50-60mph (80-112km/h) Passing Speed Test

The passing speed test is the much more useful indicator of the performance of a vehicle as it gives an indicator of the vehicles ability to overtake safely and passing slower vehicles on the motorway is probably one of the most common driving manoeuvres where a typical motorist pushes the performance capability of their vehicle.

¹ The relative 0-60mph and 70-50mph times are quoted relative to the highest performance H₂FCEV topologies, Topology B and Topology Q.

² The reference case is a 1.6l petrol ICEV production version of the vehicle, the chassis of which this simulation model was based upon.

Topology	Drivetrain Type	50-70mph (s)	Relative 50-70mph Time
<i>A</i>	H ₂ FCEV	12.01	+56.8%
<i>B</i>	H₂FCHEV	7.66	-
<i>C</i>	H ₂ FCHEV	9.19	+20.0%
<i>D</i>	H ₂ FCHEV	8.89	+16.1%
<i>E</i>	H ₂ FCHEV	9.26	+20.9%
<i>F</i>	H ₂ FCHEV	7.83	+2.2%
<i>I</i>	H ₂ FCHEV	9.81	+28%
<i>J</i>	BEV	6.79	-11.6%
<i>Q</i>	H₂FCHEV	7.66	-

Table 6.10 – 50-70mph Passing Speed Test Results

6.3.3 Gradeability

The gradeability of the vehicle is of variable importance depending on the application and perspective. For a vehicle for use on an airfield, or a city car limited to travelling around London, it is of relatively little concern. However consider that same car in some of the more hilly parts of the UK, such as the author's native Yorkshire. A driver needs to be certain that when they come ascend a 14% hill that they can get to the top and at this moment gradeability becomes the main performance metric that the driver should be concerned with.

Topology	Drivetrain Type	Gradeability
A	H₂FCEV	19%
<i>B</i>	H ₂ FCHEV	> 25%
<i>C</i>	H ₂ FCHEV	> 25%
<i>D</i>	H ₂ FCHEV	> 25%
<i>E</i>	H ₂ FCHEV	> 25%
<i>F</i>	H ₂ FCHEV	> 25%
<i>I</i>	H ₂ FCHEV	> 25%
<i>J</i>	BEV	> 25%
<i>Q</i>	H ₂ FCHEV	> 25%

Table 6.11 - Vehicle Gradeability Test Result

All vehicles passed the gradeability test with the exception of Topology A, a result that again highlights the need for hybridisation in the H₂FCEV drive train to deliver acceptable vehicle performance.

6.3.4 Vehicle Performance Summary

As would be expected, the topology with the fastest 0-96kph also had the quickest passing speed. Topology B and Q both obtained the same time, with some difference in the third decimal place. This was to be expected, as they are effectively the same topology save for the small and relatively lightweight battery charging DC-DC converter that plays no part in power delivery during acceleration.

The proportional relationship between the passing speed and acceleration would not necessarily hold true in ICEV vehicles and is worth noting that is a consequence of the torque speed profile of the electric motor. In ICEV vehicles petrol engine vehicles that can pickup and rev quickly to power will do well in 0-60mph tests. Whilst any high performance vehicle will have a good 50-70mph performance, it is not unusual for some turbo diesel vehicles to have a higher passing performance than a petrol engine vehicle that has a better 0-60mph performance. The higher torque of the diesel engine being the dominant factor once a vehicle is already moving.

The quickest 0-60mph performance is not as quick as the 1.6l ICEV version of the vehicle the chassis of which was used in the simulation model. There are a number of reasons for this, the H₂FCHEV is heavier and although the fixed gear ratio of the transmission attached to the electric motor is relatively high, the 1st gear ratio of the 1.6l ICEV is 35% higher, enabling higher initial acceleration.

6.3.5 The Need For Hybridisation

As mentioned earlier in this chapter, Topology A was unable to follow all of the driving cycles accurately and it also failed the basic gradeability test set out in [240]. The main reason for using an energy storage system to hybridise the drive train has been born out by the simulation. The slow response time of the fuel cell creates a power demand deficit in the drive train and the performance suffers as a result. Figure 6.4 shows the vehicle speed plotted against the driving cycle speed of Topology A during a section¹ of the US06 cycle. It is clear that the vehicle cannot keep up with the demanded speed of the cycle.

¹ A section is used to aid the illustrative process. The length of cycles prohibits seeing any significant detail when the whole cycle is shown in the space available.

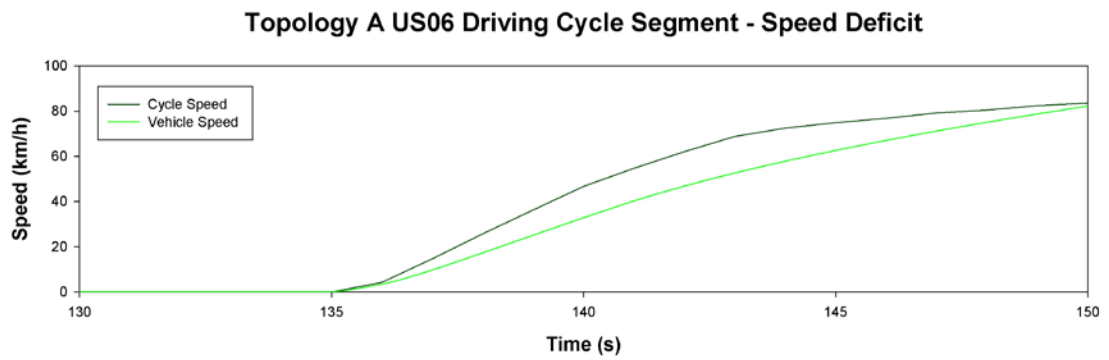


Figure 6.4 - Topology A US06 Driving Cycle Speed Deficit

Figure 6.5 overleaf shows the reason behind this. The fuel cell is at first capable of meeting the modest increase in power required by the speed profile. However when the driving cycle starts demanding higher acceleration, the rate at which the fuel cell output current can rise becomes a dominant factor and the power available is not sufficient to meet demand.

The response of the controller is to ramp up the power demand signal, ultimately beyond that which the fuel cell can provide. Since the fuel cell consumes some of its output power to power its compressor and humidification systems, it cannot meet the peak power requirements of the motor. The controller presumes that the balance of power can be met by the energy storage system however in Topology A this is absent and the power gap cannot be met.

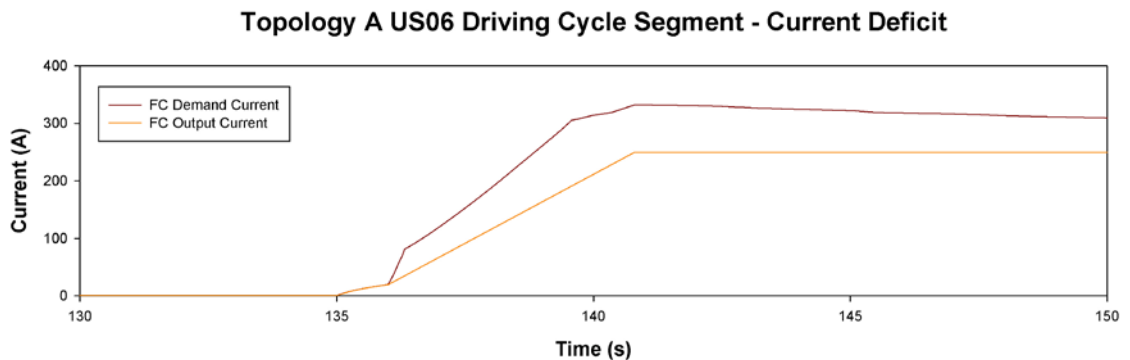


Figure 6.5 - Topology A US06 Driving Cycle Current Deficit

The demands of a cycle like the US06 are perhaps best illustrated by viewing the demands placed on the hybrid energy storage system in the hybrid topologies. Figure 6.6 shows a plot of the fuel cell and battery current during the entire US06 driving cycle.

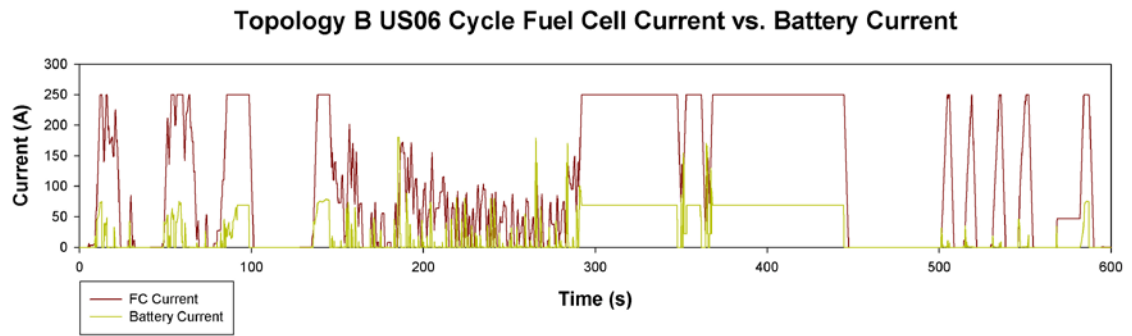


Figure 6.6 - Topology B US06 Driving Cycle Fuel Cell & Battery Currents

The periods of acceleration where the fuel cell cannot meet demand are clear, as is the battery current dropping away once the fuel cell has reached the demand set point. The graph also shows the battery meeting the gap in demand between the fuel cell output and demand power when the power demand exceeds the fuel cell capability. Examination of the US06 cycle has shown a slight distortion in the results and error in the controller. The maximum speed during the US06 cycle exceeds the maximum speed of the vehicle. The simulation model limits the maximum speed, but the controller still sees an error between actual and demanded speed and therefore continues to try and accelerate the vehicle. The US06 and Artemis Highway cycles are the only cycles where this occurs.

In some of the less arduous cycles the fuel cell response rate does not make as significant a difference, though the energy storage system is still used, though more infrequently. This highlights the differences in optimal hybridisation ratios between the different driving modes.

6.4 Drivetrain Efficiency

Ultimately the efficiency of the drivetrain is another way of expressing the range and there is a direct relationship between the efficiency and the range figures so these results do not portray a different picture of the topologies. Whilst vehicle range is a concept common to electric vehicles though, it is not one used to market ICEV. The fuel efficiency is quoted as a way for people to calculate the fuel cost per mile, a measure that is more commonly used to measure the cost of motoring. Filling stations are numerous and the standard vehicle tank sizes of 50-70l mean that most typical journeys do not require a refill.

6.4.1 Overall Efficiency by Driving Mode

The overall efficiency by driving mode was calculated by averaging the efficiency of each topology during each class of driving cycles, as previously shown in Table 5.4. Again, as expected from the range results shown earlier Topology C is the most efficient H₂FCHEV, save for the twin motor arrangement in Topology I yielding a better real world MPGe figure.

Although notable and potentially significant, Topology I exhibited certain control problems that will be discussed later in this chapter and its results should carry a certain degree of uncertainty about them as a result. The difference is also slight and when compared to the increased cost of having multiple drives in the system, may not be of any economic benefit if the accuracy of the data could be confirmed.

Topology	Drivetrain Type	MPGe (Urban)	MPGe (Extra Urban)	MPGe (Highway)	MPGe (Combined)	MPGe (Real World)
<i>A</i>	H ₂ FCEV	38.33	52.86	54.64	49.19	45.72
<i>B</i>	H ₂ FCHEV	33.91	47.52	50.05	43.97	40.96
<i>C</i>	H₂FCHEV	37.65	51.82	53.92	48.13	44.78
<i>D</i>	H ₂ FCHEV	33.57	46.92	49.68	43.45	40.59
<i>E</i>	H ₂ FCHEV	34.45	47.23	50.82	44.48	40.44
<i>F</i>	H ₂ FCHEV	31.62	45.01	48.14	41.41	38.62
<i>I</i>	H ₂ FCHEV	36.37	51.27	52.03	44.28	45.22
<i>J'</i>	BEV	87.79	120.77	127.16	110.06	101.70
<i>Q</i>	H ₂ FCHEV	33.86	47.35	50.02	43.73	40.80
<i>1.6l Ref</i> ²	ICEV	29.7	49.6	N/A	39.8	N/A

Table 6.12 - Driving Mode Efficiency

¹ The figure quoted for Topology J, the BEV, is MPGe based on 1 imperial gallon of petrol containing 40.44kWh of energy.

² The reference case is a 1.6l petrol ICEV production version of the vehicle, the chassis of which this simulation model was based upon. Figures quoted are in MPG for this case.

Topology	Drivetrain Type	MPGe (Urban)	MPGe (Extra Urban)	MPGe (Highway)	MPGe (Combined)	MPGe (Real World)
<i>A</i>	H ₂ FCEV	1.82%	2.00%	2.21%	1.33%	2.10%
<i>B</i>	H ₂ FCHEV	-9.92%	-8.31%	-8.65%	-7.18%	-8.53%
<i>C</i>	H ₂ FCHEV	-	-	-	-	-0.99%
<i>D</i>	H ₂ FCHEV	-10.82%	-9.46%	-9.73%	-7.86%	-9.35%
<i>E</i>	H ₂ FCHEV	-8.49%	-8.87%	-7.59%	-5.75%	-9.70%
<i>F</i>	H ₂ FCHEV	-16.00%	-13.14%	-13.97%	-10.72%	-13.74%
<i>I</i>	H ₂ FCHEV	-3.40%	-1.07%	-8.00%	-3.50%	-
<i>J</i>	BEV	168.17%	168.02%	162.97%	171.22%	161.20%
<i>Q</i>	H ₂ FCHEV	-10.05%	-8.63%	-9.16%	-7.23%	-8.88%

Table 6.13 – Relative Driving Mode Efficiency

6.4.2 Overall Efficiency by Market

The overall efficiency for each world market region was calculated from the average efficiency of all the legislative driving cycles of that region for each topology. Again the data bears out the differences between the European, North American and Japanese markets.

Topology	Drivetrain Type	MPGe (European)	MPGe (North American)	MPGe (Japanese)
<i>A</i>	H ₂ FCEV	55.09	49.12	45.72
<i>B</i>	H ₂ FCHEV	48.90	44.24	40.96
<i>C</i>	H₂FCHEV	53.88	48.42	44.78
<i>D</i>	H ₂ FCHEV	48.36	43.85	40.59
<i>E</i>	H ₂ FCHEV	49.42	44.84	40.44
<i>F</i>	H ₂ FCHEV	45.81	41.86	38.62
<i>I</i>	H ₂ FCHEV	51.74	45.30	45.22
<i>J</i>	BEV	124.47	113.04	101.70
<i>Q</i>	H ₂ FCHEV	48.85	44.07	40.80

Table 6.14 - Efficiency by Market

For the most efficient topology, Topology C, the difference between the European and Japanese efficiency is 16.9%. Although there is no current market price for hydrogen, since we have an equivalent measure we can express this in terms of the current market price of gasoline in the UK, which is around £1.30 a litre. To a motorist driving 12,000 miles a year

the difference in fuel cost is significant at around £270, which is approximately 1.2% of the mean UK household income.

Topology	Drivetrain Type	MPGe (European)	MPGe (North American)	MPGe (Japanese)
<i>A</i>	H ₂ FCEV	2.25%	1.45%	2.10%
<i>B</i>	H ₂ FCEV	-9.24%	-8.63%	-8.53%
<i>C</i>	H ₂ FCEV	-	-	-
<i>D</i>	H ₂ FCEV	-10.24%	-9.44%	-9.36%
<i>E</i>	H ₂ FCEV	-8.28%	-7.39%	-9.69%
<i>F</i>	H ₂ FCEV	-14.98%	-13.55%	-13.76%
<i>I</i>	H ₂ FCEV	-3.97%	-6.44%	0.98%
<i>J</i>	BEV	131.01%	133.46%	127.11%
<i>Q</i>	H ₂ FCEV	-9.34%	-8.98%	-8.89%

Table 6.15 - Relative Efficiency by Market

6.5 Electrical Performance

The electrical performance data is key to assessing the accuracy of the topology analysis carried out in Chapter 4.5 and shown in Table 4.70. It also highlights for the first time in the results, the influence of the power pathways on the overall system efficiency. The simple topology analysis showed that Topology E was the most efficient yet as is now clear from all the data shown in this chapter the results of the simulation model suggest that it is in fact Topology C.

6.5.1 Drivetrain Electrical Efficiency

The average electrical efficiency of each power pathway in the drivetrain was calculated for each topology and is shown below in Table 6.16. For the first time in the results we can see that different drive trains are optimal for the various power pathways and that despite being the most efficient overall, Topology C does not have optimal electrical characteristics across the board.

Topology	Fuel Cell Efficiency	Battery System Efficiency	Battery Charging Efficiency	Motor Drive Efficiency	Fuel Cell to Road Efficiency	Battery to Road Efficiency
<i>A</i>	44.23%	N/A	N/A	72.99%	32.28%	N/A
<i>B</i>	39.34%	80.32%	43.02%	72.11%	28.37%	57.92%
<i>C</i>	44.47%	79.15%	43.25%	72.01%	32.02%	57.00%
<i>D</i>	38.85%	73.97%	43.23%	72.31%	28.09%	53.49%
<i>E</i>	39.15%	98.8%	45.42%	71.91%	28.15%	71.05%
<i>F</i>	34.82%	94.05%	45.7%	72.31%	25.18%	68.01%
<i>I</i>	44.57%	98.52%	45.81%	65.88%	29.36%	64.90%
<i>J</i>	N/A	98.71%	N/A	73.11%	N/A	72.17
<i>Q</i>	39.42%	80.32%	45.57%	72.23%	28.47%	58.02%

Table 6.16 - Electrical Performance

Control issues aside for a moment, the twin motor arrangement, Topology I also exhibits the intrinsic electrical efficiency advantages of coupling the power sources together mechanically and not electrically, eliminating the need for power converters from the system entirely. The penalty of putting multiple power converters in the power pathway to obtain high performance is starkly illustrated by Topology F, confirming the earlier high level analysis though the 3.6% difference between the high performance Topology B and the high efficiency Topology A is also worth highlighting as it shows the economic compromise that must be made for obtaining greater performance in the H₂FCHEV.

6.5.2 Power Consumption

The MPGe figure quantified the performance of the drivetrain in terms relative to ICEVs. For electrical vehicles, a more typical, useful and readily understandable measure of the intrinsic efficiency of the drivetrain system is the power consumed per km in Wh.

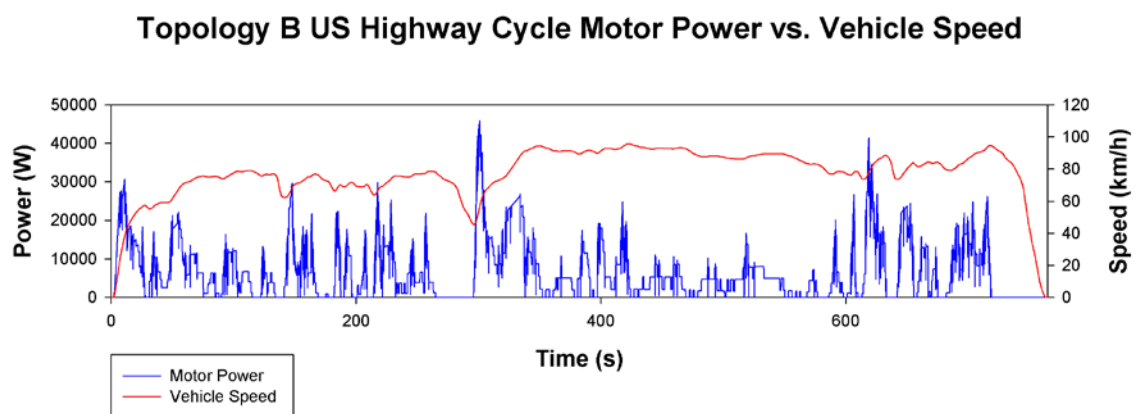


Figure 6.7 - Power Consumption During US Highway Driving Cycle

Figure 6.7 shows an example of the power consumed by the drivetrain during the US Highway driving cycle. Table 6.17 tabulates the Wh/km consumption for the different modes of driving simulated. Once again Topology C is clearly the most efficient drive train with the lowest Wh/km consumption in all modes of driving.

Topology	Drivetrain Type	Wh/km (Urban)	Wh/km (Extra Urban)	Wh/km (Highway)	Wh/km (Combined)	Wh/km (Real World)
<i>A</i>	H ₂ FCEV	452.49	328.12	317.44	352.55	457.59
<i>B</i>	H ₂ FCHEV	511.45	365.01	346.55	394.44	503.33
<i>C</i>	H₂FCHEV	460.70	334.69	321.67	360.33	465.55
<i>D</i>	H ₂ FCHEV	516.62	369.65	349.11	399.15	510.57
<i>E</i>	H ₂ FCHEV	503.42	367.26	341.29	389.93	490.63
<i>F</i>	H ₂ FCHEV	548.43	385.33	360.28	418.84	524.50
<i>I</i>	H ₂ FCHEV	476.93	338.31	333.34	391.67	485.51
<i>J'</i>	BEV	222.29	161.58	153.46	177.29	217.45
<i>Q</i>	H ₂ FCHEV	512.19	366.28	346.73	396.65	503.75

Table 6.17 - Vehicle Energy Consumption in MPGe

6.5.3 System Power Flow Visualisation

The electrical performance data has highlighted the difference between the high level review and the simulation results. The question is why did the high level review conclude Topology E to be the most efficient. The answer was obtained by visualising the power flows in the various driving cycles.

The high level review assigned an average steady state value to each of the power pathways in the topologies and then averaged them together. The steady state values are themselves an approximation and a source of potential error but the larger problem is that all the power pathways were simply averaged together with no weighting or consideration of their duty cycle. As previously stated in establishing the need for hybridisation, the utilisation of the energy storage system in the drive train varies between driving cycles. Thus the efficiency of the battery to wheel and fuel cell to battery pathways does not have the same influence on the overall system efficiency as the fuel cell to wheel pathway, which is in the majority of cases the dominant power dissipation route.

¹ The figure quoted for Topology J, the BEV, is based on the battery capacity.

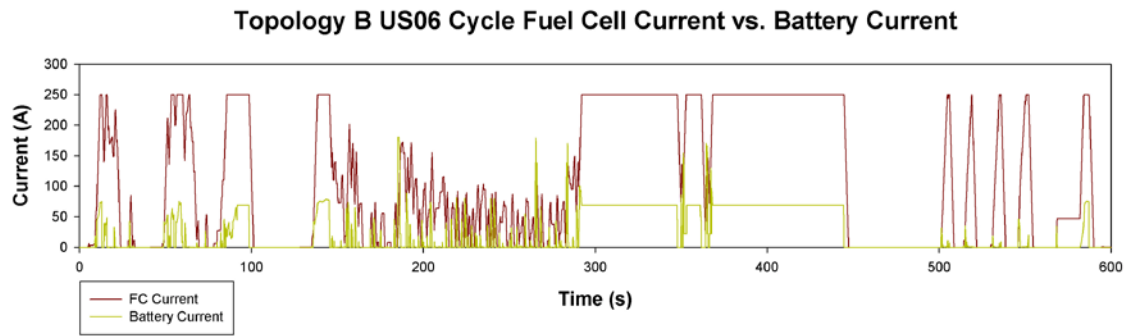


Figure 6.6 - Topology B US06 Driving Cycle Fuel Cell & Battery Currents

shows the energy storage system working hard during one of the most arduous driving cycles. However in some cycles, the data shows that the hybrid power source is barely used. The utilisation of the ESS during two of the less arduous cycles, one high speed and one low speed are shown below. The US Highway cycle in Figure 6.8 shows a high speed, yet relatively low acceleration driving cycle. It is clear that save for the initial power demand during acceleration, the ESS is barely used. In the ECE urban driving cycle, shown in Figure 6.9, where the acceleration is even less demanding the ESS is used even less and at this point can almost be considered a dead weight. It is certain that the hybridisation ratio in Topology B is not optimal for either of these driving cycles.

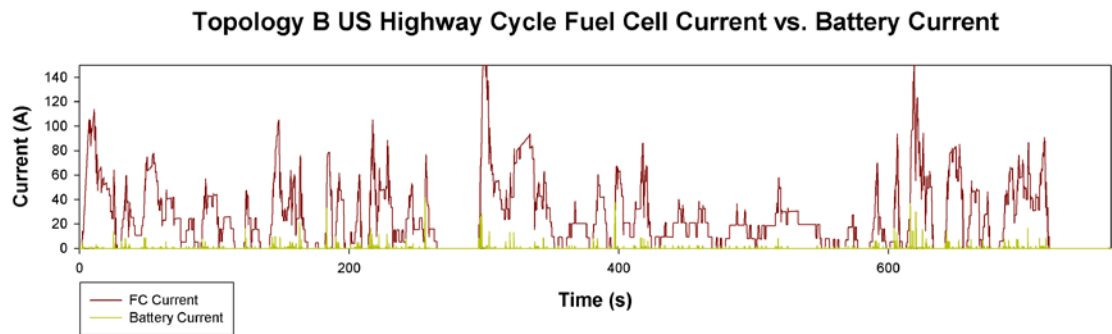


Figure 6.8 - Topology B US Highway Cycle Fuel Cell & Battery Current

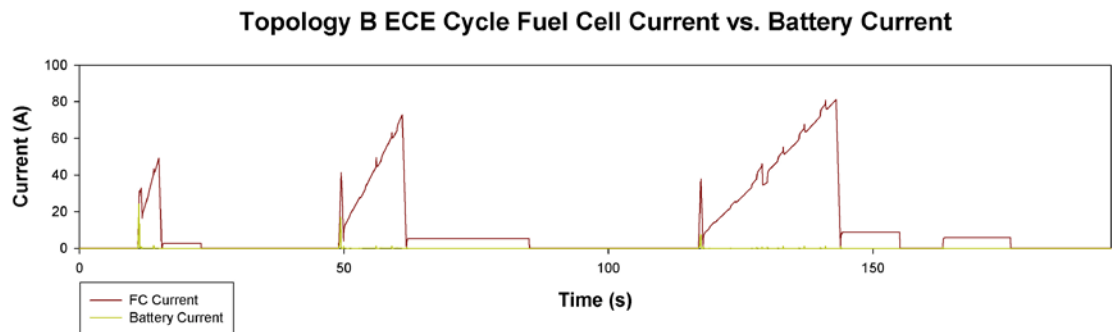


Figure 6.9 - Topology B ECE Cycle Fuel Cell & Battery Current

Topology B has been chosen to present this data as the average difference of this phenomena between topologies is not significant and a direct comparison with the same topology is the most accurate way of visualising the results.

6.5.4 Energy Source Performance Under Load

One of the main assertions of this thesis is that the IV characteristics of the energy sources require power converters to fix the voltage to obtain maximum performance from the drive. We have confirmed that a performance advantage can be gained by doing this and that it comes with an efficiency, weight and cost penalty, but as it is such a key point that there can no doubt as to the necessity. Visualising how the voltage of the energy sources behaves under load can fulfil this requirement.

The battery and fuel cell terminal voltage was measured during every cycle and two cases at opposite ends of the demand spectrum are shown below. Figure 6.10 shows the variance in the fuel cell and battery voltages during the relatively sedate yet speedy US Highway cycle and illustrates that even during this cycle, the fuel cell voltage declines by around 20% of the no-load voltage and reduces the maximum torque at full speed by around 50%.

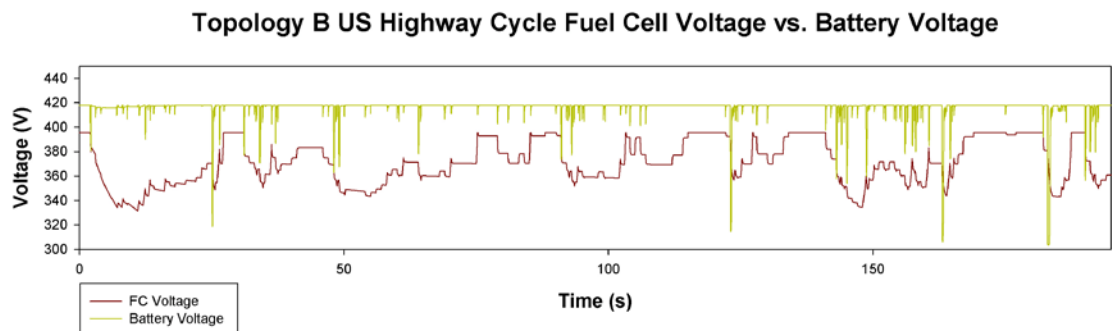


Figure 6.10 - Topology B US Highway Cycle Energy Source Terminal Voltages

Figure 6.11 shows the voltage declining even more significantly during the arduous US06 driving cycle further reducing the maximum available torque during this high speed cycle and ultimately were it not for the speed limits imposed by the motor and gear ratio combination it would be the dominant limiting factor in vehicle performance.

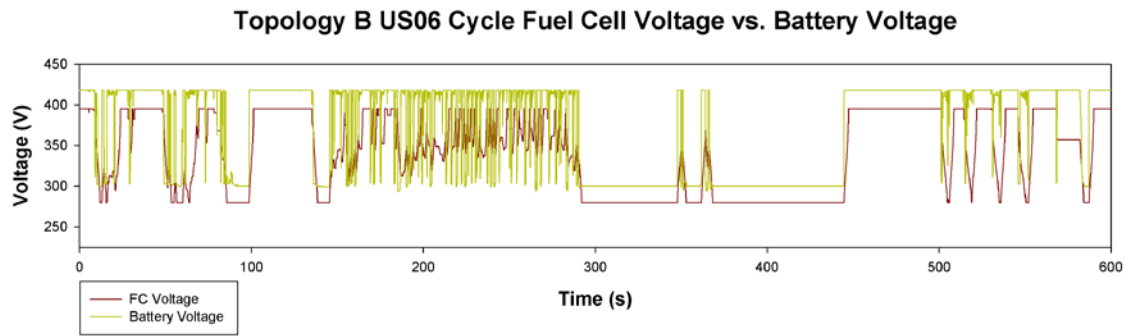


Figure 6.11 - Topology B US06 Cycle Energy Source Terminal Voltages

6.5.5 Electrical Performance Summary

The results show that the earlier high level steady state topology analysis was wrong to select Topology E as the most efficient and that it is in fact, as suggested throughout this chapter, Topology C. The simulations have highlighted that the battery system is not utilised equally during all modes of driving and that the dominant power pathway in the drive train is from the fuel cell to the wheel. The relationship between bus voltage and performance has been confirmed.

6.6 Control Performance

The accuracy of the vehicle controller that simulated the driver and followed the driving cycle during each simulation was of critical importance to this study. If any of the topologies had significantly deviated from the speed time profile of each cycle, comparisons could not be accurately drawn between them.

6.6.1 Vehicle Speed Control

The accuracy of the controller response was measured primarily by comparing the vehicles actual speed to the plot of driving cycle it was following during each simulation. Two of these plots, one for the modal New European Driving Cycle, shown below in Figure 6.13, and one for a magnified section of the real world based New York City Cycle, shown overleaf in Figure 6.15. Both clearly show the accuracy of the vehicle speed controller. The original NEDC and NYCC are shown again for ease of reference.

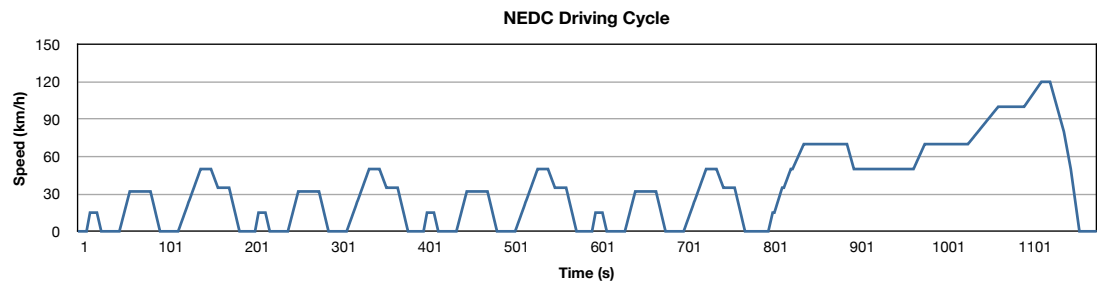


Figure 6.12 - NEDC Driving Cycle

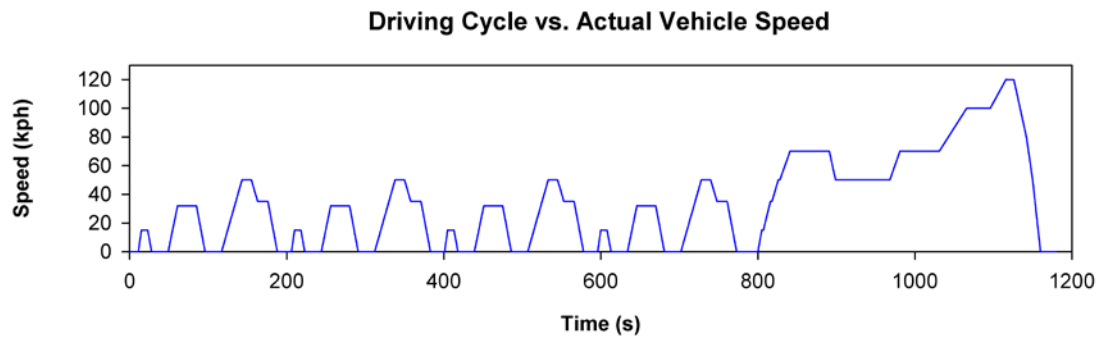


Figure 6.13 - Topology B Actual Speed During NEDC Driving Cycle Simulation

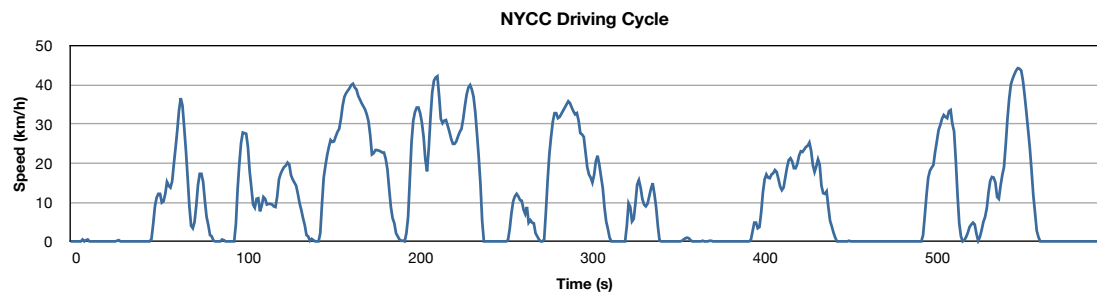


Figure 6.14 - New York City Cycle Driving Cycle

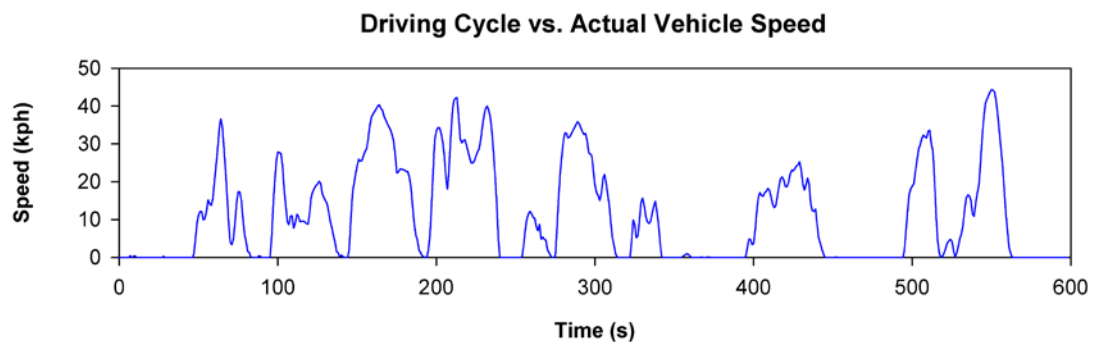


Figure 6.15 - Actual Vehicle Speed for Section of NYCC

The accuracy of these plots can also be confirmed by comparison of the distance travelled during the simulation with the calculated distance of each driving cycle. Due to controller

overshoot and vehicle inertia there will be some difference between the calculated and simulated distances, but for validity it should be negligible. Table 6.18 shows the average distance travelled to six decimal places for a selection of driving cycles and provides a secondary confirmation of the accuracy of the speed control.

Driving Cycle	Driving Cycle Distance Calculated (km)	Average Distance Travelled (km)
<i>NEDC</i>	10.93	10.929947
<i>ECE</i>	0.99	0.993216
<i>US06</i>	12.81	12.792272
<i>USHWY</i>	16.41	16.409451
<i>J10</i>	0.66	0.663041
<i>J10-15</i>	6.34	6.446725
<i>Artemis Urban</i>	4.87	4.867342

Table 6.18 - Simulation Driving Distance Accuracy

6.6.2 Controller Response

If the vehicle speed response is examined in a smaller time frame, two noteworthy elements of the control response become visible.

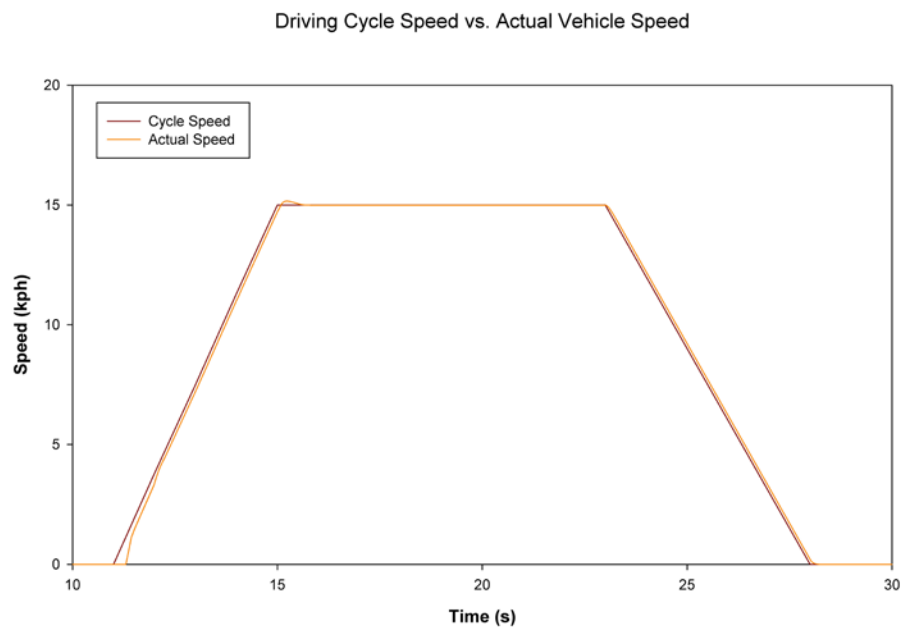


Figure 6.16 - Section of ECE Driving Cycle Simulation

Figure 6.16 shows a plot of cycle and actual vehicle speed for a section of the ECE driving cycle. It can be seen that the vehicle does not respond immediately to the cycle accelerating from rest. This is due to the vehicles inertia. The cycle is simply a speed-time profile,

unconstrained by any physical effects. The vehicle first has to overcome inertia before it can accelerate and the response from rest will always lag the driving cycle somewhat. The vehicle velocity overshoots the driving cycle response when the vehicle stops accelerating at a given speed set point for the same reason, due to inertia it cannot instantaneously change its acceleration.

Also just visible on the plot is the slight shift between the driving cycle speed and actual vehicle speed plots. The vehicle response is delayed by the requirements of the simulation calculations. There are several states in the simulation model where the state calculation relies on its output to calculate its input. At various points during the simulation this forms an algebraic loop that cannot be solved. Simulink has an “algebraic loop breaker” block, designed to break the dependency of a calculation on its own output. This block however does introduce a unit delay into the simulation process. Acceleration and deceleration are uniformly delayed, so the vehicle follows the cycle accurately and there is no impact on the simulation results.

6.6.3 Controller Accuracy

One observation when examining the performance of the vehicle controller was that although the vehicle speed profile was followed correctly, there were occasional spikes in the power demand when the vehicle was accelerating at a constant rate as shown below in Figure 6.17. This is a symptom of the controller overshooting the set point and then over correcting itself.

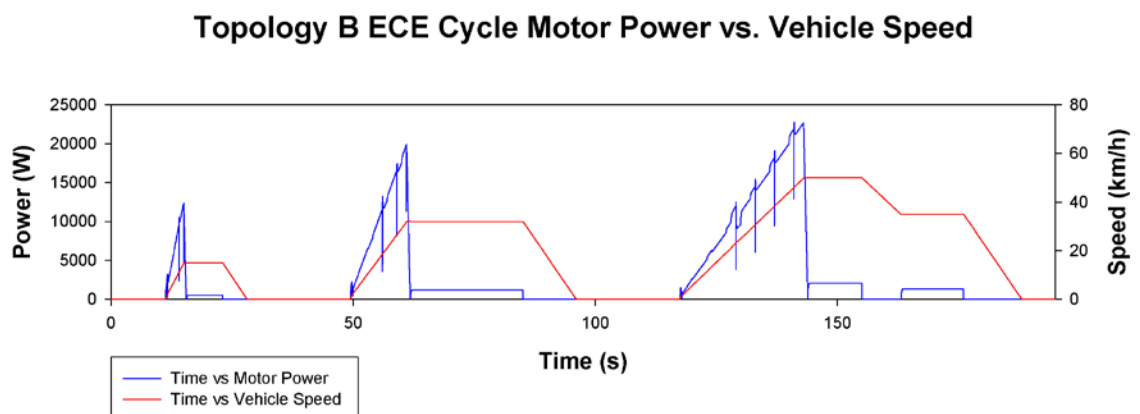


Figure 6.17 - Topology B ECE Cycle Motor Power vs. Speed

The cause was essentially the scale of the simulations. The PI controller was designed and tuned for each topology to make all the topologies follow the speed time profile of the

driving cycles. The controller was not however tuned for each driving cycle. If it were this power set point instability could be eliminated. However, that would expand the number of simulation models used in this thesis from nine to one hundred and twenty six. Furthermore due to the size of the system and the number of components involved, tuning via analytical methods proved impossible and manual tuning was found to be the quickest way of adapting the controller. It would rapidly have become impractical and change management would have become all but impossible. The inertia of the vehicle ensured that this very brief transient spikes had no effect on the accuracy of the vehicles velocity when following a given driving cycle speed time profile and no oscillation about the speed set points occurred.

6.6.4 Topology I Twin Motor Control

Topology I is an interesting case. Combining two electrical motors on a single axle it isolates the power sources and uses them to drive a separate motor. The principle method of control is therefore somewhat different. The broad principle of operation was that the controller would monitor the motor driven by the fuel cell and then command the motor driven by the battery to provide any deficit in torque at the driveshaft. Whilst the principle is relatively easy to explain the implementation proved to be somewhat more complex and at best the controller designed is somewhat of a crude implement. The main issue was, to paraphrase Donald Rumsfeld, that there were too many “unknown unknowns” to have much confidence in the accuracy of the topology model or the veracity of the results. Scaling down the single IM drive used for the other topologies derived the data used to model the two motors. This in itself introduced an initial inaccuracy, as we know the motors would likely not scale linearly. Secondly there was no data available to accurately model the interface between the two motors and the axle, so dynamic modelling of the efficiency of the transmission was not possible. Furthermore in a real system it is likely the boost motor driven by the battery would be isolated by a clutch to prevent friction losses when not being used, this was also not simulated and the motors were both connected to the drive shaft continually. Whilst useful for comparison, the inaccuracy of the controller and the method in which the simulation model was built necessitates a note of caution be attached to the data and results of Topology I.

6.7 Validation

There are several methods of validating the simulation model and the results it has generated. Model validation was defined by Schlesinger et al. in 1979 [241] as:

“Substantiation that a computerised model within its domain of applicability poses a satisfactory range of accuracy consistent with the intended application of the model”

Tsang elaborated further in 1991 [242]:

“We shall understand a model as a combination of (a) conceptual model and (b) computer code, with the relevant model parameters, which are derived from field and laboratory data and information. Only with the combination of these elements is it possible to perform modelling studies whose results may be used as a representation of the actual processes occurring in the real system.”

To the extent possible given the confidentiality and lack of data surrounding some elements of the model, validity is ensured firstly by the use of empirical data when building the models components. Empirical data was used for the motor drive, fuel cell, battery, power diode and DC-DC converters. The vehicle chassis was developed from first principles. Each individual subsystem was then tested and the output checked against the data used to construct it and with due consideration to the relevant physical laws checks were made to ensure each subsystem generated valid outputs for all known operating points.

Validation of the simulation model results as a whole is a less absolute process. The system can be easily monitored dramatic for errors in the model that cause inviolable rules, such as Ohm’s Law or Newton’s Law of Motion to be broken. However, the interconnection of the subsystems and the use of algorithmic control can introduce errors into the system that could cause discrete but nevertheless significant errors to be introduced into the simulation. The usual method of validating a power electronic system is to build the physical system and subject it to laboratory testing then compare the results to the data generated by the simulation model. This would be an undertaking that several of the worlds major automotive groups have yet to carry out and in the context of this study, building a prototype vehicle is out of the question.

The next option would be to build a static scaled hardware prototype in the lab. This however would depend on several elements that would themselves introduce uncertainty. For safety reasons the fuel cell would have to be represented by a digitally controlled power supply, programmed to react like a fuel cell. The wheels and road would be represented by a digitally controlled sink load, either a purely resistive load bank, or a friction brake acting

on the shaft of a motor. The data to control these sinks and sources would come from the simulation model and therefore if the model were erroneous the hardware test system would be invalidated. The hardware test model would allow for a more detailed examination of the transient and thermal characteristics of the power converters, battery and control system but since data from the simulation would still be involved in the hardware test environment it would not serve as a fully independent method of validation.

Another approach to validation is to compare the results of the simulation to contemporary studies in literature and existing production or prototype vehicles and see if they are within reasonable margins of the published data. As has been noted previously, the available data in the literature is by no means a complete reference, but specific excerpts exist so as to aid this method of verification. Prototype data from manufacturers pre-production development and test vehicles is used with the understanding and cautionary note that the publically published statistics are liable to reflect the most positive aspects of the vehicles.

6.7.1 Numerical Validation

To validate the simulation model analytically, Topology C was accelerated to an arbitrarily chosen speed of 70.5kph whereupon it was held at constant velocity. Once the vehicle had stopped accelerating and maintained a steady state for around 100s the relevant parameters inside the drivetrain were measured.

At 70.5kph (19.58 ms^{-1}) the wind resistance force is 44.64N and the frictional resistance force is 121.38. Since $P = Fv$, to maintain a steady speed, the drivetrain needs to deliver 3250.67W to the wheels.

The total power of the fuel cell stack was 10145W and the fuel cell system was operating at an electrical efficiency of 43.96%. The bus power was therefore 4459.74W. At 4905.6rpm ($514.192 \text{ rads}^{-1}$), generating 6.44Nm of torque at the shaft, the motor mechanical power was 3311.40W and the electrical power loss in the motor and inverter drive was measured at 1141.49W. The efficiency of the transmission is 98% therefore 3245.17W is delivered to the wheel. The error between the calculated and actual output is 5.5W or 0.17%. This is well within acceptable tolerances. Figure 6.18 shows a Sankey diagram of these losses.

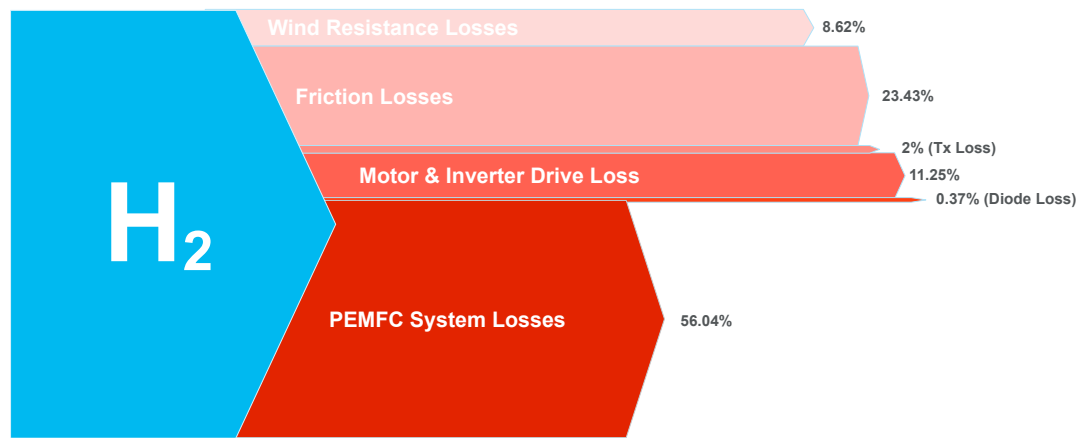


Figure 6.18 - Sankey Diagram - Validation of Power Losses in Topology C at 70.5kph

6.7.2 Validation Against Existing Prototypes

The 2010 Mercedes Benz B Class F-Cell vehicle uses an 80kW PEMFC, 1.2kWh Li-Ion battery and stores 4kg of hydrogen in a 700 bar fourth generation tank. The motor drive is more powerful than the system used in this simulation. It generates 100kW of peak power and 320Nm of torque (vs. 75kW and 260Nm in this study) [243, 244]. This accounts for its faster 0-60 time of 11.4s. The range is quoted at 400km for a 4kg tank. The new topology has a range of 505.24km for a 5kg tank and demonstrates that the range figure obtained by this study for the NEDC driving cycle is realistic and contemporary. The B class is a larger vehicle and has a kerb weight ~400kg more than the vehicle used in this study though it does have a lower drag coefficient of 0.26. The comparable range despite the extra weight would suggest the B class F-Cell drivetrain was more efficient and this is probably true, on the basis of available information the fuel cell stack will likely be 5-15% more efficient than the stack used in this study, which is now nearly 10 years old. The motor has also been changed from an AC induction motor in the previous F-Cell to a permanent magnet synchronous motor, increasing the efficiency of the motor drive as well. Overall the performance gain is claimed to be 30% [245] so the discrepancy in vehicle weight does not invalidate the comparison of vehicle range.

6.7.3 Literature Validation

Several studies in the literature detail vehicle range and efficiency for vehicles similar to the one built in this study. However the majority concentrate on describing and evaluating a single topology, rather than a broad range of topologies. The results of the simulation were compared to the available data and were found to be within acceptable boundaries of the existing published data and comparable to other contemporary works.

Ahluwalia et al. [137] simulated a slightly larger vehicle of around 2000kg that used a 120kW PEMFC system and a Li-Ion battery that could deliver 55kW of peak power. The data suggests the fuel cell system had an average efficiency as much as 20% higher than the stack used in this study. The study also made use of regenerative braking and estimated that 53% could be recovered in the J10-15 cycle, 34% in the US06 cycle and 35% in the NEDC cycle.

The increased stack efficiency and use of regenerative braking explains the discrepancies between the two datasets. Ahluwalia concurs with Sharer et al. [197] in identifying that there is little opportunity to capture regenerative energy during the USHWY cycle and the difference between the two studies is negligible for that cycle.

Given that the fuel cell stack used by Ahluwalia is more efficient, that would suggest the drivetrain arrangement of Topology C is more efficient. The vehicle efficiency for four of the driving cycles also simulated in this study is detailed below in Table 6.19.

Driving Cycle	Ahluwalia et al. MPGe	New Topology MPGe	Relative Difference
<i>NEDC</i>	64	54.57	-14.73%
<i>USHWY</i>	80	83.07	+3.83%
<i>US06</i>	43	34.91	-18.81%
<i>J10-15</i>	61	45.64	-25.18%

Table 6.19 - Vehicle Range Ahluwalia et al. vs. Topology C Validation

Hauer [125] used a fuel cell stack with similar efficiency in a fuel cell battery hybrid topology arranged as per Topology C. The study included regenerative braking and again as shown in Table 6.20 below the difference in efficiency is clear to see, though the increased efficiency for the US Highway Cycle would again suggest that the drivetrain arrangement is more efficient save for not considering regenerative braking.

Driving Cycle	Hauer MPGe	New Topology MPGe	Relative Difference
<i>US06</i>	49	34.91	-22.63
<i>USHWY</i>	70	83.07	+18.67%
<i>ECE</i>	47	44.90	-4.47%

<i>EUDC</i>	63.7	62.19	-1.51%
<i>J1015</i>	55	45.64	-9.36%

Table 6.20 – Vehicle Efficiency Hauer vs. Topology C Validation

6.8 Results Summary

This chapter has presented the results generated by computer simulation of each of the vehicle power drive train topologies selected from the earlier high-level review. Each topology has had its efficiency, performance and control characteristics measured and described herein. Several significant observations about the vehicle topologies have been made and it is clear that Topology C is the most efficient topology and that Topology B is the highest performance topology. A high performance, high efficiency topology does not exist and some key differences between the behaviour of fuel cell electric vehicles under arduous loads when compared to battery electric vehicles has been observed. Some control inaccuracy has been observed but this has not had a significant impact on the outcome. Validation has been performed in qualitative and quantitative domains and the results fall within expected boundaries.

7 Discussion

7.1 Introduction

This chapter will draw on the results shown in the previous chapter and discuss the key themes that have arisen from them and this study as a whole and then proceed to show how this analysis was applied to identify the likely optimal design of future hydrogen fuel cell vehicles, conceptualise a new drive train topology that addresses some of the shortcomings of the existing topologies and suggest further modifications to the vehicle drive trains used to obtain further performance gains.

7.2 Simulation Outcomes

Given that half way through this thesis the results of a high level study of drive trains was presented it is important to highlight the knowledge, data and experience gained from the extensive work that went beyond the high-level study to design, implement, test and eventually run the simulation model for all the different topologies.

The obvious gain from the simulation model was that it showed that the high level, steady state study was inaccurate and identified the wrong topology as the optimal drive train. The steady state analysis could not give us any provable conclusions about vehicle performance either and the wider advantage of the simulation was the wealth of data gained from methodically testing multiple drive trains against differing driving cycles. The steady state analysis could not have revealed the stark contrast between the different motorway driving cycles, nor the difference in performance between BEVs and H₂FCEVs during arduous driving, an observation that will be critical to designing vehicles with acceptable performance and endurance.

The difference between world markets highlighted by applying a broad range of driving cycles justified the decision to use an extensive range of driving cycles. Though aided by the advancing power of desktop computers, this study applied far more than was typically found in contemporary literature and has generated some significant observations as a result.

It was noted earlier that simulation is not a magic bullet in itself, but the study has shown that the optimal drive train will likely require a significant amount of design analysis to find the best sizing and ratio of power sources. Carrying this out by physical prototyping would probably be economically impossible for even a major automotive manufacturer and so simulation will likely play a key part in designing and perfecting the fuel cell vehicles of the future. Academia has much to offer in being part of this process, but the availability of data needs to improve. One regret of this study is that it was not possible to obtain empirical data for the latest fuel cell stack systems or motor drives that several manufacturers have announced since the project started to see how they would have affected the outcome of the simulation, but sadly any useful data has been kept entirely confidential and out of the public domain.

7.3 Component Sizing & Hybridisation Ratio

The results clearly show that the hybrid power source is heavily utilised during some driving cycles and barely used at all during others. This in itself asks several questions but principally what is the single optimum hybridisation ratio between the battery and the fuel cell system. The data only points to one conclusion – there isn't one.

In an ICEV, there are usually a few variants of an engine, but they are all built on the same block and simply electronically tuned or bored out to higher capacity to build higher or lower performance variants. With the fuel cell vehicle we may have an entirely different situation. The cost associated with having multiple fuel cell stack systems is likely to be prohibitive, and manufacturers thus far have generally used a single stack system across multiple prototype chassis sizes. Though this will expand, it is hard to envisage 6-10 different fuel cell engines for a single range of cars being economical. The battery pack will scale more easily, but there is a cost to carrying around a hybrid power source that is going to go largely unused. Not only is it heavy, the batteries, controllers and cooling systems all have a financial price tag attached and a fuel cell stack and lithium ion batteries all carry significantly higher cost per W than an cast metal engine block.

Conversely there is a performance disadvantage to having a vehicle with a battery that is too small or indeed a fuel cell that is too small and then the decision of which power source to make larger comes into play and the question becomes do you construct a FCEV

or a BEV with a fuel cell system that acts as a range extender and just recharges the battery. This study used the battery as a power source to compensate for the fuel cells transient response lag time but there is clearly scope for analysing a multitude of different energy management strategies to further optimise the use of each power source.

The question of how to size and control components will arise, not between model ranges but within the same model dependant upon the type of driving the user intends to do and the part of the world they are driving in. There are compromises to be had potentially and single vehicle models could be made, but they are not ideal in an economic, engineering or scientific sense. The larger question is will the way we own and use cars have to change fundamentally to enable the uptake of H₂FCEVs.

From the engineering perspective, choosing a single drive train topology and then conducting large scale, automated simulation models that have multiple different models for varying sizes of fuel cell and battery systems that change and iterate through many thousands of hybridisation ratios and generate a dataset that can be analysed to determine the optimum ratio for different forms of driving. The simulation model constructed in this thesis could be adapted for this purpose, but the lack of available data on differing sizes of fuel cell and battery packs would prove a large stumbling block to any useful simulation activity. Linear scaling of existing components could be performed, but again it leads to uncertainty as to the accuracy of the results.

7.4 Energy Storage System

This study chose to use batteries alone for its energy storage system. When the review of existing topologies was undertaken there were fuel cell battery hybrid vehicles, and fuel cell super capacitor hybrid vehicles. It is clear that the fuel cell needs electrical energy to start-up and that the super capacitors energy density and self discharge limitation mean that it cannot be used alone and provide an energy source that can be used to drive the vehicle away whilst the fuel cell is starting up.

However, since the study started, the start-up time for fuel cells has decreased significantly. With new systems starting up in a few minutes rather than the eight minutes it takes the stack in this system to start, reducing the energy density required of the battery. Lithium ion battery technology has also not advanced as far as was hoped in 2004 and still has some

significant safety limitations around how it can be used in high power charge/discharge modes. Because it is an electro-chemical device and because it is necessary to interface the battery system to the DC bus through a DC-DC converter in the optimal topologies, there is a lag in how quickly the battery can respond to large steps in demand and similar limits on how much regenerative energy the battery can safely recover from the drive system.

The ultra capacitor however is an electrostatic device and not constrained by the same safety constraints that hamper the lithium ion battery and has a much longer service life of around 1,000,000 full charge discharge cycles, compared to a few thousand for a typical lithium ion battery. In conjunction with deriving the optimal size between the battery and fuel cell it is likely that integrating an amount of super capacitor storage into the energy storage system could produce a system that requires less lithium ion battery cells but that can produce a higher peak power.

The current choice of battery is a trade off between energy density and power density, with many parallel strings of cells in series necessary to produce the required peak power and endurance. In some driving cycles though the battery is barely used, with the low performance mode of driving requiring little compensation for the fuel cells slow transient response. In these situations the battery is an expensive dead weight. Fewer, more energy dense cells could be used with a DC-DC converter stepping up the voltage and a pack of ultra capacitors added to the bus side of the converter to cope with high transient power demands and to capture large quantities of regenerative braking energy. Consideration should be given to the addition of super capacitors into the energy storage system for any component sizing exercise that is undertaken. Recent studies have adopted this approach and suggested methods for controlling the flow of energy between the two energy storage devices and succeeded in capturing more regenerative braking energy whilst using a smaller battery [246-249].

7.5 Not Such a Global Market?

The data shows a significant gap between the range/efficiency of the same topology when driven according to the driving patterns of different markets. Within each market the decline in range during urban driving of the H₂FCEV is a few percentage points worse when compared to the BEV case. Idling losses in the fuel cell system are significant during urban driving where there are long periods sat at rest and unlike the ICEV, which can be

stopped and started almost at will, the lifespan of current PEMFC technology does not allow for repeated start-up and shutdown cycles and the time taken to start-up the stack, (typically around a minute) is prohibitive anyway.

Though the hybrid energy source could be designed to provide the entirety of the fuel cells power output for short periods this will compound the problem of the battery being unnecessarily large and too expensive for the majority of its duty cycle.

Both situations suggest that an optimal topology could be designed for each market and each mode of driving, but not a single topology that could be optimal for all of them. Like the component sizing optimisation just discussed, this will lead to larger product lines and is a sea change in how cars are currently sold. There are major manufacturing and social challenges to address if this is indeed how the automotive sector is to proceed.

The manufacturing sector has already shown some signs of innovation on this front, creating common chassis like the GM Sequel, onto which different bodies can then be dropped. Adapting such a chassis concept to have different sizes of motor, battery and fuel cell would not be a revolutionary and would allow at least some commonality between models to reduce the manufacturing cost of producing so many different types of vehicle.

The consumer side of the market may face somewhat more of a shakeup. The idea of owning a vehicle that will perform your daily commute adequately and then if you so chose will also drive 800 miles across the country at the weekend could be a thing of the past. Instead, much like some car sharing schemes running in major cities, consumers may subscribe to a car pool that gives them a certain number of days per year on differing vehicle types. Given how car ownership is identified with freedom and liberty in some countries this will likely not be an easy sell though it does make long-term sense. Although hydrogen can be entirely green and emission free, it will almost certainly not be cheap, nor a return to fuel costs of bygone eras. Driving around an inefficient vehicle fleet merely for convenience or fancy akin to the cars of the 1970s and 1980s will be prohibitively expensive, similarly driving a vehicle designed for a market in a different part of the world will not be a realistic prospect.

7.6 Performance or Efficiency?

The simulation results present two clear choices of topology depending upon the desired optimal feature. Topology C where the DC bus voltage follows the fuel cell stack voltage and has no efficiency draining power converters in between the fuel cell and the drive is highly efficient. The simulations have shown that during most cycles the dominant power flow is from the fuel cell to the drive and so it is unsurprising that Topology C is the most efficient overall.

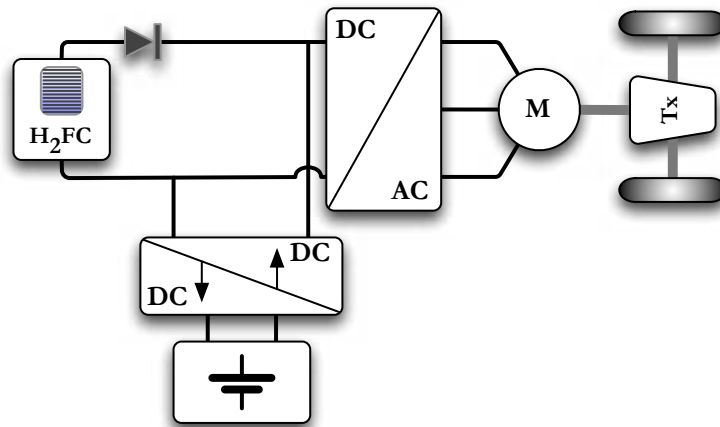


Figure 7.1 - Topology C - The Most Efficient Drivetrain

The performance of the topologies is highlighted by two cases. Topology A, the none hybrid H₂FCEV failed the gradeability test, could not accurately follow the driving cycles, takes 35% longer to get from 0-60mph than Topology B and the overtaking speed is nearly 57% greater. Topology A proves the conclusion of multiple references in literature that the FCEV drivetrain needs to be hybridised with an energy storage system to create a viable vehicle.

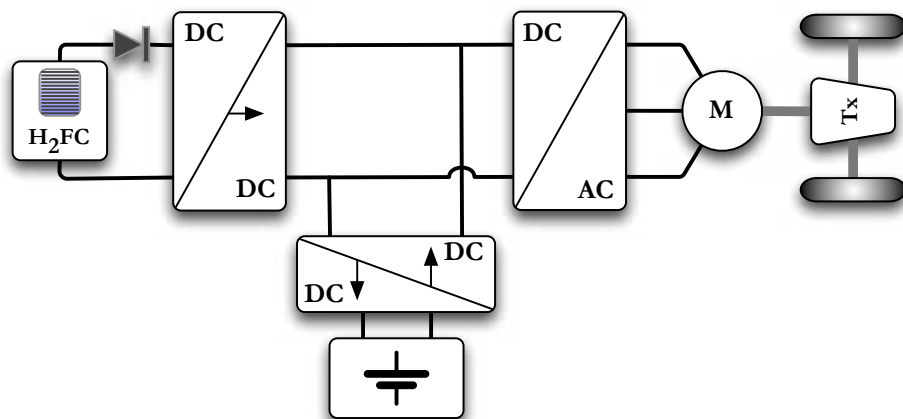


Figure 7.2 - Topology B - The Highest Performance Drivetrain

Topology B is the highest performance of the H₂FCHEV. The fixed DC bus voltage ensures the motor can generate maximum power at all times. This performance has a penalty as the range of Topology B is typically 10% less than Topology C. Topology D also attains high performance, but the arrangement of its drive train means it is even less efficient than Topology B.

Topology E is less efficient than Topology C and also impractical/unsafe when using Li-Ion batteries as the battery charging voltage is non-optimal and the battery cannot be isolated from the bus in case of a dangerous situation. Topology F is also impractical on the same grounds and much like Topology D, the arrangement of a separate converter to fix the DC bus voltage is a highly inefficient method of obtaining high performance.

Ultimately the choice is stark. Unlike a modern ICE though, tuning the FCEV for performance is not a matter of remapping an engine or adding a relatively cheap turbocharger to yield 10-40% performance gains from what is pretty much the same engine block. It's a choice between two very different power train arrangements with different costs and packaging implications.

7.7 New Topology

Topology Q was proposed by Bizon [167] as a more efficient way of charging the battery pack in Topology B (though it is equally applicable to Topology C). The idea uses a small, fixed operating point, highly efficient converter to charge the battery rather than charging the battery through the main DC-DC converter that is relatively inefficient at low loads. To prolong battery life, relatively low 1C charging rates are used and if there is heavy usage of the energy storage system then the penalty paid whilst recharging the battery could be significant over the course of an arduous driving cycle.

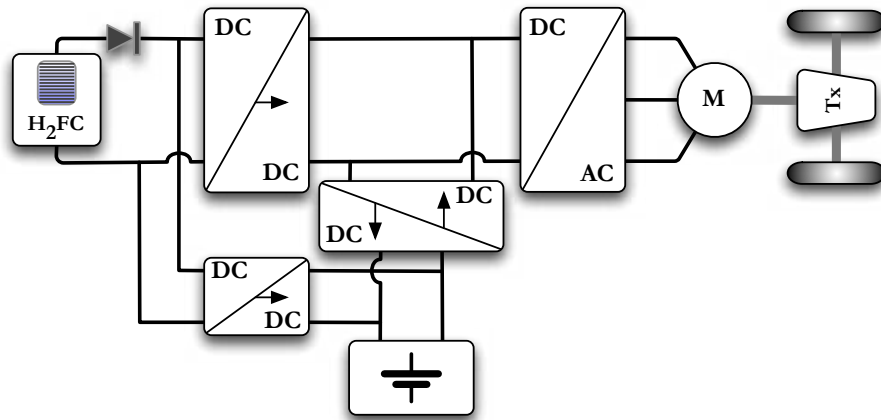


Figure 7.3 - Topology Q

Whilst analysing the results of the simulation though it became clear there was a greater opportunity for further optimising the arrangement of the power drive train. Topology C has higher efficiency because in most operating points power is flowing from the fuel cell stack through a power diode to the drive. Topology B yields high performance by fixing the bus voltage with a DC-DC converter to the maximum drive input voltage, ensuring that maximum torque is available at any given instant. In the majority of driving conditions however, maximum torque is not required.

The proposed solution was to create a topology that could do both. By bypassing the DC-DC converter when high performance was not needed with a thyristor the power pathway from the fuel cell to the drive could be maintained at efficiencies close to that of the fuel cell and power diode alone. Although the thyristor is slightly less efficient than a power diode, due to gate losses and a slightly higher on state voltage drop, it is still considerably more efficient than the DC-DC converter, especially at low loads. The arrangement of the bypass thyristor in the “New Topology” is shown overleaf in Figure 7.4.

7.7.1 New Topology Overview

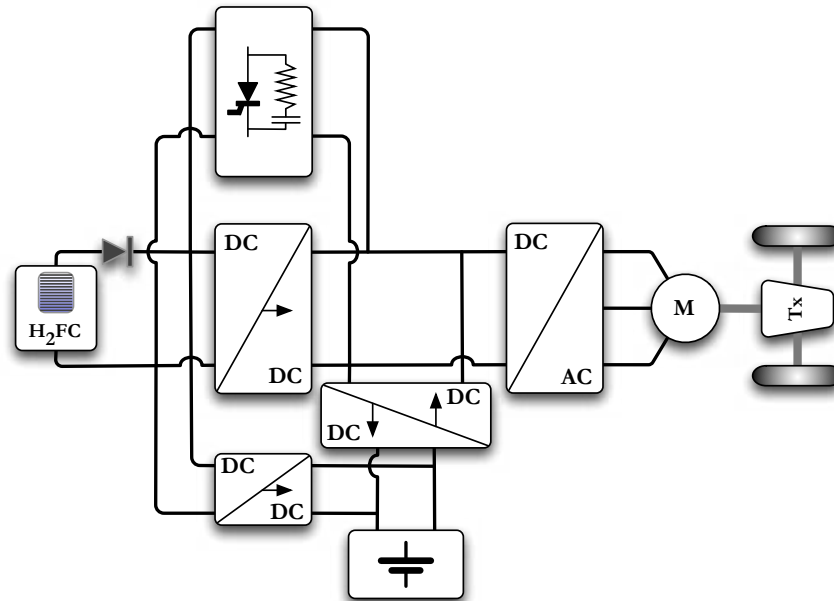


Figure 7.4 - New Topology

Once the concept had been proposed, implementing it into the simulation model was relatively straightforward. A suitable thyristor device was found, the ABB 5STF 07D1414 [250]. It was clear from the device datasheet that the rise time of the device was significantly less than a single simulation step (0.000005s vs. 0.05s). The model did not therefore need to simulate the turn on transient phase of the thyristor so long as it took into account the power dissipated by the device gate every time it is turned on and off. The model then simply has to simulate the on state voltage drop across the device and power loss in a similar way to the existing diode model. The on state voltage drop characteristic was obtained from the data sheet. Like the other models in the simulation, thermal effects are ignored and it was assumed the device was properly cooled during the simulations. It is also assumed that the gate is fired repeatedly until the thyristor device latches into its on state.

Control of the arrangement was a two-stage development process. The original method published in [251] required driving cycles to be pre-analysed. Each cycle was then matched with a control file that switched the DC-DC converter and thyristor on and off at appropriate points when high-performance or high-efficiency was required. This method proved cumbersome though and so the control process was refined. Instead the rate of change of acceleration was monitored, and when it exceeded 0.5ms^{-2} the DC-DC converter is switched into the circuit.

Since the fuel cell is a voltage source, and the DC-DC converter will raise the bus voltage above the fuel cell stack voltage, when the DC-DC converter is turned on the thyristor will become reverse biased and will turn off with no need for external control.

The MATLABSimulink model simulates both the DC-DC and thyristor at each simulation step and simply turns each one on and off as required. Once the thyristor model was constructed and validated against the manufacturers data, the new topology was simulated with the full range of driving cycles to see if it yielded any efficiency or performance gains.

7.7.2 New Topology Results

The new topology delivered a new drive train arrangement that had the positive aspects of both Topology C and Topology B/Q. The performance was an improvement over Topology C with a 0-60mph time of and the efficiency significantly improved over Topologies B & Q.

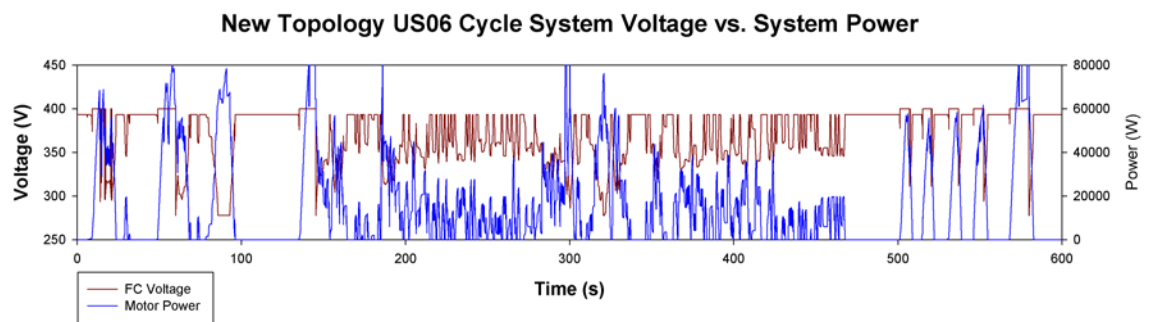


Figure 7.5 - New Topology System Voltage vs. Power

Figure 7.5 shows how the switching control schema is working, with the higher of the two flat peaks on the voltage waveform being when the DC-DC converter is active and associated with periods of peak power demand. The lower of the flat peaks is the no-load condition of the fuel cell system. By way of comparison Figure 7.6 shows the system voltage during the US06 cycle for Topology C and illustrates that during periods of similar peak demand, the voltage collapses down towards 250V.

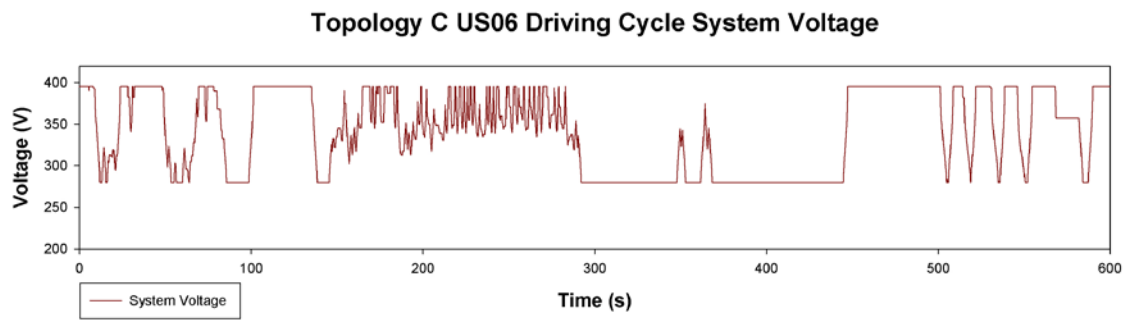


Figure 7.6 - Topology C US06 Driving Cycle System Voltage

Figure 7.7 shows the relationship between the voltage being fixed for high performance and the speed profile and confirms that once the vehicle has accelerated to a certain point and the rate of acceleration decreases the control system bypasses the DC-DC converter with the thyristor and uses the highest efficiency power pathway again.

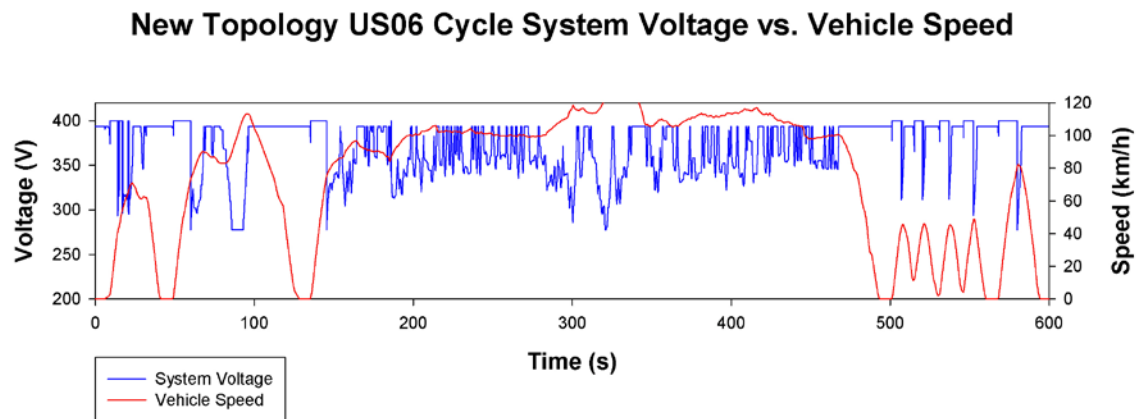


Figure 7.7 - New Topology US06 Driving Cycle Speed vs. Voltage

Table 7.1 shows the new topology efficiency data relative to the other topologies of interest highlighted in Chapter 6. Although not as efficient as Topology C, the gain over Topology B & Q is readily apparent. Table 7.2 confirms this, illustrating the more efficient utilisation of power from the fuel cell, both to the battery and drive. It also shows the benefit of fixing the bus voltage at 400V during periods of high acceleration. As stated previously, at low voltage and high load, the motor drive is relatively in efficient, by using a high voltage for high performance peaks and letting the voltage float during other periods the fuel cell to drive efficiency is actually higher than any of the other topologies simulated previously. The control mechanism is relatively crude and it could be developed further to adjust and control the system voltage in order to track the maximum efficiency point of the motor drive at any given point, potentially yielding further performance gains.

7.7.3 New Topology Efficiency & Range

Topology	Drivetrain Type	MPGe (Urban)	MPGe (Extra Urban)	MPGe (Highway)	MPGe (Combined)	MPGe (Real World)
<i>B</i>	H ₂ FCHEV	33.91	47.52	50.05	43.97	40.96
<i>C</i>	H₂FCHEV	37.65	51.82	53.92	48.13	44.78
<i>J</i>	BEV	87.79	120.77	127.16	110.06	101.70
<i>Q</i>	H ₂ FCHEV	33.86	47.35	50.02	43.73	40.80
<i>NEW</i>	H ₂ FCHEV	35.99	50.03	52.51	46.25	43.24
<i>1.6l Ref</i>	ICEV	29.7	49.6	N/A	39.8	N/A

Table 7.1 - Driving Mode Efficiency - New Topology

Topology	Fuel Cell Efficiency	Battery System Efficiency	Battery Charging Efficiency	Motor Drive Efficiency	Fuel Cell to Road Efficiency	Battery to Road Efficiency
<i>B</i>	39.34%	80.32%	43.02%	72.11%	28.37%	57.92%
<i>C</i>	44.47%	79.15%	43.25%	72.01%	32.02%	57.00%
<i>Q</i>	39.42%	80.32%	45.57%	72.23%	28.47%	58.02%
<i>NEW</i>	40.35%	79.55%	46.76%	73.11%	29.50%	58.20%

Table 7.2 - Drivetrain Electrical Efficiency - New Topology

7.7.4 New Topology Range By World Market

Topology	Drivetrain Type	Range by World Market (km)		
		EU	US	JP
<i>A</i>	H ₂ FCEV	528.83	471.53	438.91
<i>B</i>	H ₂ FCHEV	469.41	424.74	393.20
<i>C</i>	H ₂ FCHEV	517.28	464.83	429.87
<i>D</i>	H ₂ FCHEV	464.26	420.96	389.68
<i>E</i>	H ₂ FCHEV	474.45	430.48	388.19
<i>F</i>	H ₂ FCHEV	439.76	401.85	370.79
<i>I</i>	H ₂ FCHEV	496.72	434.88	434.12
<i>J</i>	BEV	223.25	202.74	182.42
<i>Q</i>	H ₂ FCHEV	468.95	423.08	391.70
<i>New Topology</i>	H ₂ FCHEV	498.98	448.82	415.12

Table 7.3 - Range by World Market - New Topology

7.7.5 New Topology Performance

Topology	Drivetrain Type	50-70mph (s)	Relative 50-70mph Time
<i>NEW</i>	H ₂ FCHEV	7.71	+0.6%
<i>B</i>	H₂FCHEV	7.66	-
<i>C</i>	H ₂ FCHEV	9.19	+20.0%
<i>J</i>	BEV	6.79	-11.6%
<i>Q</i>	H₂FCHEV	7.66	-

Table 7.4 - New Topology Passing Speed Comparison

Topology	Drivetrain Type	0-60mph (s)	Relative 0-60mph Time ¹
<i>NEW</i>	H ₂ FCEV	13.82	+0.8%
<i>B</i>	H₂FCHEV	13.71	-
<i>C</i>	H ₂ FCHEV	15.27	+11.4%
<i>J</i>	BEV	12.73	-7.2%
<i>Q</i>	H₂FCHEV	13.71	-
<i>1.6l Ref</i> ²	ICEV	11.60	-15.4%

Table 7.5 - New Topology 0-60mph Acceleration Test Comparison

¹ The relative 0-60mph and 70-50mph times are quoted relative to the highest performance H₂FCEV topologies, Topology B and Topology Q.

² The reference case is a 1.6l petrol ICEV production version of the vehicle, the chassis of which this simulation model was based upon.

7.7.6 New Topology Summary

The “New Topology” can achieve the performance of Topology B when required and it has more than halved the range deficit between Topology B and Topology C and increased the efficiency by nearly 3 MPGe. Although this increase may seem small, the control of the switching is currently an absolute. Adaptive switching may yield further performance gains. The original switching method of programming the switching to occur at certain points during the driving cycle produced around a 20km gain in urban range. The new switching method has increased that by half as much again to nearly 30km. Sensitivity analysis of the control schema for each specific driving cycle could generate a dataset that could be algorithmically integrated into the control loop to optimise each individual cycle.

It is also a relatively low cost topology to build as the thyristor is a cheap piece of electronic hardware and the control is an extension of the existing vehicle ECU. There is some associated cooling requirement, but nothing that would be beyond the capability of the existing vehicle cooling system.

7.7.7 New Topology Validation

The new topology was again validated using the available data in the literature. Since the New Topology falls between Topology C and B, the earlier validation were still expected to hold true and this is shown in Table 7.6 and Table 7.7.

Driving Cycle	Ahluwalia et al. MPGe	New Topology MPGe	Relative Difference
<i>NEDC</i>	64	52.63	-17.77%
<i>USHWY</i>	80	80.57	+0.71%
<i>US06</i>	43	34.78	-19.12%
<i>J10-15</i>	61	44.08	-27.73%

Table 7.6 - New Topology vs. Ahluwalia et. al Literature Validation

Driving Cycle	Hauer MPGe	New Topology MPGe	Relative Difference
<i>US06</i>	49	34.78	-29.02%
<i>USHWY</i>	70	80.57	+15.10%
<i>ECE</i>	47	43.10	-8.30%
<i>EUDC</i>	63.7	60.20	-5.49%
<i>J1015</i>	55	44.08	-19.85%

Table 7.7 - New Topology vs. Hauer Literature Validation

7.8 Vehicle Design Optimisation

“If I had asked people what they wanted, they would have said faster horses.”

Henry Ford (1863-1947)

Though there is some doubt as to the exact veracity of the quote, the sentiment is one Ford expressed on many occasions. Its relevance now is that it is important for this study to highlight the potential pitfalls of incremental development over step change. The large majority of future vehicle roadmaps show a steady progression towards the alternative fuelled vehicles of the future and whilst some cars have challenged the status quo, the majority build on the current design traditions that have remained largely unchanged for decades. More recently Steve Jobs went to great lengths to develop products, not that people were asking for, but that he thought they needed. Although such autocratic visionaries are probably wrong more often than they are right it does highlight the issue of whether continuous, incremental development will be the most effective way of developing alternative fuelled vehicles and introducing them to the market place or whether a more radical launch of new car designs should accompany the change in fuel.

The introduction of Hydrogen vehicles would be a disruptive step to begin with; there is no shying away from the vast scientific, engineering and social challenges that stand between mankind and a hydrogen economy. Compromising the vehicle system on the basis of marketing or manufacturing concerns alone could be a mistake. This study has analysed the, sometimes marginal, effects of different configurations of electrical and electronic components in the drivetrain. Every 1% increase in efficiency of a drivetrain is worthwhile in that ultimately the vehicle can travel further on less fuel, is cheaper to run and whilst hydrogen is generated from or with fossil fuels has less environmental impact. There are some other aspects of vehicle design that could have substantial impacts on the efficiency and performance of the H₂FCHEV. By quantifying these design changes and applying them to the simulation model some of the potential gains that could be built on by further works were highlighted and are briefly set out in this section.

7.8.1 Aerodynamics

Nearly two decades ago the General Motors EV1 had a drag coefficient of 0.19. Today, the average drag coefficient of typical passenger vehicles is around 0.30, although the Toyota Prius HEV has an optimised coefficient of 0.25.

The drag coefficient is the main area of vehicle design optimisation where there is a conflict between safety and performance. Using carbon fibre both reduces weight and increases crash survivability. Gluing body panels eliminates costly fasteners and reduces the force of impact and allows cars to crumple in a predictable manner and dissipate the energy of an impact rather than transfer it to the passengers and pedestrians. Reducing the drag coefficient though generally results in a vehicle frontal shape that can increase the risk to pedestrians involved in any collision with the vehicle.

Using the new topology as the basis for the most optimal H₂FCHEV design, the drag coefficient was reduced and a further full set of simulation tests was conducted with the new topology to quantify the efficiency gain from optimising the aerodynamic profile of the vehicle.

Topology	Drivetrain Type	MPGe (Urban)	MPGe (Extra Urban)	MPGe (Highway)	MPGe (Combined)	MPGe (Real World)
<i>B</i>	H ₂ FCHEV	33.91	47.52	50.05	43.97	40.96
<i>C</i>	H ₂ FCHEV	37.65	51.82	53.92	48.13	44.78
<i>J</i>	BEV	87.79	120.77	127.16	110.06	101.70
<i>Q</i>	H ₂ FCHEV	33.86	47.35	50.02	43.73	40.80
<i>NEW</i>	H ₂ FCHEV	35.99	50.03	52.51	46.25	43.24
<i>Low Drag</i>	H ₂ FCHEV	36.06	51.68	55.23	46.88	43.47
<i>1.6l Ref</i>	ICEV	29.7	49.6	N/A	39.8	N/A

Table 7.8 - Driving Mode Efficiency - Low Drag Vehicle

As could be expected, the most significant impact of reducing the drag coefficient is seen during highway driving as wind resistance increases with the square of velocity. For urban driving the effect is negligible.

7.8.2 Materials

Predominantly, most passenger vehicles are still made largely from steel. There has been significant advancement in construction with panel gluing techniques simplifying construction improving safety and reducing weight. Increased use of plastics has also achieved weight reduction but most of these gains have been offset by the change in vehicle size.

The average car being larger than 30 years ago is an advantage given the current packaging requirements of fuel cell engines. Unless stack and tank sizes decrease significantly, midsize and above vehicles will be needed to package the system, maintain comfort and leave useful cargo capacity and vehicle range. The battery is not so much of a concern as it can be distributed around the vehicle and the small cell size means they can, if necessary, be spread around the chassis and hidden away in all manner of places. This approach does however increase cost substantially over a single battery module system.

The aerospace industry has long made extensive use of lightweight materials. Aluminium and magnesium alloys are not new technology but they are still relatively expensive compared to steel. Carbon fibre sees extensive use in performance and racing vehicles and with improvements in the mass manufacturing techniques and reduction in cost could reduce weight even more than aluminium. This study has stressed efficiency and cost challenges facing hydrogen as a fuel and it would be amiss not to give consideration to how the material used to make the vehicle influences how efficiently that fuel can be utilised.

McKinsey & Company produced a report in January 2012 [252] that examined the application of lightweight materials, namely carbon fibre and aluminium alloys, to reduce passenger vehicle weight. The report generated three cases where the application of different mixes of materials could be used to reduce the weight of a passenger vehicle:

1. Conventional Lightweight, LW (18% Weight Reduction).
2. Moderate Lightweight, MLW (30% Weight Reduction).
3. Extreme Lightweight, ELW (35% Weight Reduction).

The material composition of these packages is shown in Figure 7.8 [252]. The reductions were applied to the basic mass of the vehicle chassis used for the simulation model. Although it is probable some weight could also be saved in the components of the drivetrain, the McKinsey study does not address this and so it is assumed the weight saving

is applied to the chassis only. Models for the three weight reduction cases were created, based on the new topology, and the full range of simulation tests was repeated for each. Additionally, the ELW vehicle was modelled for a second time with a drag co-efficient of 0.19 to model the affect of both weight and drag reduction simultaneously.

Lightweight packages apply different lightweight material mixes with different weight and cost impact

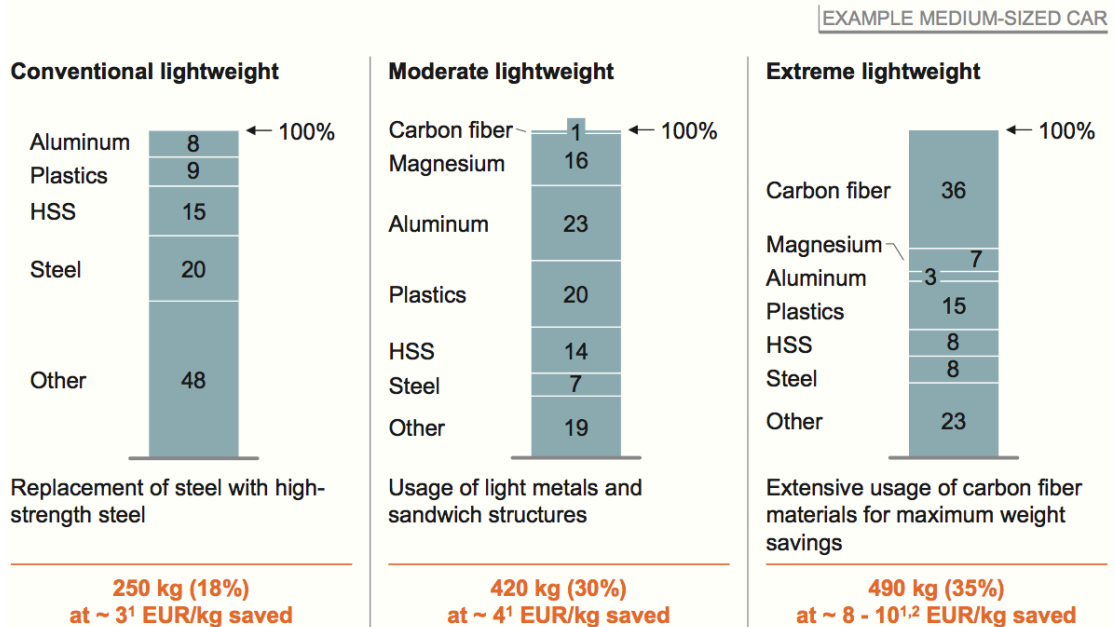


Figure 7.8 - Vehicle Weight Reduction by Application of Lightweight Materials [252]

Topology	Drivetrain Type	MPGe (Urban)	MPGe (Extra Urban)	MPGe (Highway)	MPGe (Combined)	MPGe (Real World)
<i>B</i>	H ₂ FCHEV	33.91	47.52	50.05	43.97	40.96
<i>C</i>	H ₂ FCHEV	37.65	51.82	53.92	48.13	44.78
<i>J</i>	BEV	87.79	120.77	127.16	110.06	101.70
<i>Q</i>	H ₂ FCHEV	33.86	47.35	50.02	43.73	40.80
<i>NEW</i>	H ₂ FCHEV	35.99	50.03	52.51	46.25	43.24
<i>Low Drag</i>	H ₂ FCHEV	36.06	51.68	55.23	46.88	43.47
<i>LW</i>	H ₂ FCHEV	40.33	55.61	57.75	51.50	48.03
<i>MLW</i>	H ₂ FCHEV	43.70	60.18	61.69	55.73	51.99
<i>ELW</i>	H ₂ FCHEV	45.37	62.29	63.65	57.69	53.91
<i>ELW Low Drag</i>	H ₂ FCHEV	45.65	64.37	67.21	58.93	54.51
<i>1.6l Ref</i>	ICEV	29.7	49.6	N/A	39.8	N/A

Table 7.9 - Driving Mode Efficiency

Topology	Drivetrain Type	MPGe (Urban)	MPGe (Extra Urban)	MPGe (Highway)	MPGe (Combined)	MPGe (Real World)
<i>B</i>	H ₂ FCHEV	-9.92%	-8.31%	-7.18%	-8.65%	-8.53%
<i>C</i>	H ₂ FCHEV	-	-	-	-	-
<i>J</i>	BEV	133%	133%	134%	128%	127%
<i>Q</i>	H ₂ FCHEV	10.05%	-8.63%	-7.23%	-9.16%	-8.88%
<i>NEW</i>	H ₂ FCHEV	-4.40%	-3.45%	-2.60%	-3.92%	-3.43%
<i>Low Drag</i>	H ₂ FCHEV	-4.20%	-0.28%	2.44%	-2.60%	-2.93%
<i>LW</i>	H ₂ FCHEV	7.13%	7.30%	7.10%	6.99%	7.26%
<i>MLW</i>	H ₂ FCHEV	16.08%	16.13%	14.42%	15.79%	16.11%
<i>ELW</i>	H ₂ FCHEV	20.50%	20.20%	18.05%	19.86%	20.40%
<i>ELW Low Drag</i>	H ₂ FCHEV	21.25%	24.21%	24.65%	22.42%	21.72%

Table 7.10 - Relative Driving Mode Efficiency

As Table 7.9 and Table 7.10 show, the improvement by reducing the weight of the vehicle is significant across all modes of driving with 20% gains seen nearly across the board in the ELW package. To put that into some context, a driver currently filling an ICEV with a 55l tank once a week would see an annual reduction in their fuel bill of around £800.

7.8.3 Fixed Gearing

Electric vehicles tend to use a single fixed gear transmission and differential. There are good reasons for this but it does limit acceleration performance and could adversely affect motor efficiency. The torque characteristics of an electric motor compared to petrol engines are very favourable but they are not the sole competition. Diesel engine technology has advanced more than any other in recent years and the marketplace is replete with diesel vehicles capable of 55-65mpg and sub 8 second 0-60mph times with a peak torque in excess of 500Nm. The latest iterations of the 4th generation common rail engine vehicles have gone even further, the BMW F30 330D for instance, generates 265bhp from a 3l 6-cylinder diesel engine that can achieve in excess of 50mpg on the motorway yet accelerate to 60mph in 5.6 seconds. It uses an 8 speed automatic transmission. It is reasonable to expect this performance to increase further in the years before H₂FCHEV are introduced.

The fixed gear whilst being more efficient than a multiple gear transmission reduces the available torque at the wheels at low speeds and limits the top speed of the vehicle. Ultimately, motors capable of generating higher torque will improve the acceleration

performance and probably negate the need for variable gearing, but the effect of increasing the gear ratio to that similar to 1st gear in a medium sized passenger ICEVs was simulated. The gear ratio was increased to 13.38:1 and a 10.7% reduction in the 0-60mph time was achieved as shown in Table 7.11.

Topology	Drivetrain Type	0-60mph (s)	Relative 0-60mph Time ¹
<i>B (9.8:1)</i>	H ₂ FCHEV	13.71	-
<i>B (13.38:1)</i>	H ₂ FCHEV	12.25	-10.7%
<i>J</i>	BEV	12.73	-7.2%
<i>1.6l Ref²</i>	ICEV	11.60	-15.4%

Table 7.11 - Modified Gear Ratio Performance Data

7.9 Consumer Acceptance

The primary research question identified that regardless of whether or not the fuel cell vehicle was technically possible, it being accepted by the consumer was also of critical importance to the study and to the future of the field. Having undertaken the review and simulation work it is important to consider how the public may receive the H₂FCHEV.

Existing alternative fuelled vehicles have been met with a popular response from consumers defined as innovators. Current alternative fuel vehicles, mainly consisting of HEVs and PHEVs, with a minority of EV, have a market share of 1.4% in the UK [5]. In ‘The Diffusion of Innovations’, Rogers defines ‘innovators’ as being 2.5% of the market [1]. They are classified as being willing to take risks and adopt technologies that may ultimately fail and have the financial ability to take these risks with little consequence. Though an important group in their own right, the second category of innovators is key to a technology or idea diffusing into the mass market. The second category is classified as ‘early adopters’ and they account for 13.5% of the market. They also have the greatest influence with the next category, the ‘early majority’ and it is only by capturing the early majority that an innovation can start to reach critical mass and approach 50% market share. Diesel cars currently hold 49.8% of the UK market and gasoline cars 48.8%.

¹ The relative 0-60mph and 70-50mph times are quoted relative to the highest performance H₂FCHEV topologies, Topology B and Topology Q.

² The reference case is a 1.6l petrol ICEV production version of the vehicle, the chassis of which this simulation model was based upon.

The consumer will want to be assured of several features before considering the H₂FCEV as a product ready for the mass market, namely:

- Are they safe?
- Can they do everything with it that they can in their current vehicle?
- How far can they drive in one?
- Can it easily be refuelled in as many locations as petrol and diesel cars can at a reasonable price?
- Are they affordable to purchase and maintain?
- Will they last as long as current vehicles?
- What is the environmental impact?

Safety is likely a matter of potential misperception risk alone that can be solved with proper marketing and effective public information strategies. Hydrogen gas storage cylinders will likely be safer than current steel, aluminium or plastic petrol and diesel tanks. In the event of a fire, hydrogen is much safer than petrol.

The H₂FCEV can be manufactured in a vehicle body similar to existing vehicles with a minor reduction in the volume available for storage in the passenger compartment due to the increase in size of the fuel storage system. It is likely that vehicles designed specifically to accommodate a fuel cell power train could eliminate this reduction in volume. The reduction in volume seen in prototype vehicles is due to them being built on existing combustion engine vehicle platforms that have not been designed for the purpose. From the driver experience perspective, the driver will be able to get in, press a button/turn a key, start the vehicle and press an accelerator to drive away. Performance will be in line with existing vehicles and high performance vehicles can be made for the high end of the market. Hydrogen cars can be driven for hundreds of kilometres and refuelled in less than five minutes from a fuel dispenser that is very similar to existing petrol and diesel pumps.

The affordability of the hydrogen vehicle is a question that is at this stage hard to answer definitively. Much progress has been made in recent years but the use of materials such as platinum in the fuel cell and carbon fibre in the hydrogen storage system are likely to result in a higher cost compared to ICEV technology. If the use of materials can be minimised or eliminated then the question will be how much of a cost differential remains once other costs have been brought down by the economies of scale that result from mass production.

Hybrid and electric vehicles have shown that innovators will pay a premium for alternative fuel vehicles, but cost parity with existing vehicles is likely to be necessary before mass-market penetration can occur. A 2012 study prepared for the US government estimates that at 500,000 unit volumes, a PEMFC system will cost around \$46.95/kW [253]. The UK Carbon Trust estimates that this must fall to around \$36/kW for fuel cell vehicles to compete at scale with the internal combustion engine which currently cost around \$25-35/kW [254].

The ability to refuel a vehicle in a cost effective and convenient manner is likely to be the biggest challenge for the fuel cell vehicle. Government funding will be needed to provide the hydrogen infrastructure, as without it there becomes a multi-actor chicken and egg situation. Consumers will not buy vehicles they cannot refuel, energy companies will not manufacture fuel they cannot distribute and fuel retailers will not sell a fuel in all their outlets unless there is a large customer base driving hydrogen vehicles to sell it to. A recent report by McKinsey & Company estimates the cost of infrastructure associated with H₂FCEVs to be £800 - £1600 per vehicle and that within Europe, the total capital investment required for a large scale roll out of hydrogen supply infrastructure to be around £80 billion between 2010 and 2050 [255].

The retail cost of Hydrogen fuel will likely be prohibitive unless each part of the supply chain is done at scale and without the fuel being cost competitive, the environmental benefit alone is unlikely to precipitate and achieve mass-market adoption. In a recent survey by the UK Office for Low Emission Vehicles, some 58% of private purchasers and 43% of business purchases cited saving money on fuel as the primary reason for purchasing an EV over an ICEV [6]. The European cost targets for hydrogen are £4.40/kg by 2025, at this price. Taking Topology C during the NEDC driving cycle, this would equate to a cost of £0.04/km. Taking the 1.6l reference ICEV during the NEDC driving cycle and the current cost of petrol to be £1.30/l, the cost per km for the petrol vehicle is £0.09/km. All parties seem to agree that the price of oil is only likely to increase in coming years, but assuming prices were to remain static, refuelling a H₂FCEV in 2025 will be twice as cheap as a comparable ICEV. This reduction in running cost may allow the retail price of fuel cell vehicles to be higher without damaging the mass-market appeal.

The environmental impact of running a H₂FCEV will largely be dictated by infrastructure development in the hydrogen supply chain. If the hydrogen is generated by electrolysis from renewably generated electricity then the carbon footprint of the vehicles will be zero.

If the hydrogen is made by reforming natural gas, the carbon footprint will likely be similar to that of fossil fuel vehicles however the particulate emissions by the vehicles themselves will be eliminated, delivering a benefit to local air quality around roads.

The durability of the vehicles is again mainly a question of materials technology. The current average age of the UK vehicle fleet is 7.6 years [5]. The main limitation on the lifespan of the H₂FCEV is currently the lifespan of the fuel cell stack and the endurance of the lithium ion batteries in the energy storage system. If we assume two journeys a day for a typical car, over the lifespan of the vehicle there are ~5,500 engine starts. On a typical journey it is unlikely the battery will be fully depleted and fully recharged so with careful SOC control the lifespan of the battery should be sufficient. However there is a limit to the number of times the fuel cell stack can be started up and shut down however current expectations for fuel cell technology in development are that the new generation of PEMFC systems will be able to meet durability requirements.

7.10 Manufacturing Considerations

There is no underestimating the scale of change that will be required of manufacturers in order to mass-produce fuel cell vehicles. New technologies that most manufacturers have limited or no previous experience of will need to be developed and integrated into production lines. The level of quality control required on some components will greatly exceed that currently required for internal combustion engines and many of the technologies will be being deployed at scale in an automotive application for the very first time. This will be expensive and full of risk for the automotive industry and it is not something they will do lightly.

Vehicle designs that have incorporated many common features for many years will need to be redesigned from scratch with a large change to the design methodology. Fuel cell assembly and integration will need cleanroom facilities which to date have only been built and used in production lines by very high-end sports car manufacturers.

History has shown that the stick of regulation and the carrot of government subsidy has been the greatest driver of innovation other than the primary drive of consumer demand in the automotive sector. Left with no external stimuli, new features and innovations are largely determined by what can be implemented in the most cost effective manner and sold

for the most profit. The political will to invest in this new era will be as important as the manufacturers capability to deliver it.

Beyond manufacture, entire portions of the vehicle-servicing sector will also need to retool and reskill to deal with pressurised gas systems, fuel cells, power electronics and electric drives.

Despite these impediments, nothing about the fuel cell vehicle suggests that there will be insurmountable problems in manufacturing it on a large scale and the flexibility of how the various components can be packaged compared to existing engine technologies may offer the opportunity for manufacturers to design some innovative and exciting vehicles.

The environmental benefits of fuel cell vehicles will support manufacturers in marketing them to consumers and businesses but the manufacturers will likely not build large scale production facilities without confidence that the infrastructure to support the vehicles will exist by the time they bring them to market. As with the infrastructure aspect of the hydrogen economy, this will need government investment and support to stimulate and drive innovation.

One-thing manufacturers must avoid and must be supported in, is delivering products without serious flaws or limitations that could prevent the innovation diffusing to the mass market. As the safety issue with lithium batteries on the Boeing 787 has shown, cutting edge technologies present risk as well as benefit and a major safety or performance issue with an early fuel cell vehicle could present a serious risk of consumer rejection to the whole concept.

7.11 Regenerative Braking Simulation

There are two main areas where reflection has made it apparent that the simulation model could be improved. The decision to exclude regenerative braking was taken due to the limited availability of computational power, but as became apparent in the validation that decision has reduced the efficiency of each of the topologies simulated.

Not all driving cycles offer large opportunity for regenerative braking, but that is an important area to have knowledge of itself, as it may affect the suitability of a given topology for a particular market.

Compared to 2004 when this project started, the computing power that is available for a similar investment is remarkable. 64 bit operating systems have removed the limit on RAM, meaning simulations can run entirely in memory. Processor technology has improved significantly and workstation CPUs now feature 8-12 cores where they previously had one or two. These cores are running at higher clock rates, feature hyper-threading that can in some situations double the number of calculations performed and require less power. The memory bus is running at twice the speed and solid-state disc storage has increased the speed of writing to disc by a factor of ten. Given this, it is important to state that it would no longer be necessary to exclude regenerative braking from any further work or similar study. The only grounds for excluding it were computational, and those restrictions no longer apply.

8 Conclusions

8.1 Introduction

In this final chapter the original aims of the research project will be reviewed and conclusions drawn on the basis of the work contained within this thesis. The conclusions are based on a wide-ranging review of the subject area, critical analysis of comparable work in the same field, extensive computer modelling analysis and interpretation of the results.

8.2 Analysis of Fuel Cell Vehicle Power Drive Train Topologies

The primary goal of this project was to build a tool to enable the quantitative analysis of different configurations of H₂FCEV power drive trains. A literature review was undertaken to identify all the different existing drive train architectures and methods of simulating fuel cell vehicles. After a comprehensive review of software tools MATLAB Simulink was selected as the most suitable simulation software and a vehicle model and common set of power drive train subsystem components was designed and implemented in the simulation environment. Each subsystem was tested before the different topologies were assembled into the final simulation environment for each vehicle. A BEV simulation model was also constructed to allow the H₂FCHEV to be compared directly with what is likely to be its main competitor in the future automotive marketplace. The model was validated with empirical data and by comparison against existing data and published studies. The models performance compared favourably to some of the existing works and where there were deficiencies the cause was readily identifiable.

A collection of driving cycles which represented the legislative testing cycles of the worlds three major automotive markets, Europe, North America and Japan and the Far East. In addition, newly developed real world driving cycles were used to further test the simulation model and ensure the simulation was not affected by modal cycles only testing a few of the operating points of the power drive train.

The extensive set of results and built the largest collection of different drive train architectures simulated against a common set of tests that allowed their relative

performance to be evaluated in a way the data available in the existing literature does not. Previous works have not tested multiple topologies against multiple markets cycles before and the results were revealing.

The major conclusions of this thesis are:

- 1) Hydrogen fuel cell electric vehicles need a hybrid power source in the drive train to deliver acceptable performance.
- 2) There is no single suitable power drive train for all world markets and different markets around the world will likely need different drive train topologies to be optimised to the specific local driving needs. The differences between the differing markets and modes of driving were so significant that it leads this thesis to conclude that in the future the concept of a multi-role vehicle may change and vehicles will become more task specific.
- 3) The current state of the art leads to a choice between performance and fuel economy. No single drive train currently delivers both across multiple modes of driving.
- 4) The H₂FCHEV already exceeds the range capability of the BEV and the refuelling time is minimal.
- 5) “Range anxiety” should not be a problem for the H₂FCHEV in the way it has been for the BEV.
- 6) The relative sizing of the components in the power drive train is likely of critical importance to the performance of the H₂FCHEV. The sizing of components for optimal highway driving will likely be inappropriate for optimal urban driving.

8.3 Development of New Topology

This study developed a novel H₂FCHEV drive train topology to go some way to addressing the compromise between economy and performance in existing drive train architectures. The topology, despite the relatively simple approach to controlling it first adopted, delivered tangible gains without significantly complicating the control, design or cost of the drive train. A minor improvement to the control process yielded a further 50% gain in efficiency and there is reason to be optimistic that further development may bring more gains.

8.4 Assessment of the Potential for Hydrogen

Hydrogen offers the potential answer to the clean energy question. However as this study has highlighted, the question of how, when or indeed if it will be adopted as an energy carrier on a large scale is a very difficult one to answer. There have been many promised dawns for the “hydrogen economy” that have all failed to materialise. It is not a question of its promise being misunderstood and more one of timing.

July, 1960

NEWNES PRACTICAL MECHANICS

441

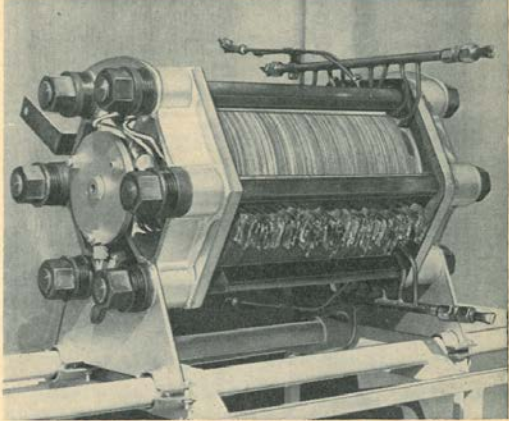
BEFORE we describe the various types of voltaic or electrolytic cell it would be as well to establish the fundamental principles underlying the electro-chemical processes involved.

Principle of Electrolysis

When a current of electricity passes through a solution of a salt or an acid some of the dissolved substance is carried to the points where the current enters and leaves the solution. The vessel in which this reaction takes place is called the electrolytic cell and the solution is known as the electrolyte. This electrochemical reaction is known as electrolysis and the conductor by which the current enters the cell is called the anode and that by which the current leaves the cell is known as the cathode.

As an illustration of the basic principles governing electrolysis, consider the experiment shown in Fig. 1. The three cells are connected in series with a battery and the contents of each cell are as named. The anodes are marked positive and the cathodes negative and the current travels from positive to negative in each cell.

When the current passes through the first cell it is found that a certain quantity of copper is deposited on the cathode and the same quantity of copper goes into solution from the anode. When the current passes through the second cell, a certain quantity of silver is deposited upon the cathode (negative electrode) and exactly the same quantity of silver goes into solution from the anode, or positive electrode. Finally, when the current



A 3kW. power unit utilising 40 hydrogen/oxygen cells linked in series.

Evolution of the FUEL CELL

The revolutionary hydrogen/oxygen fuel cell put into perspective by F. Colin Sutton

passes to the third cell, oxygen is evolved at the anode and hydrogen at the cathode. Moreover, if the respective gas bubbles are caught over inverted tubes placed over the two platinum electrodes, it will be found that the volume of hydrogen collected from the cathode is exactly twice the volume of oxygen that has been trapped in the tube suspended above the anode. In other words, the quantities of copper and silver deposited

2. The mass of any substance liberated by a given quantity of electricity is proportional to the chemical equivalent of that substance.

Before proceeding to a description of different types of cell let us consider for a moment a very elementary type and show why such a cell would not fulfil industrial requirements.

Consider the reactions arising from the

plate were connected electrically by a wire, then a current would flow from the copper plate through the wire to the zinc plate and a mass of bubbles would emanate from the copper plate and the zinc plate. This arrangement then becomes a cell and from it a current of electricity can be obtained.

$$\text{H}_2\text{SO}_4 \rightarrow \text{SO}_4 + \text{H}_2$$
$$\text{Zn} + \text{H}_2 + \text{SO}_4 \rightarrow \text{ZnSO}_4 + \text{H}_2$$

The H_2SO_4 molecules dissociate (in dilute solution) to SO_4 and hydrogen ions, the SO_4 attacks the zinc, forming zinc sulphate, and the hydrogen ions are evolved as gas on the copper plate.

It is the energy given out by this chemical reaction that maintains the output of current.

However, there is a limit to the duration of the vigour of this reaction, for gradually the copper plate becomes coated with hydrogen bubbles. This has a double effect. It increases the resistance of the cell by virtue of an increasing area of copper becoming coated with hydrogen bubbles and thus diminishing the effective area of copper, and it also lowers the E.M.F. (voltage) of the cell. The cell is then said to polarise. If some means is taken to remove the bubbles from the surface of the copper, as for instance by agitation, then the cell becomes depolarised and the reaction starts again with renewed vigour.

It follows, therefore, that an effective cell must possess within itself the power of depolarisation.

The Leclanché Cell

This well-known cell is illustrated in Fig. 2. Here depolarisation takes place through the agency of manganese dioxide. The carbon electrode in the centre is encased in a conglomerate of manganese dioxide and powdered carbon. This unit stands within a porous pot. The interspace between the porous pot and

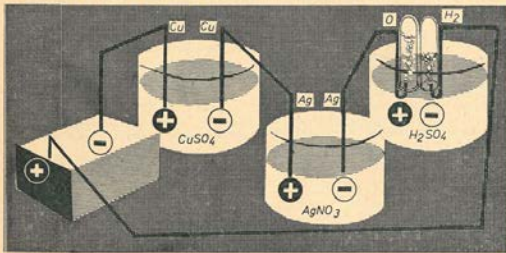


Fig. 1.—The basic principles of electrolysis.

and the quantities of oxygen and hydrogen evolved are proportional to the quantity of electricity that passes and are independent of the size and shape of the cells and electrodes or of the concentration of the solutions.

From these facts Faraday formulated two fundamental laws:

1. The mass of any substance liberated is proportional to the amount of electricity that passes.

simple case of a copper plate and a zinc plate immersed in a dilute solution of sulphuric acid contained in a glass vessel. The two plates will be at different potential and if this difference were measured it would be found to be 1.8V., the copper plate being at the higher potential. Provided that the surfaces of both plates were of perfectly pure metal, no bubbles would be found on either plate. If, however, the copper plate and the zinc

Figure 8.1 - Popular Mechanics July 1960

Popular Mechanics ran an article in July 1960 heralding the great promise of the fuel cell. Similar articles have appeared in every decade since but the interest in hydrogen generally waxes and wains with the prevailing economic climate and the oil price. As long as oil is perceived to be affordable, the hugely powerful special interest groups that surround it will likely ensure that it remains the dominant fuel source for as long as possible.

Hydrogen is unfathomably abundant, but the world powered by hydrogen will not be cheap in the way we normally assume abundant things will be. The investment required will dwarf many of mans greatest endeavours and likely only be triggered by a catastrophic event or a final realisation that our dependency on oil needs to be broken.

Hydrogen can be produced from the oceans using renewable energy from the sea, the sky and the sun. It can be used to transport and more importantly store electricity in a way that batteries are not forecast to be ever capable of. It is true that the process of converting hydrogen from water or other elements is not efficient, but if the fuel and feedstock are both free who cares about efficiency? Cost will be the predominant factor and with the world economy in such a poor state the trillions of dollars likely needed to start the transition to the hydrogen economy will not be invested anytime soon.

That is not a good reason to sit idly by though. One of the major problems with H₂FCEVs is the fuel cell technology. It will need many years of painstaking research to perfect.

The one proviso about this entire subject though is that the BEV is the ideal electric vehicle. The fuel cell can't hope to rival the efficiency of the Li-Ion battery but at the moment it doesn't need to. The BEV is hamstrung by poor range and massive recharge times. If there were to be a breakthrough in battery technology though, a fleet of BEVs powered by renewable energy, even if that renewable energy was hydrogen shipped to a hydrogen burning power station would be the best answer to human passenger transportation. This project makes no secret of that fact but all the available information suggests that such a breakthrough is neither imminent nor predicted in the near future. The car manufactures and major oil companies currently see the H₂FCEV as the ultimate solution and logical progression for passenger vehicles and all the information examined in this study leads it to draw the same conclusion. The hard question to answer is when.

8.5 The Need for Open Dialogue

One of the most prohibitive and frustrating aspects of this study has been the difficulty in obtaining data, information and materials with which to improve the study. The need for corporations to protect their intellectual property is acknowledged and understood, but a

more open dialogue between academia and industry could accelerate the development of H₂FCEVs to the benefit of both. However, more importantly it will be to the greater benefit of this planet and its people. There are some issues that should transcend politics and self-interest. The current state of the discourse on climate change does not suggest anyone would be receptive to this plea, but it is one worth making nonetheless.

8.6 Future Work

- 1) The fundamental power electronic control of the new topology bypass converter needs to be observed, described and recorded so it can be simulated with a complete set of empirical data rather than just the empirical data supplied by the device manufacturer. A scaled hardware DC-DC with thyristor bypass power converter system was conceptualised, designed and prepared for prototyping.
- 2) Regenerative braking needs to be incorporated into the simulation model and the components optimised to recapture as much energy as possible.
- 3) A simulation system needs to be developed to automate the variation of drivetrain component sizing to derive the ideal component sizing for each mode of driving and market. Appropriate sizing of the components could deliver significant cost benefits by reducing materials spend and increasing performance and efficiency. Because of the number of interactions between the subsystems, manually exploring this optimisation is likely impossible and the problem is probably best suited to automated analysis with high performance computing (HPC).
- 4) In addition to optimising the component size, consideration should be given as to whether the optimal energy storage system consists of batteries alone or a combination of batteries and super capacitors. Further investigation in this area may reduce the number of battery cells required yet increase the acceleration performance and the amount of energy that can be recaptured by regenerative braking by utilising the power density of super capacitors.
- 5) Significant advances are required in the fuel cell system and hydrogen storage system. Less significant leaps are needed in motor drive technology and battery control. The ability to shut the fuel cell down to reduce idling losses or at low efficiency operating points where the battery is better able to deliver power to the load more efficiently would be a significant step forward in drive train design but is currently prohibited by the materials technology associated with the fuel cell.

8.7 Summary

This thesis has shown that hydrogen fuel cell electric vehicles can be developed beyond the current state of the art. It has identified areas where the vehicle design can be improved both in the drivetrain and in the whole vehicle design. It is likely that we will see the adoption of such vehicles within the next 20-30 years. On what scale it is hard to predict but this study is certain that hydrogen, electric vehicles, and the fuel cell electric vehicle in particular, are the only real alternatives to fossil fuel powered mass transport that are currently foreseeable.

9 References

- [1] E. M. Rogers, *Diffusion of Innovations*, 5 ed.: New York Free Press, 1962.
- [2] "BP Statistical Review of World Energy," British Petroleum 2012.
- [3] (2013). *Reducing CO2 emissions from passenger cars*. Available: http://ec.europa.eu/clima/policies/transport/vehicles/cars/faq_en.htm
- [4] "European CO2 Emission Performance Standards for Passenger Cars and Light Commercial Vehicles," International Council on Clean Transportation 2012.
- [5] "Motor Industry Facts 2013," Society of Motor Manufacturers and Traders 2013.
- [6] M. Fallon and N. Baker, "Driving the Future Today - A strategy for ultra low emission vehicles in the UK," UK Department for Transport. Office for Low Emission Vehicles, United Kingdom September 2013 2013.
- [7] J. Struben and J. D. Sterman, "Transition Challenges for Alternative Fuel Vehicle and Transportation Systems," *Environment and Planning B: Planning and Design*, vol. 35, pp. 1070-1097, 2008.
- [8] B. G. Pollet, I. Staffell, and J. L. Shang, "Current status of hybrid, battery and fuel cell electric vehicles: From electrochemistry to market prospects," *Electrochimica Acta*, 2012.
- [9] R. H. Bezdek and R. M. Wendling, "Potential long-term impacts of changes in US vehicle fuel efficiency standards," *Energy Policy*, vol. 33, pp. 407-419, 2005.
- [10] "Briefing: German manufacturers calling for weaker car fuel efficiency targets," European Federation for Transport and Environment July 10th 2012 2012.
- [11] Y. Liu and G. E. Helfand, "The Alternative Motor Fuels Act, alternative-fuel vehicles, and greenhouse gas emissions," *Transportation Research Part A: Policy and Practice*, vol. 43, pp. 755-764, 2009.
- [12] S. Sorrell, "Fuel efficiency in the UK vehicle stock," *Energy Policy*, vol. 20, pp. 766-780, 1992.
- [13] T.-H. Kwon, "The determinants of the changes in car fuel efficiency in Great Britain (1978–2000)," *Energy Policy*, vol. 34, pp. 2405-2412, 2006.
- [14] M. Sivak and O. Tsimhoni, "Fuel efficiency of vehicles on US roads: 1923–2006," *Energy Policy*, vol. 37, pp. 3168-3170, 2009.
- [15] K. S. Whitefoot and S. J. Skerlos, "Design incentives to increase vehicle size created from the U.S. footprint-based fuel economy standards," *Energy Policy*, vol. 41, pp. 402-411, 2012.
- [16] E. Kesidou and P. Demirel, "On the drivers of eco-innovations: Empirical evidence from the UK," *Research Policy*, vol. 41, pp. 862-870, 2012.
- [17] A. Shukla, J. Pekny, and V. Venkatasubramanian, "An optimization framework for cost effective design of refueling station infrastructure for alternative fuel vehicles," *Computers & Chemical Engineering*, vol. 35, pp. 1431-1438, 2011.
- [18] S. Yeh, "An empirical analysis on the adoption of alternative fuel vehicles: The case of natural gas vehicles," *Energy Policy*, vol. 35, pp. 5865-5875, 2007.
- [19] M. Achtnicht, G. Bühler, and C. Hermeling, "The impact of fuel availability on demand for alternative-fuel vehicles," *Transportation Research Part D: Transport and Environment*, vol. 17, pp. 262-269, 2012.
- [20] D. Browne, M. O'Mahony, and B. Caulfield, "How should barriers to alternative fuels and vehicles be classified and potential policies to promote innovative technologies be evaluated?," *Journal of Cleaner Production*, vol. 35, pp. 140-151, 2012.
- [21] M. Kuby and S. Lim, "The flow-refueling location problem for alternative-fuel vehicles," *Socio-Economic Planning Sciences*, vol. 39, pp. 125-145, 2005.
- [22] H. Hu and R. Green, "Making markets for hydrogen vehicles: Lessons from LPG," *International Journal of Hydrogen Energy*, vol. 36, pp. 6399-6406, 2011.

- [23] O. D. Momoh and M. O. Omoigui, "An Overview of Hybrid Electric Vehicle Technology," presented at the IEEE Vehicle Power and Propulsion Conference, 2009.
- [24] X. Wu, B. Cao, X. Li, J. Xu, and X. Ren, "Component sizing optimization of plug-in hybrid electric vehicles," *Applied Energy*, vol. 88, pp. 799-804, 2011.
- [25] L. Houyu and Z. Guirong, "Hybrid Electric Vehicle Drive Control," *Procedia Environmental Sciences*, vol. 10, Part A, pp. 403-407, 2011.
- [26] K. Çağatay Bayindir, M. A. Gözükcük, and A. Teke, "A comprehensive overview of hybrid electric vehicle: Powertrain configurations, powertrain control techniques and electronic control units," *Energy Conversion and Management*, vol. 52, pp. 1305-1313, 2011.
- [27] A. Bredekamp, "Toyota Prius Engine Cross Section," Toyota_1NZ-FXE_Engine_01.JPG, Ed., ed. Web, 2010.
- [28] "Motor Industry Facts 2012," Society of Motor Manufacturers and Traders 2012.
- [29] A. Bandivadekar, *On the road in 2035 : reducing transportation's petroleum consumption and GHG emissions*, 1st ed. Cambridge, Mass.: Massachusetts Institute of Technology, 2008.
- [30] "Technology Roadmap - Electric and plug-in hybrid electric vehicles," International Energy Agency 2011.
- [31] A. C. UK, "UK OEM Consensus Passenger Car Technology Roadmap," Automotive Council UK 2010.
- [32] N. Bento, "Dynamic competition between plug-in hybrid and hydrogen fuel cell vehicles for personal transportation," *International Journal of Hydrogen Energy*, vol. 35, pp. 11271-11283, 2010.
- [33] "Electric and Plug-In Hybrid Vehicle Roadmap," International Energy Agency 2010.
- [34] C. Weiller, "Plug-in hybrid electric vehicle impacts on hourly electricity demand in the United States," *Energy Policy*, vol. 39, pp. 3766-3778, 2011.
- [35] R. Gilbert and A. Perl, "Grid-connected vehicles as the core of future land-based transport systems," *Energy Policy*, vol. 35, pp. 3053-3060, 2007.
- [36] G. J. Suppes, "Roles of plug-in hybrid electric vehicles in the transisition to the hydrogen economy," *International Journal of Hydrogen Energy*, vol. 31, pp. 353-360, 2006.
- [37] A. F. Burke, "Batteries and Ultracapacitors for Electric, Hybrid, and Fuel Cell Vehicles," *Proceedings of the IEEE*, vol. 95, pp. 806-820, 2007.
- [38] A. Parris, "Light Vehicle Alternative Fuels and Fuel Economy Related Technologies," US Department of Commerce International Trade Administration 2009.
- [39] "BP Energy Outlook 2030," British Petroleum 2012.
- [40] G. R. Timilsina, J. C. Beghin, D. van der Mensbrugghe, and S. Mevel, "The Impacts of Biofuel Targets on Land-Use Change and Food Supply - A Global CGE Assessment," The World Bank 2010.
- [41] C. E. Sandy Thomas, "Transportation options in a carbon-constrained world: Hybrids, plug-in hybrids, biofuels, fuel cell electric vehicles, and battery electric vehicles," *International Journal of Hydrogen Energy*, vol. 34, pp. 9279-9296, 2009.
- [42] S. Blanchette Jr, "A hydrogen economy and its impact on the world as we know it," *Energy Policy*, vol. 36, pp. 522-530, 2008.
- [43] P. A. Steenhof and B. C. McInnis, "A comparison of alternative technologies to decarbonize Canada's passenger transportation sector " *Technological Forecasting and Social Change*, pp. 12-19, 2008.
- [44] W. Shen, W. Han, D. Chock, Q. Chai, and A. Zhang, "Well-to-wheels life-cycle analysis of alternative fuels and vehicle technologies in China," *Energy Policy*, vol. 49, pp. 296-307, 2012.

- [45] S. Crutchfield. (2012). *U.S. Drought 2012: Farm and Food Impacts*. Available: <http://www.ers.usda.gov/topics/in-the-news/us-drought-2012-farm-and-food-impacts.aspx> - .UYmW1Cta224
- [46] U. Bossel, "Does a Hydrogen Economy Make Sense?," *Proceedings of the IEEE*, vol. 94, pp. 1826-1837, 2006.
- [47] "The Future of Natural Gas - An Interdisciplinary MIT Study," Massachusetts Institute of Technology 2012.
- [48] H. C. Mantripragada and E. S. Rubin, "Techno-economic evaluation of coal-to-liquids (CTL) plants with carbon capture and sequestration," *Energy Policy*, vol. 39, pp. 2808-2816, 2011.
- [49] S. Chiuta and E. Blom, "Techno-economic evaluation of a nuclear-assisted coal-to-liquid facility," *Progress in Nuclear Energy*, vol. 54, pp. 68-74, 2012.
- [50] X. Ou, X. Yan, and X. Zhang, "Using coal for transportation in China: Life cycle GHG of coal-based fuel and electric vehicle, and policy implications," *International Journal of Greenhouse Gas Control*, vol. 4, pp. 878-887, 2010.
- [51] X. Ou, X. Zhang, and S. Chang, "Scenario analysis on alternative fuel/vehicle for China's future road transport: Life-cycle energy demand and GHG emissions," *Energy Policy*, vol. 38, pp. 3943-3956, 2010.
- [52] R. Hammerschlag and P. Mazza, "Questioning hydrogen," *Energy Policy*, vol. 33, pp. 2039-2043, 2005.
- [53] E. Baker, H. Chon, and J. Keisler, "Battery Technology for Electric and Hybrid Vehicles: Expert Views about Prospects for Advancement.," *Technology Forecasting Social Change*, vol. 77, pp. 1139-1146, 2010.
- [54] "Cost and performance of EV batteries," Element Energy Limited report for The Committee on Climate Change 21st March 2012 2012.
- [55] A. Chu and P. Braatz, "Comparison of commercial supercapacitors and high-power lithium-ion batteries for power-assist applications in hybrid electric vehicles: I. Initial characterization," *Journal of Power Sources*, vol. 112, pp. 236-246, 2002.
- [56] E. Karden, S. Ploumen, B. Fricke, T. Miller, and K. Snyder, "Energy storage devices for future hybrid electric vehicles," *Journal of Power Sources*, vol. 168, pp. 2-11, 2007.
- [57] C. Sapienza, L. Andaloro, F. V. Matera, G. Dispenza, P. CretI, M. Ferraro, and V. Antonucci, "Batteries analysis for FC-hybrid powertrain optimization," *International Journal of Hydrogen Energy*, vol. 33, pp. 3230-3234, 2008.
- [58] M. Contestabile, G. J. Offer, R. Slade, F. Jaeger, and M. Thoennes, "Battery electric vehicles, hydrogen fuel cells and biofuels. Which will be the winner?," *Energy & Environmental Science*, vol. 4, pp. 3754-3772, 2011.
- [59] A. Dinger, R. Martin, X. Mosquet, M. Rabi, D. Rizoulis, M. Russo, and G. Sticher, "Batteries for Electric Cars - Challenges, Opportunities and the Outlook to 2020," Boston Consulting Group 2010.
- [60] A. Grenier and S. Page, "The impact of electrified transport on local grid infrastructure: A comparison between electric cars and light rail," *Energy Policy*, vol. 49, pp. 355-364, 2012.
- [61] K. D. Huang and S.-C. Tzeng, "A new parallel-type hybrid electric-vehicle," *Applied Energy*, vol. 79, pp. 51-64, 2004.
- [62] M. Book, M. Groll, X. Mosquet, D. Rizoulis, and G. Sticher, "The Comeback of the Electric Car?," Boston Consulting Group 2009.
- [63] G. J. Offer, M. Contestabile, D. A. Howey, R. Clague, and N. P. Brandon, "Techno-economic and behavioural analysis of battery electric, hydrogen fuel cell and hybrid vehicles in a future sustainable road transport system in the UK," *Energy Policy*, vol. 39, pp. 1939-1950, 2011.
- [64] C. E. Thomas, "Fuel cell and battery electric vehicles compared," *International Journal of Hydrogen Energy*, vol. 34, pp. 6005-6020, 2009.

- [65] X. Yan, O. R. Inderwildi, and D. A. King, "Biofuels and synthetic fuels in the US and China: A review of Well-to-Wheel energy use and greenhouse gas emissions with the impact of land-use change," *Energy & Environmental Science*, vol. 3, pp. 190-197, 2010.
- [66] I. Staffell, "The Energy and Fuel Data Sheet," University of Birmingham 2012.
- [67] J. Schoonman, "Sustainable Hydrogen, a European Perspective," presented at the GCEP Hydrogen Conference, Schwab Center, Stanford University, US, 2003.
- [68] M. Granovskii, I. Dincer, and M. A. Rosen, "Economic and environmental comparison of conventional, hybrid, electric and hydrogen fuel cell vehicles," *Journal of Power Sources*, vol. 159, pp. 1186-1193, 2006.
- [69] "Hydrogen Production - Overview of Technology Options," FreedomCAR & Fuel Partnership 2009.
- [70] S. Hadlington. (2005, March 2005) Stepping on The Gas. *IEEE Review*. 40-43.
- [71] A. G. Dutton and M. Page, "The THESIS model: An assessment tool for transport and energy provision in the hydrogen economy," *International Journal of Hydrogen Energy*, vol. 32, pp. 1638-1654, 2007.
- [72] A. T-Raissi and D. L. Block. (2004) Hydrogen: Automotive Fuel of the Future. *IEEE Power & Energy Magazine*. 40-45.
- [73] P. Kruger, "Electric power requirement for large-scale production of hydrogen fuel for the world vehicle fleet," *International Journal of Hydrogen Energy*, vol. 26, pp. 1137-1147, 2001.
- [74] D. Levitan. (2012, 14/09/2012) Nuclear Fuel From the Sea. *IEEE Spectrum*. Available: <http://spectrum.ieee.org/energy/nuclear/nuclear-fuel-from-the-sea>
- [75] H. Liu, A. Almansoori, M. Fowler, and A. Elkamel, "Analysis of Ontario's hydrogen economy demands from hydrogen fuel cell vehicles," *International Journal of Hydrogen Energy*, vol. 37, pp. 8905-8916, 2012.
- [76] M. Esteban and D. Leary, "Current developments and future prospects of offshore wind and ocean energy," *Applied Energy*, vol. 90, pp. 128-136, 2012.
- [77] R. Shinnar, "The hydrogen economy, fuel cells, and electric cars," *Technology in Society*, vol. 25, pp. 455-476, 2003.
- [78] J. H. Gurney. (2004, March/April 2004) Building a Case for the Hydrogen Economy. *IEEE Power & Energy Magazine*. 35-39.
- [79] R. Card, R. Dixon, D. Garman, T. Gross, R. S. Johnson, K. Kimball, R. Kripowicz, R. Moorer, W. Parks, and F. Wilkins, "A National Vision of America's Transition To A Hydrogen Economy To 2030 And Beyond," U.S. Department of Energy 2002.
- [80] W. W. Clark, J. Rifkin, T. O'Connor, J. Swisher, T. Lipman, and G. Rambach, "Hydrogen energy stations: along the roadside to the hydrogen economy," *Utilities Policy*, vol. 13, pp. 41-50, 2005.
- [81] J. Sinha, J. Marcinkoski, K. Randolph, and T. G. Benjamin, "DOE Hydrogen Program - FY 2010 Annual Progress Report," United States Department of Energy 2010.
- [82] "Module 3: Hydrogen Use In Internal Combustion Engines," US Department of Energy, Energy Efficiency and Renewable Energy Dec 2001 2001.
- [83] C. M. White, R. R. Steeper, and A. E. Lutz, "The hydrogen-fueled internal combustion engine: a technical review," *International Journal of Hydrogen Energy*, vol. 31, pp. 1292-1305, 2006.
- [84] S. Verhelst and T. Wallner, "Hydrogen-fueled internal combustion engines," *Progress in Energy and Combustion Science*, vol. 35, pp. 490-527, 2009.
- [85] R. Mikalsen and A. P. Roskilly, "A review of free-piston engine history and applications," *Applied Thermal Engineering*, vol. 27, pp. 2339-2352, 2007.
- [86] P. van Blarigan, "Advanced Internal Combustion Electrical Generator," in *Proceedings of the 2002 U.S. DOE Hydrogen Program Review*, 2002.

- [87] M. J. Blackwelder and R. A. Dougal, "Power coordination in a fuel-cell battery hybrid power source using commercial power controller circuits," *Journal of Power Sources*, vol. 134, pp. 139-147, 2004.
- [88] H. Xu, L. Kong, and X. Wen, "Fuel Cell Power System and High Power DC-DC converter," *IEEE Transactions on Power Electronics*, vol. 19, pp. 1250-1255, 2004.
- [89] J. Van Mierlo, P. Van den Bossche, and G. Maggetto, "Models of energy sources for EV and HEV: fuel cells, batteries, ultracapacitors, flywheels and engine-generators," *Journal of Power Sources*, vol. 128, pp. 76-89, 2004.
- [90] W. Joerg, "Example of an FC system (NuCellSYS HY-80) for an automotive drivetrain," t_58_1.jpg, Ed., ed, 2005.
- [91] S. Gelfi, A. G. Stefanopoulou, J. T. Pukrushpan, and H. Peng, "Dynamics of Low-Pressure and High-Pressure Fuel Cell Air Supply Systems," in *American Control Conference 2003*, 2003, pp. 2049-2054.
- [92] A. Brouzgou, S. Q. Song, and P. Tsiakaras, "Low and non-platinum electrocatalysts for PEMFCs: Current status, challenges and prospects," *Applied Catalysis B: Environmental*, vol. 127, pp. 371-388, 2012.
- [93] A. F. Anderson and E. J. Carlson, "Platinum Availability and Economics for PEMFC Commercialization," US Department of Energy / TIAX2003.
- [94] C. Wang, M. Waje, X. Wang, J. M. Tang, R. C. Haddon, and Y. Yan, "Proton Exchange Membrane Fuel Cells with Carbon Nanotube Based Electrodes," *Nano Letters*, vol. 4, pp. 345-348, 2004.
- [95] S. Wang, Y. Dingshan, and L. Dai, "Polyelectrolyte Functionalized Carbon Nanotubes as Efficient Metal-free Electrocatalysts for Oxygen Reduction," *Journal of The American Chemical Society*, vol. 133, pp. 5182-5185, 2011.
- [96] M. Zhang and L. Dai, "Carbon nanomaterials as metal-free catalysts in next generation fuel cells," *Nano Energy*, vol. 1, pp. 514-517, 2012.
- [97] S. G. Chalk and J. F. Miller, "Key challenges and recent progress in batteries, fuel cells, and hydrogen storage for clean energy systems," *Journal of Power Sources*, vol. 159, pp. 73-80, 2006.
- [98] H. M. Zhang, "Progress on the Composite Membranes for PEM Fuel Cells," *Advanced Materials Research*, vol. 26-28, p. 839, 2007.
- [99] N. Cele and S. S. Ray, "Recent Progress on Nafion-Based Nanocomposite Membranes for Fuel Cell Applications," *Macromolecular Materials and Engineering*, vol. 294, pp. 719-738, 2009.
- [100] S. Mekhilef, R. Saidur, and A. Safari, "Comparative study of different fuel cell technologies," *Renewable and Sustainable Energy Reviews*, vol. 16, pp. 981-989, 2012.
- [101] C. E. Borroni-Bird, "Fuel cell commercialization issues for light-duty vehicle applications," *Journal of Power Sources*, vol. 61, pp. 33-48, 1996.
- [102] K. Rajashekara, "Propulsion System Strategies for Fuel Cell Vehicles," in *SAE 2000 World Congress*, Detroit, Michigan, 2000.
- [103] M. Cifrain and K. Kordesch, "Hydrogen/oxygen (Air) fuel cells with alkaline electrolytes," *Handbook of Fuel Cells – Fundamentals, Technology and Applications*, vol. 1, pp. 267-280, 2003.
- [104] G. Pasquerella, "The Hidenburg Disaster," n/a, Ed., ed: US Navy, 1937.
- [105] T. Hua, R. K. Ahluwalia, J. K. Peng, M. Kromer, S. Lasher, K. McKenney, K. Law, and J. Sinha, "Technical Assessment of Compressed Hydrogen Storage Tank Systems for Automotive Applications " Argonne National Laboratory - Nuclear Engineering Division 2010.
- [106] V. Ananthachar and J. J. Duffy, "Efficiencies of hydrogen storage systems onboard fuel cell vehicles," *Solar Energy*, vol. 78, pp. 687-694, 2005.
- [107] S. W. Jorgensen, "Hydrogen storage tanks for vehicles: Recent progress and current status," *Current Opinion in Solid State and Materials Science*, vol. 15, pp. 39-43, 2011.

- [108] R. von Helmolt and U. Eberle, "Fuel cell vehicles: Status 2007," *Journal of Power Sources*, vol. 165, pp. 833-843, 2007.
- [109] M. Felderhoff, C. Weidenthaler, R. von Helmolt, and U. Eberle, "Hydrogen storage: the remaining scientific and technological challenges," *Physical Chemistry Chemical Physics*, vol. 9, pp. 2643-2653, 2007.
- [110] K. H. Hauer, "Dynamic Interaction Between the Electric Drive Train and Fuel Cell System for the Case of an Indirect Methanol Fuel Cell Vehicle," 2000.
- [111] S. G. Chalk, P. G. Patil, and S. R. Venkateswaran, "The new generation of vehicles: market opportunities for fuel cells," *Journal of Power Sources*, vol. 61, pp. 7-13, 1996.
- [112] B. Bowman. (2012). 1966 GM Electrovan. Available: http://history.gmheritagecenter.com/wiki/index.php/1966_GM_Electrovan
- [113] VolkswagenAG. (2012). HyMotion-Touran/Tiguan. Available: http://www.volkswagenag.com/content/vwcorp/content/en/innovation/research_vehicles/HyMotion.html
- [114] Toyota. (2012). Fuel Cell Hybrid Vehicles. Available: http://www.toyota.com/about/environment/innovation/advanced_vehicle_technology/FCHV.html
- [115] FuelCells2000. (2012). Fuel Cell Vehicles. Available: <http://www.fuelcells.org/info/charts/carchart.pdf>
- [116] J. Voelcker. (2006) Driving GM's New Hydrogen Car. *IEEE Spectrum*. Available: <http://spectrum.ieee.org/energy/renewables/driving-gms-new-hydrogen-car>
- [117] B. Eberle and T. Hartkopf, "A high speed induction machine with two speed transmission as drive for electric vehicles," in *SPEEDAM 2006 - International Symposium on Power Electronics, Electrical Dris, Automation and Motion*, 2006, pp. S34-12-17.
- [118] L. Chang, "Comparison of AC drives for electric vehicles-a report on experts' opinion survey," *Aerospace and Electronic Systems Magazine, IEEE*, vol. 9, pp. 7-11, 1994.
- [119] A. J. Mitcham, A. G. Jack, and B. C. Mecrow, "High performance permanent magnet drive for electric vehicles," 1993, pp. 8/1-8/4.
- [120] K. Lu and E. Ritchie, "Preliminary comparison study of drive motor for electric vehicle application," in *ICEMS 2001*, Shenyang, 2001, pp. 995-998.
- [121] A. G. Jack, B. C. Mecrow, and C. Weiner, "Switched reluctance and permanent magnet motors suitable for vehicle drives-a comparison," 1999, pp. 505-507.
- [122] B. C. Mecrow, A. C. Clothier, and P. G. Barrass, "High performance switched reluctance drives using novel windings," 1996, pp. 6/1-6/5.
- [123] X. D. Xue, K. W. E. Cheng, and N. C. Cheung, "Selection of electric motor drives for electric vehicles," in *Power Engineering Conference, 2008. AUPEC '08. Australasian Universities*, 2008, pp. 1-6.
- [124] Kokam, "SLPB (Superior Lithium Polymer Battery Technical Specification) - SLPB75106100," ed, 2009.
- [125] K. H. Hauer, "Analysis Tool for Fuel Cell Vehicle Hardware and Software (Controls) with an Application to Fuel Economy Comparisons of Alternative System Designs," Doctor of Philosophy, Transportation Technology & Policy, University of California Davis, 2001.
- [126] R. M. Moore, K. H. Hauer, D. Friedman, J. Cunningham, P. Badrinarayanan, S. Ramaswamy, and A. Eggert, "A dynamic simulation tool for hydrogen fuel cell vehicles," *Journal of Power Sources*, vol. 141, pp. 272-285, 2005.
- [127] K. Pill-Soo, "Cost modeling of battery electric vehicle and hybrid electric vehicle based on major parts cost," in *Power Electronics and Drive Systems, 2003. PEDS 2003. The Fifth International Conference on*, 2003, pp. 1295-1300 Vol.2.
- [128] A. Emadi and S. S. Williamson, "Fuel cell vehicles: opportunities and challenges," 2004, pp. 1640-1645 Vol.2.

- [129] S. M. N. Hasan, S. Kim, and I. Husain, "Power Electronic Interface and Motor Control for a Fuel Cell Electric Vehicle," in *19th Applied Power Electronics Conference and Exposition*, 2004, pp. 1171-1177.
- [130] M. Joeri Van, C. Yonghua, T. Jean-Marc, and B. Peter Van den, "Comparison of Fuel Cell Hybrid Propulsion Topologies with Super-Capacitor," 2006, pp. 501-505.
- [131] J. Marhsall and M. Kazerani, "Design of an efficient fuel cell vehicle drivetrain, featuring a novel boost converter," in *Industrial Electronics Society, 2005. IECON 2005. 32nd Annual Conference of IEEE*, 2005.
- [132] J. Wang, Z. Fang, J. Anderson, A. Joseph, and R. Buffenbarger, "Low Cost Fuel Cell Converter System for Residential Power Generation," *IEEE Transactions on Power Electronics*, vol. 19, pp. 1315-1322, 2004.
- [133] J. Bernard, M. Hofer, U. Hannesen, A. Toth, A. Tsukada, F. N. Büchi, and P. Dietrich, "Fuel cell/battery passive hybrid power source for electric powertrains," *Journal of Power Sources*, vol. 196, pp. 5867-5872, 2011.
- [134] P. Corbo, F. E. Corcione, F. Migliardini, and O. Veneri, "Energy management in fuel cell power trains," *Energy Conversion and Management*, vol. 47, pp. 3255-3271, 2006.
- [135] Y. Tang, W. Yuan, M. Pan, and Z. Wan, "Experimental investigation on the dynamic performance of a hybrid PEM fuel cell/battery system for lightweight electric vehicle application," *Applied Energy*, vol. 88, pp. 68-76, 2011.
- [136] D. Wu and S. S. Williamson, "Status Review of Power Control Strategies for Fuel Cell Based Hybrid Electric Vehicles," presented at the IEEE Canada Electrical Power Conference, Canada, 2007.
- [137] R. K. Ahluwalia, X. Wang, and A. Rousseau, "Fuel economy of hybrid fuel-cell vehicles," *Journal of Power Sources*, vol. 152, pp. 233-244, 2005.
- [138] H. S. Lee, K. S. Jeong, and B. S. Oh, "An experimental study of controlling strategies and drive forces for hydrogen fuel cell hybrid vehicles," *International Journal of Hydrogen Energy*, vol. 28, pp. 215-222, 2003.
- [139] G. Wasselynck, B. Auvity, J.-C. Olivier, D. Trichet, C. Josset, and P. Maindru, "Design and testing of a fuel cell powertrain with energy constraints," *Energy*, vol. 38, pp. 414-424, 2012.
- [140] F. Liu, Z. Jin, J., D. Gao, and Q. Lu, "Development and Application of Fuel Cell Hybrid Powertrain Simulation Platform," presented at the IEEE Vehicle Power and Propulsion Conference, Harbin, China, 2008.
- [141] F. Barreras, M. Maza, A. Lozano, S. Bascónes, V. Roda, J. E. Barranco, M. Cerqueira, and A. Vergés, "Design and development of a multipurpose utility AWD electric vehicle with a hybrid powertrain based on PEM fuel cells and batteries," *International Journal of Hydrogen Energy*.
- [142] D. Brown, M. Alexander, D. Brunner, S. G. Advani, and A. K. Prasad, "Drive-train simulator for a fuel cell hybrid vehicle," *Journal of Power Sources*, vol. 183, pp. 275-281, 2008.
- [143] J. Buamann and M. Kazerani, "An Improved Powertrain Topology for Fuel Cell-Battery-Ultracapacitor Vehicles," presented at the IEEE International Symposium on Industrial Electronics, 2008.
- [144] P. Bubna, D. Brunner, S. G. Advani, and A. K. Prasad, "Prediction-based optimal power management in a fuel cell/battery plug-in hybrid vehicle," *Journal of Power Sources*, vol. 195, pp. 6699-6708, 2010.
- [145] K. Ettihir, L. Boulon, K. Agbossou, S. Kelouwani, and M. Hammoudi, "Design of an energy management strategy for PEM Fuel Cell Vehicles," presented at the Industrial Electronics (ISIE), 2012 IEEE International Symposium on , 2012.

- [146] P. Fisher, J. Jostins, S. Hilmanen, and K. Kendall, "Electronic integration of fuel cell and battery system in novel hybrid vehicle," *Journal of Power Sources*, vol. 220, pp. 114-121, 2012.
- [147] Y. Hou, B. Wang, and Z. Yang, "A method for evaluating the efficiency of PEM fuel cell engine," *Applied Energy*, vol. 88, pp. 1181-1186, 2011.
- [148] J.-J. Hwang, Y.-J. Chen, and J.-K. Kuo, "The study on the power management system in a fuel cell hybrid vehicle," *International Journal of Hydrogen Energy*, vol. 37, pp. 4476-4489, 2012.
- [149] J. J. Hwang and W. R. Chang, "Characteristic study on fuel cell/battery hybrid power system on a light electric vehicle," *Journal of Power Sources*, vol. 207, pp. 111-119, 2012.
- [150] C.-Y. Li and G.-P. Liu, "Optimal fuzzy power control and management of fuel cell/battery hybrid vehicles," *Journal of Power Sources*, vol. 192, pp. 525-533, 2009.
- [151] X. Li, L. Xu, J. Hua, X. Lin, J. Li, and M. Ouyang, "Power management strategy for vehicular-applied hybrid fuel cell/battery power system," *Journal of Power Sources*, vol. 191, pp. 542-549, 2009.
- [152] M. J. Marcel, T. A. Haskew, and K. A. Williams, "Test facility for a hybrid fuel cell electric vehicle," in *SoutheastCon, 2007. Proceedings. IEEE*, 2007, pp. 734-739.
- [153] C. A. Ramos-Paja, C. Bordons, A. Romero, R. Giral, and L. Martinez-Salamero, "Minimum Fuel Consumption Strategy for PEM Fuel Cells," *IEEE Transactions on Industrial Electronics*, vol. 56, pp. 685-696, 2009.
- [154] C. A. Ramos-Paja, A. Romero, R. Giral, J. Calvente, and L. Martinez-Salamero, "Mathematical analysis of hybrid topologies efficiency for PEM fuel cell power systems design," *International Journal of Electrical Power & Energy Systems*, vol. 32, pp. 1049-1061, 2010.
- [155] A. Schell, H. Peng, D. Tran, E. Stamos, C.-C. Lin, and M. J. Kim, "Modelling and control strategy development for fuel cell electric vehicles," *Annual Reviews in Control*, vol. 29, pp. 159-168, 2005.
- [156] K. S. Jeong and B. S. Oh, "Fuel economy and life-cycle cost analysis of a fuel cell hybrid vehicle," *Journal of Power Sources*, vol. 105, pp. 58-65, 2002.
- [157] J. Baumann and M. Kazerani, "A Comparative Study of Fuel-Cell-Battery, Fuel-Cell-Ultracapacitor, and Fuel-Cell-Battery-Ultracapacitor Vehicles," *IEEE Transactions on Vehicular Technology*, vol. 57, pp. 760-769, 2008.
- [158] Q. Li, W. Chen, Y. Li, S. Liu, and J. Huang, "Energy management strategy for fuel cell/battery/ultracapacitor hybrid vehicle based on fuzzy logic," *International Journal of Electrical Power & Energy Systems*, vol. 43, pp. 514-525, 2012.
- [159] L. Xu, J. Li, J. Hua, X. Li, and M. Ouyang, "Optimal vehicle control strategy of a fuel cell/battery hybrid city bus," *International Journal of Hydrogen Energy*, vol. 34, pp. 7323-7333, 2009.
- [160] M.-J. Kim and H. Peng, "Power management and design optimization of fuel cell/battery hybrid vehicles," *Journal of Power Sources*, vol. 165, pp. 819-832, 2007.
- [161] S. Ahmed and D. J. Chmielewski, "Load characteristics and control of a hybrid fuel cell / battery vehicle," presented at the Proceedings of the 2009 conference on American Control Conference, St. Louis, Missouri, USA, 2009.
- [162] D. Feroldi, M. Serra, and J. Riera, "Energy Management Strategies based on efficiency map for Fuel Cell Hybrid Vehicles," *Journal of Power Sources*, vol. 190, pp. 387-401, 2009.
- [163] N. Henao, S. Kelouwani, K. Agbossou, and Y. Dubé, "Proton exchange membrane fuel cells cold startup global strategy for fuel cell plug-in hybrid electric vehicle," *Journal of Power Sources*, vol. 220, pp. 31-41, 2012.
- [164] G. Pede, A. Iacobazzi, S. Passerini, A. Bobbio, and G. Botto, "FC vehicle hybridisation: an affordable solution for an energy-efficient FC powered drive train," *Journal of Power Sources*, vol. 125, pp. 280-291, 2004.

- [165] S. Pischinger, C. Schönfelder, and J. Ogrzewalla, "Analysis of dynamic requirements for fuel cell systems for vehicle applications," *Journal of Power Sources*, vol. 154, pp. 420-427, 2006.
- [166] P. Thounthong, P. Sethakul, S. Rael, and B. Davat, "Performance investigation of fuel cell/battery and fuel cell/supercapacitor hybrid sources for electric vehicle applications," in *Power Electronics, Machines and Drives, 2008. PEMD 2008. 4th IET Conference on*, 2008, pp. 455-459.
- [167] N. Bizon, "A new topology of fuel cell hybrid power source for efficient operation and high reliability," *Journal of Power Sources*, vol. 196, pp. 3260-3270, 2011.
- [168] V. Paladini, T. Donato, A. de Risi, and D. Laforgia, "Super-capacitors fuel-cell hybrid electric vehicle optimization and control strategy development," *Energy Conversion and Management*, vol. 48, pp. 3001-3008, 2007.
- [169] R. M. Freinds and J. P. Kajs, "Comparison of the Matrix and DC-link Converter Topologies in a Hybrid Electric Vehicle," in *Future Transportation Technology Conference*, Costa Mesa, California, 2003.
- [170] L. Gao, Z. Jiang, and R. A. Dougal, "An actively controlled fuel cell/battery hybrid to meet pulsed power demands," *Journal of Power Sources*, vol. 130, pp. 202-207, 2004.
- [171] A. Folkesson, C. Andersson, P. Alvfors, M. Alakula, and L. Overgaard, "Real life testing of a Hybrid PEM Fuel Cell Bus," *Journal of Power Sources*, vol. 118, pp. 349-357, 2003.
- [172] S. E. Gay, H. Gao, and M. Ehsani, "Fuel Cell hybrid Drive Train Configurations and Motor Drive Selection," in *56th Annual Vehicular Technology Conference*, 2002, pp. 1007-1010.
- [173] K. Wang, C. Y. Lin, L. Zhu, D. Qu, F. C. Lee, and J. S. Lai, "Bi-Directional DC to DC converters for Fuel Cell Systems," in *IEEE Power Electronics In Transportation*, 1998, pp. 47-51.
- [174] R. Kotz, M. Bartschi, F. Buchi, R. Gallay, and P. Dietrich, "HY. Power - A Fuel Cell Car Boosted With Supercapacitors," in *12th International Seminar on Double Layer Capacitors and Similar Energy Storage Devices*, Deerfield Beach, USA, 2002.
- [175] R. Kotz, S. Muller, M. Bartschi, B. Schnyder, P. Dietrich, F. N. Buchi, A. Tsukada, G. G. Scherer, P. Rodatz, O. Garcia, P. Barrade, V. Hermann, and R. Gallay, "Supercapictors for peak-power demand in fuel-cell-driven cars," *Electrochemical Societ Proceedings*, vol. 21, pp. 564-575, 2001.
- [176] M. Marchesoni and C. Vacca, "A New DC-DC Converter Structure for Power Flow Management in Fuel-Cell Electric Vehicles with Energy Storage Systems," in *35th Annual IEEE Power Electronics Specialists Conference*, Aachen, Germany, 2004, pp. 683-689.
- [177] M. Michon, J. L. Duarte, M. Hendrix, and M. G. Simoes, "A three-port bi-directional converter for hybrid fuel cell systems," in *35th Annual IEEE Power Electronics Specialists Conference*, Aachen, Germany, 2004, pp. 4736-4742.
- [178] A. D. Napoli, F. Crescimbeni, S. Rodo, and L. Solero, "Multiple Input DC-DC Power Converter for Fuel Cell Powered Hybrid Vehicles," in *IEEE Annual Power Electronics Specialist Conference*, 2002, pp. 1685-1690.
- [179] L. Solero, A. Lidozzi, and J. A. Pomilio, "Design of Multiple-Input Power Converter for Hybrid Vehicles," in *19th Annual IEEE Applied Power Electronics Conference & Exposition*, 2004, pp. 1145-1151.
- [180] S. Aso, M. Kizaki, and Y. Nonobe, "Development of Fuel Cell Hybrid Vehicles in TOYOTA," 2007, pp. 1606-1611.
- [181] A. Emadi, K. Rajashekara, S. S. Williamson, and S. M. Lukic, "Topological overview of hybrid electric and fuel cell vehicular power system architectures and configurations," *Vehicular Technology, IEEE Transactions on*, vol. 54, pp. 763-770, 2005.

- [182] L. Gao, Z. Jiang, and R. A. Rougal, "Performance of Power Converters in Hybrid Fuel Cell/Battery Power Sources," in *35th Annual IEEE Power Electronics Specialists Conference*, Aachen, Germany, 2004.
- [183] M. Nadal and F. Barbir, "Development of a Hybrid Fuel Cell/Battery Powered Electric Vehicle," *International Journal of Hydrogen Energy*, vol. 21, pp. 497-505, 1996.
- [184] H. Yun, Y. Zhao, and J. Wang, "Modeling and simulation of fuel cell hybrid vehicles," *International Journal of Automotive Technology*, vol. 11, pp. 223-228, 2010/04/01 2010.
- [185] L. Gokdere, K. Benlayazid, R. A. Dougal, E. Santi, and C. W. Brice, "A virtual prototype for a hybrid electric vehicle," *Mechatronics*, vol. 12, pp. 575-593, 2002.
- [186] F. Z. Peng, H. Li, G. Su, and J. S. Lawler, "A New ZVS Bidirectional DC-DC Converter for Fuel Cell and Battery Application," *IEEE Transactions on Power Electronics*, vol. 19, pp. 54-65, 2004.
- [187] G. Rizzoni, L. Guzzella, and B. M. Baumann, "Unified Modeling of Hybrid Electric Vehicle Drivetrains," *IEEE/ASME Transactions On Mechatronics*, vol. 4, pp. 246-257, 1999.
- [188] A. Same, A. Stipe, D. Grossman, and J. W. Park, "A study on optimization of hybrid drive train using Advanced Vehicle Simulator (ADVISOR)," *Journal of Power Sources*, vol. 195, pp. 6954-6963, 2010.
- [189] A. Emadi, *Handbook of Automotive Power Electronics and Motor Drives*, 2005.
- [190] Toyota. (2007, 2007) aim: zero emissions. 1-22.
- [191] S. Wilkins and M. U. Lampert, "An Object-Oriented Modelling Tool of Hybrid Powertrains for Vehicle Performance Simulation," presented at the EVS19, Busan, South Korea, 2002.
- [192] W. Maurer and Z. H. Winterthur, "Modelica/Dymola - a multidomain modelling and simulation environment for fuel cells?," 2004.
- [193] M. J. Ogburn, D. Nelson, K. Wipke, and T. Markel, "Modelling and Validation of a Fuel Cell Hybrid Vehicle," *Society of Automotive Engineers*, vol. 01, 2000.
- [194] B. Sørensen, "Assessing current vehicle performance and simulating the performance of hydrogen and hybrid cars," *International Journal of Hydrogen Energy*, vol. 32, pp. 1597-1604, 2007.
- [195] D. Doerffel and S. Abu Sharkh, "System Modeling and Simulation as a Tool for Developing a Vision for Future Hybrid Electric Vehicle Drivetrain Configurations," in *Vehicle Power and Propulsion Conference, 2006. VPPC '06. IEEE*, 2006, pp. 1-6.
- [196] C.-C. Lin, Z. Filipi, Y. Wang, L. Louca, H. Peng, D. Assanis, and J. Stein, "Integrated, Feed-Forward Hybrid Electric Vehicle Simulation in SIMULINK and its Use for Power Management Studies " *Society of Automotive Engineers*, vol. 2001-01, p. 1334, 2001.
- [197] P. Sharer, R. Leydier, and A. Rousseau, "Impact of Drive Cycle Aggressiveness and Speed on HEVs Fuel Consumption Sensitivity," *Society of Automotive Engineers*, 2007.
- [198] Q. Ning, D. Xuan, and Y. Kim, "Modeling and control strategy development for fuel cell hybrid vehicles," *International Journal of Automotive Technology*, vol. 11, pp. 229-238, 2010.
- [199] J. Van Mierlo and G. Maggetto, "Innovative iteration algorithm for a vehicle simulation program," *Vehicular Technology, IEEE Transactions on*, vol. 53, pp. 401-412, 2004.
- [200] D. S. Bernstein, "From the editor - Theorem and look-up table," *Control Systems, IEEE*, vol. 24, pp. 6-6, 2004.
- [201] J. Y. Wong, *Theory of Ground Vehicles*: Wiley-Interscience, 1978.

- [202] J. Lee, "Rotating Inertia Impact on Propulsion and Regenerative Braking for Electric Motor Driven Vehicles " Master of Science, Mechanical Engineering, Virginia Polytechnic Institute and State University, 2005.
- [203] P. Fajri, R. Ahmadi, and M. Ferdowsi, "Equivalent vehicle rotational inertia used for electric vehicle test bench dynamic studies," in *IECON 2012 - 38th Annual Conference on IEEE Industrial Electronics Society*, 2012, pp. 4115-4120.
- [204] K. H. Hauer and R. M. Moore, "Fuel Cell Vehicle Simulation - Part 3: Modelling of Individual Components and Integration into the Overall Vehicle Model," *Fuel Cells* 2003, vol. 3, pp. 105-121, 2003.
- [205] G. Xu, W. Li, K. Xu, and Z. Song, "An Intelligent Regenerative Braking Strategy for Electric Vehicles," *energies*, vol. 4, pp. 1461-1477, 22-09-2011 2011.
- [206] J. Zhang, X. Lu, J. Xue, and B. Li, "Regenerative Braking System for Series Hybrid Electric City Bus," *The World Electric Vehicle Journal*, vol. 2, pp. 363-369, 2008.
- [207] M. Panagiotidis, G. Delagrammatikas, and D. Assanis, "Development and Use of a Regenerative Braking Model for a Parallel Hybrid Electric Vehicle," presented at the Society of Automotive Engineers 2000 World Congress, Detroit, Michigan, 2000.
- [208] A. A. Mukhitdinov, S. K. Ruzimov, and S. L. Eshkabilov, "Optimal Control Strategies for CVT of the HEV during a regenerative process," in *Electric and Hybrid Vehicles, 2006. ICEHV '06. IEEE Conference on*, 2006, pp. 1-12.
- [209] K. Hirose, "Challenge of Hydrogen Fuel Cell Vehicle and Hydrogen Storage Technologies Toward The Sustainable Society," presented at the StorHy 2008, PSA Poissy, France, 2008.
- [210] H. Otsubo, M. Mizuno, Y. Negishi, and N. Ogami, "High-Pressure Hydrogen Tank for FCHV," *Society of Automotive Engineers*, vol. 1, 2007.
- [211] T. Markel, K. Wipke, and D. Nelson, "Vehicle System Impacts of Fuel Cell System Power Response Capability," *Society of Automotive Engineers*, 2002.
- [212] D. Chen and H. Peng, "A Thermodynamic Model of Membrane Humidifiers for PEM Fuel Cell Humidification Control," *Journal of Dynamic Systems, Measurement, and Control*, vol. 127, pp. 424-432, 2005.
- [213] C. Dongmei and P. Hueti, "Modeling and simulation of a PEM fuel cell humidification system," in *American Control Conference, 2004. Proceedings of the 2004*, 2004, pp. 822-827 vol.1.
- [214] K. Haraldsson, "On Direct Hydrogen Fuel Cell Vehicles - Modelling and Demonstation," Doctor of Philosophy, Department of Chemical Engineering and Technology, KTH- Royal Institute of Technology, Stockholm, Sweden, 2005.
- [215] Z. M. Salameh and B. G. Kim, "Advanced lithium polymer batteries," in *Power & Energy Society General Meeting, 2009. PES '09. IEEE*, 2009, pp. 1-5.
- [216] B. Lawson, "A Software Configurable Battery," presented at the EVS26 International Battery, Hybrid and Fuel Cell Electric Vehicle Symposium, Los Angeles, California, 2012.
- [217] P. Albertus, J. Coutts, V. Srinivasan, and J. Newman, "II. A combined model for determining capacity usage and battery size for hybrid and plug-in hybrid electric vehicles," *Journal of Power Sources*, vol. 183, pp. 771-782, 2008.
- [218] D. Doerffel and S. A. Sharkh, "A critical review of using the Peukert equation for determining the remaining capacity of lead-acid and lithium-ion batteries," *Journal of Power Sources*, vol. 155, pp. 395-400, 2006.
- [219] B. Schweighofer, H. Wiegler, M. Recheis, and P. Fulmek, "Fast and accurate battery model applicable for EV and HEV simulation," in *Instrumentation and Measurement Technology Conference (I2MTC), 2012 IEEE International*, 2012, pp. 565-570.

- [220] S. W. Moore and P. J. Schneider, "A Review of Cell Equalization Methods for Lithium Ion and Lithium Polymer Battery Systems," *Society of Automotive Engineers*, vol. 1, 2001.
- [221] X. Dongping, W. Lifang, and Y. Jian, "Research on Li-ion Battery Management System," in *Electrical and Control Engineering (ICECE), 2010 International Conference on*, 2010, pp. 4106-4109.
- [222] H. Mettlach, "Cell balancing techniques using the example of the Li-Ion battery system for the Opel Ampera," presented at the EV Battery Forum 2012, Barcelona, Spain, 2012.
- [223] J. F. Reynaud, C. E. Carrejo, O. Gantet, P. Aloisi, B. Estibals, and C. Alonso, "Active balancing circuit for advanced lithium-ion batteries used in photovoltaic application," presented at the International Conference on Renewable Energies and Power Quality (ICREPQ'11), Gran Canaria, Spain, 2010.
- [224] A. Kawamura, M. Pavlovsky, and Y. Tsuruta, "State-of-the-art high power density and high efficiency DC-DC chopper circuits for HEV and FCEV applications," in *Power Electronics and Motion Control Conference, 2008. EPE-PEMC 2008. 13th*, 2008, pp. 7-20.
- [225] J. Anzicek and M. Thompson, "DC-DC boost converter design for Kettering Universitys GEM fuel cell vehicle," in *Electrical Insulation Conference and Electrical Manufacturing Expo, 2005. Proceedings*, 2005, pp. 307-316.
- [226] M. T. Aydemir, A. Bendre, and G. Venkataramanan, "A critical evaluation of high power hard and soft switched isolated DC-DC converters," in *Industry Applications Conference, 2002. 37th IAS Annual Meeting. Conference Record of the*, 2002, pp. 1338-1345 vol.2.
- [227] E. Schaltz and P. O. Rasmussen, "Design and Comparison of Power Systems for a Fuel Cell Hybrid Electric Vehicle.," in *UAS 2008 IEEE Industry Applications Society Annual Meeting*, 2008, pp. 1-8.
- [228] S. Dwari and L. Parsa, "A Novel High Efficiency High Power Interleaved Coupled-Inductor Boost DC-DC Converter for Hybrid and Fuel Cell Electric Vehicle," in *Vehicle Power and Propulsion Conference, 2007. VPPC 2007. IEEE*, 2007, pp. 399-404.
- [229] K. Sheng, B. W. Williams, X. He, Z. Qian, and S. J. Finney, "Measurement of IGBT switching frequency limits," in *Power Electronics Specialists Conference, 1999. PESC 99. 30th Annual IEEE*, 1999, pp. 376-380 vol.1.
- [230] M. Pavlovsky, Y. Tsuruta, and A. Kawamura, "Fully bi-directional dc-dc converter for EV power train with power density of 40 kW/l," in *Energy Conversion Congress and Exposition, 2009. ECCE 2009. IEEE*, 2009, pp. 1768-1774.
- [231] D. M. Bellur and M. K. Kazimierczuk, "DC-DC converters for electric vehicle applications," in *Electrical Insulation Conference and Electrical Manufacturing Expo, 2007*, 2007, pp. 286-293.
- [232] H. R. Karshenas, H. Daneshpajoo, A. Safaei, P. Jain, and A. Bakhshai, *Bidirectional DC - DC Converters for Energy Storage Systems, Energy Storage in the Emerging Era of Smart Grids*. InTech, 2011.
- [233] DieselNet. (2012). *Emission Test Cycles*. Available: <http://www.dieselnet.com/standards/cycles/>
- [234] M. Andre, M. Rapone, and R. Joumard, "Analysis of the cars pollutant emissions as regards driving cycles and kinematic parameters," Institut National De Recherche Sur Les Transports Et Leur Securite2006.
- [235] EPA. (2012). *Dynaometer Drive Schedules*. Available: <http://www.epa.gov/nvfel/testing/dynamometer.htm>
- [236] R. Stobart and R. Chen, "Duty Cycles, Standardisation and Validation of Low Carbon Power Systems," presented at the Low Carbon Vehicle Power Systems, MIRA, Nuneaton, UK, 2009.

- [237] C. C. Chan, A. Bouscayrol, and K. Chen, "Electric, Hybrid, and Fuel-Cell Vehicles: Architectures and Modeling," *Vehicular Technology, IEEE Transactions on*, vol. 59, pp. 589-598, 2010.
- [238] K. Haraldsson and P. Alvfors, "Effects of ambient conditions on fuel cell vehicle performance," *Journal of Power Sources*, vol. 145, pp. 298-306, 2005.
- [239] R. Biurrun, D. Krieg, and D. Stolten, "Systemic tradeoff analysis of fuel cell mobility systems," *International Journal of Hydrogen Energy*, vol. 37, pp. 12639-12649, 2012.
- [240] S. o. A. Engineers, "Implementation of SAE Standard J1666 May93 - Electric Vehicle Acceleration, Gradeability and Deceleration Test Procedure," ed: Electric Transportation Applications, 2004.
- [241] S. Schlesinger, "Terminology for model credibility," *Simulation*, vol. 32, pp. 103-104, 1979.
- [242] C.-F. Tsang, "The Modeling Process and Model Validation," *Ground Water*, vol. 29, pp. 825-831, 1991.
- [243] C. Louie, "Automotive Fuel Cells - The Road To Emission Free Mobility," presented at the AFCC Automotive Fuel Cell Cooperation Corp, 2011.
- [244] C. Mohrdieck, "EVS24 - Next Generation Fuel Cell Technology for Passenger Cars and Buses," *World Electric Vehicle Journal*, vol. 3, pp. 1-5, 2009.
- [245] B. Winfield. (2010) 2011 Mercedes-Benz B-Class F-Cell Test Drive. *Popular Mechanics*. Available: <http://www.popularmechanics.com/cars/alternative-fuel/cells/2011-mercedes-benz-b-class-f-cell-test-drive>
- [246] R. Clague, I. Siera, and M. Lamperth, "A Novel Hybrid Control Strategy for Maximising Regenerative Braking Capability In A Battery-Supercapacitor Energy Storage System," *World Electric Vehicle Journal*, vol. 4, pp. 511-516, 2010.
- [247] J. Marco and N. D. Vaughan, "Design of a Reference Control Architecture for the Energy Management of Electric Vehicles," *International Journal of Vehicle Design*, vol. 58, pp. 240-265, 2012.
- [248] M. Neenu and S. Muthukumaran, "A battery with ultra capacitor hybrid energy storage system in electric vehicles," in *Advances in Engineering, Science and Management (ICAESM), 2012 International Conference on*, 2012, pp. 731-735.
- [249] J. Cao and A. Emadi, "A new battery/ultra-capacitor hybrid energy storage system for electric, hybrid and plug-in hybrid electric vehicles," in *Vehicle Power and Propulsion Conference, 2009. VPPC '09. IEEE*, 2009, pp. 941-946.
- [250] ABB, "5STF 07D1414 Medium Frequency Thyristor Datasheet," ed, 2010, pp. 1-15.
- [251] S. M. Naylor and V. Pickert, "A highly modular simulation model for hybrid electric fuel cell power drive trains," in *UKACC International Conference on Control 2008*, University of Manchester, 2008.
- [252] R. Heuss, N. Muller, W. van Sintern, A. Starke, and A. Tschiesner, "Lightweight, heavy impact - how carbon fiber and other lightweight materials will develop across industries and specifically in automotive.," McKinsey & Company, Germany 2012.
- [253] B. D. James and A. B. Spisak, "Mass Production Cost Estimation of Direct H2 PEM Fuel Cell Systems for Transportation Applications: 2012 Update," Strategic Analysis Inc. / US Department of Energy 2012.
- [254] "Polymer Fuel Cells - Cost reduction and market potential," Carbon Trust 2012.
- [255] A. Reis, "A portfolio of power-trains for Europe: a fact-based analysis," McKinsey & Company 2010.
- [256] "Drivers of the Energy Scene - A Report of the World Energy Council " 2003.
- [257] D. L. Greene, "Costs of Oil Dependence: A 2000 Update," U. S. Department Of Energy 2000.
- [258] J. D. Hamilton, "Historical Oil Shocks," *National Bureau of Economic Research*, February 2011 2011.

- [259] J. Laherrère, "Future of Oil Supplies," presented at the Center of Energy Conversion, Zurich, 2003.
- [260] B. Fisher, "Review and Analysis of the Peak Oil Debate," Institute for Defence Analysis, Aug 2008.
- [261] L. Maugeri, "Oil: The Next Revolution - The Unprecedented Upsurge of Oil Production Capacity and What It Means for The World," Belfer Center for Science and International Affairs - Harvard University Kennedy School, 2012.
- [262] M. Aftabuzzaman and E. Mazloumi, "Achieving sustainable urban transport mobility in post peak oil era," *Transport Policy*, vol. 18, pp. 695-702, 2011.
- [263] N. P. F. Bere, "A Critical Review Of The Peak Oil Phenomenon," Masters, Norges Handelshøyskole, Norway, Bergen, Norway, 2010.
- [264] C. J. Campbell, "Peak Oil: A Turning Point For Mankind," Hubbert Center, April 2001.
- [265] E. Hemmingsen, "At the base of Hubbert's Peak: Grounding the debate on petroleum scarcity," *Geoforum*, vol. 41, pp. 531-540, 2010.
- [266] M. Tsoskounoglou, G. Ayerides, and E. Tritopoulou, "The end of cheap oil: Current status and prospects," *Energy Policy*, vol. 36, pp. 3797-3806, 2008.
- [267] A. Verbruggen and M. Al Marchohi, "Views on peak oil and its relation to climate change policy," *Energy Policy*, vol. 38, pp. 5572-5581, 2010.
- [268] A. f. t. S. o. P. Oil, "Growing gap between discovery and production," GrowingGap.jpg, Ed., ed, 2011.
- [269] J. Friedrichs, "Global energy crunch: How different parts of the world would react to a peak oil scenario," *Energy Policy*, vol. 38, pp. 4562-4569, 2010.
- [270] J. Benes, M. Chauvet, O. Kamenik, M. Kumhof, D. Laxton, S. Mursula, and J. Selody, "The Future of Oil: Geology versus Technology," International Monetary Fund, May 2012.
- [271] M. Höök, "Coal and Oil: The Dark Monarchs of Global Energy," Uppsala University, 2010.
- [272] "Coutts - Global Markets Weekly 17th August 2012," in *Global Markets Weekly*, ed, 2012.
- [273] "U.S. Net Petroleum Imports By Country," U. S. E. I. Administration, Ed., ed, 2012.
- [274] J. Blas, "Pipelines bypassing Hormuz Open," in *Financial Times*, ed. London, UK, 2012.
- [275] M. Izady, "Persian Gulf Region Digital Map," ed: Columbia University, US, 2011.
- [276] M. Izady, "Straits of Hurmuz Digital Map," ed: Columbia University, US, 2006.
- [277] V. Foster, W. Butterfield, C. Chen, and N. Pushak, "Building Bridges: China's Growing Role as Infrastructure Financier for Sub-Saharan Africa," The World Bank / Public-Private Infrastructure Advisory Facility, 2008.
- [278] J. Colgan, "Oil and resource-backed aggression," *Energy Policy*, vol. 39, pp. 1669-1676, 2011.
- [279] T. A. Litman, "Understanding Transport Demands and Elasticities - How Prices and Other Factors Affect Travel Behavior," Victoria Transport Policy Institute, Australia, 26/7/2012.
- [280] J. Sunyer, J. Anto, A. Tobias, and P. Burney, "Generational increase of self-reported first attack of asthma in fifteen industrialized countries. European Community Respiratory Health Study (ECRHS)," *European Respiratory Journal*, vol. 14, pp. 885-891, October 1, 1999.
- [281] R. McConnell, K. Berhane, L. Yao, M. Jerrett, F. Lurmann, F. Gilliland, N. Künzli, J. Gauderman, E. Avol, D. Thomas, and J. Peters, "Traffic, Susceptibility, and Childhood Asthma," *Environ Health Perspect*, vol. 114, 2006.

- [282] G. D'Amato, G. Liccardi, and M. D'Amato, "Environmental risk factors (outdoor air pollution and climatic changes) and increased trend of respiratory allergy," *J Investig Allergol Clin Immunol*, vol. 10, pp. 123-8, May-Jun 2000.
- [283] J. Bartra, J. Mullol, A. del Cuervo, I. Davila, M. Ferrer, I. Jauregui, J. Montoro, J. Sastre, and A. Valero, "Air pollution and allergens," *J Investig Allergol Clin Immunol*, vol. 17 Suppl 2, pp. 3-8, 2007.
- [284] D. Bray, "The scientific consensus of climate change revisited," *Environmental Science & Policy*, vol. 13, pp. 340-350, 2010.
- [285] H. R. Nilsen, "Overlapping consensus versus discourse in climate change policy: The case of Norway's Sovereign Wealth Fund," *Environmental Science & Policy*, vol. 13, pp. 123-130, 2010.
- [286] L. Whitmarsh, "Scepticism and uncertainty about climate change: Dimensions, determinants and change over time," *Global Environmental Change*, vol. 21, pp. 690-700, 2011.
- [287] N. T. Gavin and T. Marshall, "Mediated climate change in Britain: Scepticism on the web and on television around Copenhagen," *Global Environmental Change*, vol. 21, pp. 1035-1044, 2011.
- [288] G. D'Amato, M. Rottem, R. Dahl, M. S. Blaiss, E. Ridolo, L. Cecchi, N. Rosario, C. Motala, I. Ansotegui, and I. Annesi-Maesano, "Climate Change, Migration, and Allergic Respiratory Diseases: An Update for the Allergist," *World Allergy Organisation Journal*, pp. 121-125, 2011.
- [289] L. Antilla, "Climate of scepticism: US newspaper coverage of the science of climate change," *Global Environmental Change*, vol. 15, pp. 338-352, 2005.
- [290] F. A. Pasquaré and P. Oppizzi, "How do the media affect public perception of climate change and geohazards? An Italian case study," *Global and Planetary Change*, vol. 90-91, pp. 152-157, 2012.
- [291] L. Scruggs and S. Benegal, "Declining public concern about climate change: Can we blame the great recession?," *Journal of Global Environmental Change*, 2012 2012.
- [292] B. M. W. Ratter, K. H. I. Philipp, and H. von Storch, "Between hype and decline: recent trends in public perception of climate change," *Environmental Science & Policy*, vol. 18, pp. 3-8, 2012.
- [293] *The World Factbook*: US Central Intelligence Agency, 2012.
- [294] N. Banerjee, "Auto Industry Fights MPG Upgrade," *Auto industry fights mpg upgrade*, in *Chicago Tribune*, ed, 2011.
- [295] P. Stasinopoulos, P. Compston, and H. M. Jones, "Policy resistance to fuel efficient cars and the adoption of next-generation technologies," in *30th International Conference of the System Dynamics Society*, 2012.
- [296] I. Meyer and S. Wessely, "Fuel efficiency of the Austrian passenger vehicle fleet—Analysis of trends in the technological profile and related impacts on CO2 emissions," *Energy Policy*, vol. 37, pp. 3779-3789, 2009.

i.1 Oil Economics

By 2040, the worlds fleet of personal vehicles is expected to double to 1.6 billion vehicles with the most rapid expansion in car ownership coming from developing countries where car ownership is increasingly rapidly as GDP and personal wealth increase [135, 256]. Rapid industrialisation has also increased the demand for oil in developing countries and as Figure 9.1 illustrates, oil prices have been increasing for many years and some transient downward spikes aside, the trend is continuously upwards.

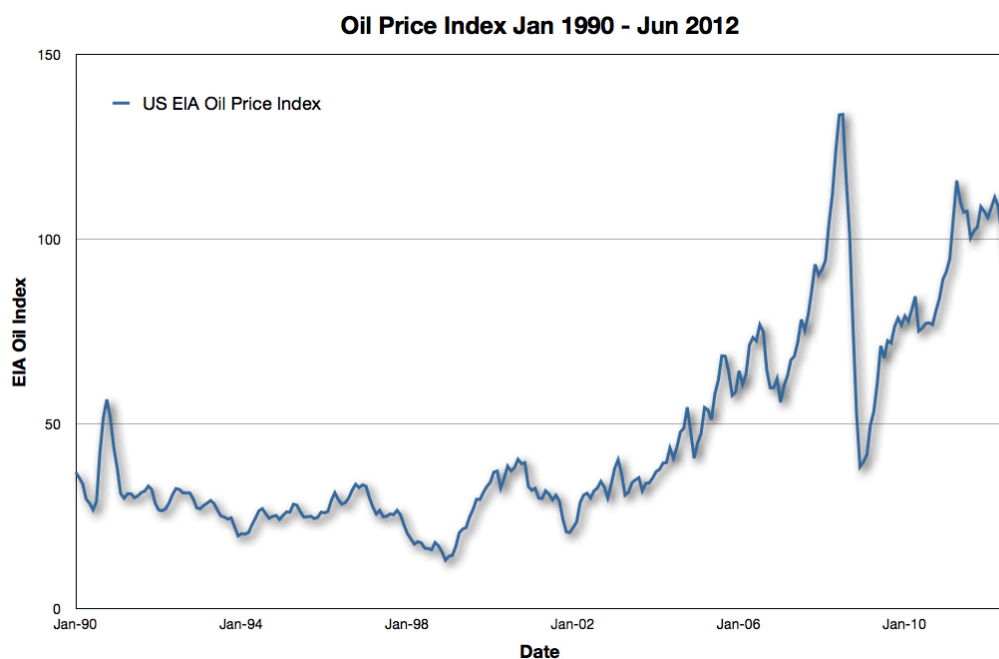


Figure 9.1 - Oil Price Index Jan 1990 - Jun 2012 (US EIA Oil Index)

In countries where there is net-importation of oil the immediate economic impact is a transfer of wealth outside of the country and the subsequent impact of GDP [257]. When the oil price increases significantly, recession generally follows shortly afterwards [258] and it has clear knock on effects on world GDP as shown in Figure 9.2.

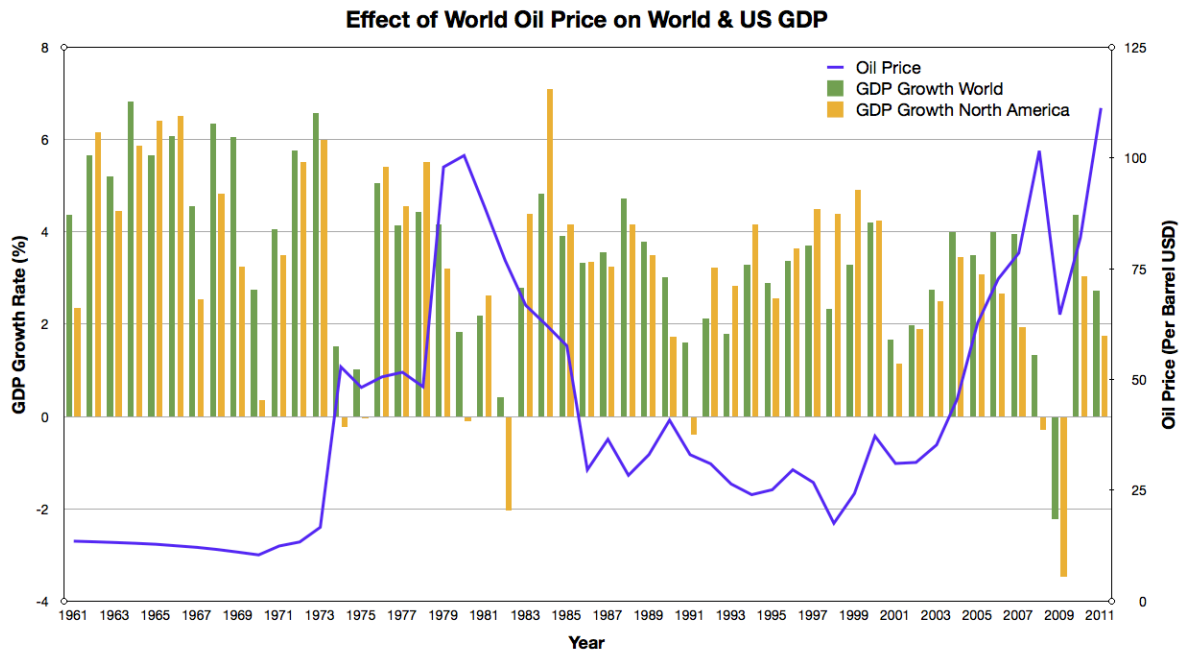


Figure 9.2 - Effect of Oil Price on US & World GDP (Data: World Bank, US EIA)

To determine whether this price rise is a historical blip or a progressive and continued trend an understanding of how much oil we have left is necessary as the main determinants on price aside from demand are how much oil has been discovered (reserves), how much oil has been extracted (cumulative production) and an estimate of how much oil is yet to be discovered.

i.2 Peak Oil

An often-quoted phrase when talking about the future of oil is ‘Peak Oil’, the point in time at which the maximum rate of oil production is reached. At this point, assuming all production capacity is being sold, the only a way any country can get more oil, is for another to get less. This will mark an economic point in history and it is important to consider it, as if we were to suppose that there were vast resources of easily extractable oil yet to be discovered and they were in large singular oils fields similar to those in Saudi Arabia then it could be hypothesised that such a scenario where they are discovered and put into production in the near future would push the price of oil sharply downward and change many of the economic assessments made in this thesis.

The Peak Oil discussion is split between ‘Peakists’ and ‘Optimists’. The Peakists contend that world oil production is limited by geology and that peak production will be reached within the next decade and when that happens it will trigger a financial crisis. They base their findings on technical data that is largely confidential. Optimists suggest that peak oil

production is driven by economics and base their work on data published about known reserves and production that is largely politically generated public data and therefore should be treated with a degree of caution [259]. Known reserves influences the price of oil, the stock price of oil producers and the wealth of oil producing nations and it could therefore be seen as expedient for any of the controlling parties to elaborate on reserves over a period of time to maintain price, or overstate reserves at such a time as it is expedient, for instance to support the share price of an oil company or the borrowing ability of a nation state. As an example, between 1986 and 1990 OPEC's declared reserves increased by 300Gbbbl (300×10^9 barrels of oil) when only 10Gbbbl was discovered in this period [259, 260].

Comparing the Peakists and Optimists views on a like-for-like basis is therefore quite difficult but it is important to consider both cases and try and best ascertain the reality of the issue. Although oil production from any given resource will deplete it, as the price of oil increases the percentage of the total resource that is economic to extract will increase, thus potentially increasing total production from that originally estimated. An increased world price also increases activity in areas where production was, due to the costs and difficulties involved, never originally envisaged until recently, (e.g. Deep Sea Wells, The Arctic Ocean, Oil Tar Sands, Shale Oil). A scenario based on this new exploration may show that the rate of production could actually increase.

Of all the expressed views, the most pessimistic is that peak oil has already happened and in contrast the most optimistic is that it will happen later this century between 2030 and 2050. There are also those even further outside the envelope that believe the concept is baseless and that the only limitation on oil is economic as the market will control supply and deliver alternatives when necessary and that production can actually increase to meet any demand [261]. Jean Laherrère, who considered both viewpoints and analysed the available data to draw a realistic conclusion came to the view that the peak will occur as early as 2015. He built upon the work of M. King Hubbert who initially developed the theory that peak oil discovery will lead peak oil production and that peak production is predictable. Hubbert developed a mathematical model that described how peak oil discovery in the United States happened in the 1930's and that this date could be used to predict peak production and derive a curve that illustrated production levels in the US oil industry. In 1956 he published the curve shown in Figure 9.3 that accurately predicted that US oil production would peak in 1970 though his estimate of a global peak between 1993

and 2000 has been proved by steady production increases over that period and the period since he formulated his idea to be too early [259, 262-267].

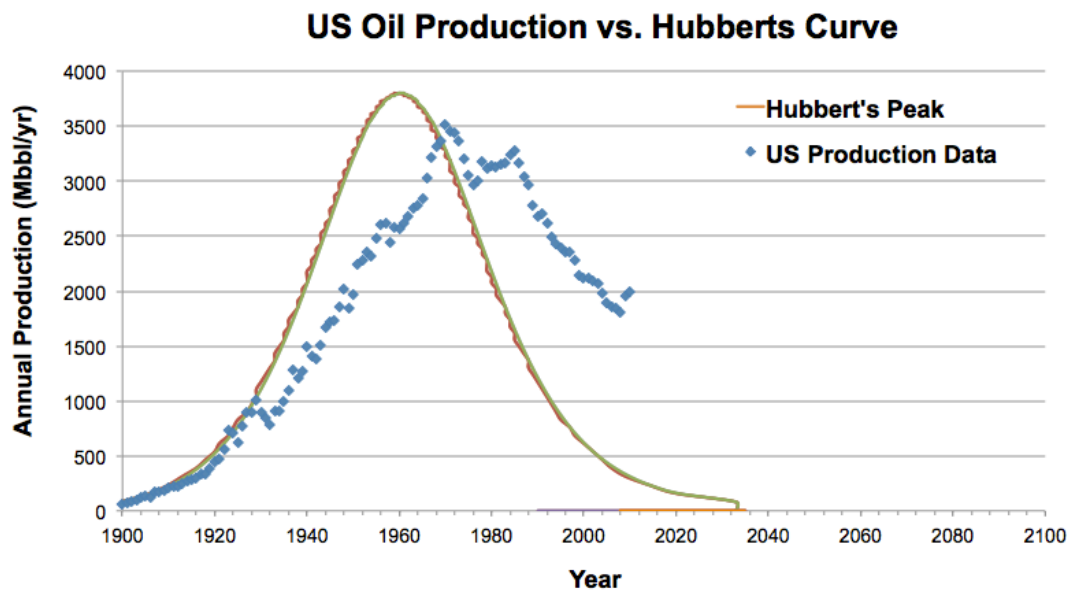


Figure 9.3 - Hubbert Curve vs Actual US Production Data [263]

Figure 9.4 shows clearly that discoveries of oil reserves have been outpaced by demand for nearly 20 years and there is a growing gap between oil production and reserves. This would further complement the arguments that suggest peak oil has been reached, or will be reached in the near future.

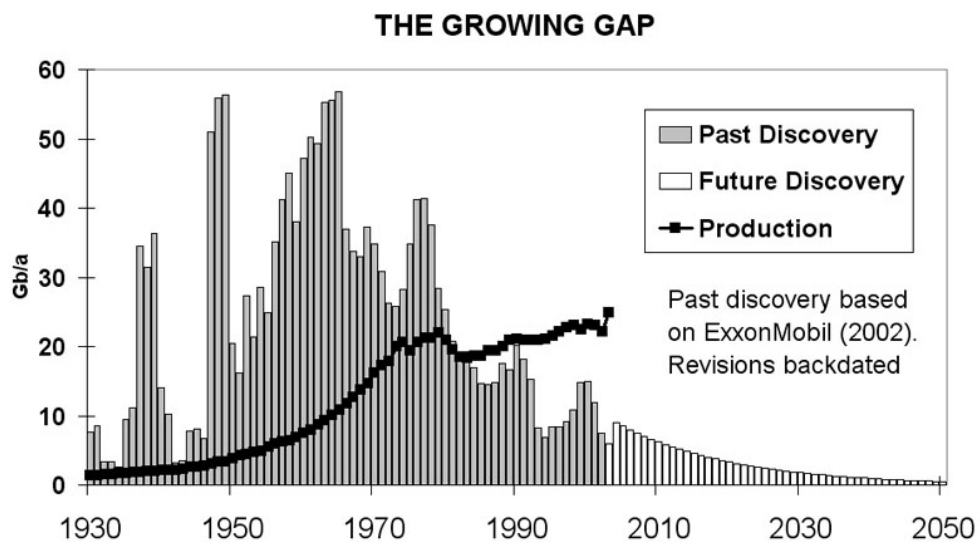


Figure 9.4 – The increasing gap between oil discovery and production [268]

If we set aside price, its wider impacts and potential conflicts caused by supply exceeding demand, how long reserves will last in total is the next question that dictates how soon alternatives to oil have to be found. What current proved reserves actually exist and how much oil has already been consumed are like the rest of this subject, both disputed. But most analysts and studies estimate that around 1 trillion barrels have been consumed and that extractable reserves total some 2-3 trillion barrels. Current consumption totals 32 billion barrels a day and with forecast increases the near or total depletion of oil reserves within a lifetime is highly likely. In 2008, the International Energy Agency said the world needed to invest \$25 trillion in energy use optimisation and alternatives to avert disaster and meet future fuel demands.

Subsequently this thesis is written on the basis that although we do not face the danger of running out of oil in the immediate future, in the face of increasing demand, the price of oil, and thus vehicle fuel is now likely to rise continually. In the face of an expanding global population, and the importance of a reasonable oil price in sustaining long-term growth and more immediately what is currently a faltering recovery from the global economic crisis, it is economically imperative that alternative fuels for vehicles are found and put into production as soon as possible.

Previous phases of mankind have not ended due to depletion, but advancement. A lack of stone did not cause the end of the Stone Age; a lack of coal did not cause the end of the Steam Age. For the first time in history, depletion of oil resources could end the Oil Age before technological gains relieve our dependency on it [269]. It cannot just be hoped that technology will provide the answer in due course as it has before without actively investing time and resources in research and development.

i.3 Oil Politics

The capability of oil to shape the world and events cannot be understated. Before the increase in demand from developing nations really took hold after 2005, previous oil prices spikes, so called “oil shocks” were nearly related to geo-political events, not concerns about reserves. The first such “oil shock” occurred due to the American Civil War, which was one of the first truly industrialised wars and caused a subsequent spike in commodity prices.

In 1894, social influences affected the price as a cholera epidemic in the Baku fields of Russia caused a massive drop in Russian oil exports. This coincided with rapidly decreasing production in the Appalachian field in the United States and oil prices subsequently spiked in 1895. It is worth noting the effect of decreasing production on price at this time but especially so in the light of the economic balance of energy in 1895. In 1900 oil consumption accounted for 0.4% of GNP. In 2008 it accounted for 4.8% of GDP. Although GNP and GDP are not strictly analogous, the difference is marked and the ramifications of a similar simultaneous decrease in production levels and demand-exceeding supply would have on both the oil price and the economic outlook would be uncharted territory [270].

History has gone on to repeat itself many times, with oil being an objective, a tool and a weapon in political struggles and civil unrest throughout the world and the oil price being strongly correlated to significant world events. War is a common factor. The end of The Great War and the Russian Revolution drove the oil price up before the Wall Street Crash and Great Depression caused it to collapse a decade later. In the Second World War, Germany and Japan both made huge expansionist drives into and toward oil rich territories. The Germans would pay a fatal price for their attempt to reach the Caucus oil fields at Stalingrad and once they had retreated beyond ready supplies of oil, both Germany and Japan failed to sustain industrial production and fuel supplies to maintain their armies [271]. Oil has also caused several wars in its own right. Had Kuwait not been sat atop one of the world's largest oil fields, and had the West not been concerned that Iraq would continue south and attack and seize the Saudi Arabian oil fields it is unlikely that the first Gulf War would have happened. The fields themselves became a weapon as Iraqi troops set them ablaze during their retreat. Likewise the closure of the Suez Canal would not have prompted France and Great Britain to invade Egypt in 1956 had their oil supply and economies not been effectively throttled by the closure. The 21st century heralded an increasingly unstable world. With the Cold War hegemony now a distant memory, on September the 11th 2001 terrorists attacked and brought down the World Trade Centre towers. Despite a large drop in demand from aviation due to a flurry of airline closures the oil price rose and another recession followed. The Arab Spring of 2011 caused further concerns about production in North Africa and the Mediterranean and questions were raised of what the risk of the civil unrest spreading to Saudi Arabia was and its possible affect on production

Embargos of oil have been used many times to try and influence world events with varying degrees of success. The US attempt to stop Japan's expansionist policies in the 1930's by removing 80% of its oil supply caused Japan to seek further expansion and attack Pearl Harbour, the act that ultimately resulted in the US laying waste to vast swathes of Japan. The majority of the G8 nations have embargoed Iranian oil exports to try and force Iran to give up its nuclear weapons program, thus far without success though the pace of advancement has been slowed somewhat. The most significant oil embargo came during the 1970s though. The oil price was increasing due to the peak in US production being reached in 1970 [265, 266]. Five Middle Eastern oil producers from OPEC (Organisation of Petroleum Exporting Countries) were of growing influence and controlled around 36% of the world supply. In 1973, when commodity prices were already on the increase in the US, the Middle Eastern members of OPEC declared an embargo on oil exports to the US in response to US support for Israel during the Yom Kippur war. OPEC then also cut production, reducing the world supply by 7.5% and, on January 1st 1974, the price of oil had more than doubled. In 2011 equivalent prices, crude jumped from \$17 a barrel to \$53. This caused inflation and recession within the world financial system that lasted into the 1980's even though the embargo was lifted in March 1974 after failing to achieve its aim – Israel won the war. This was not a problem of resources but a political act, that had huge consequences such as precipitating a change of the British government in the February 1974 General Election. This was further compounded when in 1979 the Shah of Iran was deposed during the Iranian revolution. Strikes in Iran's giant oil fields were commonplace and world production fell by around 7%. Saudi Arabia managed to increase production and restore a third of the lost output but a shortfall remained. Prices increased and at the human level shortages of fuel supplies were commonplace and global recession again followed. With oil now at \$98 a barrel, in 1980, Iran and Iraq went to war, causing the price to reach a new all time high of \$100 a barrel (prices in constant 2011 US dollars).

The experience of a turbulent decade was not forgotten easily in the major oil consuming nations and for the first time they caused a major shift in behaviour and improvements in technology that through the 1980's led to a decrease in fuel consumption. In 1974 a federal law imposed a US wide maximum speed limit of 55mph. In Britain, speed limits were reduced on previously de-restricted roads from 70mph to 60mph on dual carriageways and 70mph to 50mph on all other roads, though motorways remained at 70mph. Speeding fines were increased and enforcement stepped up. This was aimed at increasing efficiency, the United States Congress stating that a reduction from 75mph to 55mph used 17% less fuel. Automotive manufacturers were also forced to act, being forced (despite their strong

objections and intensive lobbying) in 1975, to double fuel efficiency to 27.5mpg within 10 years.

The oil price declined continually through the early 1980's despite the best efforts of some OPEC nations. Saudi Arabia shut down 75% of its production from 1981 to 1985, losing market share in the process, yet the price still fell from \$100 a barrel high in 1980 to \$58 a barrel in 1985. To regain market share Saudi Arabia ramped production back up in 1986 and the price of oil collapsed to \$29 a barrel and coincided with extensive deregulation in the financial markets that together helped fuel the global economic boom of the late 1980's.

The economic power of oil and energy was brought into sharp focus in 2001 when history's largest example of corporate malfeasance in the energy sector was exposed. Enron, in increasingly desperate efforts to obtain income to maintain its vastly over inflated share price began deliberately orchestrating blackouts on the Californian power grid to drive up the price of the energy they were trading. Despite available supply comfortably exceeding demand, Californian residents experienced rolling blackouts and sky rocketing energy prices. The human cost went further as when Enron was exposed and crashed into bankruptcy, pension funds and individual investors lost hundreds of millions of dollars they had invested in Enron stock.

The economy also served to halt a continual rise in prices when the 2008 Financial Crises triggered a massive slowdown in global trade and manufacturing and caused a reduction in oil demand for the first time in several years. Key to this sustained rise was the lack of additional production capacity after 2005 [258, 266]. The global financial crisis was only a brief moderator of price though and as recovery slowly started the price began to rise.

The past 200 years of oil shocks and the price of oil price are strikingly visualised overleaf in Figure 9.5. The price throughout history has been converted into constant 2011 US dollars to illustrate the relative economic effect that each event had but the trend of war, civil unrest, embargos and terrorism causing the oil price to spike is clear.

Crude Oil Prices 1861 - 2011

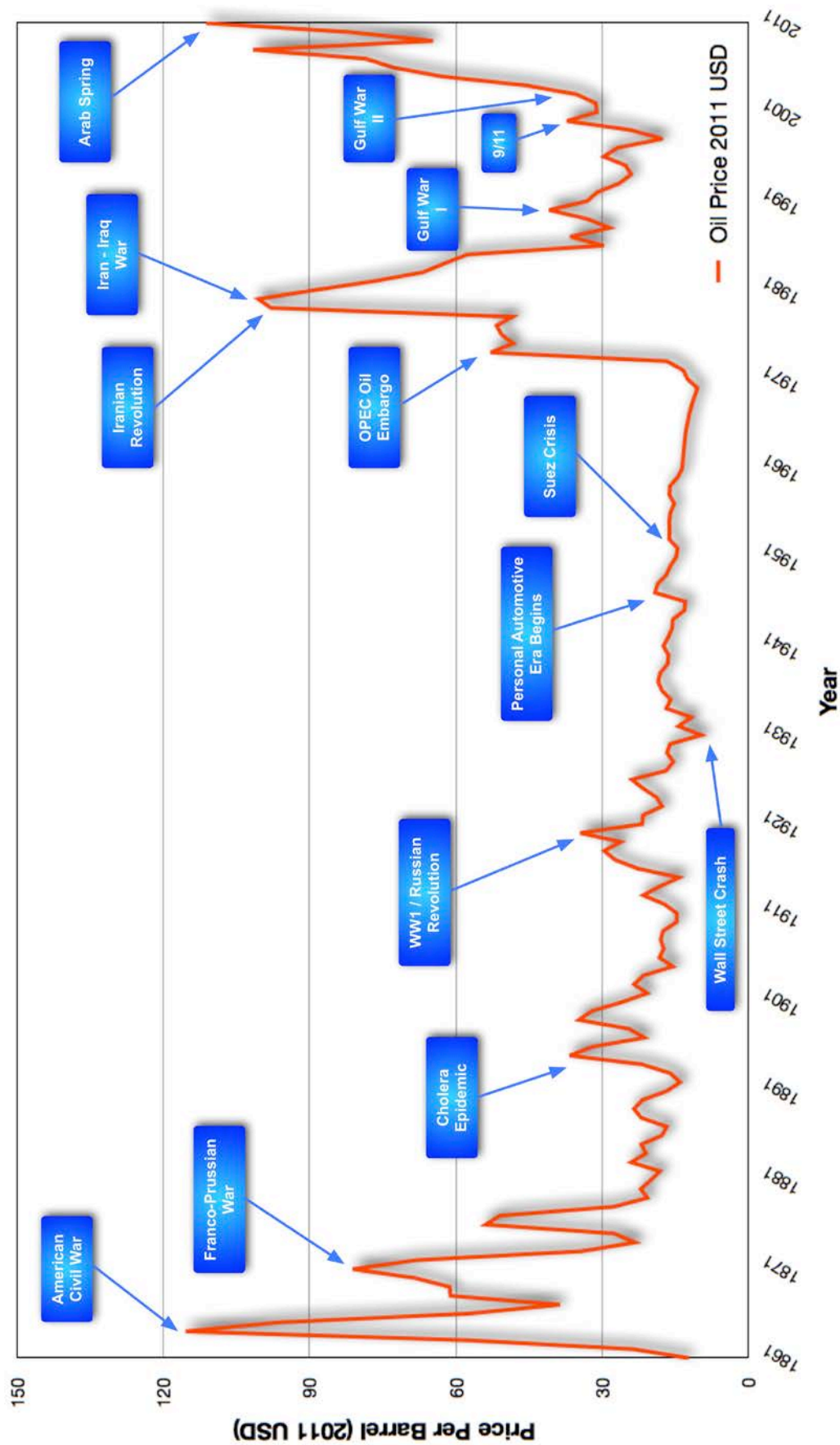


Figure 9.5 - How Oil Prices Are Linked to Geo-Political Events [2]

With rising oil prices again since the financial crises, and with little spare capacity an interesting phenomenon is observable. The economic recovery is affected by the oil price, and the oil price is affected by the recovery. Uplift in manufacturing generally causes an increase in the oil price, but that price rise then has the effect of causing the fragile growth to falter. Oil for the first time also showed some signs of behaving differently to the different commodity markets. Copper is a key commodity in most electrical and electronic items and it has been growing in price for many years however it has not followed some of oils recent price rises as it has in the past. The difference between the two commodities is that there are no long term concerns over the supply of copper [272].

The ramifications of political events on oil prices are plain to see and the economy of nations and the world as a whole are directly affected by changes in oil price. Each major oil price shock has been followed by an economic recession in the affected areas. The causes of these oil price shocks are not always controllable by the countries and areas they affect and therefore economic development should be considered a hostage to oil prices. Reducing the dependence on oil will reduce the impact of these effects and also give back some self-control over managing the impact whilst a continuance of current consumption and dependence will increase the risk to economic development. Previous shocks have been managed and mitigated by increasing productions in other areas. With global demand now normally using nearly all available production capacity, it is going to be increasingly difficult to pick up any sudden loss of capacity and the effect of the world economy will become increasingly profound. The political risks of our oil dependence are illustrated in history by war, the fall of governments and recession. Energy is a driving force of development, but it can also be the catalyst for chaos. Finding more stable ways to power the world and further social change must be found.

i.4 Security of Supply

Another key consideration of a resource on which we politically depend so highly is the country of origin. In the case of oil, much of it comes from unstable countries and autocratic regimes. The Arab spring of 2011 showed how quickly the balance of power shifts in such places and the OPEC crisis of the 1970's showed oil supplies used as leverage against those nations dependant on imports for their supply due to the whim of several large suppliers. Of the 'giant' oil fields that form much of the world supply, many are located in countries with currently active social unrest or the potential for conflict. The United States for example currently obtains around 8.1% of its oil from Venezuela with

whose government it has a long standing and public dispute; 8% from Iraq which is still beset by internal sectarian violence; 7.1% from Mexico where there is a virtual war between drug cartels and the government in the US border area; 6.1% from Nigeria, a country where corruption is rife; 4.5% from Angola, where infant mortality and the standard of living is amongst the lowest in the world; and 8% from Russia, a country that has at times frosty relations with the US. 42% of Americas oil supply of June 2012 came from unstable nations or nations that American might not be able to positively influence at all times [273].

During 2012, much political and press attention was focused on Iran being the largest threat to the wider world due to the country seemingly being set on developing a nuclear weapons program that the world largely opposes. Israel sees this as a major threat to its security as Iran has a long-standing policy of wishing to see the Jewish state eliminated. The United States also has key interests in the area. A nuclear-armed Iran would change the balance of power in the region dramatically and Iran has responded to both the perceived threat of American and/or Israeli military action to stop their nuclear program by threatening to close the Straits of Hormuz. Figure 9.6 shows how the Straits are a strategic bottleneck in the Persian Gulf. Iran's threat to close the Straits of Hormuz and the 17 million barrels of oil a day that transit through, including the 18% of the American oil supply that comes from Saudi Arabia, 8% that comes from Iraq and 5.1% that comes from Kuwait [273], has been taken seriously enough to prompt the deployment of significant multi-national naval forces and for Saudi Arabia and the United Arab Emirates to build a pipeline to bypass it that can carry 6.5 million barrels a day [274].



Figure 9.6 - The Persian Gulf & Expanded View of the Straits of Hormuz[275, 276]

Given the implications of small decrease in supply in the current world marketplace, having a very real threat to such a significant portion of the worlds oil supply has both an inflationary effect on the oil price and asks questions about whether the risk and supply security can or should be managed in the long term.

Securing supplies is often also a matter of influence. As China's need for oil supplies grew with its booming economy it began to build direct and indirect influence in many of the countries that it obtains supplies from. It has not joined the EU & US embargo on Iran for instance and has underwritten and built significant amounts of social infrastructure in countries like Nigeria, Angola and Sudan in Africa where China obtains 30% of its oil supply [277]. Western economies such as the UK, still recovering from the cost of the financial crisis, do not have the same resources to secure such influence. Although the world is not there yet, in a marketplace where supply is saturated by demand that influence will probably start to dictate who can secure sufficient oil supplies to meet their needs.

Historically it also of note that a small group of oil producing nations, where over 10% of GDP is linked to oil income, have been responsible for over a quarter of the worlds international conflicts since 1970. Conventional conflicts are not the only direct destabilising result of oil wealth. Libya funded and provided weapons to the Irish Republican Army throughout the 1980's and Iran has been the primary funder of Hamas for many years [278].

Supply security is a key factor in the oil price. As production capacity is further utilised to its limits, smaller and smaller fluctuations in the supply will have proportionally larger effects than has been the case before. Diversification in energy supply by finding alternative ways of meeting demand can help mitigate that risk and potentially avoid conflict, the need to maintain deterrence forces in hostile areas and fight costly wars in foreign lands.

i.5 Oil Technology

The "Optimists" often cite technological developments in petroleum extraction and use as the solution to our oil dependence. There is a degree of reason in such a belief but there are also causes to believe that such developments, whilst they may sustain supplies for longer than would otherwise be possible, are likely to contribute to the increasing price of oil. Many of the techniques that are now being used to increase production yield and

exploit new resources are not in fact new. Horizontal drilling for instance, is in technological terms, old. Like other enhanced recovery techniques implemented over recent decades, their development and use is a direct result of the price of oil making it an economically viable extraction technique.

Deep water drilling is another development made viable by technology and the escalating price of oil, but it carries with it-increased risks as demonstrated by the disaster in the Gulf of Mexico in April 2010. Deep Water Horizon was a drilling platform working in the Macondo Prospect field at a depth of 1,500m above the seabed and to a total expected drilling depth of 5,600m. During drilling operations a bubble of methane gas escaped up the drilling column and onto the deck of the platform. The ensuing explosion and fire killed 11 people and ultimately destroyed and sank the \$550 million drilling platform. The failure of the protection device at the wellhead on the seabed was to become the larger part of the story though. On the seabed there was a blowout preventer that was designed to prevent the escape of oil and gas in the event of a problem with the well. The blowout preventer failed and for over three months the largest marine oil spill in history occurred, with 4.9 million barrels of oil flowing into the Gulf of Mexico. The failure of a well at depths where only remotely operated vehicles can go was anticipated, but the technology designed to mitigate the risk failed. The only way to solve the problem was to drill a relief well, a lengthy and expensive process.

The tar sands of Canada now account for around a quarter of US imports [273] though this comes at a financial and environmental cost. Extraction of oil from the tar sands is an energy and water intensive process, far more so than drilling a conventional well. Nevertheless it has become a major source of oil for the United States and Canada.

Hydraulic fracturing (Fracking) of oil and gas deposits held in shale rocks has been one of the recent great hopes for energy security in many countries. Some of these hopes have been dashed; Poland had high hopes for large potential reserves but has since abandoned development. In the UK, Fracking at a test site in Cumbria is thought to be the cause of a (very) minor earthquake in 2011 though permission has subsequently been given to continue drilling. Groundwater pollution from Fracking is a continuing concern with production companies estimating that 25% of the fluid used in the process cannot be recovered. The long-term effects on the groundwater supply are as yet unknown but development of Fracking has been rapid, especially in the US as it strives to reduce its energy imports.

All of these unconventional reserves come at a higher cost, both financial and environmental and whilst current high prices make them economic and their location enables diversification of supply, they are not a panacea or solution that will end worries about supply or drive price downward.

The main beneficial improvement in oil technology can yield is in the consumption sector. Improvements in efficiency of the internal combustion engine will be discussed later in this chapter but optimising the processes that consume oil to reduce consumption is one way that consumption and dependence can be reduced reasonably significantly whilst having the simultaneous benefit of reducing greenhouse gas emissions. Historically the main driver behind efficiency has been cost, with environmental concerns a relatively recent and secondary factor. Energy intensity varies throughout the world but there is a clear correlation between the cost of oil and how efficiently it is used. There are still nations that subsidise the cost of fuel and whilst a boon for the people that benefit, in the wider view it is an unhelpful policy and does not incentivise efficiency or help promote alternatives.

i.6 Environmental and Social Impacts

The direct social costs of oil dependence will increase with price. Fuel poverty will hit those on lowest incomes the hardest and restrict their ability to travel [262, 279] which may further limit their income and social mobility. The health costs of oil are mainly related to exhaust gas emissions. Respiratory problems such as asthma have increased significantly in industrialised nations over the last 50 years [280] and exposure to vehicle exhausts is thought to be a significant risk factor [58, 281-283].

Climate change is a topic that promotes even fiercer debate than peak oil, both as to its cause and its impact. There is an overwhelming consensus though that the climate has warmed significantly in the past 50 years and that the emission of greenhouse gases by human activity involving fossil fuels is a significant factor [284-287]. Climate change could have wide reaching effects. A rise in sea level due to melting sea ice and glaciers could destroy large swathes of low-lying land causing displacement of people across the world. Increasingly frequent and violent weather phenomena cause increasing amounts of death and destruction. Changeable weather affects crop yields at a time when food commodity prices are already at high levels and changeable weather can further increase demand for

energy. Changing climate can further exacerbate air pollution problems and the health impacts and climate change itself can lead to respiratory health problems [283, 288].

The need to act to reduce greenhouse gas emissions to combat climate change is complicated by public perception and vested interests. Some major media outlets give climate change sceptics prominent feature over and above proponents, whilst others do the opposite, confusing the public about the need for urgent action [287, 289, 290]. The global economic crises has cut budgets across the world and focused investment on those areas needed for short-term economic growth. Concern about climate change has decreased as immediate personal financial concerns have come to the fore [291] and as recent changeable, often cooler, local weather patterns have changed peoples perceptions about global warming [292] .

i.7 Resistance To Change

The industry that surrounds fossil fuels is massive and the political influence it can bring to bear should not be underestimated. The immediate concern of an oil company is to generate returns for its shareholders and in times of rising prices delivering ever increasing profits, there can be no assurances that oil producers will do anything to reduce our dependence on oil and may in fact act to further it. The ‘supermajor’ oil companies BP, Shell, ExxonMobil, Total and Chevron all have active programs working towards alternative energy sources that they are keen to promote and cite as part of their policy of tackling climate change but they do not see alternative energy becoming a major part of the energy mix anytime soon. BP predicts that in 2030, renewable sources will only provide 18% of our energy, up from 5% in 2010 [39]. For many of the major petro states, particularly in the Middle East, oil is the basis of their entire economy. Saudi Arabia for instance generates 90% of its export income from oil. Although investment in diversifying the economy is increasing [293] the logical course for any such state is to maximise the returns on remaining oil reserves.

Automotive manufactures have a vast installed production capacity centred on the internal combustion engine vehicle and with significant amounts of capital invested in each new model that can continue to sell for typically 5-10 years. Previous initiatives to increase fuel efficiency have met with resistance from the industry [9, 10, 294, 295] and although nearly all the major companies have active alternative fuel vehicle programs, none has yet been taken beyond niche market levels. At the human level, the production of more fuel-

efficient internal combustion engine vehicles has had the effect of people buying larger, more powerful cars and travelling more miles rather than peoples “vehicle related behaviour” being unaffected and fuel consumption simply being modified so the net effect is only a slight reduction in fuel consumption [13, 14, 296].

ii.1 Siemens Motor Drive Parameters

```
%% Motor & Transmission Inertia (kgm^2)
J_motor = 0.049;
J_gearbox = 0.1;

%% Motor Angular Speed LUT
Motor_omega = [0 104.72 209.44 314.16 418.88 523.6 628.32 733.04 837.76
942.48 1047.2];
%% Motor Torque LUT
Motor_torque = [0 10 20 30 40 50 60 70 80 90 100 110 120 130 140 150 160 170
180 190 200 210 220 230 240 250 260 270];
%% Motor Voltage LUT
Motor_voltage = [250 300 350 400];

%% Gear Ratio
Gear_Ratio = 9.81;

%% Absolute Maximum Peak Torque (Nm)
T_max = 270;

%% Torque Control Saturation Value
T_drive_max = Gear_Ratio * T_max;

%% Max Drive Speed
Omega_limit = 1047.2 / Gear_Ratio;
U_limit = Omega_limit * r_tire;
RPM_limit = 1150.954839;

%% Max Torque vs Voltage Characteristic
T_max_speed_index = [0 104.72 209.44 314.16 418.88 523.6 628.32 733.04 837.76
942.48 1047.2];
T_max_voltage_index = [250 300 350 400];
T_max_250 = [260 260 260 260 232 174 127 100 77      62 50];
T_max_300 = [260 260 260 260 260 240 193 150 120 98 80];
T_max_350 = [260 260 260 260 260 260 244 206 169 137 116];
T_max_400 = [260 260 260 260 260 260 260 245 214 181 154];
```


ii.2 Siemens Motor Drive Loss at 250V LUT

Siemens 75kW IM Motor Drive Losses at 250V

Angular Velocity (rad/s)	0	100	200	300	400	500	600	700	800	900	1000
Torque (Nm)											
0	20	81.737176	73.252025	96.997889	121.79995	143.37410	158.52897	178.92438	196.33639	221.04206	252.27620
10	484.07642	617.66342	751.25042	927.82788	1073.5090	1196.4296	1277.8078	1417.0907	1524.9969	1728.8054	1819.0756
20	847.15405	1059.8144	1272.4747	1493.0341	1631.4762	1761.6407	1844.6049	2018.1486	2177.2243	2449.3773	2694.8199
30	1182.3507	1431.3224	1680.2942	1916.7118	2079.7490	2243.9948	2353.5441	2634.9976	3042.9776	3387.8541	3685.6674
40	1539.2327	1803.7566	2068.2805	2305.0739	2659.8575	2694.8199	2979.9447	3403.3920	3764.7859	4188.7902	4705.9823
50	1883.4817	2169.9355	2456.3893	2685.4363	2937.4070	3335.2120	3646.4915	4117.7345	4602.5553	5235.9878	6077.4858
60	2255.3606	2553.9248	2852.4890	3094.0482	3362.4302	3843.2503	4282.0817	4832.6830	5523.0663	6563.6847	8004.5089
70	2697.2272	2979.5790	3261.9308	3550.2551	3885.1859	4391.6627	4941.2814	5638.1302	6733.8188	8320.9751	10100.789
80	3115.7364	3421.8286	3727.9209	3989.7863	4354.4486	4966.5745	5585.0536	6661.0160	8198.9339	10968.585	12333.629
90	3580.1997	3887.0553	4193.9110	4488.5096	4898.7546	5587.3963	6353.0761	7822.3549	10087.291	13278.640	14594.293
100	4230.8360	4445.3685	4659.9011	4987.2328	5496.6025	6208.2181	7292.9829	9152.6715	12740.099	15495.127	16791.360
110	4678.6557	4936.7885	5194.9212	5532.4103	6105.2922	6829.0400	8281.4212	10787.797	15008.803	17666.335	18897.744
120	5234.6569	5488.7596	5742.8622	6086.1516	6724.8605	7528.5647	9414.1764	12796.682	17191.915	19752.011	20908.176
130	5814.6167	6059.2182	6303.8197	6648.4868	7355.3444	8327.0423	10613.968	15642.132	19376.781	21739.552	22817.584
140	6436.3733	6679.5046	6922.6360	7279.1214	8072.5945	9152.6715	12108.892	17761.951	21455.172	23620.105	24619.217
150	7154.4744	7358.0621	7561.6498	7927.3833	8730.6220	10005.636	13834.536	19647.397	23356.211	25379.861	26306.020
160	7788.0383	8030.5800	8273.1218	8593.3963	9486.9404	10993.205	15824.319	21531.237	25085.746	27006.853	27871.758
170	8523.9287	8768.3258	9012.7228	9350.9450	10265.891	12137.972	18554.571	23354.002	26657.898	28494.236	29311.808
180	9381.4158	9581.1468	9780.8779	10136.082	11067.629	13341.010	20132.240	24956.357	28071.306	29839.341	30623.535
190	10381.918	10479.969	10578.021	10949.101	11892.312	14603.122	21298.676	26288.980	29322.525	31042.538	31806.334
200	11181.837	11327.160	11472.483	11790.300	12851.421	16084.276	22455.847	27422.433	30417.359	32106.829	32861.441
210	11768.690	12050.877	12333.064	12659.982	13728.578	17603.124	23706.555	28432.768	31369.056	33037.400	33791.655
220	12505.334	12902.911	13300.488	13657.463	14753.094	19378.048	25021.376	29350.469	32191.111	33840.797	34600.986
230	12752.121	13489.407	14226.694	14590.281	15683.610	21586.100	26255.269	30167.150	32893.046	34524.101	35294.325
240	13623.061	14446.379	15269.697	15662.433	16774.712	22640.668	27237.536	30861.426	33480.969	35094.477	35877.150
250	14619.356	15441.586	16263.815	16775.495	17902.909	23288.717	27934.402	31422.544	33960.454	35559.140	36355.300
260	15707.652	16546.395	17385.137	17930.065	19088.594	23841.307	28433.159	31859.061	34338.907	35925.475	36734.803
270	16801.552	17625.559	18449.565	19126.755	20272.164	24457.779	28830.194	32192.883	34626.049	36201.045	37021.712

ii.3 Siemens Motor Drive Loss at 300V LUT

Siemens 75kW IM Motor Drive Losses at 300V

Angular Velocity (rad/s) Torque (Nm)	0	100	200	300	400	500	600	700	800	900	1000
0	20	88.001342	81.568959	108.953094	138.69320	168.52663	192.43318	220.75884	253.18431	277.23194	315.00560
10	510.83040	666.71006	822.58972	1036.05715	1230.0846	1400.2451	1512.3300	1652.9295	1826.5370	2013.0594	2084.3500
20	921.39297	1147.7026	1374.0122	1660.1589	1889.0622	2069.3125	2165.5996	2288.0964	2459.4731	2766.9073	2883.0695
30	1249.5763	1547.3516	1845.1269	2167.8149	2375.8061	2578.3735	2692.7937	2829.5609	3106.2939	3458.9252	3764.2824
40	1638.8862	1953.1309	2267.3756	2610.4055	2841.5185	2937.4070	3169.8953	3476.6022	3847.8965	4282.0817	4809.8706
50	1927.3949	2330.4685	2733.5422	3059.0179	3268.7091	3401.9129	3724.9309	4163.1350	4757.8686	5235.9878	5688.7672
60	2366.7774	2744.3798	3121.9822	3484.0411	3755.4671	3962.3691	4469.9171	4995.7620	5523.0663	6074.4416	6826.5206
70	2799.3139	3186.6657	3574.0175	3941.8097	4227.1315	4483.7920	5050.3641	5638.1302	6299.4209	7086.8485	8144.870
80	3250.9275	3641.9037	4032.8799	4400.4447	4656.3317	5071.6294	5709.4423	6443.5774	7199.3382	8284.599	9828.446
90	3735.1174	4136.0536	4536.9899	4911.5040	5092.1615	5705.5831	6423.1226	7167.8467	8191.825	9739.988	12126.689
100	4380.2762	4726.8278	5073.3794	5413.9991	5604.0504	6339.5367	7058.9735	7964.2741	9308.423	11411.166	14168.696
110	4880.0512	5248.1822	5616.3132	6002.9493	6164.4554	6973.4904	7850.4832	8859.919	10696.375	13604.091	16149.290
120	5445.2168	5805.5162	6165.8157	6548.6720	6854.3840	7686.5005	8564.1635	9882.563	12298.401	15657.922	18126.323
130	6048.4752	6406.3850	6764.2948	7150.7226	7566.5390	8412.8792	9277.844	11061.024	14151.958	17709.736	20079.179
140	6695.5321	7058.8872	7422.2423	7822.5287	8531.1214	9152.6715	10100.728	12425.492	16602.146	19791.132	21992.547
150	7372.5539	7736.7580	8100.9622	8446.7350	8975.9790	9905.923	11057.002	13868.292	18606.483	21825.138	23850.197
160	8080.4489	8440.5697	8800.6905	9220.2956	9662.0149	10672.679	12045.704	15540.744	20500.604	23762.878	25632.469
170	8902.0180	9211.8425	9521.6670	9946.5134	10452.761	11452.985	13201.749	17315.734	22470.281	25602.418	27320.194
180	9707.8311	10016.5328	10325.2345	10771.175	11266.401	12367.356	14264.529	19716.202	24508.641	27336.945	28895.990
190	10647.862	10903.175	11158.487	11624.268	12103.094	13309.620	15665.317	22484.949	26448.496	28936.249	30343.967
200	11540.063	11780.972	12021.882	12506.100	13074.836	14279.967	16973.872	24060.098	28089.008	30362.652	31650.735
210	12074.105	12531.848	12989.590	13416.982	13964.252	15278.588	18677.414	25217.846	29380.687	31592.864	32807.608
220	13026.006	13472.504	13919.001	14458.164	15001.714	16305.679	20290.653	26295.720	30398.556	32626.626	33812.242
230	13086.278	14024.494	14962.710	15433.455	16075.765	17519.267	22168.701	27312.183	31225.140	33480.908	34668.595
240	14070.366	15015.408	15960.450	16550.830	17186.793	18611.502	23395.383	28201.588	31910.779	34179.686	35385.424
250	15100.584	16045.769	16990.954	17592.150	18335.186	19906.405	24348.361	28943.476	32483.871	34746.816	35974.220
260	16323.401	17189.073	18054.746	18787.729	19521.343	21064.875	25236.853	29575.405	32964.746	35203.084	36447.354
270	17205.174	18229.505	19253.836	20026.197	20745.665	22442.548	26117.917	30139.783	33370.549	35565.527	36816.747

ii.4 Siemens Motor Drive Loss at 350V LUT

Siemens 75kW IM Motor Drive Losses at 350V

Angular Velocity (rad/s)	0	100	200	300	400	500	600	700	800	900	1000
Torque (Nm)											
0	20	81.712503	83.687313	116.141602	143.12381	181.15951	224.00484	274.18801	308.78287	353.13979	409.15440
10	430.52745	655.56269	880.59794	1156.07172	1381.4095	1599.5054	1792.8884	2031.5365	2133.8128	2430.2887	2520.5499
20	816.00835	1147.7026	1479.3968	1855.6558	2226.9518	2440.4481	2592.0982	2792.5268	2772.9986	3274.3360	3185.0248
30	1124.5572	1554.3605	1984.1638	2445.2195	2814.7440	3036.6230	3119.6235	3344.2761	3330.1594	3855.5910	3882.8673
40	1464.1306	1962.1499	2460.1692	2947.6672	3310.9000	3494.7316	3557.6026	3847.6218	3931.3785	4517.1388	4705.9823
50	1785.5031	2352.4003	2919.2975	3448.0895	3812.4923	4016.0690	4042.2298	4391.6627	4654.2113	5235.9878	5688.7672
60	2206.3320	2783.4602	3360.5883	3888.1472	4227.9378	4487.9895	4517.1388	4995.7620	5461.2165	6074.4416	6749.3796
70	2606.9022	3216.9306	3826.9590	4377.1351	4733.6735	4903.5441	5105.0881	5638.1302	6371.4192	7006.0296	7605.474
80	3032.4711	3676.4921	4320.5132	4858.5968	5229.9346	5389.6398	5709.4423	6371.4192	7117.2365	7822.774	8691.971
90	3519.5898	4175.1902	4830.7907	5385.5874	5783.1394	5943.5537	6353.0761	7086.8485	7914.731	8800.620	9893.413
100	4174.6042	4771.0747	5367.5452	5939.5152	6314.5169	6471.4455	7058.9735	7874.2762	8691.971	9778.467	11248.966
110	4653.5704	5297.1380	5940.7056	6484.6651	6885.0230	7191.3848	7764.8708	8661.704	9561.168	11009.475	12941.451
120	5198.2002	5859.3927	6520.5853	7074.1801	7510.9342	7765.7346	8470.7682	9449.131	10552.974	12287.737	14899.724
130	5677.7169	6435.8695	7194.0221	7663.6951	8136.8453	8412.8792	9277.844	10236.559	11565.509	13764.998	17516.329
140	6340.8516	7091.1122	7841.3728	8315.3213	8762.7565	9152.6715	9991.524	11023.987	12742.838	15644.710	19703.094
150	6920.0704	7736.7580	8553.4456	8975.9790	9471.7753	9806.434	10822.209	11946.411	14117.947	17651.581	21780.939
160	7670.0062	8478.5151	9287.0240	9717.1935	10192.0794	10566.318	11668.773	12887.155	15558.364	20368.646	23847.002
170	8381.3290	9211.8425	10042.3560	10476.9860	10923.708	11339.721	12531.269	14000.297	17064.747	22465.399	25814.125
180	9150.8477	10016.5328	10882.2179	11255.490	11767.353	12246.887	13409.751	15151.092	19019.372	24364.989	27617.997
190	10053.863	10903.175	11752.487	12052.841	12634.323	13054.431	14304.273	16339.792	21091.009	26257.138	29253.431
200	10908.308	11780.972	12653.637	12960.491	13524.781	14010.126	15214.888	17750.703	23935.944	28062.494	30719.176
210	11477.541	12531.848	13586.155	13897.554	14438.891	14993.965	16308.043	19220.610	25624.991	29605.236	32001.029
220	12199.054	13414.733	14630.412	14864.352	15376.819	16006.140	17259.323	20750.113	26822.993	30814.054	33087.122
230	12501.705	14024.494	15547.282	15861.212	16470.676	17046.846	18410.370	22556.303	27842.821	31741.705	33980.534
240	13236.832	14951.376	16665.919	16888.464	17463.125	18116.278	19402.703	23805.226	28713.724	32464.684	34698.676
250	14221.879	15977.773	17733.667	17946.445	18625.088	19214.634	20612.259	24802.450	29443.471	33040.088	35265.936
260	15398.006	17116.734	18835.462	19035.495	19672.972	20342.113	21855.797	25727.807	30070.536	33506.617	35707.089
270	16334.431	18153.144	19971.857	20286.046	20904.247	21686.773	23133.546	26629.089	30632.974	33891.015	36043.736

ii.5 Siemens Motor Drive Loss at 400V LUT

Siemens 75kW IM Motor Drive Losses at 400V

Angular Velocity (rad/s) Torque (Nm)	0	100	200	300	400	500	600	700	800	900	1000
0	20	79.913815	83.720988	107.647749	142.61166	184.10821	228.43235	289.66132	344.43302	426.18267	476.33867
10	436.57904	686.57323	936.56742	1191.63859	1494.7786	1754.6501	1973.3000	2276.9341	2446.1669	2799.3180	2936.4438
20	853.09191	1209.0672	1565.0425	1995.0562	2460.1692	2750.2158	2966.8440	3240.0471	3334.9601	3431.2430	3812.4923
30	1163.4676	1640.1313	2116.7951	2658.2707	3161.2522	3448.0895	3617.1377	3789.7993	3956.0796	4002.3030	4447.0033
40	1513.8947	2072.4807	2631.0666	3220.5271	3752.9920	3989.3240	4159.4980	4265.5607	4483.2403	4659.4408	5124.3337
50	1804.9909	2475.3344	3145.6779	3756.6752	4259.3595	4475.7272	4570.2436	4762.6781	5071.6294	5352.6022	5882.4779
60	2198.9517	2902.7581	3606.5645	4278.7336	4787.1888	4987.2328	5140.7880	5325.2109	5709.4423	6143.8686	6749.3796
70	2630.7906	3370.9060	4111.0214	4860.0707	5296.5694	5525.2023	5547.3168	5892.0915	6371.4192	7086.8485	7784.477
80	3088.7102	3852.4640	4616.2178	5331.1875	5821.0418	6093.6581	6085.9553	6515.8959	7199.3382	8006.891	8691.971
90	3616.5552	4374.3113	5132.0674	5873.4124	6393.4166	6609.1658	6634.2012	7249.0246	8006.891	8904.072	9663.775
100	4153.6799	4927.9885	5702.2971	6434.5874	6932.4966	7207.6737	7292.9829	7984.2741	8794.145	9778.467	10737.527
110	4631.6499	5470.7577	6309.8655	7027.9431	7500.8569	7779.6912	8022.2812	8760.701	9673.560	10630.152	11811.280
120	5272.7027	6078.0962	6883.4896	7666.8471	8114.8688	8406.0756	8657.7670	9557.129	10552.974	11596.529	13037.956
130	5820.2070	6705.1903	7590.1736	8305.7510	8791.1079	9019.1816	9379.248	10470.813	11432.389	12712.007	14456.887
140	6434.6165	7352.3960	8270.1755	8944.6549	9467.3470	9619.0544	10100.728	11276.260	12311.803	13689.854	15928.548
150	7147.5085	8055.9751	8964.4418	9651.8810	10143.5860	10306.130	10939.474	12081.708	13191.218	15012.921	17647.434
160	7821.6516	8747.3671	9673.0825	10368.3926	10910.3373	10993.205	11794.136	13031.792	14234.473	16383.649	19866.298
170	8631.9096	9543.8142	10455.7189	11172.2176	11785.244	11794.314	12664.765	13846.279	15298.594	17802.358	22453.425
180	9397.8728	10329.3232	11260.7737	11995.172	12581.034	12488.098	13551.416	14823.844	16383.649	19479.976	24300.059
190	10392.642	11240.576	12088.510	12837.395	13497.213	13309.620	14454.144	15819.913	17686.003	21456.409	25864.394
200	11346.524	12142.859	12939.195	13699.028	14437.331	14279.967	15373.001	16834.547	18823.929	23535.441	27289.779
210	11941.726	12915.436	13889.146	14678.688	15401.556	15136.115	16474.809	17867.808	20420.352	25048.814	28536.584
220	12774.702	13823.008	14871.313	15688.690	16518.059	16155.739	17434.424	18919.759	21852.928	26308.554	29587.717
230	12893.322	14389.766	15886.210	16729.368	17537.464	17203.960	18594.257	19990.462	23571.935	27425.510	30468.223
240	13873.516	15403.938	16934.360	17686.003	18722.849	18116.278	19787.769	21079.981	24761.447	28383.649	31208.125
250	14900.494	16458.398	18016.302	18783.376	19946.620	19386.981	21015.189	22418.960	25722.782	29183.187	31830.222
260	15976.094	17554.338	19132.582	20038.901	21209.191	20522.180	22276.748	23556.062	26616.122	29863.109	32353.014
270	17102.235	18692.998	20283.761	21205.750	22348.575	21686.773	23572.679	24807.064	27483.340	30462.599	32792.337

iii.1 Simulation Model Parameters

```
%% Vehicle Chassis Mass (kg)
Mass_vehicle = 859;

%% Topology Specific Component Total Mass (kg)
Topology_A = 355;
Topology_B = 421;
Topology_C = 383.5;
Topology_D = 426.5;
Topology_E = 392.5;
Topology_F = 435.5;
Topology_G = 465;
Topology_H = 470;
Topology_I = 490;
Topology_J = 400;
Topology_K = 647.5;
Topology_Q = 426;
Topology_New = 425;
M_vehicle = Mass_vehicle + Topology_New;

%% Drag Coefficient
C_drag = 0.30;
%% Frontal Drag Area of Vehicle Cd Measured Over (m^2)
A_vehicle = 0.6333;

%% Wheel Data
r_wheel = 0.254;
r_tire = 0.381;
m_tire = 7;
m_wheel = 7.25;

%% Wheel Inertia
J_wheel = ((m_tire * (r_tire^2)) + (m_wheel * (r_wheel^2)));

%% Maximum Breaking Force (N)
F_brake_max = 0.6*g*M_vehicle ;

%% Maximum Braking Torque (Nm)
T_brake_max = F_brake_max * r_tire;

%% Starting Speed (m/s)
u_zero = 0;
```

Appendix iv

iv.1 Fuel Cell Characterisation Data

<i>Demand Current (A)</i>	<i>Stack Current (A)</i>	<i>Stack Voltage (V)</i>	<i>H2 Consumption (kg/hr)</i>	<i>System Power (W)</i>	<i>Stack Power (W)</i>	<i>Efficiency (%)</i>
0	1.26	395.5	0.0117	0	0	20
3.52	13.9	395.5	0.1346	1392.16	4315	32.2595
11.08	17.88	382.5	0.1819	4238.1	6057.2846	69.967
18.75	26.35	374.5	0.3078	7021.875	10250.3688	68.5036
33.2	43.1	364	0.545	12084.8	18149.9863	66.583
57.34	68.94	351.5	0.9414	20155.01	31346.9945	64.2965
75.99	91.59	344	1.2475	26140.56	41542.6946	62.9246
99.84	118.34	336	1.6391	33546.24	54581.1637	61.4612
119.56	140.76	329.5	1.9628	39395.02	65361.8183	60.2722
138.42	162.72	322.5	2.2724	44640.45	75672.3226	58.9918
155.87	184.97	317	2.5589	49410.79	85211.9991	57.9857
169.11	201.51	313.5	2.7763	53015.985	92450.1262	57.3455
179.2	213.9	311	2.9419	55731.2	97966.1913	56.8882
187.77	222.87	308	3.0826	57833.16	102651.2932	56.3394
190.74	227.34	306.5	3.1314	58461.81	104274.9516	56.0651
196.9	232.9	304.5	3.2325	59956.05	107642.5394	55.6992
211.02	251.72	298.5	3.4643	62989.47	115361.7505	54.6017
222.4	264.5	295.5	3.6511	65719.2	121583.041	54.0529
228.86	272.56	293.5	3.7572	67170.41	125114.6347	53.6871
233.51	277.21	290.5	3.8335	67834.655	127656.7262	53.1383